

Morphogenesis and protein production in
Aspergillus niger

Min Jin Kwon

Morphogenesis and protein production in

Aspergillus niger

Proefschrift

ter verkrijging van
de graad van Doctor aan de Universiteit Leiden,
op gezag van Rector Magnificus Prof. Mr. C.J.J.M. Stolker,
volgens besluit van het College voor Promoties
te verdedigen op donersdag 19 Juni 2014
klokke 10:00 uur

door

Min Jin Kwon

geboren te Busan, Republic of Korea

in 1978

Promotie commissie

Promotor: Prof. Dr. C.A.M.J.J. van den Hondel
Prof. Dr. V. Meyer (Technische Universität Berlin)

Co-promotor: Dr. A.F.J. Ram

Overige leden: Prof. Dr. H.A.B. Wösten (Universiteit Utrecht)
Prof. Dr. S. Brul (Universiteit van Amsterdam)
Dr. J. Wagener (Max von Pettenkofer Institute, München, Germany)
Dr. C.M.J. Sagt (DSM)
Prof. Dr. C. ten Cate (Universiteit Leiden)
Prof. Dr. P.J. Punt (Universiteit Leiden)

This work described in this thesis was financially supported by the Kluyver Centre for Genomics of Industrial Fermentations and carried out at the Institute of Biology in the department Molecular Microbiology and Biotechnology at Leiden University

Cover design by Joohae Park:

Front Left: *A. niger* GFP-RacA localization (top), GFP-SncA (bottom)

Right: CFP-TubA (top), SlaB-YFP (bottom) in *A. niger* Δ racA strain

Back: Life-image of *A.niger* GFP-SncA strain

Printed by: Ridderprint BV

ISBN: 978-90-5335-875-7

내 사랑하는 가족들에게~

정말 고맙습니다!

Contents

Chapter 1

General introduction	9
Aim and thesis outline	18

Chapter 2

Functional characterization of Rho GTPases in <i>Aspergillus niger</i> uncovers conserved and diverged roles of Rho-proteins within filamentous fungi	21
---	----

Chapter 3

The transcriptomic signature of RacA activation and inactivation provides new insights into the morphogenetic network of <i>Aspergillus niger</i>	49
---	----

Chapter 4

The transcriptomic fingerprint of glucoamylase over-expression in <i>Aspergillus niger</i>	81
--	----

Chapter 5

Molecular genetic analysis of vesicular transport in <i>Aspergillus niger</i> reveals partial conservation of the molecular mechanism of exocytosis in fungi	109
--	-----

Chapter 6

General discussion	133
--------------------	-----

Summary	139
---------	-----

Samenvatting	141
--------------	-----

Supplementary material	143
------------------------	-----

References	147
------------	-----

Publications	163
--------------	-----

<i>Curriculum Vitae</i>	165
-------------------------	-----

General Introduction

1. The importance of filamentous fungi in product formation

The fungal kingdom is estimated to exist of over 1.5 million species among which only a small number of species have been described in detail (Hawksworth 2001). There is a huge diversity among fungi, both in their morphology as well as in the products they can produce. Morphologically, the fungal kingdom includes unicellular yeast cells as well as multi-cellular hyphal cells that form a mycelium. Hyphal cells grow exclusively at the tip of the hyphae in a highly polarized way (Momany 2002). Many filamentous fungi are saprophytes meaning that they feed on dead organic material. It is, therefore, necessary for them to secrete large amounts of extra-cellular hydrolytic enzymes to decompose these often complex organic materials in nature.

For centuries, filamentous fungi have been used in many traditional food processes such as cheese-making, sake (rice wine) and soy sauce production. Nowadays, filamentous fungi are also used as cell factories in biotechnology to produce a wide variety of products such as enzymes, primary and secondary metabolites including organic acids and antibiotics. Filamentous fungi have been explored as expression hosts for protein production of both fungal and non-fungal origin (Punt et al. 2002; Su et al. 2012). So the industrial application areas utilizing filamentous fungi are very diverse including food and beverage, pulp and paper, feed and pharmaceuticals (Fleissner and Dersch 2010; Meyer 2008; Saloheimo and Pakula 2012).

Relatively few species have been developed into a commercially exploited filamentous fungal expression system. The most frequently used industrial fungi include *Trichoderma reesei*, *Aspergillus oryzae*, *A. niger* and *Myceliophthora thermophila* (previously known as *Chrysosporium lucknowense* C1 (Berka et al. 2011; Verdoes et al. 2007; Visser et al. 2011)). *T. reesei* has mainly been used for the production of cellulases and other plant cell wall-degrading enzymes (Saloheimo and Pakula 2012; Schuster and Schmoll 2010). Fermented foods including soy sauce and sake are produced by *A. oryzae* (Machida et al. 2008) and citric acid and amylases that are used in the beverage and food industry respectively are mostly produced by *A. niger* (Pel et al. 2007). *M. thermophila* is a recently described fungal expression system for neutral cellulases and heterologous protein production (Berka et al. 2011; Visser et al. 2011). Recently, increased attention has been paid to second generation feedstocks using wheat straw or sugar cane bagasse. Compared to first generation feedstocks, these are cheaper more environmentally friendly and less competitive in

relation to food supply (Kumar et al. 2008; Zheng et al. 2012). Filamentous fungi have been shown as predominant hosts for the enzymes that are used for the saccharification process (Gusakov 2011; Sims et al. 2010) as well as for the direct microbial conversion from crude feedstock into bioproducts (Beeson et al. 2011; Lin et al. 2010; Rumbold et al. 2009; van den Brink et al. 2013). *A. niger* has also been shown as a potential and promising host for those processes (Delmas et al. 2012; Rumbold et al. 2010; Rumbold et al. 2009).

2. Factors affecting the productivity

A successful commercialization of fungal enzymes in relation to lignocellulose degradation or the production of metabolites is only possible when these proteins or metabolites are efficiently produced. Productivity is affected by many factors such as culture conditions, morphology and the fungal host strain. In the next sections, these different factors are discussed in more detail.

2.1. Culture conditions

Different culture conditions including the composition of culture medium, pH, temperature and the type of cultivation affect product formation. The carbon source is not only important as energy source, but also an important factor that decides which product is to be formed. For example, when starch or maltose is used as a carbon source, amylolytic enzymes including glucoamylase (GlaA) are highly induced and secreted, whereas xylose induces the synthesis of (hemi)cellulolytic enzymes (de Oliveira et al. 2011). Galacturonic acid, the main component of pectin induces the expression of pectinolytic enzymes (Martens-Uzunova and Schaap 2009). In addition, the carbon source affects the productivity. It has been shown that the production rate of extracellular proteins is three times higher on maltose than xylose (Jørgensen et al. 2009). Besides the carbon source of the medium, the pH, temperature and agitation speed of culture medium can affect the productivity. Withers et al. found that the GlaA productivity was not affected in the pH range 3.5-5.5 and culture temperature 30 and 37°C, but significantly reduced at pH 6.5 and at 25°C (Withers et al. 1998). In addition, the effect of pH on extracellular protease activity in relation to the heterologous protein (GFP) production was investigated using *PgpdA-GlaA-GFP* in which about ten times higher GFP was yielded at pH 6 compared to pH 3 because of lower protease activity (O'Donnell et al. 2001).

The cultivation method such as solid-state or submerged cultivation can influence the protein production (Gamarra et al. 2010; Oda et al. 2006; te Biesebeke et al. 2006). Using the same substrate (wheat bran), te Biesebeke et al. found important differences in the

secretome between submerged and solid state conditions. Whereas the enzyme α -amylase was identified under both conditions, arabinosidase and xylanase were abundantly produced in submerged cultures, while a chitinase and two new proteins that were thought to be involved in filamentous fungal-specific functions were produced in solid state cultures in *A. oryzae* (te Biesebeke et al. 2006). The culture condition in which the fungus grows can also affect the product formation. For example, Jørgensen et al. reported that transcript levels of genes encoding secondary metabolites such as potential polyketide synthase (PKS), nonribosomal peptide synthetase (NRPS) and small cysteine-rich proteins (e.g. hydrophobines) were enhanced at near-zero growth conditions. The expression of extracellular hydrolases (e.g. GluA) was strongly downregulated under these conditions (Jørgensen et al. 2010).

2.2. Fungal morphology

The morphology of filamentous fungi has a strong influence on their production properties (Grimm et al. 2005; McIntyre et al. 2001; Papagianni 2004). In submerged cultures, filamentous fungi grow either as freely dispersed mycelium including loosely intertwined hyphae (dispersed mycelium), as clumps or as pellets (Grimm et al. 2005; Riley et al. 2000). The preferred morphology cannot be generalized because it varies depending on the product. In *A. niger* pelleted forms are preferred for citric acid production while dispersed filaments of *A. niger* are favored for enzyme production (Braun and Vecht-Lifshitz 1991; Gibbs et al. 2000; Papagianni 2004). In addition, the growth-form can strongly affect mixing and mass transfer properties. Dispersed long hyphae cause high viscosity of culture broth and these long hyphae are sensitive to shear forces in a bioreactor. Grown as pellets, the mycelia is less viscous but is confronted with difficulties of nutrient and oxygen access inside the pellet (Gibbs et al. 2000; Grimm et al. 2005). Thus, the preferred fungal macromorphology would consist of loosely grown mycelia with short filaments derived from an optimum branching frequency to ensure the high productivity as well as better nutrient and oxygen supply for the cells (Grimm et al. 2005; Kaup et al. 2008; Papagianni 2007). Several studies identified multiple factors affecting fungal morphology which include agitation, medium composition, temperature and the way of inoculating cultures (Amanullah et al. 2002; Papagianni 2004; Wucherpfennig et al. 2010). In addition, a recent study showed that the age of conidia also influenced the adhesion properties thereby leading to different diameters of pellets (Colin et al. 2013). Addition of talc, alumina, or titanate microparticles was used to manipulate different morphology states to increase product formation in *A. niger* and other filamentous microorganisms (Driouch et al. 2012; Driouch et al. 2010; Kaup et al. 2008).

It is generally accepted that protein secretion occurs mainly at the hyphal apex as demonstrated by several studies e.g. localization of glucoamylase or α -amylase at hyphal tips (Gordon et al. 2000; Muller et al. 2002; Wösten et al. 1991). Some studies suggested a positive correlation between the amount of hyphal branches and protein secretion yields (Amanullah et al. 2002; Muller et al. 2002; te Biesebeke et al. 2005; Wongwicharn et al. 1999), while other reports demonstrated no correlation (Bocking et al. 1999; McIntyre et al. 2001). Our recent study showed that simply making more hyphal tips did not result in an increase of a protein production level using a hyperbranching mutant (Kwon et al. 2013b). Therefore, it is still a matter of debate whether a hyperbranching strain could improve protein production yields. Recently, it has been shown that the secretion also takes place at the septa using GFP fused α -amylase (AmyB-GFP) in *A. oryzae* (Hayakawa et al. 2011).

2.3. The fungal host strain

Filamentous fungi are main sources for the production of many commercial enzymes and organic compounds. Products of each fungal host strain can overlap but also be distinct (Table 1). *M. thermophila*, *T. reesei*, *A. oryzae* and *A. niger* are very efficient for the production of proteins. On one hand, several enzymes such as glucose oxidase, protease and phytase are produced from both *A. oryzae* and *A. niger*, or xylanase is produced from *T. reesei* and *A. niger*. Plant-polysaccharide-degrading enzymes such as cellobiohydrolases are produced from *T. reesei* and *M. thermophila* (Visser et al. 2011). On the other hand, certain products are only specifically produced from certain fungi: itaconic acid from *A. terreus*, kojic acid from *A. oryzae*, citric acid mainly from *A. niger* (Table 1). Here we focus on *A. niger* and why and/or how this fungus possesses high protein secretion capacity.

3. The protein secretion capacity of *A. niger*

A. niger is well known for its tremendous capacity to secrete proteins into the culture medium and is used as a cell factory not only for native products e.g. glucoamylase (GlaA), but also for heterologous protein production (Meyer 2008; Meyer et al. 2011b; Pel et al. 2007). The complete genome sequence comparison of several fungi including *A. nidulans* and *S. cerevisiae* revealed that the number of genes related to protein secretion do not correlate with the secretion capacity of the species (Pel et al., 2007). It still remains unknown what makes *A. niger* a good protein secretor. In the following section, a few potential mechanisms are described which could contribute to the high secretion capacity of *A. niger*.

3.1. Uncoupling of growth and secretion

Growth and secretion in fungi are considered to be tightly linked processes. The high capacity of protein secretion of *A. niger*, however, cannot be explained by a more rapid growth of *A. niger* in comparison to e.g. *S. cerevisiae* or *A. nidulans* which secrete much lower levels of proteins. Therefore, it is possible that *A. niger* has developed mechanisms in which growth and high levels of protein secretion can be uncoupled. One possible mechanism could be the existence of parallel secretory pathways that independently deliver proteins for secretion (e.g. GlaA) and proteins related to growth (e.g. plasma membrane proteins and cell wall synthesizing enzymes) to the cell surface. Several studies including studies in fungi, plants and mammalian cells show that different populations of Golgi derived vesicles exist. In *S. cerevisiae* two populations of vesicles have been described: one is characterized by the presence of an enzyme involved in cell wall biosynthesis (Bgl1p) and the major plasma membrane ATPase (Pma1p) and the other population contains secreted enzymes, invertase and acid phosphatase (Harsay and Bretscher 1995). In *Yarrowia lipolytica*, mutants have been identified that are specifically affected in the export of plasma membrane and cell wall associated proteins but not in the secretion of extracellular proteins (Titorenko et al. 1997). Also in plants, it has been demonstrated that secretory proteins and cell wall synthase complexes move to different secretory pathways (Leucci et al. 2007).

Table 1. Selected examples of industrially important acids and enzymes produced by filamentous fungi.

Compound	Organism	Main application areas
Acids		
Citric acid	<i>A. niger</i>	Food and beverage
Itaconic acid	<i>A. terreus</i>	Polymer
Kojic acid	<i>A. oryzae</i>	Food
Enzymes		
α -Amylase	<i>A. niger</i> , <i>A. oryzae</i>	Starch processing and food
Cellulase	<i>Trichoderma viride</i> , <i>T. reesei</i> , <i>M. thermophila</i>	Textile, pulp and paper
Cellobiohydrolase	<i>T. viride</i> , <i>T. reesei</i> , <i>M. thermophila</i>	Textile, pulp and paper
Glucoamylase	<i>A. phoenicis</i> , <i>Rhizopus delemar</i>	Starch processing
Glucose oxidase	<i>A. niger</i> , <i>A. oryzae</i>	Textile and Biosensor
Lipases	<i>A. niger</i> , <i>A. oryzae</i>	Food and detergent
Pectin lyase	<i>T. reesei</i>	Food
Proteases	<i>A. niger</i> , <i>A. oryzae</i> , <i>R. delemar</i>	Food and detergent
Phytase	<i>A. niger</i> , <i>A. oryzae</i>	Food
Xylanases	<i>T. reesei</i> , <i>T. konignii</i> , <i>A. niger</i> , <i>M. thermophila</i>	Textile, pulp, paper and bakery

Table is adapted from (Meyer 2008) with a small modification in which *M. thermophila* was included (Ustinov et al. 2008; Visser et al. 2011).

A study in the filamentous fungus *T. reesei* revealed the possible presence of more than one pathway for exocytosis based on spatial segregation of different SNARE complexes in the fungal tip cell (Valkonen et al. 2007). More recently, a distinct secretory route that occurs behind the apex independently of the Spitzenkörper was demonstrated in *Neurospora crassa* (Fajardo-Somera et al. 2013). There a GFP-tagged plasma membrane (PM) H⁺-translocating ATPase (PMA-1) localized at the subapical PM (>120 μm), but not at the tip or in the Spitzenkörper was described. In addition, fluorescence recovery after photobleaching (FRAP) analysis suggested that PMA-1 was incorporated directly into the PM indicating an alternative secretion pathway in filamentous fungi (Fajardo-Somera et al. 2013). Also in *A. niger*, the existence of parallel secretion pathways has been suggested based on the phenotype of the *srgA* mutant. SrgA is the ortholog of the Sec4 protein, a Rab GTPase essential for exocytosis and cell viability in *S. cerevisiae*. In *A. niger*, deletion of *srgA* is not lethal, but the extracellular protein production on glucose was severely reduced while the production on maltodextrin was only marginally reduced (Punt et al. 2001). These results might be explained by postulating the existence of the two different secretion pathways: a constitutive pathway, highly dependent on SrgA and an additional, inducible pathway that is less dependent on the function of SrgA. We postulate that these parallel secretion pathways are present in all fungi and are used by *A. niger*. Possibly also other high secretors are using parallel secretion pathways to be able to increase secretion capacity of extracellular enzymes.

3.2. More efficient COPII machinery

Secretory proteins and enzymes destined for secretion follow a conventional endoplasmic reticulum (ER)-Golgi secretory route. Once properly folded and glycosylated in the ER, secretory proteins are packed into coat protein complex II (COPII)-coated vesicles and transported to the Golgi complex. The COPII core machinery comprises five proteins; Sar1, a secretion-related RAS1 GTPase and two subcomplexes, Sec23/24 and Sec13/31 (Brandizzi and Barlowe 2013). The assembly of COPII coat is initiated by Sar1 activation in which inactive and soluble Sar1-GDP is converted into the active and membrane bound form of Sar1-GTP by a guanine nucleotide exchange factor (GEF), Sec12, which is an ER resident membrane protein (Barlowe and Schekman 1993). Activated Sar1 then recruits the ‘inner layer’, Sec23/24, through binding to Sec23 (Bi et al. 2002). Sec24 serves as a main COPII adaptor that specifically recognizes ER export signals in cargo (Brandizzi and Barlowe 2013). Finally the ‘outer layer’, Sec13/31, is recruited and formed into a cage structure and COPII-coated vesicle budding is completed by membrane curvature and fission (Brandizzi and Barlowe 2013). Although the five proteins (Sar1, Sec23/24 and

Sec13/31) are the minimal core that can form COPII vesicles from membranes *in vitro* (Barlowe et al. 1994; Matsuoka et al. 1998), other elements are also required such as Sec16 that facilitates COPII vesicle formation at the ER (D'Arcangelo et al. 2013).

One of the reasons why *A. niger* possesses such an outstanding secretion capacity could be an efficient packaging of cargo via the COPII machinery. Although the information about COPII-coated vesicle transport available for *A. niger* is sparse, our transcriptomic study using the glucoamylase (GlaA) overproducing strains hints to a role of COPII machinery under high secretion conditions. By comparing the transcriptomes of a GlaA over-producing strain to a wild-type strain (Chapter 4), it was found that the expression levels of several COPII-related genes were induced. These induced genes include the five COPII core genes (Sar1, Sec23/24 and Sec13/31), Sec16 as well as four ER vesicle proteins (Ervs, -29, -14, -41, -46). These four Ervs are ER resident proteins that are packed into COPII vesicles; Erv29 is involved in trafficking of multiple soluble cargo proteins, Erv14 is required for the ER exit of many integral membrane proteins, Erv41 and Erv46 forms a complex to be involved in the membrane fusion stage of the ER to the Golgi transport (D'Arcangelo et al. 2013; Otte et al. 2001). In total 16 of the 26 genes related to the COPII vesicle transport were differentially expressed in the GlaA overexpression strain, making it one of the most significantly enriched Gene Ontology (GO) (Chapter 4, Table A4). Although this data does not directly indicate that the COPII machinery is more efficient compared to others, it can show at least that *A. niger* can modulate its secretory machinery (or at least COPII machinery) depending on the loads of secretion which may enable this fungus to secrete high. Further studies such as the investigation of the role of cargo recruiting proteins (Sec24 and Erv proteins) or COPII-coated vesicle formation in *A. niger* could give more insights into the role of cargo recruitment in relation to efficient protein secretion.

3.3. Heterogeneity and super-secreting hyphae in *A. niger*

The two methods most often used to grow filamentous fungi are on agar plates or in liquid cultures (shake flasks or bioreactors). In *A. niger* liquid cultures, inoculation with fungal spores results in the formation of micro-pellets with a diameter size up to a few millimeter. On plates, the fungal colony can be divided into several zones covering the centre of the colony towards the edge of the colony (Levin et al. 2007). Heterogeneity in *A. niger* is observed at the colony level (zonal difference), pellet level as well as at the hyphal level with respect to growth, gene expression and protein secretion (de Bekker et al. 2011a; de Bekker et al. 2011b; Krijgsheld et al. 2012; Levin et al. 2007; Vinck et al. 2011; Vinck et al. 2005; Wösten et al. 1991). Only a limited region of a plate colony can grow and secrete

proteins namely the central and periphery zone of the colony, however, glucoamylase is secreted only at the periphery zone (Wösten et al. 1991). Secretome analysis revealed that the secreted proteins are different between zones of macro-colonies (Krijgsheld et al. 2012). Even within one zone, the peripheral zone, the secretion and expression of genes are different (Vinck et al. 2011; Vinck et al. 2005). By using a reporter strain that expresses GFP under the control of the glucoamylase promoter (*P_{glaA}*) it was demonstrated that there are two different populations of hyphae present at the periphery of the colony: one population that has high and another one with low GFP fluorescence (Vinck et al. 2005). Similar results were obtained using different promoters, *aguA*, *faeA* or *aamA* (Vinck et al. 2011). Surprisingly, even among neighboring hyphae, gene expression profiles are different (de Bekker et al. 2011a).

Heterogeneity has also been observed at the level of micro-pellets. Statistical analysis of the population of cell pellets indicated two different populations with respect to size and gene expression using GFP reporter strains under control of *P_{glaA}*. Larger pellets with an average diameter of 595 μm represented 61% of the cultures, while smaller pellets with an average diameter of 505 μm accounted for 39% (de Bekker et al. 2011b). A high fluorescent population was observed in 32% whereas 68% showed a low fluorescence (de Bekker et al. 2011b). The ratio of highly or lowly expressed populations was not the same but different among different strains e.g. *P_{faeA}*, *PaamA* (de Bekker et al. 2011b). In addition, heterogeneous mRNA accumulation was shown within the pellets showing zonal differences (de Bekker et al. 2011b). Heterogeneity of macro-colonies can also be found in other filamentous fungi such as *Neurospora crassa* and *A. oryzae* (Kasuga and Glass 2008; Masai et al. 2006; Moukha et al. 1993), however, studies are not as detailed as in *A. niger* (see above); only the difference in zonal gene expression or secretion was studied.

So what can possibly make *A. niger* a better secretor than the others? In *A. niger*, different populations of hyphae seem to be present that may act as high or low producers. It will be of interest to examine whether the heterogeneity on the hyphal level is also found in other fungi. If a higher percentage of so called ‘super secreting hyphae’ is only found in *A. niger* this might explain the difference. Yet another aspect to study the process in more detail is to try to convert all hyphae in a culture into super secreting hyphae and thereby further improve protein production. To address this, it is important to establish the molecular mechanism by which a normal hypha is converted into a ‘super secreting hypha’.

4. The future is on the dynamics

Once a secretory protein is translated, it has to travel through the secretory pathway (see above). It may be possible that *A. niger* has a higher rate of secretion compared to other

fungi. To address that, a kinetic study of protein synthesis and secretion needs to be followed in the future as has been performed in *T. reesei*. Using *in vivo* labeling experiments, the average synthesis time and secretion time of CBHI cellobiohydrolase were measured as 4 min and 11 min respectively in *T. reesei* (Pakula et al. 2000). Secretion time of *T. reesei* was somewhat slower compared to the yeast, *S. cerevisiae* in which invertase transport time was 5 min (Novick et al. 1981; Pakula et al. 2000). Since the kinetic data for the protein synthesis and secretion in filamentous fungi are scarce, it will be of interest to determine the kinetics and compare the results among fungi in the future.

Several recent studies have indicated the important interplay between endocytosis and exocytosis in relation to protein secretion. It is proposed that exocytosis occurs at the hyphal tips in filamentous fungi, whereas endocytosis occurs behind the tip (Taheri-Talesh et al. 2008). Exocytosis is visualized using GFP-tagged reporters (GFP-SynA in *A. nidulans* (Taheri-Talesh et al. 2008), AmyB-GFP in *A. oryzae* (Hayakawa et al. 2011) or GFP-SncA in *A. niger* (Kwon et al. 2013b)) showing the signals along the hyphae but more pronounced at the hyphal tips (Chapter 3 & 5). The endocytic machinery was shown to be a ring-like structure that is excluded from the hyphal apex and localized a few μm behind the growing apex (Araujo-Bazan et al. 2008; Kwon et al. 2013b). Polarized secretion and growth require the delivery of cell wall biosynthetic enzymes as well as the delivery of extracellular enzymes via secretory vesicles. The retrieval and recycling of the excess membrane used for the delivery via secretory vesicles is necessary and is taken care of via endocytic processes. Further analysis of a turn-over rate for endo/exocytosis will provide important information with respect to the secretion capacity.

Secretory related organelles e.g. ER, Golgi and secretory vesicles are most important serving as the folding, modification and delivering station, respectively. The localization of these organelles is abundantly present through the hyphae especially in the apical area (Carvalho et al. 2011b; Markina-Inarrairaegui et al. 2013; Pantazopoulou and Penalva 2009; Pinar et al. 2013). In the past few years, these organelles have been successfully labeled with fluorescent markers and following their localization and dynamics under conditions of high protein production could give further insights into the mechanism by which filamentous fungi including *A. niger* secrete high amounts of proteins.

5. Aim and Thesis Outline

The research described in this thesis aims to get more fundamental insights in the molecular mechanisms used by *Aspergillus niger* in relation to control morphology and protein secretion. Knowledge on these two aspects is highly relevant to further optimization of *A. niger* as a cell factory.

Chapter 1 introduces what is important in relation to product formation in fungal biotechnology and mechanisms are discussed to explain the high secretion capacity of *A. niger*. In **Chapter 2**, the functional analysis of all six Rho GTPases encoded in *A. niger* (RacA, CftA, RhoA, RhoB, RhoC, RhoD) is described and revealed that they exert distinct and overlapping functions during the life cycle. Interestingly, a comparison of the function of Rho-GTPases among Aspergilli (in particular the comparison between *A. niger* and *A. nidulans*) revealed interesting differences (Harris 2011). **Chapter 3** describes a follow-up study of *racA* (Chapter 2) to elucidate the impact of morphology on protein production. This study clearly showed that simply making more hyphal tips did not result in an increase of protein production levels. In **Chapter 4**, the transcriptomic effect of overexpression of a secreted enzyme (glucoamylase) is described. It is shown that overexpression of glucoamylase induced many genes that are part of the unfolded protein response. A comparison of this dataset with other datasets in which *A. niger* was triggered to induce an unfolded protein response allowed to define a core set of genes that appear to be involved in dealing with misfolded proteins or high secretion loads. In **Chapter 5**, seven genes encoding putative *A. niger* orthologs that are known to function in key aspects of the protein secretion machinery in *S. cerevisiae* were analyzed. A reporter strain was constructed in which secretory vesicles are visualized by labeling a specific vesicle-SNARE (v-SNARE) with GFP giving GFP-v-SNARE. Using that strain, the protein secretion process in wild-type and mutants was visualized and analyzed. This study revealed that the exocyst-mediated vesicle transport is only partially conserved between *S. cerevisiae* and *A. niger*.

**Functional characterization of Rho GTPases in
Aspergillus niger uncovers conserved and diverged roles of
Rho-proteins within filamentous fungi**

**Min Jin Kwon*, Mark Arentshorst*, Eelke D. Roos, Cees A.M.J.J van den Hondel,
Vera Meyer and Arthur F.J. Ram**

*: both authors equally contributed to this work
Mol Microbiol (2011) 79(5):1151-67.

Abstract

Rho GTPases are signalling molecules regulating morphology and multiple cellular functions including metabolism and vesicular trafficking. To understand the connection between polarized growth and secretion in the industrial model organism *Aspergillus niger*, we investigated the function of all Rho family members in this organism. We identified six Rho GTPases in its genome and used loss-of-function studies to dissect their functions. While RhoA is crucial for polarity establishment and viability, RhoB and RhoD ensure cell wall integrity and septum formation, respectively. RhoC seems to be dispensable for *A. niger*. RacA governs polarity maintenance via controlling actin but not microtubule dynamics, which is consistent with its localization at the hyphal apex. Both deletion and dominant activation of RacA (Rac^{G18V}) provoke an actin localization defect and thereby loss of polarized tip extension. Simultaneous deletion of RacA and CftA (Cdc42) is lethal; however, conditional overexpression of RacA in this strain can substitute for CftA, indicating that both proteins concertedly control actin dynamics. We finally identified NoxR as a RacA-specific effector, which however, is not important for apical dominance as reported for *A. nidulans* but for asexual development. Overall, the data show that individual Rho GTPases contribute differently to growth and morphogenesis within filamentous fungi.

Introduction

Small monomeric GTPases are found in all eukaryotic organisms and function as molecular switches to regulate a vast array of cellular processes including metabolism, survival, morphogenesis, differentiation and vesicle transport. Based on structural similarities, small GTPases are grouped into five subfamilies: Ras, Rho (Ras homolog), Arf/Sar, Ran and Rab/Ypt. The Rho subfamily is the most extensively characterized subfamily and comprises six members in lower eukaryotes (e.g. Rho1p, Rho2p, Rho3p, Rho4p, Rho5p, Cdc42p in the yeast *Saccharomyces cerevisiae*) and more than 20 members in higher eukaryotes, with RhoA, Rac1 and Cdc42 being most studied (Heasman and Ridley 2008; Park and Bi 2007; Ridley 2006). Most Rho GTPases cycle between a GTP-bound (active) and a GDP-bound (inactive) form which is controlled by guanine nucleotide exchange factors (GEFs) and GTPase-activating proteins (GAPs). The localization of Rho GTPases to membranes and membrane compartments is post-transcriptionally regulated by prenylation (farnesylation or geranylgeranylation) of their C-terminus. This lipid modification defines the specificity to and enhances the interaction of Rho GTPases with different membranes. Guanine nucleotide dissociation inhibitors (GDIs) bind to prenyl groups of GTPases thereby

inhibiting their membrane localization as well as preventing their interaction with effector proteins. Thus, the activity of Rho GTPases is not only dependent on a functional GTP/GDP cycle but also on a membrane/cytosol cycle (Casey 1994; Dransart et al. 2005; Ridley 2006).

Various effector pathways have been discovered in eukaryotes which lie downstream of Rho GTPases: i) Actin filament nucleation and (de)polymerization on or close to membranes is regulated by interaction of Rho proteins (e.g. Rho1p/RhoA, Rac1, Cdc42) with WASP proteins, formins and PAK kinases. Because actin dynamics is closely linked to membrane dynamics and vesicular trafficking, the function of Rho GTPases is intimately linked to exocytosis, endocytosis as well as to polarized cell shape changes and cell movement (Bosco et al. 2009; Heasman and Ridley 2008; Park and Bi 2007; Ridley 2001; Ridley 2006). ii) Localized generation of reactive oxygen species (ROS) results from Rac1-mediated activation of NADPH oxidases (note that the hemiascomycetes *S. cerevisiae* and *Schizosaccharomyces pombe* do not comprise a Rac1 homolog). The regulated synthesis of ROS plays a key role in host defense responses and differentiation of multicellular organisms (Hordijk 2006; Scott and Eaton 2008). iii) Activation of cell wall synthesizing enzymes such as β -1,3 glucan synthases in *S. cerevisiae* and *S. pombe* is mediated by Rho1 (Arellano et al. 1996; Qadota et al. 1996) and positive regulation of α -1,3 glucan synthase activities has been shown for the *S. pombe* Rho2 (Calonge et al. 2000). iv) Finally, some Rho proteins have been shown to modulate gene transcription in mammalian cells as for example documented for the transcription factors NF κ B, AP1 and c-Jun (Benitah et al. 2004; Schlessinger et al. 2009).

Based on genome mining approaches, six Rho encoding genes have been predicted in filamentous fungi – *rac1*, *cdc42* and four genes encoding putative *S. cerevisiae* homologs of Rho1p, Rho2p, Rho3p, Rho4p (<http://www.broadinstitute.org/> and (Banuett et al. 2008; Boureux et al. 2007; Harris et al. 2009; Rasmussen and Glass 2005)). Over the past years, a crucial involvement of some of these Rho GTPases in the orchestration of the highly polarized growth mode of filamentous fungi has become apparent. For example, Rac1 and Cdc42 orthologs have been demonstrated to be pivotal for morphogenetic decisions e.g. in *Aspergillus nidulans*, *Claviceps purpurea*, *Magnaporthe grisea*, *Penicillium marneffii* and *Ustilago maydis* (Boyce et al. 2003; Chen et al. 2008; Mahler et al. 2006; Rolke and Tudzynski 2008; Virag et al. 2007). Rac1-mediated activation of fungal NADPH oxidases has been shown to generate tip-localized ROS in *A. nidulans* and *Epichloë festucae* which are suspected to be essential for sustaining apical dominance (Scott and Eaton 2008; Semighini and Harris 2008; Takemoto et al. 2006). Rho1 orthologs have been shown to be essential for hyphal tip extension and cell wall biosynthesis in *A. nidulans*, *Ashbya gossypii*, *Fusarium oxysporum* and *U. maydis* (Guest et al. 2004; Martinez-Rocha et al. 2008; Pham

et al. 2009; Wendland and Philippsen 2001). Considerably less information is available on the function of Rho2, Rho3 and Rho4 orthologs in filamentous fungi. An involvement of Rho3 in polar growth control has so far been documented for *A. gossypii* and *Trichoderma reesei* (Vasara et al. 2001; Wendland and Philippsen 2001), and a role of Rho4 for actin ring formation during hyphal septation has been established for *Neurospora crassa* and *A. nidulans* (Rasmussen and Glass 2005; Si et al. 2010).

As part of our effort to understand the connection between the processes of polarized growth, cell wall biosynthesis and secretion in the industrially important fungus *A. niger*, we use genome-wide expression profiling studies to predict and identify signalling molecules and networks involved in these processes (Jacobs et al. 2009; Jørgensen et al. 2009; Meyer et al. 2009; Meyer et al. 2007b). We furthermore implement functional genomics approaches to study the cellular role of predicted protagonist coordinating these processes (Damveld et al. 2005; Meyer et al. 2009; Meyer et al. 2008; Meyer et al. 2010a; Punt et al. 2001). Here, we systematically investigated the function of all members of the Rho family for growth and morphogenesis of *A. niger*. We identified six Rho GTPases in the genome of *A. niger* and used loss-of-function studies which showed that they exert distinct and overlapping functions during the life cycle of *A. niger*. While RhoA appears to be of central importance for polarity establishment and viability of *A. niger*, RhoB and RhoD ensure cell wall integrity. Whereas RhoC seems to be of minor importance for *A. niger*, RhoD has a pivotal role during septum formation. RacA and CftA (Cdc42) collectively ensure polarity maintenance, whereby the main protagonist is RacA. We furthermore show that RacA localizes to the hyphal apex and controls actin dynamics but not microtubule integrity and finally identified two downstream targets of RacA which are not shared with CftA. Most importantly, this work uncovers lack of uniformity in how members of the Rho GTPase family are deployed in filamentous fungi.

Results

A. niger has six Rho GTPases-encoding genes

Screening of the genome sequence of *A. niger* (Pel et al. 2007) revealed the presence of six open reading frames (ORFs) (An18g05980, An16g04200, An11g09620, An14g05530, An11g10030, An02g14200), each predicted to encode a single member of the Rho subfamily. Phylogenetic comparison with (predicted) Rho GTPases from *A. nidulans*, *N. crassa*, *M. grisea*, *P. marneffeii*, *S. cerevisiae*, *S. pombe* and *U. maydis* showed that each subgroup (Rasmussen and Glass 2005) was represented by a single *A. niger* orthologous

Table 1. Expression of predicted Rho GTPase genes in *A. niger* wild-type strain N402.

Gene	ORF code	Germination ^a	Steady state ^b ($\mu = 0.16 \text{ h}^{-1}$)	Exponential growth phase ^c ($\mu = 0.24 \text{ h}^{-1}$)
<i>rhoA</i>	An18g05980	9.40 ± 1.06	11.10 ± 0.72	10.00 ± 0.62
<i>rhoB</i>	An16g04200	1.61 ± 0.37	3.51 ± 0.30	3.54 ± 0.03
<i>rhoC</i>	An11g09620	0.43 ± 0.05	0.41 ± 0.02	0.51 ± 0.02
<i>rhoD</i>	An14g05530	0.63 ± 0.01	1.28 ± 0.08	1.69 ± 0.10
<i>racA</i>	An11g10030	2.15 ± 0.00	1.58 ± 0.08	1.41 ± 0.16
<i>cftA</i>	An02g14200	2.45 ± 0.33	1.76 ± 0.02	2.08 ± 0.12

Mean expression values are given in % compared to the expression level of the actin gene *actA*. Data is taken from three independent cultivations: **a**: (Meyer et al. 2007b), **b**: (Jørgensen et al. 2009), **c**: (Jørgensen et al. 2010).

protein (Fig. S1). We thus designated the respective ORFs *rhoA*, *rhoB*, *rhoC*, *rhoD*, *racA* and *cftA* (cdc forty two), respectively.

To evaluate expression of these six predicted GTPase-encoding genes, we examined Affymetrix gene arrays obtained from young germlings (Meyer et al. 2007b), from exponentially growing cultures (Jørgensen et al. 2010) and from carbon-limited chemostat cultivations (Jørgensen et al. 2009). When compared to the expression of the actin gene *actA*, all Rho GTPase-encoding genes are rather moderately expressed (Table 1). When compared among each other, *rhoA* displays highest and *rhoC* lowest transcript levels.

Individual Rho GTPase executes distinct functions

To study the roles of the Rho GTPases in *A. niger*, respective deletion mutants were generated by employing recently described protocols (Carvalho et al. 2010; Meyer et al. 2010b). All genes but *cftA* were deleted in strain MA70.15 ($\Delta ku70$, *pyrG*⁻) using the *A. oryzae pyrG* gene as selection marker, *cftA* was deleted in strain MA78.6 ($\Delta ku70$) via hygromycin selection. We were able to obtain viable deletion mutants for five GTPases (hereafter referred to as $\Delta rhoB$, $\Delta rhoC$, $\Delta rhoD$, $\Delta racA$, $\Delta cftA$, Table 2); however, deletion of *rhoA* caused a lethal phenotype. Primary $\Delta rhoA$ transformants were only cultivable as heterokaryons containing nuclei with the genotype *rhoA/pyrG*⁻ and nuclei with the genotype $\Delta rhoA/pyrG$ ⁺ (data not shown). Deletion of the different Rho-related GTPases as well as the heterokaryotic status of *rhoA* transformants was verified by Southern analysis (data not shown) and by RT-PCR (Fig. 1).

Table 2. Strains used in this work.

Strain	Relevant genotype	Source
<i>A. niger</i>		
N402	wild-type	Lab collection
AB4.1	<i>pyrG</i> ⁻	(van Hartingsveldt et al. 1987)
AO4.13	<i>pyrG</i> ⁺ (derivative of AB4.1 containing <i>A. oryzae pyrG</i>)	This work
MA70.15	Δ <i>kusA</i> , <i>pyrG</i> ⁻ (derivative of AB4.1)	(Meyer et al. 2007a)
MA78.6	Δ <i>kusA</i> , <i>pyrG</i> ⁺ (derivative of MA70.15 containing <i>A. niger pyrG</i>)	(Carvalho et al. 2010)
MK11.4	Heterokaryon Δ <i>kusA</i> , ρ <i>hoA/pyrG</i> ⁻ , Δ <i>rhoA/pyrG</i> ⁺	This work
ER2.5	Δ <i>kusA</i> , Δ <i>rhoB::AopyrG</i>	This work
ER3.4	Δ <i>kusA</i> , Δ <i>rhoC::AopyrG</i>	This work
ER7.6	Δ <i>kusA</i> , Δ <i>rhoD::AopyrG</i>	This work
MA80.1	Δ <i>kusA</i> , Δ <i>racA::AopyrG</i>	This work
MA84.1	Δ <i>kusA</i> , Δ <i>cftA::hygR</i>	This work
MA80.1.1	Δ <i>kusA</i> , Δ <i>racA</i> , <i>pyrG</i> ⁻ (derivative of MA80.1)	This work
MK3.5	Δ <i>kusA</i> , Δ <i>racA</i> , <i>PinuE::racA</i> (derivative of MA80.1.1)	This work
MK4.1	Δ <i>kusA</i> , Δ <i>racA</i> , <i>PinuE::racA</i> , Δ <i>cftA::hygR</i> (derivative of MK3.5)	This work
MK9.4	Δ <i>kusA</i> , <i>ecfp::tubA</i> (derivative of MA70.15)	This work
MK10.2	Δ <i>kusA</i> , Δ <i>racA</i> , <i>ecfp::tubA</i> (derivative of MA80.1.1)	This work
EB6.3.1	Δ <i>kusA</i> , Δ <i>racA</i> , <i>egfp::racA</i> (derivative of MA70.15)	This work
MA61.24	<i>PinuE::racAG18V</i> (derivative of AB4.1)	This work
MA1.8	<i>PglaA::racA</i> (derivative of AB4.1)	This work
MA60.15	<i>PglaA::racAG18V</i> (derivative of AB4.1)	This work
MA75.2	Δ <i>kusA</i> , Δ <i>riaA::AopyrG</i>	This work
MA76.1	Δ <i>kusA</i> , Δ <i>riaB::AopyrG</i>	This work
MA82.2	Δ <i>kusA</i> , Δ <i>noxA::AopyrG</i>	This work
<i>S. cerevisiae</i>		
MAV203	<i>MATa</i> ; <i>leu2-3,112</i> ; <i>trp1-901</i> ; <i>his3Δ200</i> ; <i>ade2-101</i> ; <i>cyh2R</i> ; <i>can1R</i> ; <i>gal4Δ</i> ; <i>gal80Δ</i> ; <i>GAL1::lacZ</i> ; <i>HIS3_{UASGALI}::HIS3@LYS2</i> ; <i>SPAL10_{UASGALI}::URA3</i>	Invitrogen
MAsc1	MAV203; pDEST32- <i>racA</i> ; pDEST22- <i>riaA</i>	This work
MAsc2	MAV203; pDEST32- <i>racA</i> ; pDEST22- <i>riaB</i>	This work
MAsc3	MAV203; pDEST32- <i>racA</i> ; pDEST22	This work
MAsc4	MAV203; pDEST32- <i>racA</i> ^{G18V} ; pDEST22- <i>riaA</i>	This work
MAsc5	MAV203; pDEST32- <i>racA</i> ^{G18V} ; pDEST22- <i>riaB</i>	This work
MAsc6	MAV203; pDEST32- <i>racA</i> ^{G18V} ; pDEST22	This work
MAsc7	MAV203; pDEST32- <i>racA</i> ^{D124A} ; pDEST22- <i>riaA</i>	This work
MAsc8	MAV203; pDEST32- <i>racA</i> ^{D124A} ; pDEST22- <i>riaB</i>	This work
MAsc9	MAV203; pDEST32- <i>racA</i> ^{D124A} ; pDEST22	This work
MAsc10	MAV203; pDEST32- <i>cftA</i> ; pDEST22- <i>riaA</i>	This work
MAsc11	MAV203; pDEST32- <i>cftA</i> ; pDEST22- <i>riaB</i>	This work
MAsc12	MAV203; pDEST32- <i>cftA</i> ; pDEST22	This work
MAsc13	MAV203; pDEST32- <i>cftA</i> ^{G14V} ; pDEST22- <i>riaA</i>	This work
MAsc14	MAV203; pDEST32- <i>cftA</i> ^{G14V} ; pDEST22- <i>riaB</i>	This work
MAsc15	MAV203; pDEST32- <i>cftA</i> ^{G14V} ; pDEST22	This work
MAsc16	MAV203; pDEST32- <i>cftA</i> ^{D120A} ; pDEST22- <i>riaA</i>	This work
MAsc17	MAV203; pDEST32- <i>cftA</i> ^{D120A} ; pDEST22- <i>riaB</i>	This work
MAsc18	MAV203; pDEST32- <i>cftA</i> ^{D120A} ; pDEST22	This work

We analyzed the phenotypes of the deletion strains on complete and minimal medium (MM) using the following descriptors: germination rate, hyphal morphology, septum formation, radial growth rate, sporulation efficiency and cell wall integrity (see *Experimental procedures* and Fig. 2). The terminal phenotype of the $\Delta\rho A$ heterokarotic mutant was characterized by swollen spores, only a very few of which (less than 0.5%) developed into malformed germlings before stopped growing (data not shown). This suggests that RhoA is not *per se* important for the process of spore swelling but already indispensable for early events during germ tube formation.

As summarized in Fig. 2, the $\Delta\rho B$ strain was indistinguishable from the wild-type (wt) strain in terms of hyphal morphology, septum formation and radial growth rate but displayed a slightly reduced germination rate (89% of the wt rate). However, main differences were observed in terms of sporulation efficiency (about 50% fewer spores were produced by $\Delta\rho B$), implicating that RhoB is important for sustaining efficient sporulation. Moreover, $\Delta\rho B$ was hypersensitive to the cell wall disrupting agent calcofluor white (CFW). Hypersensitivity to this compound is a reflection of defects in the biosynthesis and assembly of cell wall polymers, mainly chitin and glucans (Ram et al. 2004; Ram and Klis 2006). The reduced resistance of $\Delta\rho B$ would thus suggest a potential role of RhoB in cell wall deposition and integrity, a hypothetical role that would be in agreement with the function of the *S. pombe* orthologous Rho2 protein in α -1,3 glucan synthesis and cell wall integrity signaling (Calonge et al. 2000; Perez and Rincon 2010).

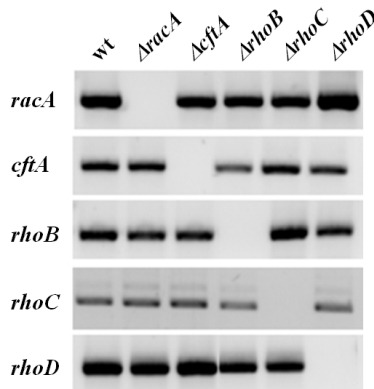


Fig. 1. RT-PCR of total RNA purified from different *A. niger* strains.

Wild-type and deletion strains were cultivated in liquid CM. Specific primer pairs were used to amplify Rho GTPase genes. The absence of a signal confirms successful deletion of a locus.

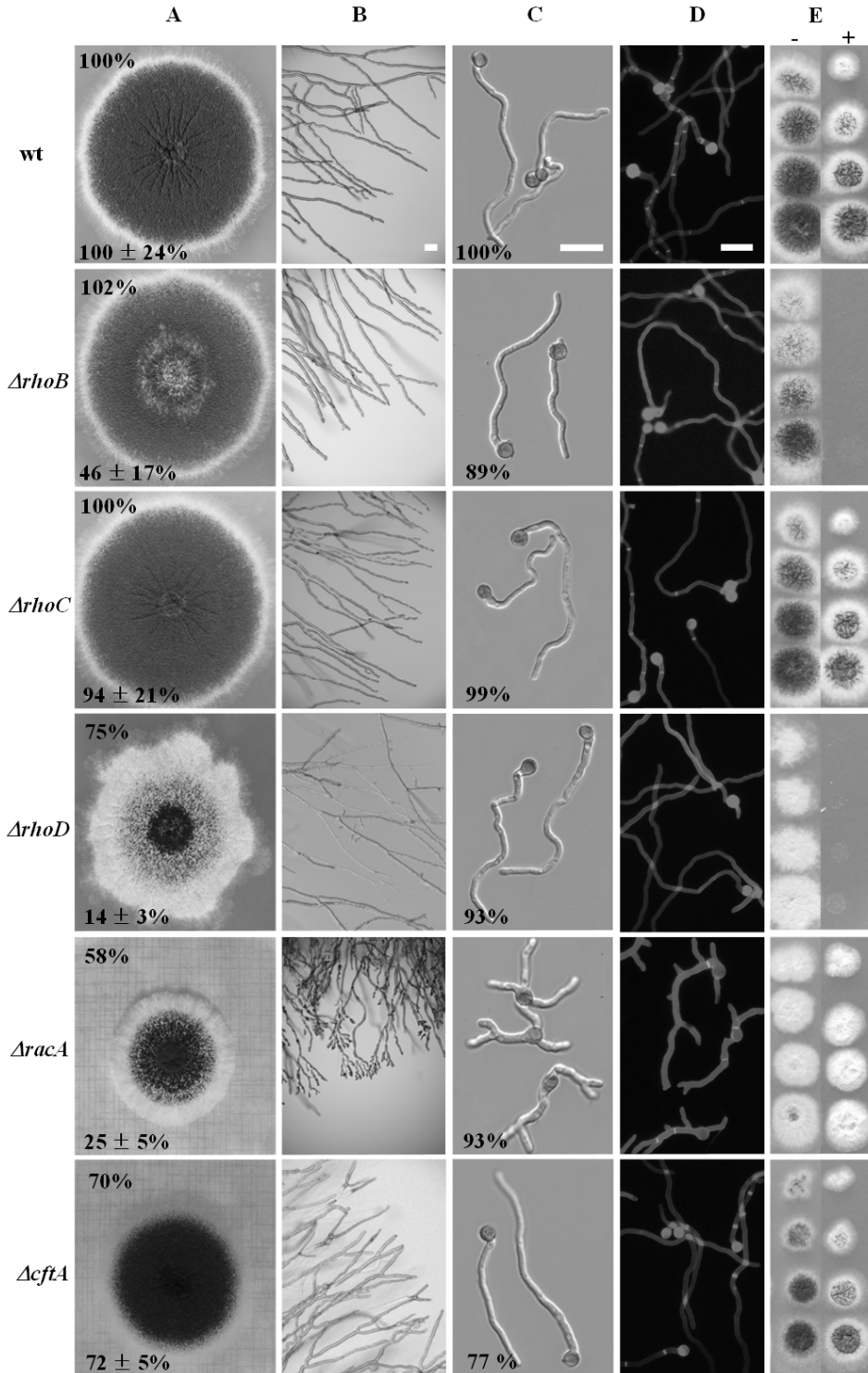


Fig. 2. Macroscopic and microscopic phenotypes of individual Rho GTPase deletion strains.

Column A: 10^5 spores were point inoculated on CM agar plates and incubated for 4 days at 30°C. The macroscopic phenotypes for the different mutants were essentially the same on MM plates (data not shown). Number in the upper left of each panel reflects relative colony growth rate, number in the lower left depicts relative sporulation rate (spores/cm²) compared with the wt strain MA78.6. Mean values of a triplicate experiment are given. Column B: Microscopic pictures with a 65x magnification from the colony edges on CM agar. Bar, 50 µm. Column C: Spores were allowed to germinate for 10 h at 30°C on cover slips in MM. Microscopic pictures were taken with a 200x magnification. Number in the lower left depicts the % of germinated spores (n > 150). Bar, 20 µm. Column D: Germlings were fixed and stained with CFW. The presence or absence of the first septum localized next to the spore was scored (n > 40). Bar, 20 µm. Higher magnification images of wt and $\Delta\rho D$ are shown in Fig. S2. Column E: Serial spore dilutions were spotted on MES-buffered CM (pH 6.0) containing 0 (-) or 100 µg/ml CFW (+). Colony pictures were taken after cultivation for 2 days at 30°C.

Deletion of *rhoC* did not have any obvious consequences for *A. niger*, suggesting that the cellular role of RhoC is rather negligible. This phenotype is completely different from the almost lethal *RHO3* deletion phenotype described for *S. cerevisiae* (Matsui and Toh-e 1992).

In the case of $\Delta\rho D$, radial growth rate was reduced compared with its parental strain (75%; Fig. 2). Moreover, septum formation, as detected by CFW staining, was almost absent in the $\Delta\rho D$ strain, a phenotype that exactly resembles the $\Delta\rho 4$ phenotype observed for *N. crassa* and *A. nidulans* (Rasmussen and Glass 2005; Si et al. 2010). Close microscopic examination of $\Delta\rho D$ hyphae revealed that many of them were empty. Such a lysing phenotype could suggest that RhoD is important for cell wall biosynthesis in *A. niger*. In such a case, one would expect a hypersensitive phenotype of $\Delta\rho D$ towards CFW, which was indeed the case (Fig. 2). Finally, the $\Delta\rho D$ strain was strongly inhibited in sporulation as the amount of conidia produced was decreased to almost 10%. Such a reduction in conidiation efficiency has previously been associated with defects in septum formation in *A. nidulans* (Harris et al. 1994).

Pleiotropic effects were caused when *A. niger* was deleted for *racA*. Spores lacking *racA* frequently developed two or three equally long germ tubes, although formation of the second germ tube is in general delayed in wt spores (Fig. 2 and Table 3). As $\Delta\rho A$ spores simultaneously established multiple polarity axes might suggest that RacA has functions in timing axis formation and/or in stabilizing established polarity axes. In consequence, the $\Delta\rho A$ strain displayed a hyperbranching phenotype (caused by dichotomous branching) and formed a compact colony which was reduced in its diameter. In general, germ tubes and hyphae had a wider hyphal diameter in the $\Delta\rho A$ strain. Furthermore, deletion of *racA* considerably compromised conidiospore formation – only 25% conidiospores were produced compared with the wild-type.

Table 3. Growth-related characteristics of different *A. niger* wild type and deletion strains.

Strain	Relevant Genotype	Germination ^a [%]				Radial growth rate ^b [%]	Sporulation ^b [%]
		N = 0	N = 1	N = 2	N = 3		
MA78.6	wt	3.0	67.7	29.3	0.0	100.0 ± 2.0	100.0 ± 28.8
MA80.1	<i>ΔracA</i>	4.9	46.7	45.7	2.7	63.1 ± 1.4	24.0 ± 11.8
MA84.1	<i>ΔcftA</i>	18.8	81.2	0.0	0.0	69.7 ± 1.4	36.3 ± 3.2
MA75.2	<i>ΔriaA</i>	0.0	73.4	26.6	0.0	103.3 ± 2.5	53.3 ± 4.0
MA76.1	<i>ΔnoxA</i>	1.0	62.6	36.4	0.0	104.9 ± 1.4	48.6 ± 2.7
MA82.2	<i>ΔriaB</i>	28.6	56.8	14.6	0.0	91.8 ± 1.4	84.5 ± 11.7

a: 1×10^5 spores were inoculated per ml liquid CM and incubated for 7 h at 37°C. The amount of germinated and non-germinated spores were counted ($n > 150$) and expressed in %. N = number of germ tubes formed. N = 0: % of non-germinated spores, $N \geq 1$: % of spores with one or more germ tubes. **b:** 1×10^5 spores were point-inoculated on CM agar plates and incubated for 3 days at 30°C. The colony diameter and the amount of spores formed per cm^2 colony were determined and expressed in %.

To our surprise, deletion of *cftA* only mildly perturbed growth of *A. niger* and did not resemble the *A. nidulans Δcdc42* phenotype (Virag et al. 2007). Basically, germ tube formation was delayed and reduced in *ΔcftA* (77% compared with wild-type) as was the growth rate (70%) and sporulation efficiency (72%; Fig. 2 and Table 3). Also, hyphal morphology remained unaffected, which could suggest that CftA has apparently no role in hyphal morphogenesis. In order to confirm that the deletion phenotypes observed were indeed caused by non-functional Rho genes, the *ΔrhoB*, *ΔrhoD*, *ΔracA*, *ΔcftA* strains were retransformed with functional gene copies. In all cases, the wt phenotype became restored back after reintroducing the respective Rho gene (Fig. S3).

RacA and CftA share overlapping functions

The closest homolog of RacA in the yeasts *S. cerevisiae* and *S. pombe* is Cdc42p, which is an essential protein for both organisms (Johnson and Pringle 1990; Miller and Johnson 1994). One explanation why RacA or CftA is not essential for *A. niger* might be that both proteins have related functions which are executed in yeast only by Cdc42p. Hence, deletion of one protein in *A. niger* might be compensated by the presence of the other. Such an allocation of cellular tasks has recently been described for RacA and ModA (Cdc42) in *A. nidulans* (Virag et al. 2007). To examine whether this scenario is also valid for *A. niger*, we followed two genetic approaches. First, we transformed the *ΔracA* strain with the *cftA*

deletion construct. None of the primary transformants obtained yielded in any viable homokaryotic double deletion mutant on uridine-deplete medium ($\Delta racA$) supplemented with hygromycin ($\Delta cftA$), implying that loss-of-function mutations in both genes are synthetically lethal (data not shown).

In the second approach, we aimed to express *racA* under control of an inducible promoter in a $\Delta cftA\Delta racA$ background strain. In doing so, we constructed an expression cassette, where *racA* gene expression is under control of the *inuE* promoter, and transformed it into the $\Delta racA$ strain, which was made *pyrG*⁻ using 5'-fluorouracil (FOA) counter selection (see *Experimental procedures*, Fig. 3). The *inuE* promoter itself is a strongly inducible promoter in the presence of sucrose but repressed by glucose (Yuan et al. 2008a). We confirmed that *PinuE*-driven *racA* expression rescued the multi-germination phenotype of $\Delta racA$ mutant on sucrose medium (Fig. 3C) but not on glucose medium (Fig. 3D). In general, *PinuE*-driven (over)expression of *racA* did not have any negative impact on hyphal morphology. This strain (*PinuE::racA*, $\Delta racA$) was eventually used as a recipient strain to delete *cftA*. Transformants were selected and purified on uridine-deplete sucrose medium (*PinuE::racA* expression) supplemented with hygromycin ($\Delta cftA$). Southern analysis on selected transformants confirmed that these strains were homokaryons successfully deleted for both *racA* and *cftA* (data not shown). Spore germination and morphology of these strains (*PinuE::racA*; $\Delta racA$; $\Delta cftA$) were completely rescued on sucrose medium but not on glucose medium (Fig. 3E-F), which demonstrated that RacA is capable of substituting for CftA, thereby implying that both proteins share at least one function required for polarity establishment/maintenance. Notably, the malformed germlings phenotype observed in glucose medium (Fig. 3F) is reminiscent of the phenotype observed for the *A. nidulans* fimbrin deletion mutant (Upadhyay and Shaw 2008) and in general resembles the phenotype of *A. nidulans* and *A. niger* wt germlings when treated with cytochalasin A ((Taheri-Talesh et al. 2008) and our own unpublished observations). As cytochalasin A blocks polymerization of actin at its barbed end (Cooper 1987), we suspected that one overlapping function of CftA and RacA might be related to the elongation of actin filaments.

RacA is important for actin but not tubulin organization

RacA appeared to be the most critical Rho GTPase important for maintaining hyphal polarity in *A. niger*. We thus focused our research interest on RacA to specifically learn more about its contribution to hyphal morphogenesis of *A. niger*. As discussed above, one function of RacA might probably be linked to the actin cytoskeleton – as also documented

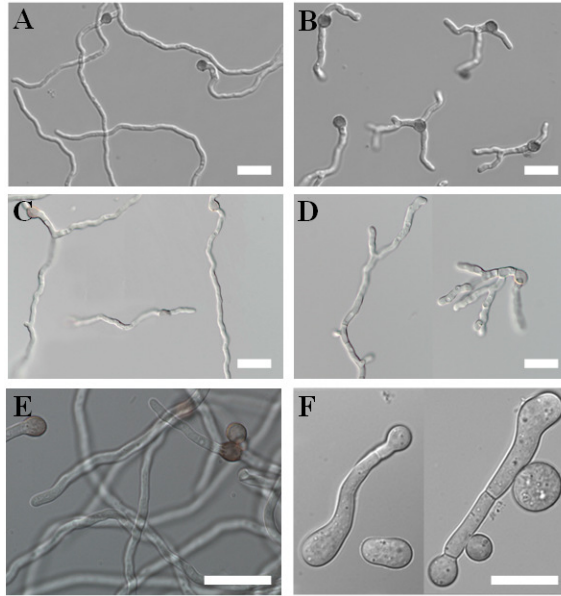


Fig. 3. Conditional expression of the *racA* gene (*PinuE::racA*) in a $\Delta racA$ and $\Delta racA\Delta cftA$ genetic background. Spores of the different strains were allowed to germinate for 16 h at 25°C in MM. A, wt (strain MA78.6). B, $\Delta racA$ (strain MA80.1). C, $\Delta racA$ transformed with *PinuE::racA* (strain MK3.5) in MM containing sucrose as carbon source. D, $\Delta racA$ transformed with *PinuE::racA* (strain MK3.5) in MM containing glucose as carbon source. E, $\Delta racA\Delta cftA$ strain transformed with *PinuE::racA* (strain MK4.1) in MM containing sucrose as carbon source. F, $\Delta racA\Delta cftA$ strain transformed with *PinuE::racA* (strain MK4.1) in MM containing glucose as carbon source. Bar, 20 μ m. Note: the *inuE* promoter is not completely tight under non-inducing condition (glucose). Its residual activity thus allows spores to germinate.

for RacA orthologs in higher eukaryotes (Bosco et al. 2009). To substantiate that presumption, we immunolabelled actin in the wt strain and in $\Delta racA$. As shown in Fig. 4, actin signals are evenly distributed at cortical spots throughout wt hyphae and are concentrated near hyphal apices (Fig. 4), an actin distribution pattern that has also been described for *A. nidulans* (Harris et al. 1994). However, in the $\Delta racA$ strain, actin was hyperpolarized at the hyphal tip and moreover, the amount of actin in the subapical/lateral regions was reduced (Fig. 4), indicating that RacA controls actin polarization.

We also examined the consequences of a *racA* null mutation on the organization of the microtubule cytoskeleton and expressed for this purpose an CFP::TubA fusion protein in both the wt and the $\Delta racA$ strain. We could, however, not observe any remarkable differences in microtubule formation and localization between both strains (Fig. 4 and

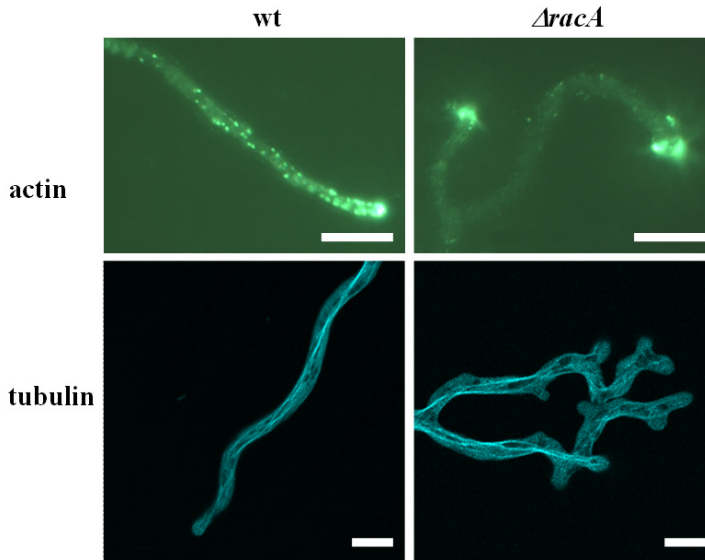


Fig. 4. Actin and tubulin localization in wt and $\Delta racA$ strain.

Actin was immunostained in strain MA78.6 (wt) and MA80.1 ($\Delta racA$). Spores were cultivated on cover slips for 20 h at 25°C in MM. After cell fixation and cell wall digestion, samples were immunolabelled and analyzed by fluorescence microscopy. Tubulin (CFP::TubA) was visualized by fluorescence microscopy in strains MK9.4 (wt) and MK10.2 ($\Delta racA$). Life-images were taken from cultures grown for 2 days at 20°C on MM agar. Bar, 10 μ m.

data not shown). In addition, the $\Delta racA$ strain did not exhibit any increased sensitivity to microtubule inhibitors benomyl and nocodazole (data not shown), altogether suggesting that RacA controls actin dynamics at the hyphal tip but plays a minor if any role in microtubule organization.

RacA localizes to the hyphal apex and ensures polarized tip growth

The data described above strongly indicated that the *A. niger* RacA secures hyphal tip growth via controlling the actin cytoskeleton. This however, is suggestive of a mainly tip-localized distribution of RacA. To test this prediction, we generated an expression construct *gfp::racA*, which we targeted to the *racA* genomic locus in such a way that the endogenous *racA* gene became replaced by the fusion construct and *gfp::racA* expressed under control of the endogenous *racA* promoter. Comparison of the phenotypes of wt, $\Delta racA$ and GFP::RacA strains uncovered that expression of GFP::RacA was not fully able to

complement the deletion phenotype of the $\Delta racA$ strain (Fig. 5A), suggesting that the GFP::RacA fusion protein was only partially functional. However, GFP::RacA was strongly polarized at the apex of germinating cells and mature hyphae and displayed a crescent-like form (Fig. 5B). Remarkably, GFP::RacA localized at hyphal apices only in actively growing cells. The signal immediately disappeared when cells stopped growing but reappeared when growth was resumed (Movie S1 and data not shown). Very rarely, we also noticed some GFP::RacA fluorescence at septa or sites destined for septum formation.

To further elucidate the role of RacA in the control of cell polarity, we wished to study the effects of *racA* overexpression on hyphal tip growth. Induced overexpression of RacA by the *inuE* promoter did not interfere with polarized tip growth (see above), pointing to the possibility that the activity of a RacA-GAP might be sufficient to inactivate RacA. We thus generated a dominant active allele of RacA, which carries the GTPase-negative G12V mutation (G18V in RacA) in the predicted GTP binding and hydrolysis domain. This mutation has been shown to trap Rho GTPases in their “on-state” (Warne et al. 1993; Ziman et al. 1991). Expression of *racA*^{G18V} was put under control of the *inuE* promoter (sucrose-inducible, high activity during germination) or the *glaA* promoter (induced by maltose, repressed by xylose; high activity during exponential growth phase) and the three constructs generated (*PglaA::racA*, *PglaA::racA*^{G18V}, *PinuE::racA*^{G18V}) were targeted to the *pyrG* locus of *A. niger*. As shown in Fig. 6, *PinuE* – driven expression of RacA^{G18V} resulted in the formation of clavate-shaped germlings which were abnormally large, unpolarized and

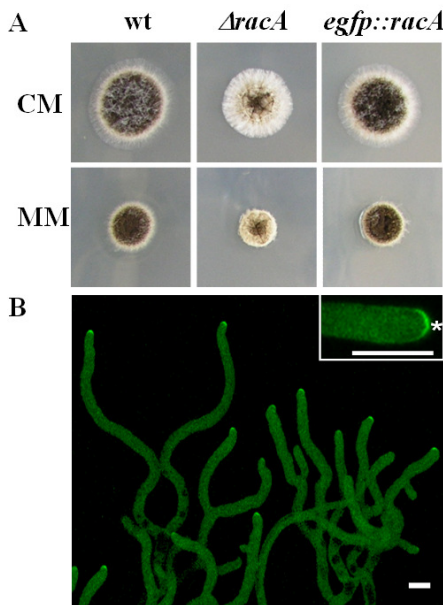


Fig. 5. RacA localization in growing hyphae of *A. niger*.

A, Colony pictures of wt (MA78.6), $\Delta racA$ (MA80.1) and GFP::RacA (EB6.3.1) on CM agar. B, Life-images of the GFP::RacA strain were taken from cultures grown for 2 days at 25°C on MM agar. The cap-like distribution of GFP::RacA is indicated with a star. Bar, 10 μm .

contained extremely large vacuoles (Fig. 6A and B). When expression of *racA*^{G18V} was under control of the *glaA* promoter, hyphae showed a pronounced swollen-tip phenotype and formed bulbous lateral branches (Fig. 6D and F). Thus, both strains expressing constitutive active RacA^{G18V} are defective in tip elongation, indicating that controlling RacA activity is inevitable for polarity maintenance. To test whether this loss of polarity might be a consequence of disturbed actin localization, we immunolabelled actin in the *PglaA::racA*^{G18V} and *PinuE::racA*^{G18V} strains. As depicted in Fig. 7, actin polarization was indeed lost in both strains and actin signals were randomly scattered intracellularly or at the cell periphery.

RacA interacts with a protein of unknown function and with NoxR

In order to identify potential downstream effectors of RacA, a yeast two-hybrid screen was

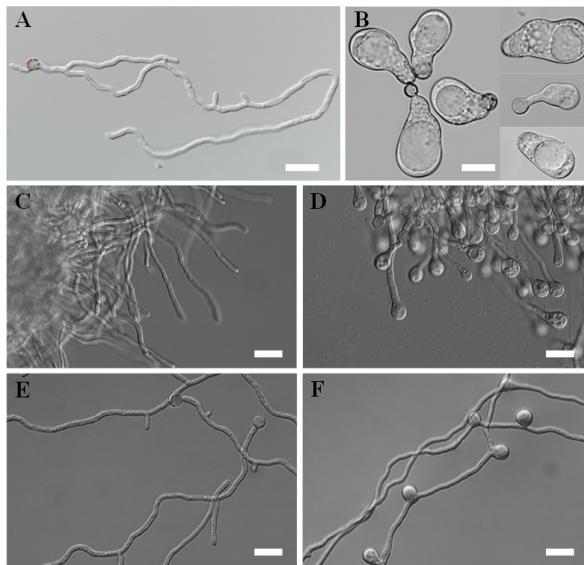


Fig. 6. Microscopic analysis of RacA^{G18V} strains.

A and B, Microscopic phenotypes of wt (AO4.13) and the *PinuE::racA*^{G18V} strain MA61.24, respectively, when cultivated in MM with 1% sucrose as carbon source. C and D, Microscopic phenotypes of wt (AO4.13) and the *PglaA::racA*^{G18V} strain (MA60.15), respectively, when cultivated in shake flasks till the mid-exponential growth phase using 2% maltose as carbon source. E and F, Microscopic phenotypes of wt (AO4.13) and the *PglaA::racA*^{G18V} strain (MA60.15), respectively, when grown on cover slips in MM with maltose as carbon source. Bar, 20 μ m.

performed using RacA^{G18V} as bait and different prey libraries. The libraries used harbored mRNA populations isolated from different morphological stages of *A. niger* (germination, vegetative growth, conidiation) and from stressed mycelium (see *Experimental procedures*). Interestingly, RacA^{G18V} interacting proteins (Ria) were only identified from the conidiation and the stressed cDNA library and altogether only two Ria proteins were isolated. RiaA (An16g05550) was isolated from the conidiation library and displayed strong interaction with RacA^{G18V}, RiaB (An12g06420) was identified from the stress library and interacted only weakly with RacA^{G18V} (Fig. 8). *riaB* encodes a zinc knuckle domain protein, having no apparent homolog outside the fungal kingdom and whose function is unknown. The interaction of RiaB is, although weak in its nature, specific for RacA^{G18V} as we have not detected any interaction of RiaB with RacA and RacA^{D124A} nor with CftA, CftA^{G14V} and CftA^{D120A}, suggesting that RiaB binds to RacA only when in its activated, GTP-bound form (Fig. 8, note that the D124A mutation in RacA and D120A mutation in CftA, respectively, are dominant negative (Ziman et al. 1991)).

To study the function of both RiaA and RiaB, we deleted the respective genes in *A. niger*, which was verified by Southern analysis (data not shown). Surprisingly, deletion of *riaB* did not manifest in a strong phenotype (Fig. S4A). Only germination of Δ *riaB* was delayed and the growth rate slightly reduced when compared with the wt situation (Table 3). These observations might hint at the possibility that RiaB's function and its interaction with activated RacA are necessary for securing maximal polar growth rate of *A. niger*.

The *riaA* gene codes for a protein with strong sequence similarity to the NADPH

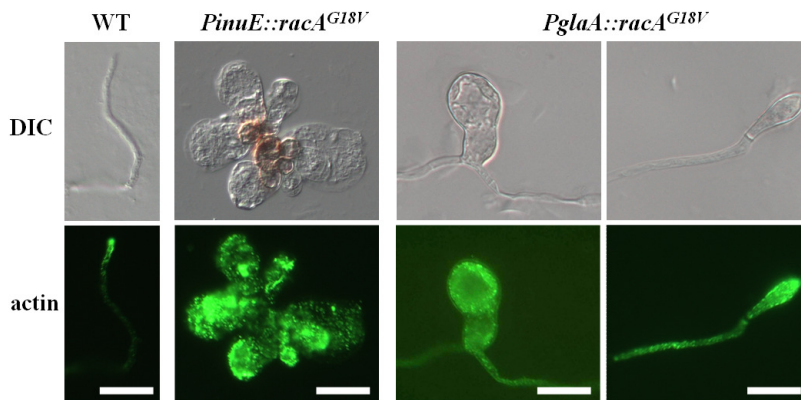


Fig. 7. Actin distribution in RacA^{G18V} strains. Actin staining of young hyphae from wt strain (AO4.13), strains MA61.24 (*PinuE::racA^{G18V}*) and MA60.15 (*PglA::racA^{G18V}*) was performed as described in Fig. 4. DIC micrographs are shown for comparison.

oxidase regulator NoxR/p67^{phox} (68% identity to the *A. nidulans* NoxR, 36% identity to the human p67^{phox}). In mammals, NADPH oxidases (Noxs) are members of a multi-protein complex to which, among others, p67^{phox} and Rac1 are bound and which generate ROS (Lambeth 2004). In filamentous fungi, it was recently shown that a tip-proximal gradient of ROS is essential to sustain apical dominance and that interaction of RacA and NoxR is required to activate Nox activities (Cano-Dominguez et al. 2008; Rolke and Tudzynski 2008; Scott and Eaton 2008; Semighini and Harris 2008; Tanaka et al. 2008). Interestingly, the interaction of RiaA (NoxR) with RacA was specific for RacA but independent from its GTP/GDP status: RiaA (NoxR) interacted with RacA, RacA^{G18V} and dominant negative RacA^{D124A} but not with CftA, dominant active CftA^{G14V} and dominant negative CftA^{D120A} (Fig. 8). Unexpectedly, deletion of *riaA* as well as deletion of the predicted NoxA protein (An08g10000; *A. niger* possesses only a single *nox* gene) did not cause any morphological defects in *A. niger* (Fig. S4A, for complementation analyses of $\Delta noxA$ and $\Delta riaA$ (*noxR*), see Fig. S3). Only sporulation efficiency was reduced in $\Delta riaA$ and $\Delta noxA$ strains to about 50% (Table 3). Moreover, we could not detect any differences in the discrete tip localization of ROS using nitro blue tetrazolium (NBT) staining of wt, $\Delta riaA$ and $\Delta noxA$ hyphae (Fig. S4B), implying that an interaction of RacA with RiaA is rather important for asexual developmental processes but not for hyphal tip growth as shown for *A. nidulans* (Semighini and Harris 2008).

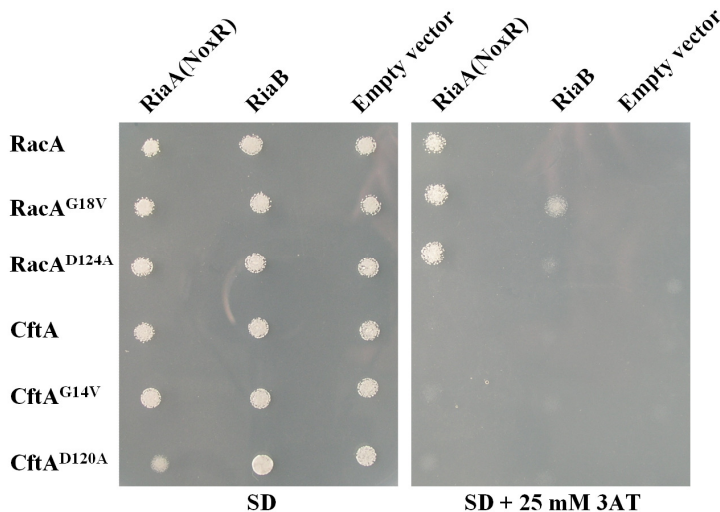


Fig. 8. Yeast-two hybrid interactions of RacA or CftA with RiaA and RiaB, respectively.

A total of 10^3 yeast cells from logarithmically growing cultures were spotted on minimal medium lacking leucine, tryptophan and histidine (SD) and cultivated for 24 h at 30°C. Growth on SD + 25 mM 3-AT is indicative for a protein-protein interaction. All interactions were confirmed using *lacZ* as reporter (data not shown).

Discussion

Rho GTPases are intracellular signalling molecules present from lower eukaryotes up to mammals but absent in eubacteria and archaea. They are key regulators of cell shape and polarity and were first described as modulators of the actin cytoskeleton (Hall 1998). Later it became evident that Rho GTPases interact not only with actin but with multiple target proteins, thus participating in many distinct processes such as metabolism, vesicular transport, proliferation, survival and even gene expression (Ridley 2001; Ridley 2006).

Recently, the ontogeny of Rho GTPases was reconstructed from major eukaryotic clades and the chronology of their emergence revisited. Basically, Rac is the founder of the Rho family, and Cdc42 and Rho1 diverged from Rac about 1.5 billion years ago. Duplications, gene loss, gene rearrangements and horizontal gene transfer of Rac, Rho1 and Cdc42 descendants finally resulted in varying repertoires of Rho family members in different eukaryotes (Boureau et al. 2007). For example, *S. cerevisiae* does not harbor a Rac homolog, Cdc42 is not present in *Arabidopsis thaliana* and *Dictyostelium discoideum* and some eukaryotes such as filamentous fungi and mammals comprise both Rac and Cdc42 proteins (Boureau et al. 2007). The evolution of Rho family members has profound consequences on their involvement in polar growth control in different model systems. Although the three hierarchical steps are the same (polar site selection by internal or external cues, establishment of the polar axis, maintenance of the polar axis coupled with polar growth), the specific GTPase(s) involved can differ and the specific mechanism that governs these steps as well. For example, the three hierarchical processes are orchestrated by three different GTPases in *S. cerevisiae* (Ras, Cdc42, Rho1) but only by a single Rac-like GTPase (Rop) in plants (Fu and Yang 2001). Within the group of filamentous Ascomycetes, the relative requirement for RacA for polar growth control differs as well ((Chen et al. 2008; Rolke and Tudzynski 2008; Virag et al. 2007) and this work).

Rho GTPases of *A. niger* exert distinct and mutual functions

Recent advances in genomics and gene targeting tools for *A. niger* has allowed us to identify and selectively inactivate all predicted Rho GTPases in this industrial model organism thereby getting insights into their physiological roles (Figs. 2 and 3). Given the phenotypic traits of the $\Delta\rho A/\rho A$, $\Delta\rho B$, $\Delta\rho C$, $\Delta\rho D$, $\Delta\rho A$, $\Delta cftA$ and $\Delta\rho A\Delta cftA$ strains during the life cycle of *A. niger*, we propose the following model (Fig. 9): RhoA occupies a central role in controlling polarity establishment and additionally exerts functions which are essential for the viability of *A. niger*. RhoB and RhoD are important for

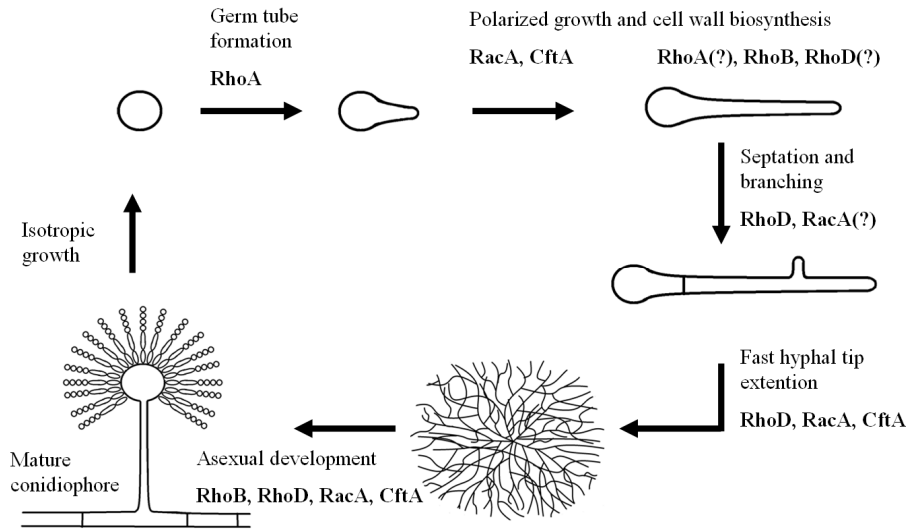


Fig. 9. Predicted functions of different Rho GTPases during the life cycle of *A. niger* as deduced from phenotypic traits of respective loss-of-function mutations. For details see Discussion.

cell wall biosynthesis, RhoD governs cytokinesis (septation and sporulation) and RacA controls polarity maintenance, which can partially also be accomplished by CftA. Altogether, the activities of RhoD, RacA and CftA contribute to and ensure fast hyphal tip growth rate in *A. niger*.

Thus, all six Rho GTPases exert distinct and overlapping functions, which, when compared with data from other filamentous fungi, are only partially conserved. Even within a genus, there is no consistent pattern for the physiological function of Rho GTPases. For example, RhoD is required for septum formation in both *A. nidulans* and *A. niger*, but RacA and CftA differently contribute to polarity maintenance in both species ((Si et al. 2010; Virag et al. 2007) and this work). Similar and differing requirements of Rho GTPases for growth and morphogenesis of filamentous fungi are most probably a consequence of species differentiation during evolution (see above). Although fungal Rho GTPases are highly related (Fig. S1), their interaction with other molecules can differ and can cause varying species-specific outputs. Hence, studying different model systems will give comprehensive insights into the roles of Rho GTPases for fungal growth and development.

RacA and CftA control actin dynamics in *A. niger*

The phenotypic analyses of the six different Rho GTPase deletion strains uncovered that apical dominance in young germlings and mature hyphae of *A. niger* is predominantly controlled by RacA. To understand more about the underlying mechanisms of RacA activity, we visualized RacA by GFP tagging, studied the cellular consequences of dominant activation of RacA (RacA^{G18V}), followed actin and tubulin distribution in wt, $\Delta racA$ and RacA^{G18V} strains and generated a conditional $\Delta racA\Delta cftA$ double deletion strain. The data shows that RacA localizes to the apex of actively growing cells, where it seems to be crucial for the organization of actin distribution (Figs. 4, 5 and 7; Movie S1). Both deletion and dominant activation of RacA provoke an actin localization defect and thereby loss of polarized tip extension (Figs. 5 and 7). In the case of RacA deletion, actin becomes hyperpolarized, whereas constitutive active RacA causes actin depolarization. Interestingly, the dichotomous branching phenotype of $\Delta racA$ suggests that loss of apical dominance can easily be overcome by the establishment of two new sites of polarized growth. This phenotype is reminiscent of the *ramosa-1* mutant of *A. niger*, which results from a transient contraction of the actin cytoskeleton and thereby transient displacement of the Spitzenkörper (Meyer et al. 2009; Reynaga-Pena and Bartnicki-Garcia 1997; Reynaga-Pena and Bartnicki-Garcia 2005). Frequent dichotomous branching is also a characteristic of the actin (*act1*) and actinin mutants in *N. crassa* and *A. nidulans* (Virag and Griffiths 2004; Wang et al. 2009) as well as of the *A. nidulans* $\Delta sepA$ mutant (Harris et al. 1994), which would be in agreement with the concept that RacA is important to stabilize polarity axes via controlling actin. When RacA is trapped in its active, GTP-bound form (RacA^{G18V}), however, loss of apical dominance can not be overcome by *A. niger*. Imaginable is a mechanism similar to the control circuit shown for plant pollen tubes (Klahre and Kost 2006): A hypothetical, subapically localized, RacA-dependent GAP ensures that the activity of RacA is spatially restricted to the hyphal apex thereby maintaining a stable polarity axes. In the RacA^{G18V} mutant strain, however, this hypothetical control mechanism is leveraged off.

Our data also showed that RacA can substitute for CftA (Fig. 3) and that deletion of both genes is lethal to *A. niger*, whereas deletion of each single gene is not (Fig. 2). These observations suggest that RacA and CftA share functions with respect to the control of the actin cytoskeleton. Basically, Rac1 and Cdc42 of higher eukaryotes can affect actin dynamics by three ways: They induce polymerization and branching of actin filaments by stimulating the Arp2/3 complex and formins. They support actin polymerization by activating WASP/WAVE proteins which prevent capping of the barbed (plus) end of actin filaments. And thirdly, they inhibit the actin depolymerizing factor cofilin, thereby controlling the disassembly of actin filaments at the minus end. Hence, Rac1 and Cdc42 govern actin dynamics by adjusting the assembly and disassembly rates of actin filaments

(for details see recent reviews (Heasman and Ridley 2008; Ridley 2006)). The actin hyperpolarization phenotype of the $\Delta racA$ strain could imply that actin turnover rates are disturbed in this strain, i.e. actin filaments disassemble too quickly. If so, it would follow that RacA and CftA can substitute each other with respect to actin polymerization but that actin depolymerization is mainly under control of RacA (Fig. 10). As a result, a *racA* deletion mutant will not be affected in actin polymerization (because secured by CftA) but will be disturbed in actin depolymerization and thus apical dominance. In contrast, a *cftA* deletion mutant is not affected in both actin polymerization and actin depolymerization as both processes can be guaranteed by RacA. Hence a *cftA* deletion strain will not be affected in the maintenance of polar tip growth, which indeed is the case (Fig. 2).

RiaA and RiaB are downstream targets of RacA

We finally showed that RacA physically interacts with two proteins, namely RiaA, which is a predicted NoxR homolog, and RiaB, a protein of unknown function. As both proteins do not interact with CftA (Fig. 7), we suspect that they are specific downstream targets of RacA (Fig. 10). Loss-of-function analyses of RiaB showed that this protein rather fulfils a moderate physiological role and apparently ensures optimal tip extension rate (Table 3).

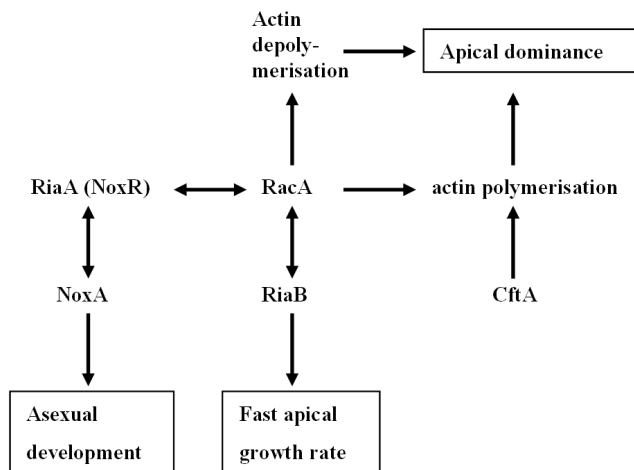


Fig. 10. Tentative mechanistic model explaining the function of RacA and CftA for growth, morphogenesis and development of *A. niger*. RacA interaction with effector proteins are indicated with double arrows. For details see Discussion.

As RacA interacted with RiaA, we also analyzed the consequences of *riaA* and *noxA* deletion for *A. niger*. A requirement of NoxA/NoxR proteins in hyphal tip extension and (a)sexual reproduction has been reported for different fungal species (Cano-Dominguez et al. 2008; Lara-Ortiz et al. 2003; Malagnac et al. 2004; Scott and Eaton 2008; Semighini and Harris 2008). Our phenotypic analyses of Δ *riaA* and Δ *noxA* strains strongly imply that an involvement of RiaA (NoxR) and NoxA in tip-localized ROS generation is rather unlikely in *A. niger* (Fig. S4). Although the well-developed ROS gradient towards hyphal apices still suggests that regulated synthesis of ROS is important for hyphal tip growth of *A. niger* hyphae, we propose that this is not mediated by NoxA and RiaA (NoxR). Several observations support this reasoning. First, the Δ *noxA* and Δ *riaA* strains do not display any polarity defects. Second, radial growth rate is not affected in *A. niger* when deleted for Δ *noxA* or Δ *riaA*. And third, ROS staining is not reduced in Δ *noxA* or Δ *riaA* strains when compared with the wt situation. As deletion of both proteins resulted in a strong reduction in conidia formation, we rather consider that NoxA and RiaA play an important role in asexual development of *A. niger*. Notably, the relative contribution of Nox proteins to these processes seems to be strongly species-dependent. For example, deletion of NoxA results in reduced conidiation in *N. crassa* (Cano-Dominguez et al. 2008) but not in *A. nidulans* (Semighini and Harris 2008). We currently undertake efforts to understand to which extent NoxA and RiaA contribute to developmental decisions in *A. niger*.

Experimental Procedures

Strains, culture conditions and molecular techniques

A. niger and *S. cerevisiae* strains used in this study are given in Table 3. *Escherichia coli* strain XL1-blue served as host for all plasmid work. General cloning procedures in *E. coli* were done according to (Sambrook and Russell 2001). *A. niger* strains were cultivated in minimal medium (MM) (Bennett and Lasure 1991) containing 1% glucose, as a carbon source (if not otherwise stated) or in complete medium (CM), consisting of MM supplemented with 1% yeast extract and 0.5% casamino acids. Then 10 mM uridine or 100 μ g/ml hygromycin was added when required. Transformation of *A. niger*, selection procedures, heterokaryon rescue, genomic DNA extraction, diagnostic PCR and Southern analyses were performed using recently described protocols (Carvalho et al. 2010; Meyer et al. 2010b). The Δ *racA* strain was rendered uridine-requiring (*pyrG*⁻) using FOA counter selection (Meyer et al. 2010b). Sensitivity of *A. niger* strains towards CFW was tested using the protocol according to (Ram and Klis 2006). The effect of the microtubule inhibitors

benomyl and nocodazole on the growth of *A. niger* strains was tested using different concentrations up to 0.25 µg/ml.

Phenotypic analyses and staining procedures

Defined spore titres of *A. niger* strains were used to inoculated MM or CM and incubated for 1-4 days at 25-30°C. All quantitative measurements (growth rate, germination rate, sporulation efficiency) were performed in triplicates. To determine the amount of spores produced by a colony, all spores formed were carefully taken off with physiological salt solution and a cotton stick and counted using a Neubauer chamber.

Actin immunostaining, CFW and NBT staining were performed according to (Meyer et al. 2009; Meyer et al. 2008). For actin immunostaining, cells were fixed with a PBS buffer containing 3.7% p-formaldehyde, 5% DMSO, 25 mM EGTA pH 7.0 and 5 mM MgSO₄. Cell walls were digested for 60 min using lysing enzyme from *Trichoderma harzianum* (Sigma-Aldrich). The monoclonal antibody against actin was obtained from MP Biomedicals. For CFW staining, germlings were fixed in PBS buffer containing 3.7% p-formaldehyde and 0.2% Triton X-100, rinsed with PBS buffer and incubated in 10 µg/ml of Fluorescent Brightener 28 (CFW, Sigma-Aldrich) for 5 min after which they were rinsed again and subjected to microscopy. For NBT staining, germlings were incubated for 1 hour in 50 mM sodium phosphate buffer containing 0.5 mg/ml NBT (Sigma-Aldrich), washed once with 100% methanol and once with water and immediately subjected to microscopy.

Microscopy

Light and fluorescence microscopic pictures were captured with 20x or 40x objectives and using an Axioplan 2 (Zeiss) equipped with a DKC-5000 digital camera (Sony). DIC and GFP settings were used and images were processed using Adobe Photoshop 6.0 (Adobe Systems).

For time-lapse microscopy, conidia were pre-grown on MM agar plate at 30°C for 2 days. An agar piece containing mycelium was transferred upside down onto an objective glass. To prevent drying-out of the agar, a small volume of CM was applied between the colony and the objective glass. After cells resumed growth, time-lapse images were captured with 40x C-apochromatic objective on an inverted LSM 5 microscope equipped with a laser scanning-disk confocal system (Zeiss). In total, eleven z stacks (0.6 µm interval) were taken in 30 s time intervals. The time-lapse movie showing 4 frames per second was assembled using ZEN 2009 software (Zeiss).

Construction of deletion cassettes, mutant alleles and expression cassettes

Standard PCR and cloning procedures were used for the generation of all constructs (Sambrook and Russell 2001) and all cloned fragments were confirmed by DNA sequencing. Details on cloning protocols and primers used can be requested from the authors.

The *rhoA*, *rhoB*, *rhoC*, *rhoD*, *racA*, *cftA*, *riaA*, *riaB* and *noxA* deletion constructs were made by PCR amplification of the 5'- and 3'- flanks of the respective ORFs (at least 0.9 kb long). Genomic DNA of *A. niger* served as template DNA. The sequences were cloned upstream and downstream of the *A. oryzae pyrG* selection marker obtained from pAO4-13 (de Rooter-Jacobs et al. 1989). In the case of *cftA*, the hygromycin resistance cassette isolated from pAN7-1 (Punt et al. 1987) was used to replace the *cftA* ORF.

The *PglaA::racA::TrpC-pyrG** construct was made based on pAN52-7 (Verdoes et al. 1994a) which already contained *PglaA::TrpC*. Next to this cassette, the *pyrG** allele of plasmid pAB94 (van Gorcom and van den Hondel 1988) was cloned to facilitate integration of the constructs at the endogenous *pyrG* locus of *A. niger*. Finally, the *racA* ORF was cloned downstream of *PglaA*. The *PinuE::racA::TrpC-pyrG** construct was generated by exchanging *PglaA* with *PinuE*, which was gained by PCR amplification of the 1.5 kb *inuE* upstream region from genomic DNA.

*PtubA::ecfp::tubA::TtubA-pyrG** was generated using a fusion PCR approach recently described (Meyer et al. 2008). *PracA::egfp-AopyrG-egfp::racA::TracA* was made according to (Hazan and Liu 2002). Note, N-terminal tagging of small GTPases is favoured over C-terminal tagging, as the C-terminal isoprenyl group is essential for GTPase function.

Mutant alleles of *racA* and *cftA* (encoding RacA^{G18V}, RacA^{D124A}, CftA^{G14V} and CftA^{D120A}), were generated by PCR using primers carrying respective point mutations. The DNA fragment encoding for RacA^{G18V} was used to replace the *racA* gene in *PinuE::racA::TrpC-pyrG** and *PglaA::racA::TrpC-pyrG**, respectively. For the yeast two-hybrid assay, wt and mutant alleles of *racA* and *cftA* were cloned into pDEST32 (Invitrogen) according to the supplier's instructions.

Complementation analyses

Complementation cassettes were generated for the deletion strains $\Delta\rho B$, $\Delta\rho D$, $\Delta racA$, $\Delta cftA$, $\Delta riaA$, $\Delta riaB$ and $\Delta noxA$, respectively. The ORFs including 1000 bp of their up- and downstream regions were amplified by PCR using genomic DNA of *A. niger* as template. The DNA fragments gained were either integrated into an autonomously replicating pAMA-based vector (Carvalho et al. 2010) or into pAN7-1 (Punt et al. 1987) and thereafter

transformed into the individual deletion strains. For complementation analyses, the strongest deletion phenotype was selected in order to analyze whether the wt phenotype became restored.

Construction of cDNA libraries and yeast two-hybrid analysis

Four *A. niger* cDNA libraries were constructed using the CloneMiner cDNA library construction kit from Invitrogen. Library A ('vegetative growth library') was made using pooled RNA populations isolated from liquid CM cultures harvested after 4, 6, 8, 16 and 32 h of incubation. Library B ('morphological mutant library') was constructed by pooling RNAs from the hyperbranching mutant strain *ramosa-1* ((Meyer et al. 2009); cultivated in liquid CM for 16 h at permissive and 2 h at restrictive temperature) with mRNAs isolated from the *PglaA::racA^{G18V}* strain (propagated for 16 h in liquid CM). Library C ('stress library') was established using RNAs extracted from 5 hour old germlings stressed for 1 h with 2 mM DTT and stressed for 1, 2 or 4 h with 200 µg/ml CFW). Library 4 ('conidiation library') was established from a culture that was pregrown for 16 h in liquid CM and transferred to a CM agar plate covered with a polycarbonate filter. RNA from sporulating mycelia was harvested after 8 h and 27 h of incubation.

For each library, equal amount of RNA from the different condition was pooled and used for reverse transcription. Each of the cDNAs obtained was cloned into the donor vector pDONR222 (Invitrogen) to create four entry libraries (each ~ 7×10⁶ clones, average insert size 1.4-1.7 kb). The two-hybrid libraries were constructed by transferring the libraries from pDONR222 to pDEST22 via LR reactions (Invitrogen). At least 3×10⁶ clones were isolated for each library. The yeast two-hybrid screen (screening procedure, confirmation of positive interactors using the reporter genes *HIS3*, *URA3* and *lacZ* and respective controls) was performed according to the manufacturer's instructions (ProQuest™ Two-Hybrid System with Gateway® Technology, Invitrogen). Putative interactions of RacA and CftA versions (RacA, RacA^{G18V}, RacA^{D124A}, CftA, CftA^{G14V} and CftA^{D120A}) with RiaA and RiaB were repeatedly analyzed using *HIS3* (3-Amino-1,2,4-triazole; 3-AT) and *lacZ* as reporters following the manufacturer's instructions.

Acknowledgements

The authors would like to acknowledge Benjamin Nitsche for bioinformatics support and Xiao-Lian Yuan for microscopic assistance. We are grateful to Erica Bernard and Robbert Damveld for help in cloning experiments. This project was carried out within the research

programme of the Kluyver Centre for Genomics of Industrial Fermentation which is part of the Netherlands Genomics Initiative / Netherlands Organization for Scientific Research.

The transcriptomic signature of RacA activation and inactivation provides new insights into the morphogenetic network of *Aspergillus niger*

Min Jin Kwon, Benjamin M Nitsche, Mark Arentshorst, Thomas R Jørgensen, Arthur FJ Ram and Vera Meyer

PLoS one, 2013 Jul 24;8(7).

Abstract

RacA is the main Rho GTPase in *Aspergillus niger* regulating polarity maintenance via controlling actin dynamics. Both deletion and dominant activation of RacA (Rac^{G18V}) provoke an actin localization defect and thereby loss of polarized tip extension, resulting in frequent dichotomous branching in the $\Delta racA$ strain and an apolar growing phenotype for Rac^{G18V}. In the current study the transcriptomics and physiological consequences of these morphological changes were investigated and compared with the data of the morphogenetic network model for the dichotomous branching mutant *ramosa-1*. This integrated approach revealed that polar tip growth is most likely orchestrated by the concerted activities of phospholipid signaling, sphingolipid signaling, TORC2 signaling, calcium signaling and CWI signaling pathways. The transcriptomic signatures and the reconstructed network model for all three morphology mutants ($\Delta racA$, Rac^{G18V}, *ramosa-1*) imply that these pathways become integrated to bring about different physiological adaptations including changes in sterol, zinc and amino acid metabolism and changes in ion transport and protein trafficking. Finally, the fate of exocytotic (SncA) and endocytotic (AbpA, SlaB) markers in the dichotomous branching mutant $\Delta racA$ was followed, demonstrating that hyperbranching does not *per se* result in increased protein secretion.

Introduction

Filamentous fungi such as *Aspergillus niger* are widely used in biotechnology for the production of various proteins, enzymes, food ingredients and pharmaceuticals (Fleissner and Dersch 2010; Meyer 2008; Meyer et al. 2011b; Saloheimo and Pakula 2012). During recent years, *A. niger* became an industrial model fungus, due to its well annotated genome sequence, sophisticated transcriptomics and proteomics technologies and newly established gene transfer systems allowing efficient and targeted genetic and metabolic engineering approaches (Carvalho et al. 2010; Jacobs et al. 2009; Meyer et al. 2011b; Pel et al. 2007).

The morphology of filamentous fungi strongly affects the productivity of industrial fermentations (Grimm et al. 2005; McIntyre et al. 2001; Papagianni 2004). Basically, *Aspergilli* and all other filamentous fungi grow either as pellets or as freely dispersed mycelium during submerged growth. Both macromorphologies depend among other things on hyphal branching frequencies – pellets are formed when hyphae branch with a high frequency, dispersed mycelia are a result of low branching frequencies. Whereas the formation of pellets is less desirable because of the high proportion of biomass in a pellet that does not contribute to product formation, long, unbranched hyphae are sensitive to

shear forces in a bioreactor. Lysis of hyphae and the subsequent release of intracellular proteases have thus a negative effect on protein production. Hence, from an applied point of view, the preferred fungal macromorphology would consist of dispersed mycelia with short filaments derived from an optimum branching frequency. It is generally accepted that protein secretion occurs mainly at the hyphal apex (Gordon et al. 2000; Hayakawa et al. 2011; Muller et al. 2002; Wösten et al. 1991). Some studies suggested a positive correlation between the amount of hyphal branches and protein secretion yields (Amanullah et al. 2002; Muller et al. 2002; te Biesebeke et al. 2005; Wongwicharn et al. 1999), whereas other reports demonstrated no correlation (Bocking et al. 1999; McIntyre et al. 2001). Therefore, it is still a matter of debate whether a hyperbranching production strain would considerably improve protein secretion rates.

Different mutations can lead to a hyperbranching phenotype in filamentous fungi. For example, dichotomous branching (tip splitting) is a characteristic of the actin (*act¹*) and actinin mutants in *Neurospora crassa* and *A. nidulans* (Virag and Griffiths 2004; Wang et al. 2009), a consequence of deleting the formin SepA in *A. nidulans* (Harris et al. 1994) or the polarisome component SpaA in *A. nidulans* and *A. niger* (Meyer et al. 2008; Virag and Harris 2006a) and a consequence of inactivating the Rho GTPase RacA or the TORC2 complex component RmsA protein in *A. niger* (Kwon et al. 2011; Meyer et al. 2009). Common to these different gene mutations is not only the phenotype they provoke but that they also disturb the dynamics of the actin cytoskeleton. Actin is crucial for polarized hyphal growth in filamentous fungi and controls many cellular processes, including intracellular movement of organelles, protein secretion, endocytosis and cytokinesis (Berepiki et al. 2011; Lanzetti 2007).

We have recently analyzed the function of all six Rho GTPase encoded in the genome of *A. niger* (RacA, CftA, RhoA, RhoB, RhoC, RhoD) and uncovered that apical dominance in young germlings and mature hyphae of *A. niger* is predominantly controlled by RacA (Kwon et al. 2011). Both RacA and CftA are not essential for *A. niger* (in contrast to RhoA) but share related functions which are executed in unicellular fungi only by Cdc42p (Kwon et al. 2011). The data showed that RacA localizes to the apex of actively growing filaments, where it is crucial for actin distribution. Both deletion and dominant activation of RacA (RacA^{G18V} expressed under control of the maltose-inducible glucoamylase promoter *glaA*) provoke an actin localization defect and thereby loss of polarized tip extension. In the case of RacA inactivation, actin becomes hyperpolarized, leading to frequent dichotomous branching. Dominant activation of RacA, however, causes actin depolarization, leading to a swollen-tip phenotype and the formation of bulbous lateral branches. Interestingly, the dichotomous branching phenotype suggested that loss of apical dominance in $\Delta racA$ can frequently be overcome by the establishment of two new sites of polarized growth. This

phenotype resembles the phenotype of the *ramosa-1* mutant of *A. niger*, which harbors an temperature-sensitive mutation in the TORC2 component RmsA causing a transient contraction of the actin cytoskeleton (Meyer et al. 2009; Reynaga-Pena and Bartnicki-Garcia 1997; Reynaga-Pena and Bartnicki-Garcia 2005).

Altogether, the data supported the model that RacA is important to stabilize polarity axes of *A. niger* hyphae via controlling actin (de)polymerization at the hyphal apex. The aim of the present study was to unravel the genetic network into which RacA is embedded and which, when disturbed due to deletion or dominant activation of RacA, leads to loss of polarity maintenance and in the case of $\Delta racA$, to reestablishment of two new polarity axes. To determine whether the hyperbranching phenotype of $\Delta racA$ leads to an increase in the amount of secreted proteins, the transcriptomes of our previously established RacA mutant strains ($\Delta racA$, *PglaA::racA^{G18V}*) were compared with the transcriptomes of the respective reference strains (wt, *PglaA::racA*). By applying defined culture conditions in bioreactor cultivations, branching morphologies as well as physiological parameters including specific growth rate and protein production rate were characterized. Finally, the implication of $\Delta racA$ on endocytosis and exocytosis in *A. niger* were examined by analyzing reporter strains harboring fluorescently tagged SlaB and AbpA (markers for endocytotic actin) and SncA (marker for secretory vesicles) was examined. The data obtained were compared with transcriptomic and physiological data of the dichotomous branching mutant *ramosa-1* (Meyer et al. 2009), thereby providing new insights into the morphogenetic network of *A. niger*.

Results

Physiological consequences of RacA inactivation

As previously reported, deletion of *racA* in *A. niger* provokes hyperbranching germ tubes and hyphae, which are shorter in length but wider in hyphal diameter. This frequent branching results on solid medium in a more compact colony with a reduced diameter due to slower tip extension rates (Kwon et al. 2011). In order to further characterize the implications of loss of RacA function, the reference strain (wild-type N402) and the $\Delta racA$ strain were cultivated in triplicate batch cultures using maltose as growth-limiting carbon source. Propagation of both strains gave rise to homogeneous cultures of dispersed mycelia, whereby loss of RacA resulted in an about 30% higher branching frequency (Fig. 1 and Table 1). Physiological profiles including growth curves, maximum specific growth rates and specific protein secretion rates were obtained with high reproducibility and were nearly

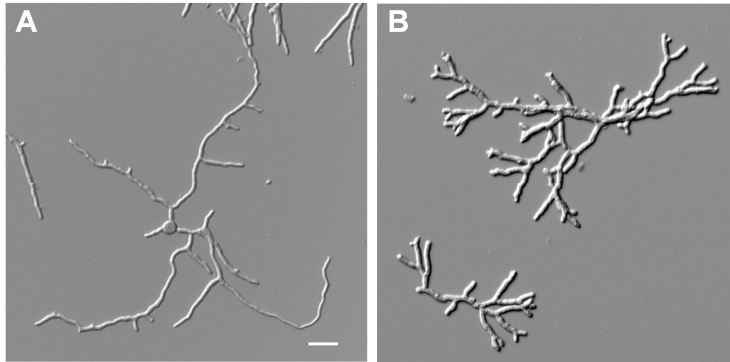


Fig. 1. Hyphal morphology during dispersed growth. Mycelial samples of the wild-type strain N402 (A) and the $\Delta racA$ mutant strain (B) were taken during the mid-exponential phase when approximately 75% of the carbon source was consumed. Bar, 20 μm .

Table 1. Comparative image analysis of branching morphologies.

	N402 (n=38)	$\Delta racA$ (n=13)
Mycelium length (μm)	510 \pm 177	507 \pm 184
No. of hyphal apices	17 \pm 6	22 \pm 8
Branch length (μm)	32 \pm 6	23 \pm 2
Central hyphal length (μm)	257 \pm 63	162 \pm 41

Morphological samples were taken from the exponential growth phase and the individual mycelium was randomly selected to measure the length of the mycelium and the number of branching tips using imageJ. Mean values \pm standard deviations are given. Bold letters indicate significant differences (two tailed t-test, $p < 0.01$).

Table 2. Physiological characterization of N402 and $\Delta racA$ strains.

	N402	$\Delta racA$
Maximum specific growth rate (h^{-1})	0.22 \pm 0.01	0.24 \pm 0.01
Yield ($\text{g}_{\text{dw}} \text{g}_{\text{maltose}}^{-1}$)	0.60 \pm 0.02	0.63 \pm 0.03
Respiratory quotient (RQ)	0.97 \pm 0.05	1.03 \pm 0.03
Acidification ($\text{mmol}_{\text{base}} \text{g}_{\text{dw}}^{-1} \text{h}^{-1}$)	1.19 \pm 0.06	1.17 \pm 0.02
Specific protein secretion rate ($\text{mg}_{\text{protein}} \text{g}_{\text{dw}}^{-1} \text{h}^{-1}$)	0.49 \pm 0.07	0.53 \pm 0.02

Biomass samples were taken from triplicate independent batch cultivations using maltose as carbon source (Fig. 2). Mean values \pm standard deviations are given. No significant difference was observed with any of the variables (two tailed t-test, $p < 0.01$). RQ, respiratory quotient calculated as the ratio of CO_2 production and O_2 consumption rates.

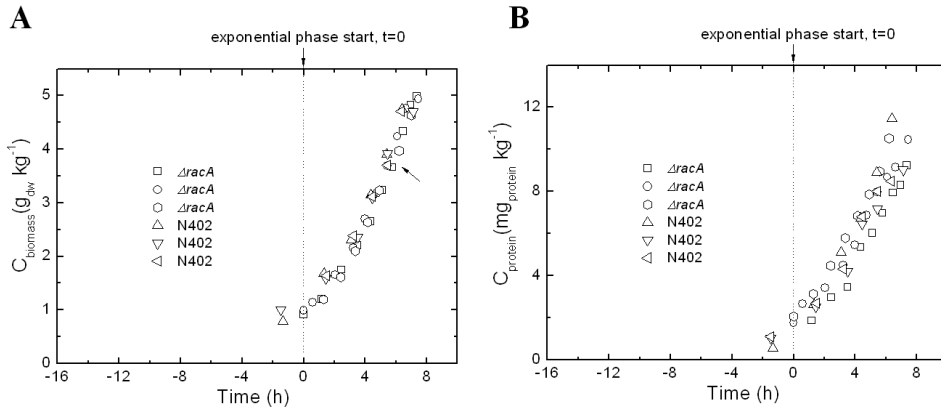


Fig. 2. Biomass (A) and extracellular protein (B) accumulation for the wild-type strain N402 and the $\Delta racA$ strain. The arrow indicates the time point when biomass samples were harvested for transcriptomics analyses. The graphs represent data for three independent biological replicate cultures per strain.

identical for both strains despite the significant difference in their morphology (Fig. 2 and Table 2). This result might come with surprise because of the negative effect of the *racA* deletion on radial colony growth on solid medium (Kwon et al. 2011). However, growth on solid media can only be assessed based on colony diameter (reflecting tip extension) and not on biomass accumulation (i.e. increase in cell volume per time). During exponential growth, growth yield on substrate ($Y_{x/s}$) was comparable in both strains; 0.63 ± 0.03 and 0.60 ± 0.02 $g_{biomass} g_{maltose}^{-1}$ for $\Delta racA$ and N402, respectively. Notably, the amount of extracellular protein was not altered in $\Delta racA$ strain compared to N402 (Table 2). Hence, an increased branching frequency is the only highly significant consequence of *racA* disruption, which, however, does not *per se* result in higher protein secretion rates.

Consequences of RacA inactivation on exo- and endocytosis

We previously showed that RacA is important for actin localization at the hyphal tip (Kwon et al. 2011). As actin is important for both exo- and endocytosis, the consequences of *racA* deletion on both was assessed in *A. niger* by following the localization of fluorescently-labelled reporter proteins SncA, AbpA and SlaB, respectively, was assessed in this study. SncA is the vesicular-SNARE that is specific for the fusion of Golgi derived secretory vesicles with the plasma membrane (Chen and Scheller 2001) and used as a marker for exocytosis in *A. nidulans* (Taheri-Talesh et al. 2008; Taheri-Talesh et al. 2012).

Abp1/AbpA and Sla2/SlaB are actin binding proteins and well characterized endocytic markers in yeast and filamentous fungi (Araujo-Bazan et al. 2008; Quintero-Monzon et al. 2005; Taheri-Talesh et al. 2008). Screening of the genome sequence of *A. niger* (Pel et al. 2007) predicted for each of the established marker proteins a single ortholog for *A. niger*: An12g07570 for SncA, An03g06960 for Abp1/AbpA and An11g10320 for Sla2/SlaB.

We constructed a reporter strain expressing a fusion of GFP with the v-SNARE SncA as described elsewhere (Kwon et al. 2013a). In brief, physiological expression levels of GFP-SncA was ensured by fusing GFP between the N-terminus and the promoter of *sncA* and used this cassette to replace it with the endogenous *sncA* gene (giving strain FG7). As depicted in Fig. 3A, GFP-SncA is visible as punctuate intracellular structures representing secretory vesicles. These vesicles accumulate towards the hyphal tip, overlap with the Spitzenkörper and are highest at the extreme apex, which is proposed to be the site of exocytosis in filamentous fungi (Taheri-Talesh et al. 2008). This localization of GFP-SncA in *A. niger* was very similar to the localization previously reported for other filamentous fungi (Furuta et al. 2007; Hayakawa et al. 2011; Kuratsu et al. 2007; Taheri-Talesh et al. 2008; Valkonen et al. 2007). Importantly, the amount of secretory vesicles per hyphal tip was affected in the $\Delta racA$ strain. Although the localization of GFP-SncA was similar to the wild-type strain, the intensity of the signal was considerably lower.

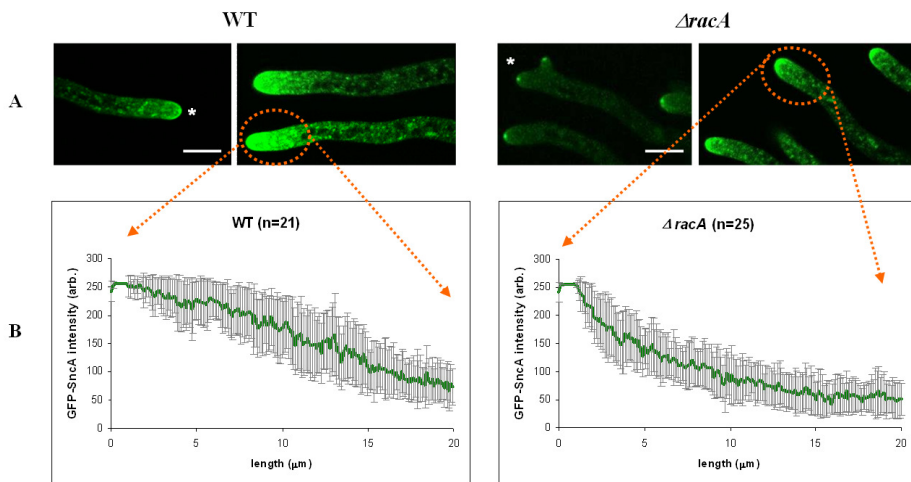


Fig. 3. Localization of secretory vesicles and fluorescent intensity distributions in the wild-type strain N402 and the $\Delta racA$ mutant strain using GFP-SncA as fluorescent marker. (A) CLSM images showing the localization of GFP-SncA in hyphal tips. The Spitzenkörper is indicated with a star. (B) Fluorescent intensity distributions along hyphal tip compartments ($n > 20$) within a region of 20 μm . Bar, 10 μm .

Quantification of the GFP signal intensities in both strains revealed that the tips of wild-type hyphae display a GFP-SncA gradient of ~20-25 μm but only about ~10 μm in the *racA* deletion strain (Fig. 3B). Both strains, however, do not differ in their specific protein secretion rates (Table 2), implying that the total amount of secretory vesicles is the same in both strains. This discrepancy can most easily be explained by the assumption that secretory vesicles in the hyperbranching ΔracA strain are merely distributed to more hyphal tips, which in consequence lowers the amount of vesicles per individual hyphal tip.

To follow the effect of *racA* deletion on endocytosis, AbpA and SlaB were labeled using a C-terminal labeling strategy as previously reported for *A. nidulans* (Taheri-Talesh et al. 2008). Importantly, both AbpA-CFP and SlaB-YFP were expressed at physiological levels by using the respective endogenous promoter and by replacing the constructs with the endogenous *abpA* and *slaB* gene, respectively (Fig. 4B). AbpA-CFP (strain MK6.1) and SlaB-YFP (strain MK5.1) transformants were phenotypically indistinguishable from the recipient strain, indicating that both AbpA-CFP and SlaB-YFP are functionally expressed (Fig. 4 and data not shown). Although AbpA-CFP and SlaB-YFP fluorescence signals were only weakly detectable (which is a direct consequence of their low endogenous expression level), both proteins were visible in the wild-type background as peripheral punctate structures and formed a subapical ring likely reflecting the endocytic machinery (Fig. 4A-C). Fluorescent signals were excluded from the hyphal apex which is in agreement with previous reports for *A. nidulans* showing that endocytosis occurs behind the tip (Araujo-Bazan et al. 2008; Taheri-Talesh et al. 2008). The signal of SlaB-YFP but not AbpA-CFP seemed to be intimately associated with the plasma membrane (data not shown), which would be in agreement with the function of both proteins - Sla2/SlaB is involved in early endocytic site initiation while Abp1/AbpA is important for invagination, scission and release of endocytotic vesicles (Kaksonen et al. 2006). SlaB-YFP and AbpA-CFP fluorescence was also occasionally observed at septa or sites destined for septum formation (Fig. 4D), probably suggesting an involvement of endocytotic events at septa as recently reported for *A. oryzae* (Hayakawa et al. 2011). Importantly, the intensity and distribution of SlaB-YFP and AbpA-CFP differed slightly in the wild-type and the ΔracA strain (Fig. 4E-G). The endocytotic actin ring as visualized by AbpA-CFP was sharper formed in the wild-type background but more diffuse in the ΔracA strain, an observation which, however, was not so evident for SlaB-YFP (Fig. 4 F-G). Still, the endocytotic ring formed by both SlaB-YFP and AbpA-CFP seemed to be positioned closer to the hyphal apex in the ΔracA strain (Fig. 4G), suggesting that deletion of *RacA* affected endocytotic processes and provoked a slight mislocalization of the endocytotic ring.

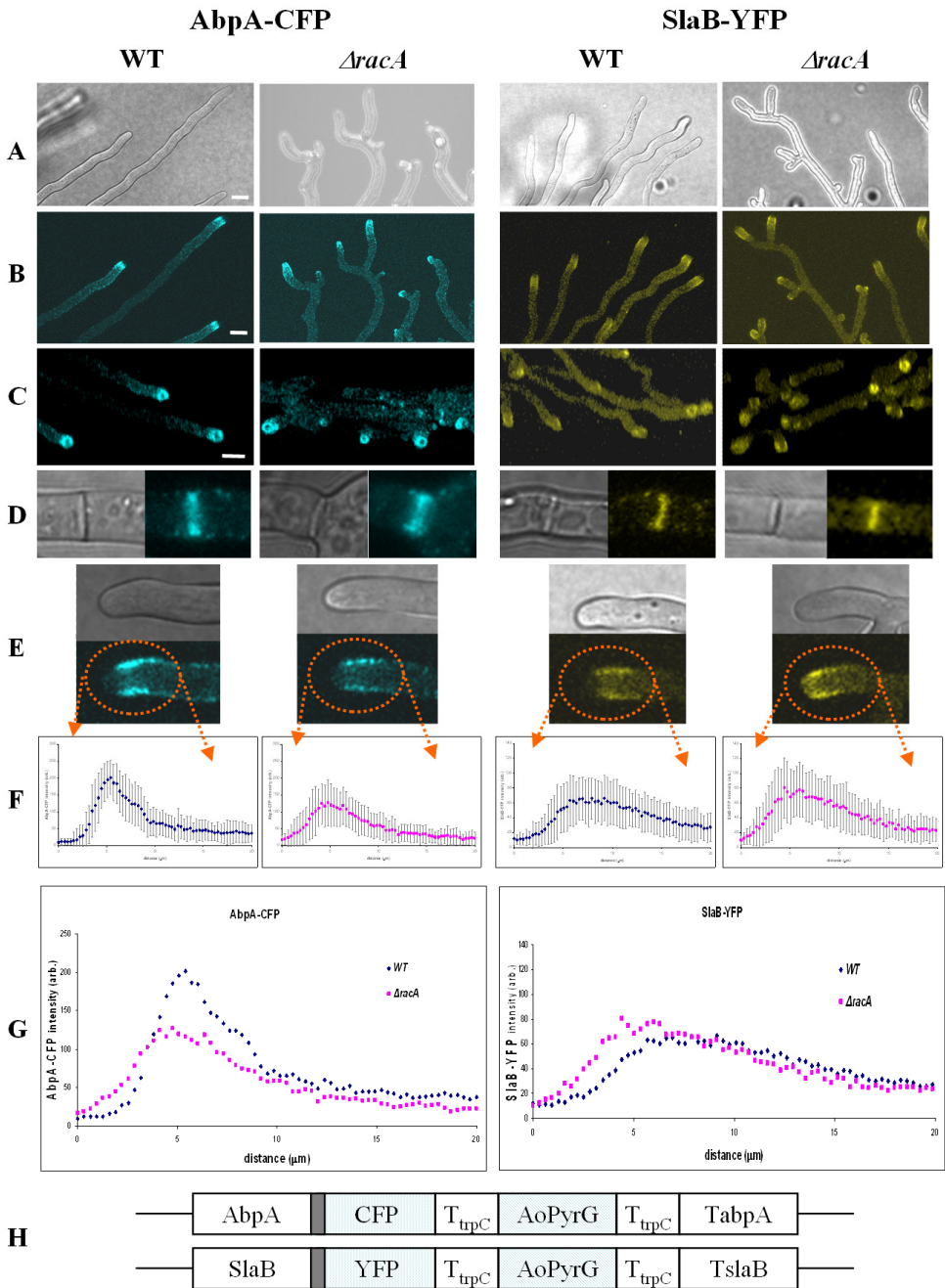


Fig. 4. Localization of endocytic ring structures in the wild-type strain N402 and the $\Delta racA$ mutant strain using AbpA-CFP and SlaB-YFP as fluorescent markers. The cultures were grown for two days at 22°C on MM agar. (A) Transmission light images, (B) two dimensional fluorescent confocal images and (C) three dimensional reconstructions from z-sectional confocal images are shown for both strains. (D, E) depict selected light and fluorescent images at sites of septation (D) and at sites of endocytosis (E). (F, G) Fluorescent intensity distribution of endocytotic ring structures. Fluorescence was measured in at least 25 hyphal tips of each strain. Mean values with (F) or without (G) standard deviation is shown. (H) Schematic representation of the AbpA-CFP and SlaB-YFP constructs designed for integration at the endogenous *abpA* and *slaB* loci, respectively. The *A. oryzae pyrG* gene served as selection marker, a sequence encoding 5x Gly-Ala as peptide linker (grey box) and the 3' region from the *A. nidulans trpC* gene as terminator. Bar, 10 μm .

The transcriptomic fingerprint of hyperbranching in $\Delta racA$

To study the transcriptomic consequences due to deletion of *racA*, RNA samples from triplicate bioreactor cultivations were taken after both wt and $\Delta racA$ cultures reached the mid-exponential growth phase (biomass concentration 3.7 gr kg⁻¹). A total of 139 genes out of 14,165 *A. niger* genes were identified as differentially expressed, 44 of which displayed increased and 95 genes decreased expression levels in $\Delta racA$ (FDR < 0.05). The complete list of differentially expressed genes, including fold change and statistical significance is given in Table S1 and S2. Interestingly, the modulated gene set in $\Delta racA$ is very small (139 genes, i.e. 1% of all *A. niger* genes) but in the same range as the differentially expressed gene set in the dichotomous branching mutant *ramosa-1* of *A. niger* (136 genes; (Meyer et al. 2009)). Although the affected gene sets had opposite signs (44 up / 95 down in $\Delta racA$, 109 up / 27 down in *ramosa-1*), similar processes were affected in both hyperbranching strains (Table 3): (i) (phospho)lipid signaling, (ii) calcium signaling, (iii) cell wall integrity (CWI) signaling and cell wall remodeling, (iv) γ -aminobutyric acid (GABA) metabolism and (v) transport phenomena. Specific responses for $\Delta racA$ but not *ramosa-1* included genes related to actin localization and protein trafficking.

In the case of (phospho)lipid signaling, genes encoding enzymes for the synthesis of the key regulatory lipid molecules diacylglycerol (DAG) and inositolpyrophosphates (IP6 and IP7) were differentially expressed in both $\Delta racA$ and *ramosa-1*. These molecules play important roles in the regulation of actin polarisation, CWI and calcium signaling in lower and higher eukaryotes (see discussion). Notably, expression of An04g03870 predicted as ortholog of the *S. cerevisiae* Dpp1p (DAG pyrophosphate phosphatase) is affected in both strains; however, down-regulated in $\Delta racA$ but up-regulated in *ramosa-1*. The same opposite response was observed for two *A. niger* ORFs predicted to encode inositol hexaki-/heptaki-phosphate kinases synthesizing the signaling molecules inositol pyrophosphates

IP6 or IP7: An14g04590 (Ksc1p ortholog) is down-regulated in $\Delta racA$, whereas An16g05020 (Vip1p ortholog) is up-regulated in *ramosa-1*. Inositol polyphosphates IP4-IP6 are known to bind to the C2B domain of the calcium sensor protein synaptotagmin (Joung et al. 2012). This binding inhibits exocytosis of secretory vesicles, whereas binding of calcium to the C2A domain of synaptotagmin activates exocytosis (Mikoshihba et al. 1999). In the $\Delta racA$ strain, four calcium transporters are down-regulated compared to the wild-type situation, two of which (An01g03100, An05g00170) code for the ortholog of the *S. cerevisiae* Vcx1p protein, which is also differentially expressed under hyperbranching conditions in *ramosa-1* (Table 3). This observation hints at the possibility that reduced GFP-SncA fluorescence at $\Delta racA$ hyphal tips is somehow linked with changes in IP6/IP7 and calcium levels in $\Delta racA$, which would be in agreement with a recent report which demonstrated that calcium spikes accompany hyphal branching in *Fusarium* and *Magnaporthe* hyphae (Kim et al. 2012). Changes in the intracellular calcium distribution also affect the homeostasis of other ions. Congruently, 12 genes putatively encoding transport proteins for ions (Na^+ , K^+ , Fe^{2+}) and small molecules (phospholipids, amino acids, peptides, hexoses) displayed differential transcription in $\Delta racA$ as also observed for *ramosa-1* (Table 3), suggesting that ion homeostatic and/or metabolic control systems are also important to maintain polar growth. Reduced exocytotic GFP-SncA signals at hyphal tips of the $\Delta racA$ strain would imply that less cell wall biosynthetic/remodeling enzymes are transported to the tip. Indeed, expression of ten ORFs encoding cell membrane and cell wall genes and three ORFs involved in protein trafficking were down-regulated in $\Delta racA$ (Table 3). Whatever the consequences of reduced expression of cell wall or ion homeostasis genes are, none of these changes led to increased sensitivity of the $\Delta racA$ strain towards cell wall stress agents (calcofluor white), different salts (MgCl_2 , KCl, NaCl) or oxidative conditions (H_2O_2 , menadion; data not shown), suggesting that the integrity of the cell wall or cell membrane is not disturbed in the *racA* strain.

Inactivation of RacA, however, has considerable consequences on actin localization as previously reported (Meyer et al. 2008). Congruently, five ORFs involved in actin polarization were down-regulated in the $\Delta racA$ strain (Table 3). Of special importance are the polarisomal component SpaA, whose deletion has been shown to cause a hyperbranching phenotype and reduced growth speed in *A. niger* (Meyer et al. 2008) and two ORFs which are homologous to the *S. cerevisiae* amphiphysin-like proteins Rvs161p and Rvs167p. The latter function as heterodimer in *S. cerevisiae*, bind to phospholipid membranes and have established roles in organization of the actin cytoskeleton, endocytosis and cell wall integrity (Friesen et al. 2006).

Table 3. Selected genes whose expression profile respond to hyperbranching in $\Delta racA$ (this work) and *ramosa-1* (Meyer et al. 2009). Genes are ordered into different processes and functions.

Predicted protein function*	$\Delta racA$ versus wt			<i>ramosa-1</i> versus wt		
	Open reading frame code	Up / Down	Closest <i>S. cerevisiae</i> ortholog	Open reading frame code	Up / Down	Closest <i>S. cerevisiae</i> ortholog
(Phospho)lipid metabolism and signaling						
phosphatidyl synthase, synthesis of phosphatidyl alcohols				An02g08050	↑	
sterol 24-C-methyltransferase, ergosterol synthesis	An04g04210	↑	Erg6			
C-14 sterol reductase, ergosterol synthesis	An01g07000	↓	Erg24	An01g07000	↑	Erg24
inositol hexaki-/heptaki-phosphate kinase, synthesis of IP6, IP7	An14g04590	↓	Kcs1	An16g05020	↑	Vip1
plasma membrane protein promoting PI4P synthesis				An18g06410	↑	Sfk1
phospholipase B, synthesis of glycerophosphocholine	An18g01090	↓	Plb3			
phospholipase D, synthesis of phosphatidic acid	An02g13220	↓	Plb1	An15g07040	↑	Spo14
diacylglycerol pyrophosphate phosphatase, synthesis of DAG	An04g03870	↓	Dpp1	An04g03870	↑	Dpp1
choline / ethanolamine permease	An02g01180	↓	Dpp1	An11g05330	↑	
	An16g01200	↑	Hnm1			
	An01g13290	↓	Hnm1			
transcription factor important for sterol uptake	An02g09780	↓	Upc2			
mannosyl-inositol phosphorylceramide (MIPC) synthase	An12g00680	↓	Upc2			
	An05g02310	↓	Sur1			
Calcium homeostasis and signaling						
Ca ²⁺ /calmodulin dependent protein kinase				An02g05490, An16g03050	↑ ↑	Cmk2 Cmk2
vacuolar Ca ²⁺ /H ⁺ exchanger	An01g03100	↓	Vcx1	An01g03100	↑	Vcx1
	An05g00170	↓	Vcx1	An05g00170	↑	Vcx1
	An14g02010	↓	Vcx1			
Ca ²⁺ transporting ATPase	An19g00350	↓	Pmc1	An02g06350	↑	Pmc1
Ca ²⁺ / phospholipid-transporting ATPase				An04g06840	↑	Drs2
Cell wall remodeling and integrity						
membrane receptor, CWI signaling	An01g14820	↑	Wsc2			
MAP kinase kinase, CWI signaling, MkkA				An18g03740	↑	Mkk1/2
plasma protein responding to CWI signaling	An07g08960	↓	Pun1			
	An08g01170	↓	Pun1			
α-1,3-glucanase	An04g03680	↑		An08g09610	↑	
β-1,3-glucanosyltransferase (GPI-anchored)				An16g06120	↑	Gas1
β-1,4-glucanase	An03g05530	↓		An03g05530	↑	
chitin synthase class II, similar to ChsA of <i>A. nidulans</i>				An07g05570	↑	
chitin transglycosidase (GPI-anchored)	An07g01160	↓	Crh2	An13g02510	↑	Crh1

Table 3. Cont.

Predicted protein function*	AracA versus wt			ramosa-1 versus wt		
	Open reading frame code	Up / Down	Closest <i>S. cerevisiae</i> ortholog	Open reading frame code	Up / Down	Closest <i>S. cerevisiae</i> ortholog
chitinase (GPI-anchored), similar to ChiA of <i>A. nidulans</i>				An09g06400	↓	Cts1
β-mannosidase				An11g06540	↑	
endo-mannanase (GPI-anchored), DfgE	An16g08090	↓	Dfg1	An16g08090	↑	Dfg1
α-1,2-mannosyltransferase				An14g03910	↑	Kre2
				An18g05910	↑	Kre2
α-1,3-mannosyltransferase	An15g04810	↓	Mnt2			
α-1,6-mannosyltransferase	An05g02320	↓				
cell wall protein	An14g01840	↓	Tir3	An04g05550	↑	Flo11
	An11g01190	↓	Sps22	An11g01190	↑	Sps22
				An03g05560	↑	
				An04g03830	↑	
				An02g11620	↓	
plasma membrane protein	An02g08030	↓	Pmp3			
<i>GABA metabolism</i>						
glutaminase				An11g07960	↑	
γ-aminobutyrate transaminase				An17g00910	↑	Uga1
NAD(+)-dependent glutamate dehydrogenase				An02g14590	↑	Gdh2
GABA permease	An16g01920	↑				
transcription factor for GABA genes	An02g07950	↓				
<i>Transporter</i>						
mitochondrial phosphate translocator				An02g04160	↑	Mir1
mitochondrial ABC transporter during oxidative stress	An12g03150	↓	Mdl1			
vacuolar glutathione S-conjugate ABC-transporter				An13g02320	↑	Ycf1
plasma membrane Na ⁺ /K ⁺ -exchanging ATPase alpha-1 chain	An09g00930	↓		An09g00930	↑	
plasma membrane K ⁺ transporter	An03g02700	↓	Trk1			
multidrug transporter	An01g05830	↓	Qdr1	An02g01480	↑	
low-affinity Fe(II) transporter of the plasma membrane	An16g06300	↓	Fet4	An16g06300	↑	Fet4
vacuolar H ⁺ -ATPase subunit, required for copper and iron homeostasis	An10g00680	↓	Vma3			
siderophore-iron transporter				An12g05510	↓	Taf1
mitochondrial carrier protein				An14g01860	↓	Rim2
vacuolar zinc transporter				An15g03900	↓	Zrc1
allantoin permease				An18g01220	↓	Dal5
oligopeptide transporter	An13g01760	↑	Opt1	An15g07460	↓	Opt1
	An11g01040	↓	Opt1			
hexose / glucose transporter	An06g00560	↑	Hxt13	An09g04810	↓	
amino acid transporter	An03g00430	↑				
galactose transporter	An01g10970	↓	Gal2			
FAD transporter into endoplasmatic reticulum, CWI-related	An01g09050	↓	Fic2			

Table 3. Cont.

Predicted protein function*	<i>ΔracA versus wt</i>			<i>ramosa-1 versus wt</i>		
	Open reading frame code	Up / Down	Closest <i>S. cerevisiae</i> ortholog	Open reading frame code	Up / Down	Closest <i>S. cerevisiae</i> ortholog
Protein trafficking						
GTPase activating protein involved in protein trafficking	An01g02860	↓	Gyp8	An15g01560	↑	Gyp7
t-SNARE protein important for fusion of secretory vesicles with the plasma membrane	An02g05390	↓	Sec9			
vacuolar protein important for endosomal-vacuolar trafficking pathway	An11g01810	↓	Rcr2			
Actin localisation						
polarisome component SpaA	An07g08290	↓	Spa2			
actin-binding protein involved in endocytosis	An03g01160	↓	Lsb4			
protein required for normal localization of actin patches	An16g02680	↓	Apd1			
Amphysin-like protein required for actin polarization	An17g01945	↓	Rvs161			
Amphysin-like protein required for actin polarization	An09g04300	↓	Rvs167			
Other signaling processes						
Ser/Thr protein kinase important for K ⁺ uptake	An17g01925	↓	Sat4			
transcription factor for RNA polymerase II	An16g07220	↓	Tfg2			
negative regulator of Cdc42				An12g04710	↓	Vtc1
putative C ₂ H ₂ zinc-finger transcription factor				An04g01500	↑	
SUN family protein involved in replication				An08g07090	↓	Sim1
similar to <i>A. nidulans</i> transcription factor RosA				An16g07890	↓	Ume6
Others						
hypothetical aspergillosis allergen rAsp	An03g00770	↓		An03g00770	↑	

Genes up-regulated are indicated with ↑, genes down-regulated with ↓. Differential gene expression was evaluated by moderated t-statistics using the Limma package (Smyth 2004) with a FDR threshold at 0.05 (Benjamini and Hochberg 1995). Identical ORFs which are differentially expressed in both *ΔracA* and *ramosa-1* are indicated in bold. Fold changes and statistical significance is given in Table S1 and S2. *: Protein functions were predicted based on information inferred from the *Saccharomyces* genome data base SGD (<http://www.yeastgenome.org/>) and the *Aspergillus* genome database AspGD (<http://www.aspergillusgenome.org/>).

The transcriptomic fingerprint of apolar growth in RacA^{G18V}

Next, we wished to dissect the transcriptomic adaptation of *A. niger* to dominant activation of RacA. Batch cultures of our previously established RacA mutant strains *PglaA::racA^{G18V}* and *PglaA::racA* (reference strain) were started with xylose (0.75%) as repressing carbon source. After the cultures reached the exponential growth phase and xylose was consumed, maltose (0.75%) was added to induce expression of genes under control of *PglaA*.

Hypothetically, a so far unknown RacA-dependent GAP ensures that the activity of RacA is spatially restricted to the hyphal apex in the *PglaA-racA* strain thereby maintaining a stable polarity axes even under inducing conditions (Fig. 5). However, this control mechanism is leveraged off in the *PglaA-racA*^{G18V} mutant strain, as the GTPase-negative G18V mutation traps RacA in its active, GTP-bound form (Kwon et al. 2011). Hence, the switch from xylose to maltose leads to a loss of polarity maintenance in the *PglaA-racA*^{G18V} strain and the formation of clavate-shaped hyphal tips and bulbous lateral branches (Fig. 5). RNA samples were extracted from duplicate cultures 2 and 4 h after the maltose shift and used for transcriptomic comparison. Expression of 3,757 (506) genes was modulated after 2 h (4 h) of induction, 1,906 (282) of which showed increased and 1,851 (224) decreased expression levels in the *PglaA-racA*^{G18V} strain when compared to the *PglaA-racA* reference strain (FDR < 0.05). The complete list of differentially expressed genes, including fold change and statistical significance is given in Table S1 and S2. GO enrichment analysis using the FetGOat tool (Nitsche et al. 2011) discovered that most of these genes belong to primary metabolism, suggesting that both strains differed in their ability to quickly adapt to the new carbon source (Table S3).

To identify those genes which only relate to the difference between polar to apolar morphology in *PglaA-racA*^{G18V} but are independent from time and carbon source, a Venn

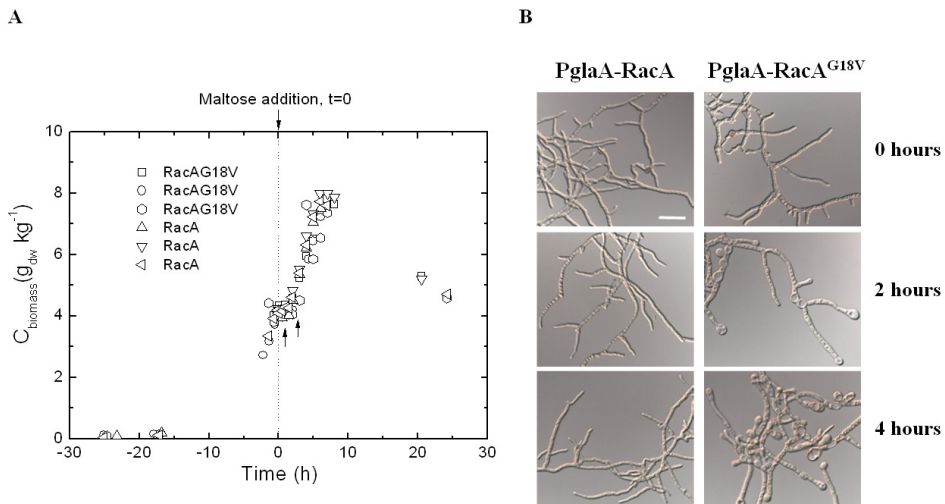


Fig. 5. Biomass accumulation and morphology during submerged cultivation of *PglaA-RacA*^{G18V} and *PglaA-RacA* mutant strains. (A) Growth curve for both mutant strains. The dashed line indicates the time point when the inducing carbon source maltose was added. The two arrows indicate the time points at which samples for transcriptome analysis were taken. (B) Dispersed hyphal morphology at the time point of maltose addition as well as 2 and 4 h after maltose addition. Bar, 20 μm .

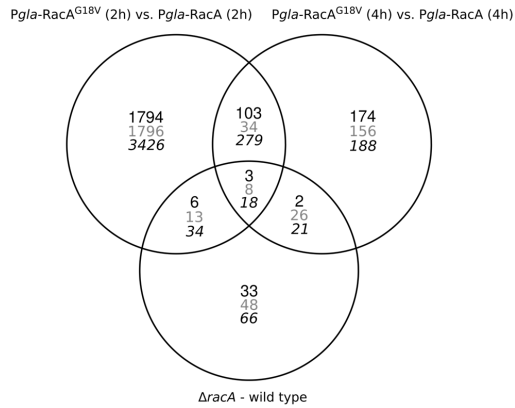


Fig. 6. Venn diagrams of induced (black numbers), repressed (grey numbers) and up- or down-regulated (italics numbers) genes for the *PglA-RacA*^{G18V}/*PglA-RacA* and Δ *racA*/N402 comparisons.

diagram was constructed (Fig. 6) and the intersection determined representing genes which are differently expressed after both 2 and 4 h in *PglA-racA*^{G18V} when compared to the 2 h and 4 h data sets of the *PglA-racA* reference strain. Overall, 148 genes showed different expression, 106 of which were up-regulated and 42 of which were down-regulated in *PglA-racA*^{G18V} (Table S4). Again, only a small set of genes (about 1% of the *A. niger* genome) show different expression levels during polar and apolar growth. Table 4 highlights the most interesting genes of this compilation, which could be grouped into several regulatory processes including (i) (phospho)lipid signaling, (ii) calcium signaling, (iii) CWI signaling and (iv) nitrogen signaling. In addition, metabolic processes including primary metabolism (amino acid biosynthesis) and secondary metabolism (polyketide synthesis, non-ribosomal peptide synthesis) were affected as well.

The transcriptomic fingerprint indicated that the turgor pressure is increased during apolar growth and thereby an osmotic and cell wall stress is sensed in the *PglA-racA*^{G18V} strain. An14g02970, an ORF with strong similarity to the Sln1p histidine kinase osmosensor of *S. cerevisiae* which forms a phosphorelay system to activate the Hog1 MAP kinase cascade (Posas et al. 1996), showed increased expression. In agreement, some cell wall genes which have been shown to respond to caspofungin-induced cell wall stress in *A. niger* (Meyer et al. 2007b) were up-regulated as well: *agtA*, a GPI-anchored alpha-glucanosyltransferase and two putative cell wall protein encoding genes *phiA* and An12g10200. In addition, other proteins, known to be up-regulated under cell wall and osmotic stress in *S. cerevisiae* showed enhanced expression in *PglA-racA*^{G18V}: An16g02850 (ortholog of the chitin transglycosylase Crh1p, (Bermejo et al. 2008),

Table 4. Selected genes whose expression profiles differ between polar and apolar growth in *PglaA-racA*^{G18V} versus *PglaA-racA* in a time- and carbon source-independent manner. Genes are ordered into different processes and functions.

Predicted protein function*	Open reading frame code	Up / Down	Closest <i>S. cerevisiae</i> ortholog
(Phospho)lipid metabolism and signaling			
dehydrogenase involved in sphingosin 1-phosphate breakdown	An01g09260	↑	Hfd1
Lysophospholipase, synthesis of glycerophosphocholine	An16g01880	↑	
plasma membrane flippase transporting sphingoid long chain bases	An02g06440	↑	Rsb1
glycerophosphocholine phosphodiesterase, synthesis of phosphocholine	An18g03170	↑	Gde1
lanosterol 14A-demethylase	An11g02230	↓	Erg11
C-14 sterol reductase, ergosterol synthesis	An01g07000	↓	Erg24
choline / ethanolamine permease	An01g13290	↓	Hnm1
Calcium homeostasis and signaling			
Ca ²⁺ /calmodulin dependent protein kinase	An02g05490	↓	Cmk2
Cell wall remodeling and integrity			
endo-glucanase EglA	An14g02760	↑	
endo-glucanase EglB	An16g06800	↑	
endo-glucanase similar to <i>Trichoderma reesei</i> egl4	An14g02670	↑	
alpha-glucanosyltransferase AgtA (GPI-anchored)	An09g03100	↑	
chitin synthase ChsL	An02g02340	↑	Chs3
chitin transglycosidase	An16g02850	↑	Crh1
chitinase	An01g05360	↑	Cts2
cell wall protein similar to <i>A. nidulans</i> PhiA	An14g01820	↑	
cell wall protein with internal repeats	An12g10200	↑	
cell wall protein (flocculin)	An12g00140	↑	Flo11
protein involved in β-1,3 glucan synthesis	An05g00130	↓	Knh1
α-1,2-mannosyltransferase	An04g06730	↓	Mnn2
Primary metabolism			
isocitrate lyase AcuD	An01g09270	↑	Icl1
citrate lyase	An11g00510	↑	
	An11g00530	↑	
succinate dehydrogenase	An16g07150	↑	Osm1
aspartate transaminase, synthesis of glutamate	An16g05570	↑	
acetyl-CoA carboxylase, synthesis of fatty acids	An12g04020	↑	
homo-isocitrate dehydrogenase, synthesis of lysine	An15g02490	↓	Lys12
arginosuccinate synthetase, synthesis of arginine	An15g02340	↓	Arg1
acetylmithine aminotransferase, synthesis of arginine	An15g02360	↓	Arg8
arginyl-tRNA synthetase	An02g04880	↓	
aspartic beta semi-aldehyde dehydrogenase, synthesis of threonine and methionine	An11g09510	↓	Hom2
homoserine kinase, synthesis of threonine	An17g02090	↓	Thr1
threonine synthase	An16g02520	↓	Thr4
phosphoribosylglycinamide formyltransferase, synthesis of purines	An02g02700	↓	Ade8
Secondary metabolism			
polyketide synthase	An11g07310	↑	
similar to plant zeaxanthin epoxidase ABA2	An03g06500	↑	
similar to enniatin synthase esyn1 of <i>Fusarium scirpi</i>	An13g03040	↑	
similar to enoyl reductase LovC of the lovastatin biosynthesis <i>A. terreus</i>	An13g02940	↑	
	An09g01880	↑	
similar to HC-toxin peptide synthase HTS of <i>Cochliobolus carbonum</i>	An16g06720	↑	
Transporter			
polyamine transporter	An11g07300	↑	Tpo3
	An12g07400	↓	Tpo3
	An13g03220	↓	Tpo1
vacuolar basic amino acid transporter	An06g00770	↑	Vba5
oligopeptide transporter	An11g01040	↓	Opt1

Table 4. Cont.

Predicted protein function*	Open reading frame code	Up / Down	Closest <i>S. cerevisiae</i> ortholog
hexose transporter	An02g07610	↑	Hxt5
galactose transporter	An01g10970	↓	Gal2
low-affinity Fe(II) transporter of the plasma membrane	An16g06300	↓	Fet4
siderophore transporter	An03g03560	↓	Arn1
plasma membrane multidrug transporter	An07g01250	↑	Pdr5
multidrug transporter	An13g03060	↑	Snq2
Protein trafficking			
protein kinase involved in exocytosis	An08g03360	↑	Kin1
Other signaling processes			
zinc finger transcriptional repressor	An04g08620	↑	Oaf3
protein recruiting the SAGA complex to promoters	An07g04540	↑	Cti6
histidine kinase osmosensor	An14g02970	↑	Sln1
transcriptional regulator involved in nitrogen repression	An02g11830	↑	Ure2
transcription factor similar to <i>A. nidulans</i> MedA	An02g02150	↑	
transcription factor	An02g06180	↑	
transcription factor important for salt stress resistance	An12g09020	↑	Hal9
DNA damage checkpoint protein during replication	An03g06930	↓	Rad24
SUN family protein involved in replication	An08g07090	↓	Sim1
transcription factor important for Zn ²⁺ homeostasis	An08g01860	↓	Zap1
alpha subunit of the translation initiation factor	An18g04650	↓	Gcn3
Others			
pathogenesis-related protein	An08g05010	↑	Pry1
hypothetical aspergillus allergen rAsp	An03g00770	↓	

Genes up-regulated are indicated with ↑, genes down-regulated with ↓. Differential gene expression was evaluated by moderated t-statistics using the Limma package (Smyth 2004) with a FDR threshold at 0.05 (Benjamini and Hochberg 1995). Identical ORFs which are differentially expressed in *PglaA-racA^{G18V}* and *ΔracA* are indicated in bold. Fold changes and statistical significance is given in Table S1 and S2. *: Protein functions were predicted based on information inferred from the *Saccharomyces* genome data base SGD (<http://www.yeastgenome.org/>) and the *Aspergillus* genome database AspGD (<http://www.aspergillusgenome.org/>).

An02g05490 (Ca²⁺/calmodulin dependent protein kinase Cmk2p, (Dudgeon et al. 2008) and An07g01250 (ortholog of the multidrug transporter Pdr5p, (Ernst et al. 2005). Furthermore, increased expression was also observed for An03g06500 encoding an ortholog of the plant zeaxanthin epoxidase, which catalyses one step in the biosynthetic pathway of the plant hormone abscisic acid, known to protect plant cells against dehydration under high-salinity stress (Xiong et al. 2002).

The expression of many transporters and permeases (iron, hexoses, amino acids and peptides) was also modulated in *PglaA-racA^{G18V}* as well as the expression of several amino acid biosynthetic genes, most of which were down-regulated (lysine, arginine, threonine, methionine; Table 4). As also some ORFs predicted to function as important activators in replication (An03g06930, An08g07090) and translation (An18g04650) displayed decreased expression suggests that reduced tip extension during apolar growth slows down basic cellular processes. In this context, it is interesting to note that An01g09260 predicted to break down sphingosin 1-phosphate (S1P) showed increased expression during apolar growth. S1P is a sphingolipid acting as second messenger in lower and higher eukaryotes

regulating respiration, cell cycle and translation (Cowart et al. 2010) and is also important for the sole sphingolipid-to-glycerolipid metabolic pathway (Nakahara et al. 2012). As also expression of An02g06440, a predicted ortholog of the *S. cerevisiae* sphingosin flippase Rsb1p which extrudes sphingosin into the extracytoplasmic side of the plasma membrane, was increased during apolar growth might suggest that reduced levels of S1P are present in apolar growing hyphal tips (see discussion).

Interestingly, none of the extracted 148 genes (Table S4) showed any link to actin filament organization, although actin polarization is lost in the *PglaA-racA*^{G18V} strain and actin patches are randomly scattered intracellularly or at the cell periphery (Kwon et al. 2011). One explanation might be that transcription of actin-related genes was immediately altered after maltose addition which induced the switch from polar to apolar growth in *PglaA-racA*^{G18V}. To still get a glimpse on genes involved in actin patch formation, the 2 h dataset of *PglaA-racA*^{G18V} versus *PglaA-racA* was screened for the presence of enriched GO terms related to actin (Table S3). Using this approach, 10 actin-related genes were extracted which are summarized in Table 5. Most interestingly, An18g04590, an ortholog of the *S. cerevisiae* Rho GDP dissociation inhibitor Rdi1p displayed increased expression. Rdi1p regulates the Rho GTPases Cdc42p, Rho1p and Rho4p, localizes to polarized growth sites at specific times of the cell cycle and extracts all three proteins from the plasma membrane to keep them in an inactive cytosolic state (Johnson et al. 2009; Richman et al. 2004; Tiedje et al. 2008). Overexpression of Rdi1p causes slightly rounder cell morphology in *S. cerevisiae* (Tcheperegine et al. 2005). Another interesting actin-related gene showing increased expression in strain *PglaA-racA*^{G18V} is An11g02840, the predicted homolog of the *S. cerevisiae* Slm2 protein. Slm2p binds to the second messenger phosphatidylinositol-4,5-

Table 5. GO term enriched actin-related genes whose expression responds to the switch from polar to apolar growth in *PglaA-racA*^{G18V}.

Predicted protein function*	Open reading frame code	Up / Down	Closest <i>S. cerevisiae</i> ortholog
Rho GDP dissociation inhibitor	An18g04590	↑	Rdi1
TORC2 and phosphoinositide PI4,5P(2) binding protein	An11g02840	↑	Slm2
Arp2/3 complex subunit	An02g06360	↑	Arc15
Arp2/3 complex subunit	An01g05510	↑	Arc35
Arp2/3 complex subunit	An18g06590	↑	Arc40
tropomyosin 1	An13g00760	↑	Tpm1
actin cortical patch component	An02g14620	↑	Aip1
twinfilin	An04g09020	↑	Twf1
actin-capping protein	An01g05290	↑	Cap2
protein recruiting actin polymerization machinery	An10g00370	↑	Bzz1

Genes up-regulated are indicated with ↑. Differential gene expression was evaluated by moderated t-statistics using the Limma package (Smyth 2004) with a FDR threshold at 0.05 (Benjamini and Hochberg 1995). Fold changes and statistical significance is given in Table S1 and S2. *: Protein functions were predicted based on information inferred from the *Saccharomyces* genome data base SGD (<http://www.yeastgenome.org/>) and the *Aspergillus* genome database AspGD (<http://www.aspergillusgenome.org/>).

bisphosphate (PIP2) and to the TORC2 signaling complex and integrates inputs from both signaling pathways to control polarized actin assembly and cell growth (Fadri et al. 2005). In addition, it is also a target of sphingolipid and calcium signaling during heat stress response in *S. cerevisiae* and promotes cell survival by coordinating cell growth and actin polarization (Daquinag et al. 2007). Both An18g04590 (Rdi1p ortholog) and An11g02840 (Slm2p ortholog) might thus be two key proteins important to sustain tip growth and proper actin polarization in *A. niger*. The other eight GO enriched proteins of strain *PglaA-racA^{G18V}* are orthologs of *S. cerevisiae* proteins with a function in cortical actin patch formation (Table 5). For example, subunits of the Arp2/3 complex which is required for the motility and integrity of cortical actin patches are up-regulated in apolar growing hyphal tips of strain *PglaA-racA^{G18V}*, one of which (An18g06590, Arc40p ortholog) also responds to caspofungin-induced loss of cell polarity in *A. niger* (Meyer et al. 2007b). Another interesting gene showing increased expression was An04g09020, the ortholog of twinfilin. Twf1p has been shown to localize to cortical actin patches in *S. cerevisiae*, forms a complex with the capping protein Cap2 (An01g05290, up-regulated in *PglaA-racA^{G18V}*), sequesters actin monomers to sites of actin filament assembly and is regulated by PIP2 (Palmgren et al. 2001), providing an additional hint that re-structuring of the actin cytoskeleton in *PglaA-racA^{G18V}* might be orchestrated by PIP2 signaling. Taken together, the transcriptomic fingerprint of *A. niger* hyphae expressing dominant active RacA suggests that several signaling pathways and secondary messengers might orchestrate the morphological switch from polar to apolar growth.

The RacA effector gene set

We finally compared the transcriptomic dataset of $\Delta racA$ versus wt with the dataset of *PglaA-racA^{G18V}* versus *PglaA-racA* (4 h after maltose addition) to identify those genes whose transcription is generally affected by morphological changes independently whether provoked by RacA inactivation or by RacA hyperactivation. Overall, 38 genes fulfill this criterion (Fig. 6, Table S4) and are summarized in Table 6. The affected gene list covered processes such as (i) (phospho)lipid signaling, (ii) CWI and remodeling, (iii) actin localization, (iv) transport phenomena and (v) protein trafficking. Most interestingly, 12 out of the 38 genes were also differentially expressed during apical branching in *ramosa-1* (Meyer et al. 2009), including two orthologs of diacylglycerol pyrophosphate phosphatase (Dpp1p), which synthesizes the secondary messenger diacylglycerol (DAG), the activator of mammalian and fungal protein kinase C, which in fungi is a component of the CWI pathway localized upstream of the MAP kinase kinase Mkk1/2 (MkkA in *A. niger*; for

review see (Singh and Del Poeta 2010)). Targets of the CWI signaling pathway are cell wall remodeling genes, five of which were differentially expressed in RacA hyper- or inactivation strains (Table 6). From these five genes, three are of special importance as these were also effector genes in the hyperbranching mutant *ramosa-1* (Meyer et al. 2009). Although calcium signaling genes seemed not be among the extracted 38 genes, its indirect involvement might be conceivable. For example, An18g01090 encoding the predicted ortholog of the *S. cerevisiae* phospholipase B (Plb3p) is among this gene set. Plb3p is activated at high concentrations of Ca^{2+} and specifically accepts phosphatidylinositol as a substrate to keep its concentration on the outer membrane leaflet low (Merkel et al. 2005). Finally, 17 RacA effector genes encode proteins of unknown function, most of which have no predicted orthologs in *S. cerevisiae*. As their function, however, seems to be important for morphological changes in *A. niger*, they are highly interesting candidate genes for future analyses.

Discussion

The fungal actin cytoskeleton is highly dynamic and fulfils multiple functions important for cell polarity regulation, endocytosis, exocytosis and septation. Central regulators of actin polymerization and depolymerization are Rho GTPases whose activity is regulated by their membrane-cytoplasmatic shuttling which itself is modulated by external or internal morphogenetic signals. Actin dynamics is thus controlled by a network of signaling pathways that sense and integrate different stimuli (Lichius et al. 2011). We have recently proposed that the *A. niger* GTPases RacA and CftA (Cdc42p) can substitute each other with respect to actin assembly but that actin disassembly is mainly under control of RacA. A *racA* deletion mutant is thus not affected in actin polymerization (because is secured by CftA) but impaired in actin disassembly. In consequence, maintenance of apical dominance can become frequently lost in the *racA* deletion strain resulting in a hyperbranching phenotype. In contrast, RacA trapped in its active, GTP-bound form (RacA^{G18V}) provokes the formation of higher-order actin structures, i.e. actin patches, which cause loss of polarity maintenance and the formation of round, apolar growing cells (Kwon et al. 2011). The purpose of the current study was to identify the transcriptional signature associated with morphological changes in hyphal tip growth of *A. niger*. The transcriptional response of *A. niger* provoked by inactivation and hyperactivation of RacA, respectively, was determined and compared with the transcriptomic fingerprint of the apical branching transcriptome of the *ramosa-1* mutant (Meyer et al. 2009). The data obtained allowed us to

Table 6. Complete list of genes whose expression respond to hyperbranching in $\Delta racA$ versus wild-type and to the switch from polar and apolar growth in $PglaA-racA^{G18V}$ versus $PglaA-racA$ (4 h after induction).

Predicted protein function*	Open reading frame code	Up / Down in $PglaA-racA^{G18V}$ versus $PglaA-racA$	Up / Down in $\Delta racA$ versus wt	Closest <i>S. cerevisiae</i> ortholog
(Phospho)lipid metabolism and signaling				
phospholipase B, synthesis of glycerophosphocholine	An18g01090	↓	↓	Plb3
diacylglycerol pyrophosphate phosphatase, synthesis of DAG	An02g01180	↓	↓	Dpp1
	An04g03870	↓	↓	Dpp1
sterol 24-C-methyltransferase, ergosterol synthesis	An04g04210	↑	↑	Erg6
C-14 sterol reductase, ergosterol synthesis	An01g07000	↓	↓	Erg24
transcription factor important for sterol uptake	An02g07950	↓	↓	Upc2
	An12g00680	↓	↓	Upc2
Cell wall remodeling and integrity				
α-1,3-mannosyltransferase	An15g04810	↓	↓	Mnt2
endo-mannanase (GPI-anchored), DfgE	An16g08090	↓	↓	Dfg1
β-1,4-glucanase	An03g05530	↓	↓	
cell wall protein	An11g01190	↓	↓	Sps22
plasma membrane protein	An02g08030	↓	↓	Pmp3
Actin localization				
amphysin-like protein required for actin polarization	An17g01945	↓	↓	Rvs161
actin-binding protein involved in endocytosis	An03g01160	↓	↓	Lsb4
Transporter				
choline / ethanolamine permease	An01g13290	↓	↓	Hnm1
low-affinity Fe(II) transporter	An16g06300	↓	↓	Fet4
oligopeptide transporter	An11g01040	↓	↓	Opt1
galactose/glucose permease	An01g10970	↓	↓	Gal2
Protein trafficking				
GTPase activating protein involved in protein trafficking	An01g02860	↓	↓	Gyp8
protein important for endosomal-vacuolar trafficking	An11g01810	↓	↓	Rcr2
peptidase	An03g02530	↓	↓	
Others				
hypothetical aspergillosis allergen rAsp	An03g00770	↓	↓	
cytochrome P450 protein	An11g02990	↓	↓	Dit2
isoamyl alcohol oxidase	An03g06270	↓	↓	
protein with strong similarity to penicillin V amidohydrolase	An12g04630	↓	↓	
oxidoreductase	An03g00280	↑	↑	
protein with nucleotide binding domain	An01g08150	↑	↑	Irc24
protein with methyltransferase domain	An09g00160	↑	↑	
protein with unknown function	An15g03880	↓	↓	
protein with unknown function	An01g10900	↓	↓	
protein with unknown function	An07g05820	↓	↓	
protein with unknown function	An18g00810	↓	↓	
protein with unknown function	An04g04630	↓	↓	
protein with unknown function	An06g00320	↓	↓	
protein with unknown function	An07g04900	↓	↓	
protein with unknown function	An01g13320	↓	↓	
protein with unknown function	An16g07920	↑	↑	
protein with unknown function	An01g03780	↓	↓	

Genes up-regulated are indicated with ↑, genes down-regulated with ↓. Differential gene expression was evaluated by moderated t-statistics using the Limma package (Smyth 2004) with a FDR threshold at 0.05 (Benjamini and Hochberg 1995). Identical ORFs or proteins with predicted similar function being also differentially expressed in *ramosa-1* are indicated in bold. Fold changes and statistical significance is given in Table S1 and S2. *: Protein functions were predicted based on information inferred from the *Saccharomyces* genome data base SGD (<http://www.yeastgenome.org/>) and the *Aspergillus* genome database AspGD (<http://www.aspergillusgenome.org/>).

reconstruct the transcriptomic network that helps *A. niger* to adapt to abnormal morphologies and to secure the integrity of its cell wall.

A transcriptomic perspective on the morphogenetic network of *A. niger*

A central result of our comparative transcriptomics approach is the finding that several lipid molecules are likely involved in the maintenance of polar growth in *A. niger* (Fig. 7). The synthesis of important phospho- and sphingolipid molecules (phosphatidic acid, DAG, PIP2, inositolphosphates (IP), glycerophosphocholine, mannose-inositol-phosphoceramide (MIPC) and S1P seem to be modulated during apical branching ($\Delta racA$, *ramosa-1*) and apolar growth (*PglaA-racA^{G18V}*), as genes encoding respective synthetic or degrading enzymes showed differential expression in comparison to the wild-type (Tables 3, 4 and 6). Many of these molecules function as secondary messengers in eukaryotes (DAG, PA, IP, PIP2, S1P), others are essential components of fungal membranes (plasma membrane, organelles, lipid droplets), whereby sphingolipids (e.g. MIPC) and ergosterol are worth highlighting as they concentrate to form lipid rafts in plasma membranes which organize and regulate signaling cascades involved in polar growth control of *S. cerevisiae* (Wachtler and Balasubramanian 2006). Lipid rafts have been shown to form ordered subdomains of eukaryotic plasma membranes into which monomeric and trimeric G proteins associate in a dynamic and selective manner to organize signal transduction complexes (Moffett et al. 2000). It is therefore intriguing that expression of An01g07000, the ortholog of the ergosterol synthesizing enzyme Erg24p, is modulated in all three strains $\Delta racA$, *ramosa-1* and *PglaA-racA^{G18V}*, and being also among the cell wall stress responsive genes when *A. niger* is exposed to caspofungin or fenpropimorph (Meyer et al. 2007b). This suggests that ergosterol metabolism is of main importance for polarized growth and cell wall integrity in *A. niger*.

Unfortunately, data on fungal lipid signaling networks are sparse. So far, it is known that sphingolipids play a key role in pathogenicity in *Cryptococcus neoformans*, that the quorum sensing molecule farnesol is involved in mycelial growth, biofilm formation and

stress response of *Candida albicans*, that both sphingolipids and farnesol are important for maintaining cell wall integrity and virulence of *A. fumigatus* (for review see (Singh and Del Poeta 2010)) and that the activity of two ceramide synthases is important for the formation of a stable polarity axis in *A. nidulans* (Li et al. 2006). In *Schizosaccharomyces pombe*, MIPC was shown to be required for endocytosis of a plasma-membrane-localized transporter and for protein sorting into the vacuole (Nakase et al. 2010). As $\Delta racA$ is affected in endocytosis (see below) and the MIPC synthesizing enzyme Sur1p (An05g02310) is down-regulated as well might suggest that MIPC has a similar function in *A. niger*. Notably, the sphingolipid synthesizing protein inositol-phosphoryl ceramide synthase (Ipc1) plays a major role in both establishment and maintenance of cell polarity in *A. nidulans* by regulating actin dynamics (Cheng et al. 2003; Cheng et al. 2001). However, it is not known whether this is mediated by the sphingolipid inositol-phosphoryl ceramide (IPC) or by other products of the ceramide synthetic pathway such as DAG, MIPC or sphingosines. Anyhow, inhibition of sphingolipid synthesis in *A. nidulans* caused wider hyphal cells, abnormal branching and tip splitting and is not suppressible by the addition of sorbitol (Cheng et al. 2003; Cheng et al. 2001) - observations which also hold true for $\Delta racA$ and *ramosa-1* (Kwon et al. 2011; Meyer et al. 2009), suggesting that sphingolipid mediated control of hyphal cell polarity is not mediated by the CWI pathway in *Aspergillus*. Still, *S. cerevisiae* strains defective in CWI signaling (e.g. *pkc1* Δ , *mpk1* Δ) also exhibit severe defects in lipid metabolism, including accumulation of phosphatidylcholine, DAG, triacylglycerol, and free sterols as well as aberrant turnover of phosphatidylcholine, suggesting that CWI signaling and lipid homeostasis are nevertheless closely linked in fungi (Nunez et al. 2008).

A second important outcome of this study is that not only calcium signaling seems to be of utmost importance for morphological decisions in all three mutant strains $\Delta racA$, *ramosa-1* and *PglaA-racA*^{G18V}, but ion homeostasis in general (Fig. 7). Many ion transport proteins are differentially expressed in all three strains when compared to the wild-type situation including transport proteins for Na⁺, K⁺, Ca²⁺, Fe²⁺, Zn²⁺ and Co²⁺. Of special importance is An16g06300, a predicted Fe(II) transporter, homologous to the *S. cerevisiae* plasma membrane transporter Fet4p, whose transcriptional regulation is affected in all three strains. Fet4p is a low-affinity Fe(II) transporter also transporting Zn²⁺ and Co²⁺ and is under combinatorial control of iron (Atf1p transcriptional activator), zinc (Zap1p transcriptional factor) and oxygen (Rox1p repressor) (Waters and Eide 2002), being for example important for *S. cerevisiae* to tolerate alkaline pH (Serrano et al. 2004). It has been postulated that changes in the phospholipid composition govern the function of membrane-associated zinc transporters such as Fet4p (Carman and Han 2007). Vice versa, the

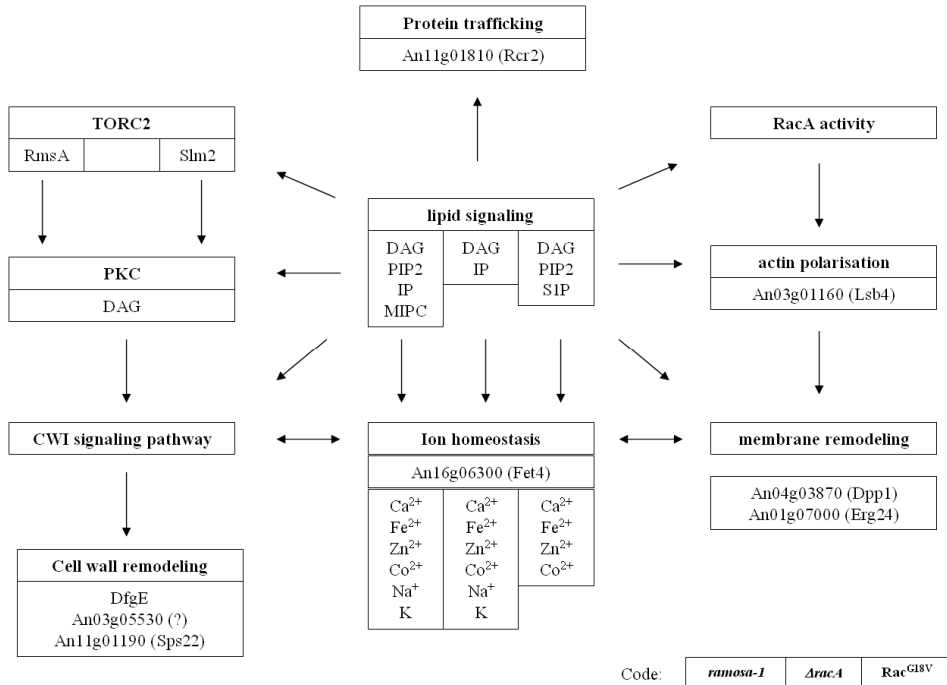


Fig. 7. A reconstructed model for the morphogenetic network of *A. niger* based on the transcriptomic fingerprints determined for the apical branching mutant *ramosa-1* (Meyer et al. 2009), the apical branching mutant *ΔracA* (this work) and the apolar growing mutant *PglaA-RacA^{G18V}* (this work). The model also rests on cell biological and phenotypic data obtained for all three strains (this work and (Meyer et al. 2009) as well as on literature data for conserved mechanisms from yeast to humans (see discussion for references). Indicated are signalling and metabolic processes, which showed transcriptional responses in all three strains, some deduced key players and the hypothetical connection of these processes.

transcriptional factor Zap1p controls not only expression of zinc-related transporters but also expression of the DAG pyrophosphate phosphatase Dpp1p (Carman and Han 2007). This is a very interesting observation in view of the fact that one predicted Dpp1p ortholog (An04g03870) shows differential expression in all three morphological mutant strains of *A. niger*, an analogy which might suggest that polarized growth of *A. niger* might be orchestrated by (phospho)lipid signaling which is somehow interconnected with zinc metabolism.

Finally, our transcriptomics comparison uncovered that endocytotic processes are likely to be involved in the morphogenetic network of *A. niger*. In all three strains, *ΔracA*, *ramosa-1* and *PglaA-racA^{G18V}*, expression of An03g01160, a predicted ortholog of the *S. cerevisiae* Lsb4p was modulated (Table 6, Fig. 7). Lsb4p is an actin-binding protein,

conserved from yeast to humans, binds to actin patches and promotes actin polymerization together with the WASP protein Lsb17 in an Arp2/3-independent pathway thereby mediating inward movement of vesicles during endocytosis (Robertson et al. 2009). Lsb4p is also a PIP binding protein due to a phosphoinositide-binding domain (SYLF), which is highly conserved from bacteria to humans. The human homolog of Lsb4p (SH3YL1) binds to PIP3 and couples the synthesis of PIP2 with endocytotic membrane remodeling, whereas Lsb4p binds directly to PIP2 (note that PIP3 is believed to be absent in yeast). Thus, Lsb4p homologs are predicted to couple PIP2 with actin polymerization to regulate actin and membrane dynamics involved in membrane ruffling during endocytosis (Hasegawa et al. 2011). Beside An03g01160 (Lsb4p ortholog), An17g01945 is worth highlighting in this context as well. An17g01945 encodes an ortholog of the amphysin-like lipid raft protein Rvs161p and is differentially expressed in both $\Delta racA$ and $PglaA-racA^{G18V}$. Rvs161p affects the membrane curvature in *S. cerevisiae* and mediates in conjunction with Rvs167 and PIP2 membrane scission at sites of endocytosis (Youn et al. 2010).

Taken together, the transcriptomic signature of the three morphological mutants predicts that the morphological changes are brought about the interconnection of several signaling and metabolic pathways. Remarkably, the responding gene set in $\Delta racA$ and *ramosa-1* seems to be, although substantially overlapping, oppositely regulated. One explanation might be that inactivation of RacA and TORC2 induces dichotomous branching in different manners. As the subcellular distribution of actin is different in both strains (the *ramosa-1* mutant shows scattered actin patches at hyphal tips, whereas actin is concentrated at hyphal apices in the $\Delta racA$ mutant) might suggest that different causes (loss of actin polarization / actin hyperpolarization) provoke different responding transcriptional changes, which, however, eventually result in the same phenotypic response, namely tip splitting. Similarly puzzling is the observation that the core set of 38 genes which are responsive in both $\Delta racA$ and $PglaA-racA^{G18V}$ respond in the same direction (Table 6), although they are associated with excessive polar growth (hyperbranching) in the $\Delta racA$ strain but with the absence of polar growth (tip swelling) in strain $PglaA-racA^{G18V}$. A plausible explanation might be that loss of polarity maintenance in both strains is connected with similar transcriptional changes controlling actin dynamics and vesicle flow, but that reestablishment of polar growth in the *racA* deletion strain requires genes which are not important for tip swelling in the $PglaA-racA^{G18V}$ strain.

Does a hyperbranching strain secrete more proteins?

In filamentous fungi, it is believed that protein secretion occurs at the hyphal tip. This holds true for glucoamylase (GLA), the most abundant secreted enzyme in *A. niger* (Gordon et al. 2000; Wösten et al. 1991). Another example is α -amylase, the major secretory protein of *A. oryzae* (Hayakawa et al. 2011). Hence, one might expect that a higher branching frequency would result in higher secretion yields. However, our study demonstrated that more tips in the $\Delta racA$ strain do not necessarily increase protein secretion; instead, protein yields were the same in both mutant and wild-type (Table 2). The most logical explanation is that the same amount of secretory vesicles is merely distributed to more tips in the $\Delta racA$ strain, resulting in less secretory vesicles per individual tip. The quantitative data obtained for the exocytotic marker GFP-SncA and the endocytotic marker AbpA-CFP and SlaB-YFP clearly demonstrate that fewer vesicles are transported to the apex of an individual tip (Fig. 3) and that endocytosis is slowed down as well – the endocytotic ring seems to be less well defined and the fluorescence intensity of both endocytotic markers is decreased (Fig. 4). This data is corroborated by the transcriptomic fingerprint of the $\Delta racA$ strain. The transcription of genes predicted to function in protein trafficking and actin localization is down-regulated as well as expression of genes governing phospholipid signaling and cell wall remodeling. Remarkably, biomass formation is the same in both $\Delta racA$ and wt. This suggests that the amount of secreted vesicles is adjusted in both strains just to ensure hyphal tip growth but that the capacity of a hyphal tip growing apparatus to accommodate vesicles is much higher (at least in $\Delta racA$). Hence, challenging the $\Delta racA$ strain to overexpress a certain protein of interest might increase the number of secretory vesicles thus resulting in higher secretion yields. We currently run respective experiments to test this hypothesis. In any case, the hyperbranching $\Delta racA$ mutant could already be of value for high-density cultivation during industrial processes: it forms a less shear stress-sensitive, compact macromorphology but does not form pellets. It thus exhibits improved rheological properties without any apparent disadvantages with respect to growth rate and physiology.

Conclusions

The transcriptomic signature of the three individual mutants $\Delta racA$, *ramosa-1* and *PglaA-racA^{G18V}* uncovered specific and overlapping responses to the morphological changes induced and suggests the participation as well as interconnectedness of several regulatory and metabolic pathways in these processes. The data obtained predict a role for different signaling pathways including phospholipid signaling, sphingolipid signaling, TORC2 signaling, calcium signaling and CWI signaling in the morphogenetic network of *A. niger*. These pathways likely induce different physiological adaptations including changes in

sterol, zinc and amino acid metabolism and changes in ion transport and protein trafficking. Central to the morphological flexibility of *A. niger* is the actin cytoskeleton whose dynamics can be precisely controlled in these mutants. Future attempts are necessary to address important issues which cannot be resolved by transcriptomics. For example, how is the lipid composition in apical and subapical regions of *A. niger* hyphae? Which morphogenetic proteins are also parts of the network whose expression is regulated post-transcriptionally and can thus not be detected by transcriptomics approaches? Where are they localized during (a)polar growth? What are the metabolic prerequisites to sustain fast polar growth coupled with high secretion rates? Clearly, a comprehensive understanding of the morphogenetic network of *A. niger* will require an integrated systems biology approach where transcriptomics analyses will be combined with proteomics, metabolomics and lipidomics approaches and linked with cell biological studies.

Material and Methods

Strains, culture conditions and molecular techniques

Aspergillus strains used in this study are given in Table 7. Strains were grown on minimal medium (MM) (Bennett and Lasure 1991) containing 1% (w v⁻¹) glucose and 0.1% (w v⁻¹) casamino acids or on complete medium (CM), containing 0.5% (w v⁻¹) yeast extract in addition to MM. When required, plates were supplemented with uridine (10 mM). Transformation of *A. niger* and fungal chromosomal DNA isolation was performed as described (Meyer et al. 2010b). All molecular techniques were carried out as described earlier (Sambrook and Russell 2001).

Bioreactor cultivation conditions

Maltose-limited batch cultivation was initiated by inoculation of 5 L (kg) ammonium based minimal medium with conidial suspension to give 10⁹ conidia L⁻¹. Maltose was sterilized separately from the MM and final concentration was 0.8% (w/v). Temperature of 30°C and pH 3 were kept constant, the latter by computer controlled addition of 2 M NaOH or 1 M HCl, respectively. Acidification of the culture broth was used as an indirect growth measurement (Iversen et al. 1994). Submerged cultivation was performed with 6.6 L BioFlo3000 bioreactors (New Brunswick Scientific, NJ, USA). A more detailed description of the fermentation medium and cultivation is given in (Jørgensen et al. 2010). Batch cultivation for *PglaA-RacA*^{G18V} or *PglaA-RacA* were run similarly as the maltose-limited batch cultivations of $\Delta racA$ cultures except that 0.75% xylose was used as an initial carbon

Table 7. Strains used in this work.

Strain	Relevant genotype	Source
N402	<i>cspA1</i> (derivative of ATCC9029)	(Bos et al. 1988)
AB4.1	<i>pyrG</i> ⁻	(van Hartingsveldt et al. 1987)
MA70.15	Δ <i>kusA pyrG</i> ⁻ (derivative of AB4.1)	(Meyer et al. 2007a)
MA80.1	Δ <i>kusA, \Delta</i> <i>racA::AopyrG</i>	(Kwon et al. 2011)
FG7	Δ <i>kusA pyrG</i> ⁺ <i>egfp::sncA</i> (derivative of MA70.15)	Kwon et al, submitted
MA1.8	<i>PglaA::racA</i> (derivative of AB4.1)	(Kwon et al. 2011)
MA60.15	<i>PglaA::racAG18V</i> (derivative of AB4.1)	(Kwon et al. 2011)
MK5.1	Δ <i>kusA, slaB::eyfp</i> (derivative of MA70.15)	This work
MK6.1	Δ <i>kusA, abpA::ecfp</i> (derivative of MA70.15)	This work
MK7.1	Δ <i>kusA, \Delta</i> <i>racA, slaB::eyfp</i> (derivative of MA80.1)	This work
MK8.1	Δ <i>kusA, \Delta</i> <i>racA, abpA::ecfp</i> (derivative of MA80.1)	This work

source instead of maltose. When the exponential growth phase was over (indicated by a sharp rise of the dissolved oxygen tension and the pH value), 0.75% maltose was added to induce expression of *PglaA-RacA*^{G18V} or *PglaA-RacA*, respectively. Samples for the analysis of morphological characteristics, biomass formation, protein yield and RNA were taken every hour.

Analysis of culture broth

Dry weight biomass concentration was determined by weighing lyophilized mycelium separated from a known mass of culture broth. Culture broth was filtered through GF/C glass microfiber filters (Whatman). The filtrate was collected and frozen for use in solute analyses. The mycelium was washed with demineralised water, rapidly frozen in liquid nitrogen and lyophilized. Glucose concentration was measured as previously described (Bergmeyer et al. 1974) with slight modifications: 250 mM triethanolamine (TEA) was used as buffer (pH 7.5). Extracellular protein concentration was determined using the Quick Start Bradford Protein Assay (Bio-Rad) using BSA as standard. The total organic carbon in the culture filtrate was measured with a Total Organic Carbon Analyzer (TOC-Vcsn; Shimadzu, Japan), using glucose as standard.

Microarray analysis

Total RNA extraction, RNA quality control, labeling, Affymetrix microarray chip hybridization and scanning were performed as previously described (Meyer et al. 2009). Background correction, normalization and probe summarization steps were performed according to the default setting of the robust multi-array analysis (RMA) package as

recently described (Nitsche et al. 2012b). Differential gene expression was evaluated by moderated t-statistics using the Limma package (Smyth 2004) with a threshold of the Benjamini and Hochberg False Discovery Rate (FDR) of 0.05 (Benjamini and Hochberg 1995). Fold change of gene expression from different samples was calculated from normalized expression values. Geometric means of the expression values as well as fold change for all strains and comparisons are summarized in Table S1 and S2 and have been deposited at the GEO repository (<http://www.ncbi.nlm.nih.gov/geo/info/linking.html>) under the accession number GSE42258. Transcriptomic data for the exponential growth phase of the reference strain N402 was published recently (Nitsche et al. 2012a).

Gene Ontology (GO) and enrichment analysis

Over-represented GO terms in sets of differentially expressed genes were determined by Fisher's exact test (Fisher 1922) as implemented in FetGOat (Nitsche et al. 2011) using a FDR of $q < 0.05$. An improved GO annotation for *A. niger* CBS513.88 was applied based on ontology mappings from *A.nidulans* FGSCA4 (Nitsche et al. 2011).

Construction of AbpA-CFP and SlaB-YFP expression cassettes

Standard PCR and cloning procedures were used for the generation of the constructs (Sambrook and Russell 2001). All PCR amplified DNA sequences and cloned fragments were confirmed by DNA sequencing (Macrogen). Primers used in this study are listed in Table S5. Correct integrations of constructs in *A. niger* were verified by Southern analysis (Sambrook and Russell 2001). The expression vectors, AbpA-CFP and SlaB-YFP were constructed using the fusion PCR approach as described previously (Meyer et al. 2008) with slight modifications. Plasmid pVM3-1 (Meyer et al. 2008) harboring the GA₅ peptide linker followed by the CFP, T_{trpC} and the selection marker *pyrG* from *A. oryzae* was used as starting point. A second T_{trpC} terminator sequence was generated by PCR and ligated via a *SalI* restriction site into pVM3-1 which would later allow looping out of the *pyrG* marker by FOA counter-selection (Meyer et al. 2010b). The resulting plasmid was named pMK3. For the fusion PCR, three separate fragments were amplified by PCR: the C-terminal part of *abpA* ORF (~1 kb), the module containing CFP-T_{trpC}-*AopyrG* (~3.5 kb) and the terminator region of *abpA* (~1 kb). Subsequently, the three individual fragments were fused together by a fusion PCR and the resulting amplicon (~5.6 kb) was cloned into pJET (Fermentas) to give plasmid pMK5. SlaB-YFP was also constructed in a similar way and the final plasmid was named pMK6.

Microscopy

Light microscopic pictures were captured using an Axioplan 2 (Zeiss) equipped with a DKC-5000 digital camera (Sony). For light and fluorescence images for SlaB-YFP and AbpA-CFP transformants, pictures were captured with 40x C-apochromatic objective on an inverted LSM5 microscope equipped with a laser scanning confocal system (Zeiss Observer). The observation conditions for the life-imaging of hyphae were described previously (Kwon et al. 2011). To determine branching frequencies, the lengths of hyphae and branches were measured and evaluated using the program Image J. For the quantification of GFP-SncA, AbpA-CFP and SlaB-YFP signals, a single section of individual hyphal tip was captured (n> 20).

Acknowledgements

This project was carried out within the research programme of the Kluyver Centre for Genomics of Industrial Fermentation which is part of the Netherlands Genomics Initiative / Netherlands Organization for Scientific Research.

Author Contributions

Conceived and designed the experiments: MJK TRJ AFJR VM. Performed the experiments: MJK BMN MA TRJ. Analyzed the data: MJK BMN TRJ VM. Contributed reagents/materials/analysis tools: BMN AFJR VM. Wrote the paper: MJK AFJR VM.

The transcriptomic fingerprint of glucoamylase over-expression in *Aspergillus niger*

Min Jin Kwon, Thomas R Jørgensen, Benjamin M Nitsche, Mark Arentshorst, Joohae Park, Arthur FJ Ram and Vera Meyer

BMC Genomics (2012),13, 701.

Abstract

Background: Filamentous fungi such as *Aspergillus niger* are well known for their exceptionally high capacity for secretion of proteins, organic acids and secondary metabolites and they are therefore used in biotechnology as versatile microbial production platforms. However, system-wide insights into their metabolic and secretory capacities are sparse and rational strain improvement approaches are therefore limited. In order to gain a genome-wide view on the transcriptional regulation of the protein secretory pathway of *A. niger*, we investigated the transcriptome of *A. niger* when it was forced to over-express the *glaA* gene (encoding glucoamylase, GlaA) and secrete GlaA to high level.

Results: An *A. niger* wild-type strain and a GlaA over-expressing strain, containing multiple copies of the *glaA* gene, were cultivated under maltose-limited chemostat conditions (specific growth rate 0.1 h^{-1}). Elevated *glaA* mRNA and extracellular GlaA levels in the over-expressing strain were accompanied by elevated transcript levels from 772 genes and lowered transcript levels from 815 genes when compared to the wild-type strain. Using GO term enrichment analysis, four higher-order categories were identified in the up-regulated gene set: i) endoplasmic reticulum (ER) membrane translocation, ii) protein glycosylation, iii) vesicle transport and iv) ion homeostasis. Among these, about 130 genes had predicted functions for the passage of proteins through the ER and those genes included target genes of the HacA transcription factor that mediates the unfolded protein response (UPR), e.g. *bipA*, *clxA*, *prpA*, *tigA* and *pdiA*.

In order to identify those genes that are important for high-level secretion of proteins by *A. niger*, we compared the transcriptome of the GlaA overexpression strain of *A. niger* with six other relevant transcriptomes of *A. niger*. Overall, 40 genes were found to have either elevated (from 36 genes) or lowered (from 4 genes) transcript levels under all conditions that were examined, thus defining the core set of genes important for ensuring high protein traffic through the secretory pathway.

Conclusion: We have defined the *A. niger* genes that respond to elevated secretion of GlaA and, furthermore, we have defined a core set of genes that appear to be involved more generally in the intensified traffic of proteins through the secretory pathway of *A. niger*. The consistent up-regulation of a gene encoding the acetyl-coenzyme A transporter suggests a possible role for transient acetylation to ensure correct folding of secreted proteins.

Introduction

Due to its well annotated genome sequence, newly established gene transfer systems, and the availability of high-quality tools for obtaining and evaluating transcriptomic and proteomic data, *Aspergillus niger* has become a model fungus for industrially exploited filamentous fungi (Meyer 2008; Meyer et al. 2007a; Meyer et al. 2011b; Pel et al. 2007). Its impressive natural capacity to secrete high amounts of hydrolytic proteins into the environment combined with its ability to synthesize and secrete various organic acids makes it highly suitable for the production of various food ingredients, pharmaceuticals and industrial enzymes (Fleissner and Dersch 2010; Meyer 2008; Meyer et al. 2011b). As it is also capable of efficiently degrading plant-derived polysaccharides such as starch, cellulose, hemicellulose, pectin and inulin, the biotechnological importance of *A. niger* will probably rise even more in the near future. For example, *A. niger*-derived (hemi)cellulases might be used to improve the efficiency of the saccharification process of second-generation feedstock used for bioethanol production (de Souza et al. 2011; Pel et al. 2007).

To analyze and eventually control the secretory capabilities of *A. niger*, several attempts have been undertaken to identify the key players and regulatory mechanisms involved in protein secretion. For example, galacturonic acid, xylose and maltose were shown to induce expression of secretory proteins, including pectinolytic, (hemi)cellulolytic and glucan-hydrolyzing enzymes, respectively, whereas sorbitol acts as a repressing carbon source (Adav et al. 2010; Braaksma et al. 2010; de Oliveira et al. 2011; Lu et al. 2010). Xylose is the main inducer of XlnR, the master transcription factor that regulates expression of all major enzymes involved in the degradation of (hemi)cellulose (de Oliveira et al. 2011; Lu et al. 2010; Mach-Aigner et al. 2012). Among those, endoxylanase (XynB) and ferulic acid esterase (FaeA) are the most abundant, secreted proteins of *A. niger* (Lu et al. 2010). When starch or maltose are used as carbon source, the synthesis of amylolytic enzymes is induced, a step that is mediated by the transcription factor AmyR. The most abundant enzyme secreted under these conditions is a glucan 1,4- α -glucosidase (glucoamylase, GluA), which is an exo-enzyme that releases glucose from the non-reducing end of starch or maltose and accounts for more than 50% of the extracellular proteome (Lu et al. 2010). Induction of extracellular hydrolytic enzymes is thus mainly regulated at the transcriptional level in *A. niger*, and either repressed by carbon catabolite repression via CreA (Yuan et al. 2006) or activated by AmyR or XlnR depending on the presence of maltose or xylose, respectively (Tsukagoshi et al. 2001).

A. niger proteins and enzymes destined for secretion into the culture medium follow the secretory pathway. The journey of secretory proteins starts with protein translocation into the lumen of the endoplasmic reticulum (ER) via a translocon that forms a channel

through the ER membrane (Romisch 1999). In the ER lumen, several ER-resident chaperones and foldases, including the binding protein (BipA), protein disulfide isomerase (PdiA) and calnexin (ClxA), assist secretory proteins in proper folding (Maattanen et al. 2010). Most secretory proteins become glycosylated in the ER, both through the attachment of a conserved, pre-assembled oligosaccharide to specific asparagine residues (*N*-glycosylation) and by the initiation of *O*-glycosylation of serine and threonine residues. After proper folding and glycosylation, secretory proteins are packed into COPII-coated vesicles and transported to the Golgi complex, where protein glycosylation is completed, and subsequently through another vesicle-mediated process delivered to the cell surface where the vesicles release their cargo into the periplasmic region. High protein flux through the ER or expression of heterologous proteins can result in the accumulation of misfolded proteins. This misfolding, however, is recognized by a quality control system known as ER-associated degradation (ERAD). The aim of ERAD is to direct misfolded proteins to the cytosol where they become degraded by the proteasome. In addition, another cellular protein quality system, the unfolded protein response (UPR), is induced, which aims at proper refolding of misfolded proteins via induced expression of chaperones and foldases (Fleissner and Dersch 2010; Geysens et al. 2009). For this purpose, the UPR transcription factor HacA becomes activated via splicing of an unconventional 20-nt intron out of the *hacA* mRNA. This subsequently facilitates translation of *hacA* mRNA and formation of HacA, which in turn induces transcription of a number of UPR target genes including *bipA*, which encodes the major ER chaperone protein and *pdiA*, which encodes for protein disulfide isomerase (Guillemette et al. 2007; Mulder et al. 2004). Hence, both ERAD and UPR are crucial for effective functioning of the secretory pathway - not only in filamentous fungi but also in yeasts and mammals (Kaufman 1999; Saloheimo and Pakula 2012; Saloheimo et al. 2003; Yoshida et al. 2001).

Interestingly, the UPR can be viewed as a general response of *A. niger*, which becomes activated when the secretion machinery becomes challenged by metabolic changes or ER stress conditions. For example, transcript levels of UPR genes become strongly enhanced, when *A. niger* is exposed to the reducing compound dithiothreitol (DTT), which blocks the formation of disulfide bridges, or to tunicamycin, which inhibits *N*-glycosylation, especially when forced to express heterologous proteins or when cultivated in carbon sources, which differentially induce expression and secretion of homologous proteins (Carvalho et al. 2011a; Guillemette et al. 2007; Jørgensen et al. 2009). These observations suggest that the UPR functions act as a homeostatic control mechanism that allows *A. niger* to flexibly adapt its protein secretion capacity to change in environmental conditions.

In this study, we investigated the transcriptomic fingerprint of *A. niger* when forced to overexpress and secrete a specific hydrolytic enzyme. We chose glucoamylase (GlaA) as a

model enzyme, because it is a naturally highly abundant and secreted enzyme used in the food industry (Kumar and Satyanarayana 2009). For comparison, we used two strains, a wild-type strain expressing a single copy of the *glaA* gene, and a mutant strain expressing multiple copies of *glaA*. In order to reduce the number of conflicting variables, such as changes in growth rates and fluctuations in environmental conditions, maltose-limited chemostat cultures were used. Maltose was selected as carbon source to transcriptionally induce expression of the *glaA* gene. Physiological and transcriptomic data were collected from both wild-type and overexpressing strains and analyzed to identify the *glaA*-specific overexpression transcriptome. Finally, we compared these global transcriptional changes with previously published transcriptomic data related to secretion stress in *A. niger*. This analysis allowed us to distinguish condition-specific responses from general transcriptomic responses of *A. niger* that are important to overcome different triggers of secretion stress. We could identify a core set of 40 genes whose expression is key to ensure high protein fluxes through the secretory route of *A. niger*, independently of the cause of the secretion stress.

Results and Discussion

Growth physiology of maltose-limited chemostat cultures of *A. niger*

In order to identify the transcriptomic adaptations of *A. niger* to forced overproduction of GlaA, we compared the transcriptomes of chemostat-grown cultures of strain B36 (overproducing strain) and wild-type strain N402 (reference strain). Strain B36 was selected as GlaA overproducer, because it is reported to contain multiple copies of the *glaA* gene at chromosome V (Verdoes et al. 1993; Verdoes et al. 1994b).

Maltose-limited chemostat cultures were used to induce expression of the *glaA* gene, to control the specific growth rate and to obtain highly reproducible data due to well-defined steady state conditions. Initial chemostat experiments were conducted using three different dilution rates ($D = 0.05, 0.1$ and 0.15 h^{-1}); however, steady state conditions for both strains were only reached at $D = 0.1 \text{ h}^{-1}$. At a higher dilution rate ($D = 0.15 \text{ h}^{-1}$), N402 reached a steady state, but the B36 strain was washed out before reaching a steady state. Although the morphology of the N402 strain at the lowest dilution rate ($D = 0.05 \text{ h}^{-1}$) was similar to the higher dilution rates, and no sign of mycelial aggregation was apparent (data not shown), N402 was not able to reach a steady state at this dilution rate. Maltose-limited chemostat cultures were therefore run in triplicate at $D = 0.1 \text{ h}^{-1}$ for both strains. The cultures were highly reproducible and gave rise to homogenous cultures of dispersed mycelial

morphologies (Fig. 1, Table 1 and data not shown). The initial batch cultivation (duration about 30 h) was followed by approximately 50 h of continuous cultivation. After four volume changes ($4 \times D^{-1}$), the cultures reached a steady state as reflected by a constant alkali addition rate and constant CO_2 , O_2 and biomass concentrations (Fig. 1 and data not shown). Biomass concentrations for both strains stabilized at about 4 g kg^{-1} with a small relative standard deviation (RSD) (approx. 0.002 for N402 and 0.02 for B36). In both strains, the respiratory quotient (RQ) was lower than 1, probably due to high production of organic acids in parallel to GlaA secretion. Notably, the RQ value calculated for B36 cultures was slightly but significantly lower than the RQ value obtained for N402 cultures (Table 1), suggesting that protein and acid production is somewhat higher in B36 compared to N402. In agreement, the carbon concentration in culture filtrates obtained from steady state samples was also higher in B36 compared to N402 (data not shown) and the specific productivity of extracellular protein ($q_{\text{protein-EC}}$) was five- to six-fold higher in B36 than N402, demonstrating that B36 indeed secretes more protein than the wild-type strain.

Protein secretion and glucoamylase production during steady state

The GlaA overproducer strain B36 was previously estimated to contain about 80 copies of the *glaA* gene as inferred from Southern analysis (Verdoes et al. 1993). As multiple gene copies can cause frequent recombination in *A. niger* resulting in genetic instability and loss of *glaA* copies (Verdoes et al. 1994b), we decided to re-determine the number of *glaA* copies present in B36 using quantitative real time PCR (qPCR). As summarized in Table 2,

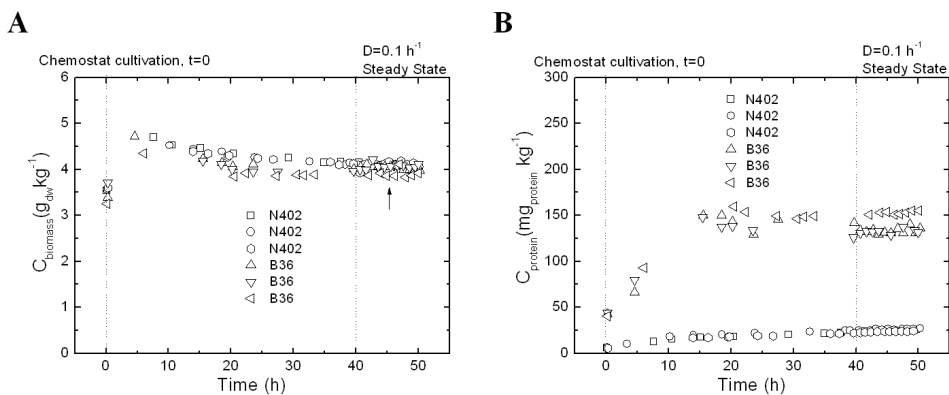


Fig. 1. Growth profiles (A) and extracellular protein production (B) of N402 and B36. The growth curves presented are based on (A) dry-weight biomass concentration and on (B) total protein concentration in culture filtrates. An arrow indicates RNA sampling for transcriptomics. All six independent cultures are shown.

Table 1. Physiology of N402 and B36 in chemostat cultures.

	N402	B36
C_{biomass} ($\text{g}_{\text{DW}} \text{kg}^{-1}$)	4.09 ± 0.01	4.01 ± 0.09
$Y_{x/s}$ ($\text{g}_{\text{DW}} \text{g}_{\text{maltose}}^{-1}$)	0.49 ± 0.02	0.47 ± 0.01
$Y_{x/c}$ ($\text{g}_{\text{DW}} \text{g}_{\text{carbon}}^{-1}$)	1.22 ± 0.05	1.17 ± 0.03
q_{CO_2} ($\text{mmol g}^{-1}\text{h}^{-1}$)	2.11 ± 0.05	2.05 ± 0.07
q_{O_2} ($\text{mmol g}^{-1}\text{h}^{-1}$)	2.38 ± 0.06	2.51 ± 0.14
RQ	0.88 ± 0.03	0.82 ± 0.03
$q_{\text{protein-EC}}$ ($\text{mg g}^{-1}\text{h}^{-1}$)	0.60 ± 0.03	3.49 ± 0.37
C-recovery (%)	92 ± 0.8	89 ± 0.3

Steady state results of maltose-limited chemostat cultures. Mean values \pm standard deviations are given for N402 and B36 from triplicate independent steady-state cultures. Bold letters indicate significant differences based on a two tailed t-test ($p < 0.001$). C_{biomass} , dry weight of biomass concentration; $Y_{x/s}$ and $Y_{x/c}$, growth yield on substrate and carbon; q_{CO_2} and q_{O_2} , specific carbon dioxide evolution rate and oxygen consumption rate; RQ, respiratory quotient; $q_{\text{protein-EC}}$, specific extracellular protein production rate; C-recovery, carbon recovery.

B36 contains about 32 *glaA* gene copies based on the fact that N402 contains only a single copy of *glaA* (Pel et al. 2007). We also determined *glaA* mRNA levels by qPCR and observed that *glaA* transcript levels in B36 were about seven times higher compared to N402. Consistent with this observation, under steady state conditions extracellular GluA production in B36 was about seven- to eight-fold higher than in N402 as estimated by Western analysis and measuring glucoamylase activity (Table 2). These data confirm previous observations that the amount of GluA produced correlates well with the amount of *glaA* mRNA but is not proportional to the number of *glaA* gene copies, a well-known phenomenon in filamentous fungi, where protein overproduction is often limited at the transcriptional level (Tsukagoshi et al. 2001; Verdoes et al. 1994b). It should be noted, however, that the increased glucoamylase production in the B36 strain is still significantly lower compared to industrial strains which produce glucoamylase up to 30 gram/liter (Finkelstein et al. 1989).

The GluA-overexpression transcriptome

RNA samples for microarray analysis were taken from triplicate steady-state cultures of both strains. The average RSD of all genes expressed was about 0.06, indicating high reproducibility of all six chemostat cultures and transcript profiles. The expression of 1,587 genes out of 14,165 *A. niger* genes was changed: 772 displayed increased expression levels in the strain B36, and 815 genes were down-regulated in B36 (significance: FDR, q value < 0.005). Although the majority of differentially expressed genes (1,280 genes) showed fold-

Table 2. Glucoamylase assessments in N402 (wild-type strain) and B36 (overexpressing strain).

	N402	B36
glucoamylase gene copy number ^a	1	32 ± 5
glucoamylase transcripts level ^a	1	6.9 ± 0.9
glucoamylase protein detection (g ⁻¹) ^b	1	8.3 ± 1.8
glucoamylase activity (U g ⁻¹) ^c	154 ± 68	1057 ± 398

Glucoamylase was assessed using steady-state samples. Mean values ± standard deviations for N402 and B36 were calculated from triplicate measurements of respective triplicate steady-state samples. **a:** Glucoamylase gene copy number and relative glucoamylase transcripts level were assessed by qPCR using genomic DNA and cDNA as templates. **b:** Western blot analysis of glucoamylase protein. Culture filtrate samples corrected for equal amounts of biomass were loaded onto SDS-PAGE. The amount of glucoamylase protein was represented as relative values based on N402. **c:** Glucoamylase activity was determined by measuring liberated glucose from starch.

changes in gene expression <2, these values are considered to be significant in view of the identical culture conditions used, the identical specific growth rates of both strains during steady state conditions, and the stringent statistical analysis of the data. A comprehensive list of all differentially expressed genes is depicted in Additional file 1.

An enrichment analysis was performed to identify gene ontology (GO) terms which were over-represented in the differentially expressed gene set. We used the recently published improved GO annotation tool for *A. niger* (Fisher's exact test Gene Ontology annotation tool, FetGOat (Nitsche et al. 2011)), an open source tool accessible at <http://www.broadinstitute.org/fetgoat/index.html>. GO terms (up- or down-regulated) with FDR values < 0.05 were defined as over-represented. Overall, 129 enriched GO terms were identified among the differentially expressed gene set, 54 of which belonged to 'biological processes' (BP), 63 to 'cellular components' (CC) and 12 to 'molecular functions' (MF). The corresponding network maps and gene lists are depicted in the Additional file 2 and 3.

Predicted up- and down-regulated biological processes inferred from the GlaA-overexpression transcriptome

In order to deduce biological information out of the GO term enrichment analysis, we focused on the BP gene list and removed redundant and less detailed annotations. Among the remaining GO terms in the up-regulated gene set, the following four higher-order categories were identified: i) translocation, ii) protein glycosylation, iii) vesicle transport

and iv) ion homeostasis (see Additional file 4). The translocation category included GO terms such as ‘posttranslational protein targeting to membrane’, ‘SRP-dependent co-translational protein targeting to membrane’, ‘translocation’ and ‘protein targeting to ER’. The protein glycosylation category included the GO terms ‘related to glycosylation’, ‘protein N-linked glycosylation’, ‘oligosaccharide biosynthetic process’, ‘dolichol-linked oligosaccharide biosynthetic process’ and ‘oligosaccharide-lipid intermediate biosynthetic process’. The vesicle transport category included the GO terms ‘vesicle-mediated transport’, ‘COPII-coated vesicle budding’, ‘membrane budding’, ‘vesicle organization’, ‘vesicle coating’, ‘vesicle targeting (rough ER to cis-Golgi)’, ‘COPII vesicle coating’ and ‘retrograde vesicle-mediated transport (Golgi to ER)’. The last category, ion homeostasis, contained GO terms involved in iron, calcium and zinc homeostasis (e.g. ‘iron homeostasis’, ‘inorganic cation homeostasis’, ‘cellular response to iron starvation’ and ‘ion transport’, see Additional file 4).

As three out of the four major categories were related to the secretory pathway, the corresponding genes lists were examined in more detail. The expression of at least 130 predicted secretory pathway genes were changed in the *GlaA*-overexpressing strain B36 (Table 3). Importantly, this set of genes is causatively linked to *GlaA* overexpression and does not depend on the growth rate or the carbon source, because both strains were in steady state at the same specific growth rate in maltose-limited chemostat cultures. Only 16 of the 130 genes were down-regulated, indicating that the capacity of the protein secretion machinery is increased compared to the wild-type situation. Among the secretory pathway-related genes, the majority of the induced genes belonged to ER-related processes, including translocation into the ER, protein folding, glycosylation, ERAD, UPR, COPI- and COPII-mediated transport processes (Table 3). Notably, the gene with the most significantly increased transcript level in B36 was the *bipA* gene (FDR, 1.1×10^{-7}), which is under transcriptional control of HacA (Mulder et al. 2004), and encodes the main chaperone in the ER and is thus important for protein overproduction in *A. niger* (van Gemeren et al. 1997). The increased expression of *bipA* gene in the B36 strain was previously reported by Northern blot analysis in a shake flask culture (Punt et al. 1998). In agreement, other important HacA-dependent ER chaperones and foldases such as *clxA*, *prpA*, *tigA* and *pdiA* (Table 3) were also significantly higher expressed in B36 (Mulder et al. 2004).

As up-regulation of these genes pointed towards slow or aberrant folding of *GlaA* and thus induction of UPR in strain B36, we tested whether the central activation mechanism of appropriate and sufficient for *A. niger*, because strain B36 is better adapted to grow on starch compared to the wild-type strain. Interestingly, starch- and maltose-responsive genes such as the transcription factor AmyR and AmyR-dependent hydrolase genes (Yuan et al. 2008b) are down regulated in B36 except *glaA* (Table 4). As previously suggested, a possible explanation for the reduced expression could be the titration of the AmyR

Table 3. Differential expression of genes encoding secretory pathway related proteins.

DSM code	DSM annotation	FC B36/N402	P	FDR
Protein folding				
An02g14800*	protein disulfide isomerase A <i>pdiA</i> - <i>Aspergillus niger</i>	1.72	5.98E-08	3.43E-06
An18g02020*	disulfide isomerase <i>tigA</i> - <i>Aspergillus niger</i>	1.89	1.61E-08	1.17E-06
An01g04600*	PDI related protein A <i>prpA</i> - <i>Aspergillus niger</i>	2.08	2.21E-09	2.40E-07
An16g07620*	strong similarity to endoplasmatic reticulum oxidising protein Ero1 - <i>Saccharomyces cerevisiae</i>	1.97	1.02E-08	8.15E-07
An18g04260*	similarity to secreted protein HNTME13 from patent WO9839446-A2 - <i>Homo sapiens</i>	2.46	1.06E-09	1.28E-07
An18g06470*	strong similarity to DnaJ-like protein MTJ1 - <i>Mus musculus</i>	1.48	1.34E-06	3.70E-05
An05g00880*	strong similarity to dnaJ protein homolog Scj1 - <i>Saccharomyces cerevisiae</i>	1.79	1.02E-07	5.04E-06
An01g08420*	strong similarity to calcium-binding protein precursor clx1p - <i>Schizosaccharomyces pombe</i>	2.42	8.96E-10	1.13E-07
An04g02020*	strong similarity to cyclophilin cypB - <i>Aspergillus nidulans</i>	1.69	1.19E-07	5.60E-06
An01g06670*	strong similarity to peptidyl-prolyl isomerase FKBP-21 - <i>Neurospora crassa</i>	1.66	4.71E-07	1.57E-05
An11g04180*	dnaK-type molecular chaperone bipA - <i>Aspergillus niger</i>	2.32	8.63E-10	1.11E-07
An01g13220*	strong similarity to 150 kDa oxygen regulated protein ORP150 - <i>Rattus norvegicus</i>	2.26	1.34E-09	1.58E-07
Signal recognition/cleavage				
An04g06890	similarity to 72-kD protein of the signal recognition particle SRP72 - <i>Canis lupus</i>	1.33	1.14E-04	1.37E-03
An15g06470*	similarity to signal sequence receptor alpha chain - <i>Canis lupus</i>	1.86	4.49E-08	2.72E-06
An01g00560*	strong similarity to signal peptidase subunit Sec11 - <i>Saccharomyces cerevisiae</i>	1.84	5.70E-07	1.84E-05
An16g07390*	strong similarity to endoplasmatic reticulum signal peptidase subunit Spc2 - <i>Saccharomyces cerevisiae</i>	1.90	7.99E-09	6.74E-07
An09g05420*	similarity to signal peptidase subunit Spc3 - <i>Saccharomyces cerevisiae</i>	1.99	6.90E-09	6.03E-07
Translocation into ER				
An03g04340*	strong similarity to ER membrane translocation facilitator Sec61 - <i>Yarrowia lipolytica</i>	1.68	9.76E-08	4.90E-06
An01g03820	strong similarity to ER protein-translocation complex subunit Sbh2 - <i>Saccharomyces cerevisiae</i>	1.62	2.60E-06	6.33E-05
An01g11630*	strong similarity to translocation complex component Sss1 - <i>Saccharomyces cerevisiae</i>	1.71	1.88E-07	8.11E-06
An02g01510*	strong similarity to component of the endoplasmic reticulum protein translocation machinery Sec62 - <i>Saccharomyces cerevisiae</i>	1.57	7.50E-06	1.49E-04
An01g13070*	strong similarity to signal recognition particle receptor Sec63 - <i>Saccharomyces cerevisiae</i>	2.02	2.17E-08	1.47E-06
An16g08830*	strong similarity to component of ER protein-translocation subcomplex Sec71 from patent WO9949028-A1 - <i>Saccharomyces cerevisiae</i>	1.80	3.47E-08	2.17E-06
An15g01670	strong similarity to signal sequence receptor alpha subunit SRP101 - <i>Yarrowia lipolytica</i>	1.29	1.14E-04	1.37E-03
An05g00140*	similarity to signal recognition particle receptor beta chain Srp102 - <i>Saccharomyces cerevisiae</i>	1.39	2.57E-05	4.16E-04
Glycosylation				
An02g07650	strong similarity to phosphoglucomutase pgmB - <i>Aspergillus nidulans</i>	0.80	5.29E-04	4.81E-03
An03g05940*	strong similarity to glutamine-fructose-6-phosphate transaminase Gfa1 - <i>Saccharomyces cerevisiae</i>	0.66	2.20E-06	5.58E-05

Table 3. Cont.

DSM code	DSM annotation	FC B36/N402	P	FDR
An04g04990*	strong similarity to mannose-1-phosphate guanyltransferase MPG1 - <i>Trichoderma reesei</i>	1.46	1.44E-05	2.57E-04
An11g02380*	strong similarity to GTP:alpha-D-mannose-1-phosphate guanylyltransferase MPG1 - <i>Hypocrea jecorina</i>	1.35	5.47E-05	7.67E-04
An02g08660	strong similarity to hypothetical protein H04M03.4 - <i>Caenorhabditis elegans</i>	1.25	2.90E-04	2.91E-03
An03g06940*	strong similarity to UPD-GlcNAc transporter MNN2-2 - <i>Kluyveromyces lactis</i>	1.35	2.72E-05	4.38E-04
An02g14560*	oligosaccharyltransferase alpha subunit ostA - <i>Aspergillus niger</i>	2.05	2.27E-09	2.40E-07
An07g04190*	strong similarity to dolichyl-diphosphooligosaccharide--protein glycosyltransferase 48kD chain DDOST - <i>Gallus gallus</i>	1.69	1.03E-07	5.04E-06
An18g03920*	strong similarity to defender against apoptotic cell death DAD1 - <i>Homo sapiens</i>	2.04	2.49E-09	2.56E-07
An02g14930*	strong similarity to dolichyl-diphosphooligosaccharide-protein glycotransferase gamma chain Ost3 - <i>Saccharomyces cerevisiae</i>	1.47	1.51E-06	4.08E-05
An16g08570*	strong similarity to translation initiation factor 3 47 kDa subunit stt3p - <i>Schizosaccharomyces pombe</i>	1.78	2.74E-07	1.07E-05
An16g04330*	strong similarity to mannose phospho-dolichol synthase dpm1 - <i>Hypocrea jecorina</i>	1.63	2.72E-07	1.07E-05
An01g05200*	strong similarity to DPM2 - <i>Mus musculus</i>	1.43	4.84E-05	6.98E-04
An03g04410*	strong similarity to UDP-glucose:dolichyl-phosphate glucosyltransferase Alg5 - <i>Saccharomyces cerevisiae</i>	1.78	3.47E-07	1.26E-05
An02g03240*	strong similarity to UDP-N-acetylglucosamine--dolichyl-phosphate N-acetylglucosaminophosphotransferase Alg7 - <i>Saccharomyces cerevisiae</i>	1.92	1.76E-08	1.24E-06
An06g01100*	strong similarity to mannosyltransferase Alg1 - <i>Saccharomyces cerevisiae</i>	1.27	1.50E-04	1.70E-03
An14g05910*	strong similarity to mannosyltransferase Alg2 - <i>Saccharomyces cerevisiae</i>	1.93	2.28E-08	1.53E-06
An18g05910*	strong similarity to hypothetical glycosyl transferase SPCC330.08 - <i>Schizosaccharomyces pombe</i>	1.49	7.14E-05	9.49E-04
An02g14940*	strong similarity to human transmembrane protein HTMPN-23 from patent WO9961471-A2 - <i>Homo sapiens</i>	1.49	2.62E-06	6.38E-05
An04g03130	strong similarity to mannosylation protein Lec35 - <i>Cricetulus griseus</i> [putative sequencing error]	1.56	4.25E-07	1.46E-05
An18g02360*	strong similarity to Dol-P-Man dependent alpha(1-3) mannosyltransferase Alg3 - <i>Saccharomyces cerevisiae</i>	1.92	1.74E-08	1.24E-06
An08g07020*	similarity to mannosyl transferase Alg9 - <i>Saccharomyces cerevisiae</i>	1.48	7.80E-06	1.53E-04
An01g08460*	strong similarity to the mannosyltransferase Alg12 - <i>Saccharomyces cerevisiae</i>	1.37	4.69E-04	4.36E-03
An02g12630*	strong similarity to glucosyltransferase Alg6 - <i>Saccharomyces cerevisiae</i>	1.37	1.35E-05	2.44E-04
An04g08820*	strong similarity to glucosyltransferase Alg8 - <i>Saccharomyces cerevisiae</i>	1.24	3.24E-04	3.22E-03
An02g02980*	strong similarity to protein influencing Itr1 expression Die2 - <i>Saccharomyces cerevisiae</i>	1.42	4.53E-05	6.58E-04
An15g01420*	strong similarity to glucosidase I Cwh41 - <i>Saccharomyces cerevisiae</i>	1.81	2.90E-08	1.84E-06
An18g05620	strong similarity to glucosidase II alpha subunit AAF66685.1 - <i>Homo sapiens</i>	0.80	4.70E-04	4.37E-03
An01g10930*	strong similarity to enzyme with sugar transferase activity from patent JP11009276-A - <i>Acremonium sp.</i>	0.45	2.27E-09	2.40E-07
An04g06920*	extracellular alpha-glucosidase agIU - <i>Aspergillus niger</i>	0.60	7.55E-08	4.07E-06

Table 3. Cont.

DSM code	DSM annotation	FC B36/N402	P	FDR
An09g03300	strong similarity to alpha-xylosidase XylS - <i>Sulfolobus solfataricus</i>	0.80	4.19E-04	3.98E-03
An09g05880*	strong similarity to alpha-glucosidase ModA - <i>Dictyostelium discoideum</i>	1.75	4.77E-08	2.86E-06
An13g00620*	strong similarity to 80K protein H precursor G19P1 - <i>Homo sapiens</i>	1.53	1.24E-06	3.47E-05
An07g06430*	strong similarity to glycoprotein glucosyltransferase gpt1p - <i>Schizosaccharomyces pombe</i>	1.64	3.96E-07	1.39E-05
An01g12550	strong similarity to mannosyl-oligosaccharide 1,2-alpha-mannosidase msdS - <i>Aspergillus saitoi</i>	0.32	2.29E-11	8.76E-09
An06g01510	strong similarity to class I alpha-mannosidase AAB62720.1 - <i>Spodoptera frugiperda</i>	0.74	4.29E-05	6.31E-04
An12g00340*	similarity to alpha 1,2-mannosidase IB - <i>Homo sapiens</i>	1.54	7.61E-06	1.50E-04
An05g01750	strong similarity to alpha-1,6-mannosyltransferase Hoc1 - <i>Saccharomyces cerevisiae</i>	0.52	1.04E-08	8.30E-07
An11g07490	similarity to alpha-1,6-mannosyltransferase Hoc1 - <i>Saccharomyces cerevisiae</i>	0.66	8.04E-07	2.46E-05
An15g03330	strong similarity to galactosyltransferase Bed1 - <i>Saccharomyces cerevisiae</i>	1.42	9.62E-05	1.20E-03
An11g09890*	strong similarity to mannosyltransferase 1 PMT1 - <i>Candida albicans</i>	1.36	1.27E-04	1.49E-03
An07g10350*	protein O-mannosyl transferase pmtA - <i>Aspergillus niger</i>	1.50	4.45E-06	9.69E-05
An16g08490*	strong similarity to dolichyl-phosphate-D-mannose--protein O-mannosyltransferase Pmt4 - <i>Saccharomyces cerevisiae</i>	1.49	1.89E-06	4.90E-05
An15g04810	similarity to alpha-1,3-mannosyltransferase Mnt2 - <i>Saccharomyces cerevisiae</i>	0.75	2.96E-05	4.66E-04
An02g11720	strong similarity to alpha-mannosidase msd2 - <i>Aspergillus nidulans</i>	0.71	1.64E-05	2.85E-04
An01g06500	strong similarity to filamentous growth protein Dfg5 - <i>Saccharomyces cerevisiae</i>	0.58	1.44E-05	2.56E-04
An02g02660	strong similarity to hypothetical protein Dcw1 - <i>Saccharomyces cerevisiae</i>	0.78	2.74E-04	2.79E-03
An11g01240*	similarity to filamentous growth protein Dfg5 - <i>Saccharomyces cerevisiae</i>	2.17	1.48E-08	1.10E-06
Protein misfolding (UPR and ERAD associated degradation)				
An08g00830	strong similarity to protein phosphatase type 2C Ptc2 - <i>Saccharomyces cerevisiae</i>	1.31	5.07E-04	4.65E-03
An11g11250*	strong similarity to interferon-induced double-stranded RNA-activated protein kinase inhibitor P58 - <i>Homo sapiens</i>	1.80	2.58E-07	1.03E-05
An01g14100*	weak similarity to stress protein Herp - <i>Mus musculus</i>	1.61	1.12E-06	3.21E-05
An03g04340*	strong similarity to ER membrane translocation facilitator Sec61 - <i>Yarrowia lipolytica</i>	1.68	9.76E-08	4.9E-06
An04g00360*	strong similarity to transport vesicle formation protein Sec13 - <i>Saccharomyces cerevisiae</i>	1.84	1.28E-08	9.9E-07
An15g00640*	strong similarity to hypothetical protein GABA-A receptor epsilon subunit - <i>Caenorhabditis elegans</i>	2.03	6.20E-08	3.53E-06
An16g07970*	similarity to autocrine motility factor receptor Amfr - <i>Mus musculus</i>	1.60	1.09E-05	2.02E-04
An12g00340*	similarity to alpha 1,2-mannosidase IB - <i>Homo sapiens</i>	1.54	7.61E-06	1.50E-04
An15g01420*	strong similarity to glucosidase I Cwh41 - <i>Saccharomyces cerevisiae</i>	1.81	2.90E-08	1.84E-06
An18g06220*	strong similarity to alpha-mannosidase Mns1 - <i>Saccharomyces cerevisiae</i>	2.10	3.47E-06	8.05E-05
An01g12720*	similarity to tumour suppressor protein TSA305 from patent WO9928457-A1 - <i>Homo sapiens</i>	1.69	3.91E-07	1.38E-05

Table 3. Cont.

DSM code	DSM annotation	FC B36/N402	P	FDR
Protein complex involved in protein transport				
An01g03190	similarity to protein Sec3 - <i>Saccharomyces cerevisiae</i>	1.30	7.93E-05	1.03E-03
An08g05570*	similarity to secretory protein Sec5 - <i>Saccharomyces cerevisiae</i>	1.54	1.97E-06	5.07E-05
An04g06180	strong similarity to exocyst subunit Sec6 - <i>Saccharomyces cerevisiae</i>	1.38	7.87E-05	1.03E-03
An08g07370	similarity to exocyst protein Exo84 - <i>Saccharomyces cerevisiae</i>	1.42	9.83E-05	1.22E-03
An02g14400*	strong similarity to hypothetical protein SPCC338.13 - <i>Schizosaccharomyces pombe</i>	1.43	8.59E-06	1.66E-04
An16g01630	strong similarity to enoyl reductase of the lovastatin biosynthesis lovC - <i>Aspergillus terreus</i>	0.35	1.66E-10	3.53E-08
An04g08690*	similarity to polynucleotide sequence SEQ ID NO:3913 from patent WO200058473-A2 - <i>Homo sapiens</i>	1.37	7.88E-05	1.03E-03
An02g07090*	strong similarity to ASNA1 product arsenite translocating ATPase - <i>Homo sapiens</i>	1.30	1.46E-04	1.66E-03
An01g14250*	strong similarity to delta subunit of the coatomer delta-coat protein CopD - <i>Bos taurus</i>	1.46	3.66E-06	8.35E-05
An08g01250*	weak similarity to COP1-interacting protein 7 CIP7 - <i>Arabidopsis thaliana</i>	1.75	4.69E-07	1.57E-05
An16g05370*	similarity to zinc-finger protein Glo3 - <i>Saccharomyces cerevisiae</i>	1.59	1.28E-05	2.34E-04
An16g02460*	strong similarity to alpha subunit of the coatomer complex Ret1 - <i>Saccharomyces cerevisiae</i>	1.67	2.40E-07	9.68E-06
An01g14260*	strong similarity to delta subunit of the coatomer delta-coat protein CopD - <i>Bos taurus</i> [deleted ORF]	1.51	1.15E-06	3.27E-05
An12g04830*	strong similarity to coatomer protein zeta chain Ret3 - <i>Saccharomyces cerevisiae</i>	1.47	7.15E-06	1.44E-04
An07g06030*	strong similarity to coatomer gamma subunit 2 copg2 - <i>Homo sapiens</i>	1.65	4.32E-06	9.45E-05
An02g05870*	strong similarity to coatomer beta subunit copB2 - <i>Homo sapiens</i> [putative frameshift]	1.50	1.17E-04	1.40E-03
An01g04040*	secretion-associated GTP-binding protein sarA - <i>Aspergillus niger</i>	1.27	1.99E-04	2.13E-03
An08g03270*	strong similarity to beta-COP Sec26 - <i>Saccharomyces cerevisiae</i>	1.48	2.84E-06	6.82E-05
An04g00360*	strong similarity to transport vesicle formation protein Sec13 - <i>Saccharomyces cerevisiae</i>	1.84	1.28E-08	9.90E-07
An02g01690*	strong similarity to p150 component of the COPII coat of secretory pathway vesicles Sec31 - <i>Saccharomyces cerevisiae</i>	1.60	2.05E-07	8.64E-06
An01g04730*	strong similarity to secretory protein Sec23 - <i>Saccharomyces cerevisiae</i>	1.62	2.83E-07	1.08E-05
An08g10650*	strong similarity to transport protein Sec24 - <i>Saccharomyces cerevisiae</i>	1.55	6.97E-07	2.18E-05
An16g03320*	strong similarity to transport protein Sec24A - <i>Homo sapiens</i>	1.56	2.27E-06	5.69E-05
An15g01520*	strong similarity to multidomain vesicle coat protein Sec16 - <i>Saccharomyces cerevisiae</i>	1.53	1.74E-06	4.55E-05
ER to Golgi and intra-Golgi transport				
An08g03590*	strong similarity to precursor of protein Emp24 - <i>Saccharomyces cerevisiae</i>	1.39	7.73E-06	1.52E-04
An09g05490*	strong similarity to COP-coated vesicle membrane protein P24 homolog lbrA - <i>Polysphondylium pallidum</i>	1.42	4.30E-06	9.43E-05
An07g09160	strong similarity to pattern formation protein cni - <i>Drosophila melanogaster</i>	1.28	1.30E-04	1.52E-03
An01g08870*	strong similarity to component of COPII-coated vesicles Erv25 - <i>Saccharomyces cerevisiae</i>	1.39	7.23E-06	1.45E-04

Table 3. Cont.

DSM code	DSM annotation	FC B36/N402	P	FDR
An08g03960*	strong similarity to hypothetical edoplasmic reticulum associated protein - <i>Schizosaccharomyces pombe</i>	1.55	7.36E-06	1.47E-04
An03g04940*	strong similarity to Erv41 - <i>Saccharomyces cerevisiae</i>	2.12	1.20E-08	9.44E-07
An01g04320*	strong similarity to COPII vesicle coat component protein Erv46 - <i>Saccharomyces cerevisiae</i>	2.12	7.61E-09	6.57E-07
An02g02830	strong similarity to protein RER1 - <i>Homo sapiens</i>	1.30	5.22E-05	7.42E-04
An07g02190	strong similarity to protein Sec7 - <i>Saccharomyces cerevisiae</i>	1.44	9.50E-06	1.81E-04
An08g06780*	strong similarity to transport protein Uso1 - <i>Saccharomyces cerevisiae</i>	1.52	2.93E-06	7.00E-05
An18g06440	strong similarity to COPII vesicle component Yip3 - <i>Saccharomyces cerevisiae</i>	1.67	2.58E-06	6.30E-05
An04g01780*	strong similarity to hypothetical protein YAR002c-a - <i>Saccharomyces cerevisiae</i>	1.54	1.03E-06	3.00E-05
An04g08830*	similarity to Golgi membrane protein Emp47 - <i>Saccharomyces cerevisiae</i>	1.69	9.30E-07	2.78E-05
An02g04250*	similarity to protein p58 - <i>Rattus norvegicus</i>	1.77	2.01E-08	1.39E-06
An04g01990*	similarity to protein ZW10 homolog HZW10 - <i>Homo sapiens</i>	1.32	1.06E-04	1.29E-03
An04g06090	similarity to geranylgeranyltransferase type-II alpha chain Bet4 - <i>Saccharomyces cerevisiae</i>	0.77	2.69E-04	2.75E-03
An08g00290*	strong similarity to golgin-160 related protein Rud3 - <i>Saccharomyces cerevisiae</i>	1.52	1.11E-05	2.05E-04
An08g06330*	strong similarity to epsilon-COP - <i>Cricetulus griseus</i>	1.39	1.84E-05	3.14E-04
An07g07340*	strong similarity to luminal ER-protein retention receptor ERD2 - <i>Kluyveromyces marxianus</i>	1.65	2.00E-07	8.46E-06
Other processes in the secretory pathway				
An07g02170*	similarity to transport protein Bos1 - <i>Saccharomyces cerevisiae</i>	1.91	1.65E-08	1.18E-06
An15g01380*	strong similarity to Synaptobrevin homolog v-SNARE Sec22 - <i>Saccharomyces cerevisiae</i>	1.30	2.74E-04	2.78E-03
An18g02490*	strong similarity to ARF guanine-nucleotide exchange factor 2 Gea2 - <i>Saccharomyces cerevisiae</i>	1.31	1.52E-04	1.71E-03
An07g08220*	strong similarity to clathrin associated epsin 2A - <i>Homo sapiens</i>	1.39	1.58E-05	2.76E-04
An02g08450*	secretory gene nsfA - <i>Aspergillus niger</i>	1.27	2.86E-04	2.89E-03
An02g14450*	secretory pathway Ca2+-ATPase pmrA - <i>Aspergillus niger</i>	1.51	3.12E-06	7.38E-05
An16g08470*	similarity to hypothetical cell growth regulator OS-9 - <i>Homo sapiens</i>	1.76	8.57E-07	2.58E-05
An02g03460*	similarity to hypothetical protein YIL041w - <i>Saccharomyces cerevisiae</i>	1.31	1.49E-04	1.68E-03
An04g02070	strong similarity to clathrin heavy chain - <i>Bos taurus</i>	1.30	1.09E-04	1.33E-03
An06g01200*	strong similarity to endosomal protein Emp70 - <i>Saccharomyces cerevisiae</i>	1.55	1.37E-06	3.77E-05
An01g11960	similarity to brefeldin A resistance protein Bfr1 - <i>Saccharomyces cerevisiae</i>	1.44	1.27E-05	2.33E-04
An04g01950*	strong similarity to zinc-metalloprotease Ste24 - <i>Saccharomyces cerevisiae</i>	1.63	1.61E-07	7.12E-06

DSM code: ORF identifier in *A. niger* CBS 513.88 genome sequence (Pel et al. 2007). Genes in bold are also found in maltose/xylose transcriptomic comparison (Jørgensen et al. 2009). * Indicates genes that were also identified in strains with constitutively active *hacA^{CA}* (Carvalho et al. 2012).

transcription factor due to the high number of *glaA* promoter copies in this strain (Verdoes et al. 1994b). Alternatively, the biosynthesis of an inducer through one of the enzymes under control of AmyR might be reduced. Lower inducer levels could then lead to lower levels of active AmyR transcription factor, leading to a negative feedback loop. Down-regulation of AmyR targets (except for *glaA*, Table 4) could also be explained by the RESS (repression under secretion stress) phenomenon, described for *Trichoderma reesei* (Pakula et al. 2003; Saloheimo and Pakula 2012) and *Arabidopsis thaliana* (Martinez and Chrispeels 2003), and predicted for *A. niger* (Carvalho et al. 2012). RESS is a transcriptional feedback mechanism that is activated in response to impairment of protein folding or transport and aims at lowering the protein load in the secretory route when ER stress conditions are sensed (Pakula et al. 2003). As we have observed that GlaA overexpression induces a mild UPR (Fig. 2A), we propose that down-regulation of AmyR and its target genes reflects a negative feedback mechanism similar to RESS in *T. reesei*.

Notably, enriched GO terms of the ‘ion homeostasis’ category indicated an increased demand for iron, calcium and zinc. In the context of increased fluxes of GlaA through the secretory pathway in strain B36, several explanations are conceivable. First, the mature GlaA protein contains nine cysteine residues, eight of which are involved in disulfide bridge formation (Lee and Paetzel 2011; Sorimachi et al. 1996). Hence, in B36 there is an increased demand for disulfide bond formation, which requires increased activity of protein disulfide isomerases. Increased amounts of PdiA, however, might result in sequestration of

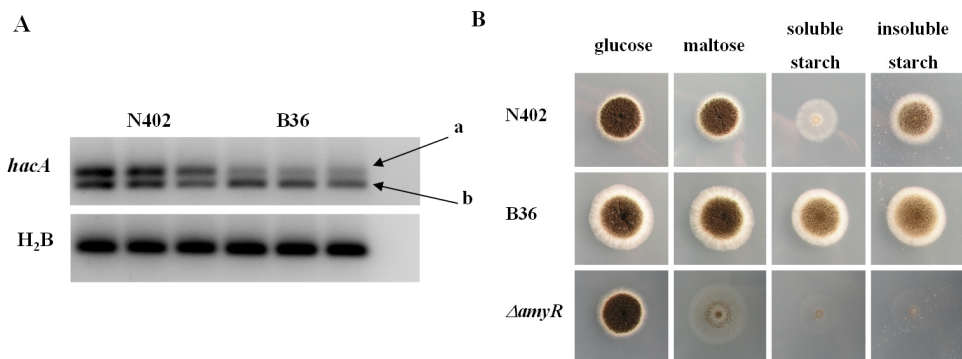


Fig. 2. RT-PCR analysis (A) and plate growth assay (B) of N402 and B36. A, RT-PCR analysis of expression and transcript processing of the UPR transcription factor gene, *hacA*. The ratio between unspliced, a (220 bp), and spliced, b (200 bp), of *hacA* transcript is similar in all three N402 steady states of maltose-limited chemostat cultures while in B36 there is more spliced *hacA* present. The H₂B control shows that there is no contamination with genomic DNA ; genomic DNA, 181-bp amplicons; mRNA, 131-bp amplicons. B, plate growth assay of N402 and B36 using different carbon sources. 10⁴ spores were point-inoculated on MM plates and incubated for 4 days at 30°C.

Table 4. Expression values of genes involved in starch metabolism.

Gene ID	Name	DSM annotation	FC B36/N402	P	FDR
An04g06910	<i>amyR</i>	transcription factor of starch utilization <i>amyR</i> – <i>A. niger</i>	0.64	1.06E-06	3.06E-05
An11g03340	<i>aamA</i>	acid alpha-amylase – <i>A. niger</i>	0.23	1.24E-09	1.48E-07
An04g06920	<i>agdA</i>	extracellular alpha-glucosidase <i>aglU</i> – <i>A. niger</i>	0.60	7.55E-08	4.07E-06
An01g10930	<i>agdB</i>	strong similarity to enzyme with sugar transferase activity from patent JP11009276-A - <i>Acremonium</i> sp.	0.45	2.27E-09	2.40E-07
An03g06550	<i>glaA</i>	glucan 1,4-alpha-glucosidase <i>glaA</i> – <i>A. niger</i>	1.23*	3.94E-04	3.80E-03
An04g06930	<i>amyC</i>	strong similarity to extracellular alpha-amylase <i>amyA/amyB</i> – <i>A. niger</i>	0.54	7.68E-08	4.13E-06
An04g06920	<i>aglU</i>	extracellular alpha-glucosidase <i>aglU</i> – <i>A. niger</i>	0.60	7.55E-08	4.07E-06
An09g03100	<i>amyA</i>	strong similarity to alpha-amylase precursor <i>amy</i> – <i>A. niger</i>	0.32	7.34E-08	3.99E-06

FC: fold change. *Fold difference in *glaA* is under-estimated due to the saturation of array signals. Transcript level of *glaA* in B36 was about 7-fold higher than N402 based on qPCR results.

zinc ions in the ER (Lee and Paetzel 2011; Solovyov and Gilbert 2004), thus preventing it from binding to other proteins and causing a cellular shortage of zinc. Second, chaperones such as ClxA needs calcium as co-factor (Wang et al. 2003), hence enhanced expression of *clxA* in B36 calls for higher calcium concentrations in the ER. Third, calcium is of general importance for vesicle fusions and the function of the ER and Golgi (Dolman and Tepikin 2006; Stojilkovic 2005). Hence, the cells have to mobilize calcium from internal or external stores to ensure higher fluxes through the secretory pathway in B36. Finally, the activity of GlaA is known to be positively affected by the presence of Mn^{2+} , Ca^{2+} and Fe^{2+} ions (Kumar and Satyanarayana 2009), which are also required for many other protein activities including heme or iron-sulfur-cluster (Fe-S) proteins (Lill 2009; Stojilkovic 2005; Waldron et al. 2009). In this context, it is interesting to note that protein secretion in *A. fumigatus* has most recently been shown to require controlled uptake of iron. Basically, the transcription factor PrtT not only positively regulates expression of protease genes but also strengthens expression of iron uptake genes (Hagag et al. 2012). We thus compared the published expression data of iron uptake genes in *A. fumigatus* (wt versus $\Delta prtT$) with the expression data of their predicted orthologs in *A. niger* (B36 versus N402). Twelve out of 15 iron-uptake genes showed similar expression profiles (Additional file 5), i.e. their up-regulation in wt versus $\Delta prtT$ was mirrored in B36 versus N402. In agreement, expression profiles of the main iron transcription factors also matched, i.e. up-regulation/down-regulation of the activator HapX/repressor SreA in wt versus $\Delta prtT$ were comparably up-/down-regulated in B36 versus N402. Hence, both independent observations from two *Aspergilli* strongly

indicate that proper function of the protein secretion machinery and high fluxes through the secretory pathway mandate optimal iron supply and assuring proper ion homeostasis.

GO enrichment analysis of the down-regulated gene set in B36 uncovered three major categories: i) 'carbon catabolism', ii) 'amino acid catabolism' and iii) 'response to oxidative stress' (Additional file 3). The first two categories might be causatively linked to the RESS phenomenon discussed above, i.e. increased GlaA secretion is only possible at the cost of other secreted proteins. As AmyR targets related to starch degradation are down-regulated in B36 (see Table 4), processes related to polysaccharide degradation have consequently to be down-regulated as well. In a recent study, 19 proteases of *A. niger* were identified in the extracellular medium, when the strain was cultivated under sorbitol-, galacturonic acid- or carbon-starvation conditions (Braaksma et al. 2010). Expression of 12 of them was reduced in B36 compared to N402, two of the genes were up-regulated and expression of five genes was unaltered (Additional file 6). Hence, overall reduction in protease activity in B36 will in turn decelerate amino acid catabolic processes. An additional explanation for reduced expression of carbon and amino acid catabolic processes is that many enzymes involved in these processes are iron-dependent. Iron deficiency has been shown to trigger a metabolic response in *Saccharomyces cerevisiae* or *Schizosaccharomyces pombe*, which includes down-regulation of enzymes involved in carbon and amino acid metabolism and respiration (Lill 2009; Mercier and Labbe 2010; Philpott et al. 2012; Philpott and Protchenko 2008). Assuming that this also holds true for *A. niger*, reduction in catabolic processes would lower the fluxes into the citric acid cycle and into the respiratory chain, which in turn would also lower the amount of radical oxygen species produced. Hence, oxidative stress would be diminished, which in turn would result in down-regulation of oxidative stress genes as observed in B36. A slight but significantly reduced RQ in B36 compared to N402 (Table 1) supports this hypothesis. Taken together, the enriched GO term set of down-regulated genes in B36 can hypothetically be viewed as a consequence of the RESS phenomenon and reduced iron availability due to increased GlaA secretion.

Two *A. niger* proteins lacking an N-terminal signal peptide for entering the secretory route were recently determined to be abundantly present in the secretome of *A. niger* (Braaksma et al. 2010). It was thus proposed that proteins can also be exported out of the cell by the so-called non-classical secretion pathway (Braaksma et al. 2010). Interestingly, transcript levels of both protein-encoding genes were lowered in B36 *versus* N402 (An01g09980, fold-change B36/N402 = 0.15, FDR = 8.65×10^{-9} ; An01g00370, fold-change = 0.54, FDR = 0.0001). This could mean that an accelerated activity of the classical secretory machinery is only possible at the expense of the non-classical secretion pathway –

which could be another potential example for the existence of the RESS regulatory feedback loop in *A. niger*.

Comparison of the GlaA overexpression transcriptome with the maltose transcriptome

In order to identify genes whose transcript levels are generally important for high-level secretion in *A. niger*, i.e. independent of the conditional trigger, we first compared the GlaA transcriptomic fingerprint with two other recently determined fingerprints from our laboratory. First, we compared the GlaA overexpression transcriptome with the maltose transcriptome of *A. niger*. The maltose transcriptome was recently obtained by comparing carbon-limited chemostat cultures supplied with different carbon sources (maltose and xylose) but with the same specific growth rate ($D = 0.16 \text{ h}^{-1}$) (Jørgensen et al. 2009). This comparison showed that the production rate of extracellular proteins was about three-fold higher in maltose-grown cultures compared to xylose (Jørgensen et al. 2009). As shown in the Venn diagram depicted in Fig. 3, 150 genes were commonly induced in both B36 *versus* N402 and maltose *versus* xylose and thus represent the most interesting genes with respect to high-level secretion in *A. niger*. GO enrichment analysis of this set of genes confirmed that genes related to ER import, translocation, N-glycosylation and COPII transport are of utmost importance for ensuring high protein traffic through the secretory pathway (Additional file 7).

Genes that are induced in B36 *versus* N402, but not in maltose *versus* xylose, are likely to be genes that are mainly related to GlaA overexpression per se. There are 640 such genes and GO enrichment analysis uncovered two main categories (Additional file 7), one of which is the ‘ion homeostasis’ category, as expected due to the high iron, calcium and zinc demand for GlaA overexpression (see former section). The second category involves

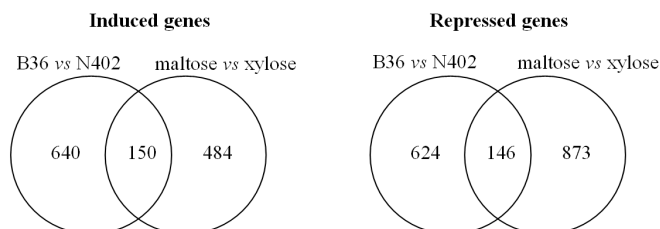


Fig. 3. Venn diagrams of the number of overlapping and non-overlapping induced and repressed genes on B36/N402 and maltose/xylose (Jørgensen et al. 2009) chemostat cultures.

genes involved in ‘DNA repair and DNA replication’ and could hypothetically also be linked to the iron deficiency in B36 *versus* N402, as many proteins involved in nucleotide excision repair and DNA replication are iron-dependent (Lill 2009). Genes that induced in maltose *versus* xylose but not in B36 *versus* N402 are likely to be genes, which are important for starch/maltose degradation but not for xylose catabolism. Indeed, the enriched GO categories of this gene set (484 genes) contained ‘starch metabolic processes’ and other catabolic process related to ‘carbon source oxidation’, ‘amino acid metabolism’ and ‘respiration and oxidative stress’ (Additional file 7). These are processes important for (or related to) high ATP generation during oxidative phosphorylation in the respiratory chain and do likely form the energetic basis for the observed higher secretory flux in maltose cultures compared to xylose cultures despite similar growth rates. There were 146 commonly repressed genes in B36 *versus* N402 and in maltose *versus* xylose, but only a small fraction of these genes could be assigned to enriched GO terms related to ‘saccharide catabolic processes’ (Additional file 7).

Comparison of the GlaA overexpression transcriptome with other high-secretion transcriptomes

In order to determine so far unknown HacA targets and their involvement in UPR, we have recently determined the HacA transcriptome by expressing a constitutively active form of HacA (*hacA^{CA}*) in *A. niger* (Carvalho et al. 2012). Using bioreactor-controlled batch cultures, we compared the genome-wide expression profiles of a strain expressing *hacA^{CA}* with a wild-type strain (*hacA^{WT}*) at three different time points during the exponential growth phase. At each of the three time points the up-regulated gene set of the *hacA^{CA}* cultures contained genes related to protein traffic through the secretory pathway, and to the UPR and ERAD response (Carvalho et al. 2012). When comparing these data with the GlaA-overexpression transcriptome, one might expect a considerably overlap due to the fact that overexpression of GlaA induced splicing of the *hacA* mRNA (Fig. 2) and thus activation of HacA. Indeed, the transcriptional response in B36 had more in common with *hacA^{CA} versus hacA^{WT}* (578 genes) than with maltose *versus* xylose (296 genes, data not shown). Commonly induced genes in B36 *versus* N402 and *hacA^{CA} versus hacA^{WT}* were predicted to function in ‘vesicle coating’, ‘targeting from the ER to the Golgi’, ‘N-glycosylation’ and ‘COPII transport’.

For a more condition-independent view on how the *A. niger* transcriptome ensures high-level secretion, we finally compared the transcriptomic dataset of seven independent studies performed with *A. niger*: i) the GlaA-overexpression transcriptome obtained from

chemostat cultures of B36 *versus* N402 (this study), ii) the maltose-high secretion transcriptome obtained from chemostat cultures of maltose *versus* xylose (Jørgensen et al. 2009), iii) the HacA transcriptome reflecting permanent activation of UPR and obtained from batch cultures comparing *hacA^{CA}* *versus* *hacA^{WT}* (Carvalho et al. 2012) and iv) three UPR stress transcriptomes obtained from *A. niger* batch cultures stressed with DTT, tunicamycin, or forced to express the heterologous protein t-PA (Guillemette et al. 2007).

This analysis uncovered 40 genes whose transcript levels were commonly modified under all seven secretion stress conditions: 36 genes were up-regulated, and 4 genes were down-regulated (Table 5). The genes from this set thus probably represent genes that are crucial for coping with stress conditions that target the secretion machinery. This gene set includes ER chaperones and foldases (*prpA*, *clxA*, *lhs1*, *pdiA*, *bipA*, *tigA*), genes important for translocation of secretory proteins into the ER (*sec63*, *sec11*, *sss1*, *spc3*, *sec71*) and genes important for protein glycosylation and COPII-based vesicle trafficking (Table 5). Fascinatingly, a gene encoding the predicted acetyl-coenzyme A transporter (An02g13410) was consistently up-regulated under all seven conditions. In higher eukaryotes, this protein was shown to be involved in translocation of membrane-impermeable coenzyme A from the cytosol into the ER lumen, where it is used for transient acetylation of ER-based proteins, thus improving the folding efficiency of nascent secretory proteins (Jonas et al. 2010). It becomes therefore important to examine whether the predicted *A. niger* CoA transporter fulfills the same function. Similarly, the set of core genes included six hypothetical proteins, whose precise relevance for the secretory machinery remains to be elucidated in future studies.

Conclusions

The evidence is accumulating that the secretory machinery of *A. niger* is equipped with a high inherent flexibility, which enables the fungus to dynamically respond to changes in the secretory protein load. Irrespective of whether different amounts of a homologous protein or a heterologous protein have to be accommodated and escorted, or a specific step in the secretory pathway becomes blocked, *A. niger* follows general and specific strategies to adapt to these challenges. On the one hand, the burden of high protein loads is in general dealt with increased transcript levels of genes involved in stabilizing the secretory pathway, including chaperone-encoding and foldase-encoding genes, transport genes and UPR- and ERAD-related genes. In addition, it seems likely that for the efficient secretion of individual proteins (either overexpressed or a heterologous proteins) an additional, particular set of genes becomes up-regulated, whose expression is important to deal with

Table 5. The list of common transcriptional response from all compared conditions.

DSM code	DSM annotation	FC B36/N402	P	FDR
Protein folding				
An01g13220	similar to the chaperone Lhs1	2.26	1.34E-09	1.58E-07
An02g14800	Protein disulfide isomerase PdiA	1.72	5.98E-08	3.43E-06
An01g04600	Protein disulfide isomerase PrpA	2.08	2.21E-09	2.40E-07
An01g08420	calnexin ClxA	2.42	8.96E-10	1.13E-07
An11g04180	chaperone BipA	2.32	8.63E-10	1.11E-07
An16g07620	similar to ER oxidising protein Ero1	1.97	1.02E-08	8.15E-07
An18g02020	Protein disulfide isomerase TigA	1.89	1.61E-08	1.17E-06
An11g11250	similar to the chaperone P58IPK <i>Homo sapiens</i>	1.80	2.58E-07	1.03E-05
Translocation/Signal peptidase complex				
An01g13070	similar to ER protein-translocation complex subunit SEC63	2.02	2.17E-08	1.47E-06
An16g08830	similar to component of subcomplex SEC71	1.80	3.47E-08	2.17E-06
An01g11630	similar to translocation complex component SSS1	1.71	1.88E-07	8.11E-06
An09g05420	similar to signal peptidase subunit SPC3	1.99	6.90E-09	6.03E-07
An01g00560	similar to signal peptidase subunit SEC11	1.84	5.70E-07	1.84E-05
An15g06470	similar to signal sequence receptor α -subunit	1.86	4.49E-08	2.72E-06
Glycosylation				
An14g05910	similar to mannosyltransferase ALG2	1.93	2.28E-08	1.53E-06
An03g04410	similar to glucosyltransferase ALG5	1.78	3.47E-07	1.26E-05
An02g03240	similar to N-acetylglucosaminophosphotransferase ALG7	1.92	1.76E-08	1.24E-06
An07g04190	similar to glycosyltransferase WBP1	1.69	1.03E-07	5.04E-06
An02g14560	oligosaccharyltransferase alpha subunit OSTA	2.05	2.27E-09	2.40E-07
An18g03920	similar to oligosaccharyltransferase subunit OST2	2.04	2.49E-09	2.56E-07
An18g04260	similar to UDP-galactose transporter HUT1	2.46	1.06E-09	1.28E-07
An13g00620	similar to beta subunit of an ER alpha-glucosidase	1.53	1.24E-06	3.47E-05
An15g01420	similar to glucosidase I CWH41	1.81	2.90E-08	1.84E-06
An02g14940	similar to flippase RFT1	1.49	2.62E-06	6.38E-05
Vesicle trafficking/transport				
An03g04940	similar to COPII vesicle coat component protein ERV41	2.12	1.20E-08	9.44E-07
An01g04320	similar to COPII vesicle coat component protein ERV46	2.12	7.61E-09	6.57E-07
An02g04250	similar to ER protein P58 (lectin family) <i>Rattus norvegicus</i>	1.77	2.01E-08	1.39E-06
An08g06780	similar to ER to Golgi transport protein USO1	1.52	2.93E-06	7.00E-05
Lipid metabolism				
An02g13410	similar to acetyl-coenzyme A transporter AT-1	2.10	4.55E-09	4.23E-07
Stress related				
An12g03580	similar to glutathione S-transferase 3 MGST3 <i>H. sapiens</i>	1.51	1.21E-05	2.23E-04
An01g14100	weakly similar to stress protein HERP <i>Mus musculus</i>	1.61	1.12E-06	3.21E-05
Cell cycle and DNA processing				
An01g08170	similar to DNA repair endonuclease RAD1 <i>S. pombe</i>	2.05	1.62E-08	1.17E-06
Phosphate metabolism				
An12g01910	similar to phytase PHYA3 <i>Aspergillus fumigatus</i>	0.56	2.09E-07	8.76E-06
Cell rescue. Defense and virulence				
An18g00980	similar to membrane protein PTH11 <i>M. grisea</i>	0.41	1.32E-08	1.01E-06

Table 5. Cont.

DSM code	DSM annotation	FC B36/N402	P	FDR
Unclassified				
An08g03960	hypothetical endoplasmic reticulum associated protein	1.55	7.36E-06	1.47E-04
An08g03970	hypothetical protein	1.87	2.87E-08	1.83E-06
An07g10280	hypothetical protein	1.43	6.40E-06	1.31E-04
An09g06130	hypothetical protein	1.64	4.24E-07	1.46E-05
An18g01000	hypothetical protein	0.56	1.05E-06	3.03E-05
An13g01520	hypothetical protein	0.49	3.57E-06	8.23E-05

DSM code: ORF identifier in *A. niger* CBS 513.88 genome sequence (Pel et al. 2007). The list of common transcriptional response from B36/N402 (this study), maltose/xylose (Jørgensen et al. 2009), *hacA^{CA}/hacA^{WT}* (Carvalho et al. 2012) and ER stress with at least 2 types of protein folding stress (Guillemette et al. 2007).

the specific requirements of the respective protein. On the other hand, *A. niger* attempts to avoid exceeding the maximum capacity of the secretory machinery. In doing so, the RESS regulatory system offers a flexible way to lower transcript levels of those genes whose function is less important for growth and survival under the given circumstances.

Materials and Methods

Strains and inoculums

The laboratory strain *Aspergillus niger* N402 (Bos et al. 1988) was used as a reference strain and B36 (Verdoes et al. 1993), which contains multiple copies of the glucoamylase gene, was used as an overproducer strain. Strains were grown on solidified Complete Medium (CM) containing 1% (w v⁻¹) glucose, 0.1% (w v⁻¹) casamino acids and 0.5% (w v⁻¹) yeast extract in addition to Minimal Medium (MM) (Alic et al. 1991). Spore plates were incubated for four or five days at 30°C and stored for no more than three months at 4°C. Conidia were harvested from CM agar plates with a sterile detergent solution containing 0.05% (w/v) Tween 80 and 0.9% (w/v) NaCl.

Bioreactor cultivation conditions

Maltose-limited batch and chemostat cultivations were performed as described previously for *A. niger* (Jørgensen et al. 2009) with slight modifications. The N402 and B36 strains were both grown in triplicate in maltose-limited chemostat cultures.

(i) Batch cultures

Batch cultivation was initiated by inoculation of 5 kg ammonium-based minimal medium with a conidial suspension to give 10^9 conidia L^{-1} . Maltose was heat sterilized separately from the MM and the final concentration was 0.8% (w/v). Germination was induced by addition of 0.003% (w/w) yeast extract. During the first six hours of cultivation the culture was aerated (air flow = $1 L min^{-1}$) through the headspace of the reactor and the stirrer speed was kept low at 250 rpm to avoid loss of the hydrophobic conidia. After six hours when most conidia had germinated, air was sparged into the culture broth, mixing was intensified (750 rpm) for more efficient oxygen transfer, and 0.01% (v/v) of polypropylene glycol (PPG) was added as an antifoaming agent. The temperature was 30°C and the pH was kept constant at pH = 3 by computer-controlled addition of 2 M NaOH or 1 M HCl. Acidification of the culture broth was used as an indirect growth measurement (Iversen et al. 1994). Submerged cultivation was performed with 6.6 L BioFlo3000 bioreactors (New Brunswick Scientific, NJ, USA).

(ii) Chemostat cultures

Continuous cultivation was started in the late-exponential growth phase, when 90 mmol of NaOH had been added to the batch culture (75% of maltose had been consumed, at a biomass concentration of about 3.5 g dry weight per kg of culture). The dilution rate (D) was set at $0.1 h^{-1}$. Steady-states, where the specific growth rate (μ) is equal to the dilution rate, were defined by constant alkali addition rate and constant CO_2 , O_2 and biomass concentrations after four residence times ($\sim 40 h$). Samples were taken regularly to monitor growth and to determine if a steady-state had been reached. All samples were quickly frozen in liquid nitrogen. Mycelium harvested during steady-state conditions was used for micro-array analysis.

Analysis of culture broth

Dry weight biomass concentration was determined by weighing lyophilized mycelium separated from a known mass of culture broth. Culture broth was filtered through GF/C glass microfiber filters (Whatman). The filtrate was collected and frozen for use in solute analyses. The mycelium was washed with demineralised water, rapidly frozen in liquid nitrogen, and stored at -80°C until lyophilization. Extracellular protein concentration was determined using the Quick Start Bradford Protein Assay (Bio-Rad) with BSA as a standard. The total organic carbon in the culture filtrate was measured with a Total Organic Carbon Analyzer (TOC-Vcns; Shimadzu, Japan), using glucose as a standard.

RNA isolation and quality control

Total RNA was extracted by modified Trizol extraction. Frozen ground mycelium (~200 mg) was directly suspended in 800 μ l Trizol reagent (Invitrogen) and vortexed vigorously for 1 min. After centrifugation for 5 min at 13000 rpm, 450 μ l of the supernatant was transferred to a new tube. Chloroform (150 μ l) was added and after 3 min incubation at room temperature, samples were spun down for 15 min at maximum speed. The upper aqueous phase was transferred to a new tube to which 400 μ l of isopropanol was added, followed by 10 min incubation at room temperature and centrifugation for 10 min at 13000 rpm. Pellet was washed with 75% ethanol and finally precipitated in 100 μ l H₂O. RNA samples for micro-array analysis were additionally purified on NucleoSpin RNA II columns (Machery-Nagel) according to manufacturer's instructions. RNA quantity and quality was determined on Nanodrop spectrophotometer.

Microarray analysis

Probe synthesis and fragmentation were performed at ServiceXS (Leiden, The Netherlands) according to the GeneChip Expression Analysis Technical Manual (Affymetrix inc., 2002). DSM (Delft, The Netherlands) proprietary *A. niger* gene chips were hybridized, washed, stained and scanned as described in the GeneChip Expression Analysis Technical Manual (Affymetrix inc., 2002).

Normalization, filtering, statistical significance and comparisons

Transcriptomic analysis was basically performed using Bioconductor and statistical programming language R (Nitsche et al. 2012b). Two experimental conditions (N402 vs B36) were compared to each other; each condition was represented by independent triplicate cultures. Using the robust multi-array analysis (RMA) package (Irizarry et al. 2003), background correction, normalization and probe summarization steps were performed according to the default setting of the RMA package. Differential gene expression was evaluated by moderated t-statistics using the Limma package (Smyth 2004) with a threshold of the Benjamini and Hochberg (BH) False Discovery Rate (FDR) (Benjamini and Hochberg 1995) at 0.005. A minimal fold-change criterion was not applied for the identification of differentially expressed genes, as fold-changes are not necessarily related to biological relevance (van den Berg et al. 2010; van den Berg et al. 2006). Fold-changes of gene expression from N402 to B36 (B36/N402) were calculated from normalized expression values. Means of the expression values for B36 and N402 as well as classifiers for the moderated t-statistics are summarized in Additional file 1.

Gene Ontology (GO) and enrichment analysis

Controlling the FDR at $q < 0.05$, over-represented GO terms in sets of differentially expressed genes were determined by Fisher's exact test (Fisher 1922). An improved GO annotation for the *A. niger* CBS513.88 was applied that is based on ontology mappings from *A.nidulans* FGSCA4 (<http://www.broadinstitute.org/fetgoat/index.html>) (Nitsche et al. 2011).

Quantitative real-time PCR (qPCR)

Quantitative real-time PCR was performed as described (Nowrousian et al. 2005) with slight modifications. After a DNase treatment (DNA-freeTM Kit Applied Biosystems) of 10 μg of total RNA, 600 ng were used for cDNA synthesis using the iScriptTM cDNA Synthesis Kit from BioRad according to the manufactures instructions. Real time PCR was performed in PTC-200 Peltier Thermal Cycler with a Chromo4 Continuous Fluorescence detection system from Bio-Rad with a SYBRgreen mix (iQTM SYBR[®] Green supermix) in a volume of 25 μl . Each reaction was carried out in triplicate with ~ 200 ng of cDNA and each oligonucleotide primer at 0.3 μM . Oligonucleotide primers used for real time PCR are listed in Additional file 8. Two reference genes, H₂B and Cox5 were used for normalization. The PCR program was as follows: 95°C for 3 min, followed by 39 cycles of 95°C for 15 sec and 60°C for 1 min, followed by a melting curve analysis. The efficiency of each primer pair and mean Ct (threshold cycles) values were calculated and used for determination of glucoamylase RNA transcript levels (Pfaffl 2001). Estimation of glucoamylase gene copy number was also performed by qPCR as well but with genomic DNA as a template.

Analysis of glucoamylase activity

One unit of glucoamylase activity was expressed as the amount of enzyme that liberates one micromole of glucose per minute from starch. Filtrates from steady-state cultures were mixed with 1% soluble starch (Sigma, S9765) in 50 mM NaAc buffer at pH 4.5 and incubated at 37°C for 3.75 min. Liberated glucose was determined with the glucose kit from ABX (Pentra Glucose HK CP).

Western blot analysis of glucoamylase

Protein concentrations of the samples were determined with the Bradford assay using BSA as a standard. For each sample, culture filtrate samples corrected for equal amounts of biomass were mixed with 2x loading buffer (0.5 M HCl, 25% glycerol, 10% SDS, 0.5% bromophenol blue, 5% β -mercaptoethanol) and boiled for 5 min at 95°C. Protein samples were loaded on 9% SDS-PAGE gels and blotted to a nitrocellulose membrane through semi-dry electrotransfer. The membrane was blocked for 1 h with 5% low-fat dried milk in TPBS (PBS, 0.05% Tween20) and glucoamylase protein was detected using a glucoamylase-specific primary antibody (1:3,000) for 1 h at room temperature, followed by a goat anti-mouse-HRP secondary antibody (1:20,000) for 1 h at room temperature. Detection was performed using a chemiluminescence kit (Bio-Rad) according to the manufacturer's instructions. Analysis and quantification of band intensities were performed using Image J software based on N402 signal as one.

Competing interests

The authors declare that they have no competing interests.

Authors' contributions

MJK, TRJ, MA and JP performed the chemostat experiments. MJK carried out the physiological and transcriptomic analyses and drafted the manuscript. BMN participated in initial transcriptomic analyses and the statistical analysis. MJK, VM and AFJR were involved in writing the manuscript. MJK, TRJ, VM and AFJR designed the experiments and interpreted the results. All authors read and approved the final manuscript.

Acknowledgements

The authors would like to acknowledge Nick van Biezen in HAN BioCentre for glucoamylase activity analysis. We are grateful to Peter Punt (TNO, The Netherlands) for kindly providing the B36 strain and helpful discussions. We thank David Archer and Frans Klis for critically reading the manuscript and their helpful comments. This project was carried out within the research programme of the Kluyver Centre for Genomics of Industrial Fermentation which is part of the Netherlands Genomics Initiative/Netherlands Organization for Scientific Research.

**Molecular genetic analysis of vesicular transport in
Aspergillus niger reveals partial conservation of the
molecular mechanism of exocytosis in fungi**

**Min Jin Kwon, Mark Arentshorst, Markus Fiedler, Florence L.M. de Groen, Peter J.
Punt, Vera Meyer and Arthur F.J. Ram**

Microbiology 2014 Feb;160(Pt 2):316-329

Abstract

The filamentous fungus *Aspergillus niger* is an industrially exploited protein expression platform, well known for its capacity to secrete high levels of proteins. To study the process of protein secretion in *A. niger*, we established a GFP-v-SNARE reporter strain in which the trafficking and dynamics of secretory vesicles can be followed *in vivo*. The biological role of putative *A. niger* orthologs of seven secretion-specific genes, known to function in key aspects of the protein secretion machinery in *S. cerevisiae*, was analyzed by constructing respective gene deletion mutants in the GFP-v-SNARE reporter strain. Comparison of the deletion phenotype of conserved proteins functioning in the secretory pathway revealed common features but also interesting differences between *S. cerevisiae* and *A. niger*. Deletion of the *S. cerevisiae* Sec2p ortholog in *A. niger* (SecB), encoding a guanine exchange factor for the GTPase Sec4p (SrgA in *A. niger*), did not have an obvious phenotype, while *SEC2* deletion in baker's yeast is lethal. Similarly, deletion of the *A. niger* ortholog of the *S. cerevisiae* exocyst subunit Sec3p (SecC) did not result in a lethal phenotype as in *S. cerevisiae*, although severe growth reduction of *A. niger* was observed. Deletion of *secA*, *secH* and *ssmA* (the *A. niger* orthologs of *S. cerevisiae* Sec1p, Sec8p and Sso1/2p, respectively) showed that these genes are essential for *A. niger*, similarly to the situation in *S. cerevisiae*. These data demonstrate that the orchestration of exocyst-mediated vesicle transport is only partially conserved in *S. cerevisiae* and *A. niger*.

Introduction

As a member of the black aspergilli, *Aspergillus niger* is an important industrial microorganism. It is used for the production of various food ingredients, pharmaceuticals and industrial enzymes (Fleissner and Dersch 2010; Meyer et al. 2008; Meyer et al. 2011b). Its high protein secretion capacity together with high production of organic acids, like citric acid has stimulated the development of both genetic and genomic tools for *A. niger* to get insights into the molecular basis of these special properties. (Carvalho et al. 2010; Fleissner and Dersch 2010; Jacobs et al. 2009; Meyer et al. 2007a; Meyer et al. 2008; Meyer et al. 2010b; Meyer et al. 2011b; Pel et al. 2007). Using these tools, also more complex processes such as the protein secretion process can now systematically be studied (Carvalho et al., 2011, 2012, Kwon et al., 2012).

A. niger is well known for its outstanding capacity to secrete proteins into the growth medium. However, the number of genes predicted to function in protein secretion in *Aspergilli* (including *A. niger* and *A. nidulans*) or *S. cerevisiae* does not explain differences

among the secretion capacities of these species (Pel et al. 2007). Up to now, the mechanisms to explain the difference in secretion efficiency, which might include higher levels of secretory vesicles, more efficient packing of cargo load in vesicles or faster trafficking through the secretory pathway, are not known. Growth and secretion are considered to be tightly connected processes. Experiments in *A. niger* in chemostat cultures grown at identical growth rates on different carbon sources (xylose or maltose) revealed different protein production rates. The specific production rate of extracellular proteins on maltose was about three times higher compared to xylose at identical growth rates (Jørgensen et al., 2009). One possible mechanism to explain this uncoupling of growth and secretion in *A. niger* can be the existence of two parallel secretory pathways that independently deliver proteins destined for secretion (e.g. glucoamylase) and proteins destined for growth (e.g. plasma membrane proteins and cell wall synthesizing enzymes) to the cell surface. Several studies including studies in yeasts, plants and mammalian cells show that different populations of Golgi derived vesicles exist (Harsay and Bretscher 1995; Leucci et al. 2007; Titorenko et al. 1997; Yoshimori et al. 1996). Also in filamentous fungi, a study using *Trichoderma reesei* revealed the possible presence of more than one pathway for exocytosis based on spatial segregation of different SNARE complexes in the fungal tip cell (Valkonen et al. 2007).

The secretion process involves an ordered transport of proteins via various organelles which is mediated via secretory vesicles trafficking from one compartment to the next. The different transport steps along the secretory pathway involved in vesicle trafficking are mediated by the action of secretion-related small GTPases of the Ypt/Rab family (Segev 2001a). *A. niger* contains 11 different secretion-related GTPases that are expected to be involved in specific transport steps in the secretory pathway (Pel et al. 2007; Segev 2001a). One of those, SrgA, the ortholog of Sec4p was described earlier to be involved in protein secretion but not being essential for the viability of *A. niger* (Punt et al. 2001). Another secretion related GTPase, SrgC, an ortholog of Rab6/Ypt6 was recently described to be required for maintaining the integrity of Golgi equivalents in *A. niger* (Carvalho et al. 2011b).

Other important factors involved in the secretion pathway as mediators of vesicle docking and fusion with the membrane are soluble NSF (N-ethylmaleimide sensitive factor) attachment protein receptors (SNAREs) (Bonifacino and Glick 2004; Chen and Scheller 2001). Like the Ypt/Rab proteins, these proteins are highly conserved in eukaryotic cells and most SNAREs are C-terminally anchored transmembrane (TM) proteins present on vesicles (v-SNAREs) and target (t-SNAREs) membranes (Bonifacino and Glick 2004; Chen and Scheller 2001; Gupta and Brent Heath 2002). SNAREs are categorized into two classes based on whether they contain an arginine (R) or glutamine (Q) residue in their

SNARE central domain. Q-SNARE are further subclassified into Qa, Qb or Qc- types (Bock et al. 2001). Monomeric R-SNARE (v-SNARE) on the vesicle membrane and oligomeric Q-SNAREs on the target membrane form a stable four helices complex called as the SNARE complex at each fusion site (Bonifacino and Glick 2004). The localization of SNARE proteins have been systematically analysed in *A. oryzae* and supports the localized distribution of specific SNARE proteins at specific membranes (Kuratsu et al., 2007). In filamentous fungi, the localization of v-SNARE Snc1 and t-SNAREs Sso1 and Sso2 have been studied in detail in *T. reesei* (Valkonen et al., 2007). This SNARE-complex plays an important role in the fusion of Golgi-derived vesicles with the plasma membrane. The vesicle fusion event to the plasma membrane is promoted by the exocyst complex which provides the spatio-temporal information for the initial recruitment and tethering of Golgi-derived secretory vesicles to the plasma membrane. The exocyst is a conserved eukaryotic multi-subunit complex composed of eight protein members: Sec3, Sec5, Sec6, Sec8, Sec10, Sec15, Exo70 and Exo84. It is localized to limited regions of the plasma membrane by the interaction of Exo70p and Sec3p to Rho-GTPases and phosphatidylinositol 4,5-bisphosphate (PIP2) (see for a recent review (Heider and Munson 2012)).

The availability of temperature sensitive (ts) secretion mutants in *S. cerevisiae* has formed a strong basis for understanding and identification of secretion pathway genes including the Sec components of the exocyst complex (Novick et al. 1980; Schekman 2010). However, tools and strategies for selecting secretion mutants in filamentous fungi are lacking so far which is one reason why little is known about the regulation of the secretory pathway in filamentous fungi. In this study, we constructed an *A. niger* reporter strain expressing GFP-tagged v-SNARE to visualize secretory vesicle and used this strain to explore the function of seven predicted *A. niger* genes, which are homologous to *S. cerevisiae* genes playing a key role in the secretory pathway. The data obtained show that some genes are essential in both organisms, but also indicate interesting differences. The finding that some genes were not essential in *A. niger* but in *S. cerevisiae* indicates differences in the molecular mechanisms underlying the protein secretion process. For the essential *ssoA* gene, several approaches were undertaken to create a conditional secretion mutant of *A. niger*. Whereas attempts to introduce conserved temperature-sensitive mutations of the *S. cerevisiae* Sso1/Sso2p in the *A. niger* SsoA ortholog failed, a conditional *ssoA* mutant was obtained by controlled expression of *ssoA* in a *ssoA* deletion strain. Such a strain will facilitate synthetic lethal screens and the identification of high-copy number suppressors in future secretion-related studies.

Results

Localization of secretory vesicles in *A. niger*

The polarized delivery of secretory vesicles to the hyphal tips involves SNARE proteins as mediators of vesicles docking and fusion with the plasma membrane. SNARE proteins are organelle-specific thereby ensuring the fusion of a vesicle to the correct target membrane (Chen and Scheller 2001). In *S. cerevisiae* a redundant pair of highly homologous vesicular-SNARE (v-SNARE) proteins, Snc1p and Snc2p are required for the fusion of Golgi derived secretory vesicles with the plasma membrane (Protopopov et al. 1993). In order to examine the localization of secretory vesicles in *A. niger*, we constructed a reporter strain expressing a fusion protein of GFP and the v-SNARE protein, the homolog of the *S. cerevisiae* Snc1p/Snc2p proteins, named SncA in *A. niger* (Sagt et al. 2009). To minimize risks of non-functional protein expression and to prevent possible interference arising from non-physiological expression levels of the GFP-SncA fusion protein, GFP was fused to the open reading frame (ORF) of *sncA* at the N-terminus under control of its endogenous *sncA* promoter and used to replace the endogenous *sncA* gene. Notably, N-terminal tagging of SNAREs is favored over C-terminal tagging, as the C-terminal transmembrane (TM) domain is required for proper localization and function of SNAREs (Taheri-Talesh et al. 2008; Ungar and Hughson 2003). The expression cassette that targeted the fusion gene to the genomic locus of *sncA* in *A. niger* was constructed as depicted in Fig. 1a. After transformation, selected transformants were analyzed by Southern analysis and strain FG7 was selected as it contained the correct gene replacement (data not shown). FG7 was phenotypically indistinguishable from the wild-type strain with respect to growth at different temperatures as well as germination (data not shown).

The reporter strain FG7 was further analyzed by fluorescence microscopy. Bright GFP-SncA signals were observed along the hyphae but were more pronounced at the hyphal tips (Fig. 1b). The highest intensity of fluorescence was visible at the very apex of growing hyphae and at newly formed branches reminiscent of the Spitzenkörper, a vesicle-rich region present at actively growing hyphal tips of filamentous fungi also known as the vesicle supply center (Fig. 1b) (Harris et al. 2005; Steinberg 2007). The dynamic movement of vesicles in growing *A. niger* cells and the movement of the Spitzenkörper along the hyphal tip during growth were observed from four-dimensional image sets (Z-series captured over time, Supplemental video1) similar as described for *A. nidulans* and *A. oryzae* (Taheri-Talesh et al. 2008). To examine the role of the tubulin and actin cytoskeleton on the localization of secretory vesicles, the GFP-SncA reporter strain was treated with benomyl and latrunculin B, respectively, known to disrupt the

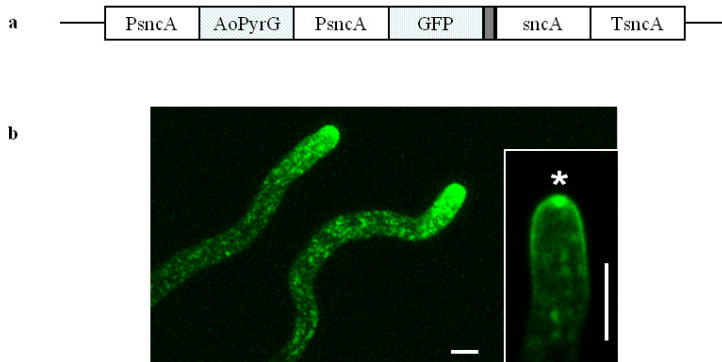


Fig. 1. Localization of v-SNARE protein SncA in living cells of *A. niger*. a) Schematic representation of the approach to label v-SNARE protein SncA with GFP. The GFP part was fused to the N-terminus of SncA and separated from SncA by a NPAFLYKVG-linker derived from the Gateway cloning technology. The construct is designed for integration at the *sncA* locus using the *A. oryzae pyrG* (*pyrG*) as a selection marker. The promoter region in front of the GFP-SncA fusion protein is about 800 bp to allow proper transcription and no interference of the *pyrG* gene. b) Confocal images of SncA localization in tip cells expressing GFP-SncA. The image represents a Z-stack of the entire hyphae showing the intracellular staining (representing secretory vesicles) as well as labeling of the plasma membrane. A clear gradient of GFP-SncA labeling towards the tip is visible. The Spitzenkörper is indicated with a star. Bar, 5 μ m.

integrity and function of the cytoskeleton (Roca et al. 2010). As a control, GFP-tubulin (Kwon et al., 2011) and SlaB-YFP (Kwon et al., 2013) reporter strains were treated with the same concentration of benomyl and latrunculin B to confirm disruption of both the tubulin and actin networks by the concentrations used (Supplemental Fig. 2). As shown in Fig. 2, benomyl treatment of the GFP-SncA strain resulted in wider and curled hyphae and reduced the polar distribution of secretory vesicles at hyphal tips. Similarly, polar distribution of secretory vesicles was also lost when the function of the actin cytoskeleton was impaired by latrunculin B. Here, lower fluorescence and reduced polar accumulation of secretory vesicles at the hyphal tip was observed. These data demonstrate that the tubulin and actin cytoskeletal networks are crucial for targeted transport of secretory vesicles towards hyphal tips of *A. niger*.

Deletion of secretion-related genes in the GFP-SncA reporter strain

To identify proteins important for the delivery of vesicles to the plasma membrane, seven candidate genes covering different aspects of polarized protein secretion in *S. cerevisiae* including SNARE proteins, secretion related GTPase and members of the exocyst complex

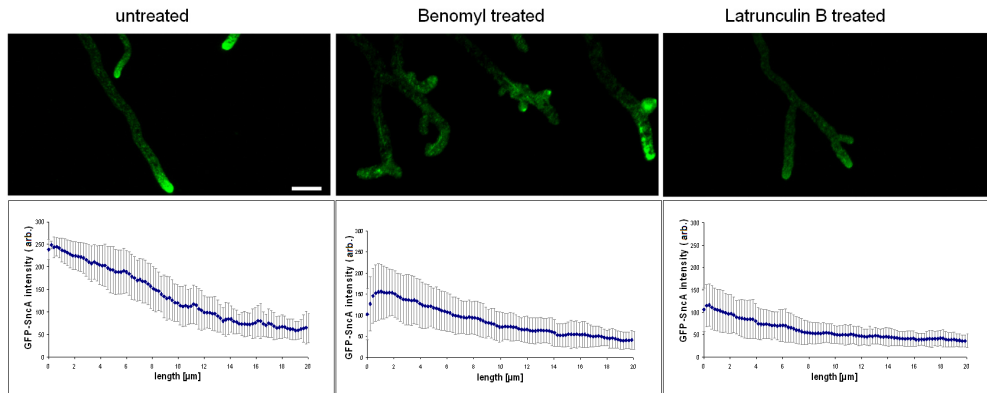


Fig. 2. Localization of v-SNARE protein SncA in living cells of *A. niger* after treatment with cytoskeleton disturbing compounds. Top panels: CLSM images showing the localization of GFP-SncA in hyphal tips. Left: untreated hyphae, middle: benomyl treated cells, right: latrunculin B treated cells. Lower panels: fluorescent intensity distributions along hyphal tip compartments ($n > 20$) within a region of 20 μm from the tip. Conidia of GFP-SncA strain were pre-grown on a MM agar plate for 2 days at 22°C and placed on a cover glass bottom culture dish containing MM media with 5 $\mu\text{g/ml}$ of benomyl or 2 $\mu\text{g/ml}$ of latrunculin B. After an additional hour incubation, the cells were examined using an inverted confocal microscope. Bar, 10 μm .

were selected (Table 1). These proteins were all selected based on high amino-acid sequence similarities with *S. cerevisiae* homologs (Pel et al., 2007, Table S2). Expression analysis of the different genes confirmed that all chosen genes are actively expressed during germination and exponential growth (Table 1). To study the roles of the seven genes and their effects on the localization of secretory vesicles in *A. niger*, respective deletion mutants were generated in both wild-type and GFP-SncA background strains. We were able to obtain viable deletion mutants for *secB*, *secC*, *srgA* and *sncA*; however, deletion of *secA*, *secH* or *ssoA* caused a lethal phenotype both in the wild-type as well as in the GFP-SncA background. Primary transformants for *secA*, *secH* or *ssoA* survived only as heterokaryons containing transformed ($\Delta secA/pyrG^+$) and untransformed nuclei (*secA/pyrG*⁻) in the absence of uridine in the medium (data not shown). Correct deletion of the target genes in purified transformants (non-essential genes) or heterokaryons (essential genes) was verified by Southern analysis (Supplemental Fig. 1 and data not shown).

The growth phenotype as well as GFP-SncA localization for the viable deletion mutants was analyzed using plate growth assays and *in vivo* fluorescence microscopy. As shown in Fig. 3, deletion of the GTPase SrgA strongly reduced the growth rate of *A. niger* and resulted in the formation of a compact colony as previously reported (Punt et al. 2001). However, the localization of GFP-SncA in young germlings was not dramatically perturbed

Table 1. Expression and predicted function of selected secretion related genes in *A. niger*.

<i>A. niger</i>	<i>S. cerevisiae</i>	ORF code	Exponential growth phase ^a	Germination ^b	Predicted function
<i>secA</i>	<i>SEC1</i>	An14g03790	0.48 ± 0.02	0.48 ± 0.03	SNARE binding protein
<i>secB</i>	<i>SEC2</i>	An11g09910	0.74 ± 0.04	1.22 ± 0.30	Guanine exchange factor of SrgA
<i>secC</i>	<i>SEC3</i>	An01g03190	0.37 ± 0.01	0.43 ± 0.02	Subunit of the exocyst complex
<i>srgA</i>	<i>SEC4</i>	An14g00010	5.40 ± 0.23	1.97 ± 0.26	Rab GTPase
<i>secH</i>	<i>SEC8</i>	An03g04210	0.69 ± 0.03	0.57 ± 0.02	Subunit of the exocyst complex
<i>ssoS</i>	<i>SSO1/2*</i>	An12g01190	1.14 ± 0.14	1.71 ± 0.04	t-SNARE
<i>sncA</i>	<i>SNC1/2*</i>	An12g07570	5.18 ± 0.19	4.00 ± 0.03	v-SNARE

Mean expression values are given in % compared to the expression level of the actin gene *actA*. Data are taken from three independent cultivations: **a**: (Jørgensen et al. 2010), **b**: (Meyer et al. 2007b). * Sso1p and Sso2p as well as Snc1p and Snc2p are paralogs and have a redundant function. Deletion of both genes is lethal in *S. cerevisiae* (Protopopov et al., 1993; Jannti et al., 2002).

in the Δ *srgA* strain despite the strong reduction in radial growth (Fig. 3). GFP-SncA localization was generally more intense along the hyphae but the majority of the signal resembled wild-type localization of secretory vesicles. SecB is the predicted guanine exchange factor (GEF) functioning as an activator of the GTPase SrgA. Interestingly, deletion of *secB* only mildly perturbed growth and did not resemble the expected Δ *srgA* phenotype. We thus examined whether another *sec2* homolog is present in the genome of *A. niger*. We noticed the presence of an uncharacterized protein of 257 amino acids in the *A. niger* genome (An15g06770) which contains a GDP/GTP exchange factor Sec2p domain (pfam06428) (Table S2). It will be of interest to determine whether this hypothetical protein which has orthologs in other filamentous fungi has an overlapping role with SecB. In agreement with the mild phenotype of the Δ *secB* strain, the localization of GFP-SncA in the Δ *secB* strain did not differ from the wild-type localization (Fig. 3).

The deletion of v-SNARE encoding gene *sncA* displayed a mild but significant phenotype with reduced radial growth (72%) when compared to the wild-type strain (Fig. 3). Morphologically, Δ *sncA* strain was identical to the wild-type strain. This was somewhat surprising since only a single copy of the *sncA* gene was found in the genome of *A. niger* ((Pel et al. 2007) and Table S2)).

In the case of Δ *secC*, predicted to encode a subunit of the exocyst complex, the observed growth defect phenotype was very severe and characterized by strongly reduced growth and aberrant morphologies of young germlings (Fig. 4a). The Δ *secC* strain in the wild-type background was able to grow on secondary selection plates only as a very

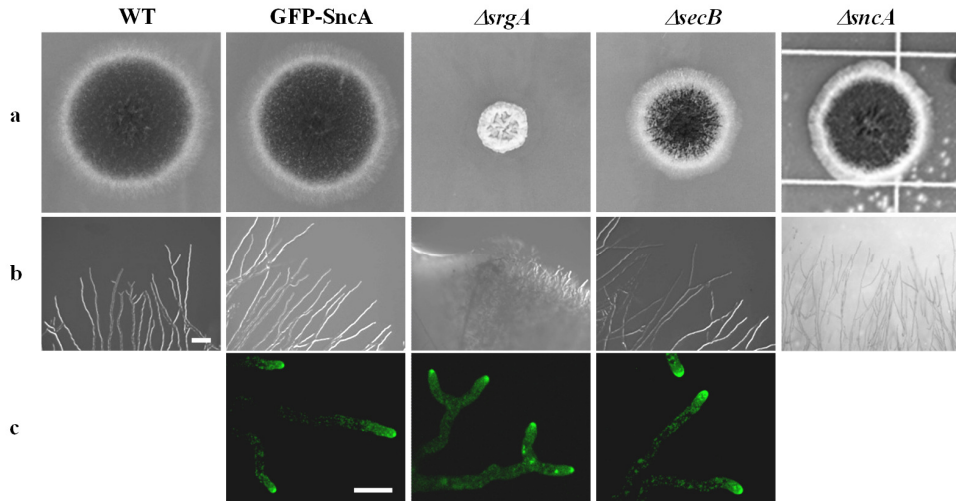


Fig. 3. Phenotypic analysis of *srgA*, *secB* and *snca* gene deletion mutants. a) Colony morphology of wild-type, GFP-SncA, $\Delta srgA$, $\Delta secB$ and $\Delta snca$ mutants after 3 days at 30°C on CM agar plates, b) hyphal morphology of the colony edge on CM agar plates (100x magnification, Bar, 100 μ m) and c) localization of GFP-SncA in hyphal tip cells on MM agar plates. Bar, 10 μ m.

compact colony after prolonged incubations at 30°C on minimal medium or on minimal medium supplemented with 1.2 M sorbitol. The primary transformants of the $\Delta secC$ in the GFP-SncA background were not able to form colonies on minimal medium and the supplementation with sorbitol was required to obtain $\Delta secC$ colonies. Although the replacement of SncA with GFP-SncA did not cause any growth-related phenotype (see above), the combination with the *secC* deletion was synthetic lethal, indicating that the function of SncA might partially be disturbed when fused to GFP. Interestingly, growth and germination of the $\Delta secC$ mutant was improved by lowering the temperature to 22°C (Fig. 4) but still partially unable to maintain polar growth as indicated by the presence of abnormally swollen hyphal tip cells. In agreement, the localization of GFP-SncA was highly affected in the $\Delta secC$ mutant. Large fluorescent spots were present not only apically but also subapically, indicating that SecC is important for correct GFP-SncA localization at the hyphal apex. However, since GFP-SncA fluorescence was still preferentially localized at swollen hyphal tips, polarity was not completely lost in the $\Delta secC$ mutant (Fig. 4b). The growth defect of the $\Delta secC$ mutant was partially remediated by supplementing the growth medium with the osmotic stabilizer sorbitol, which was paralleled by partial repolarisation of GFP-SncA signals at hyphal tips (data not shown). The partial loss of polarization of GFP-SncA in the *secC* null mutant, indicates the importance of SecC for the maintenance of the polarity axis in growing *A. niger* hyphae (Fig. 4b).

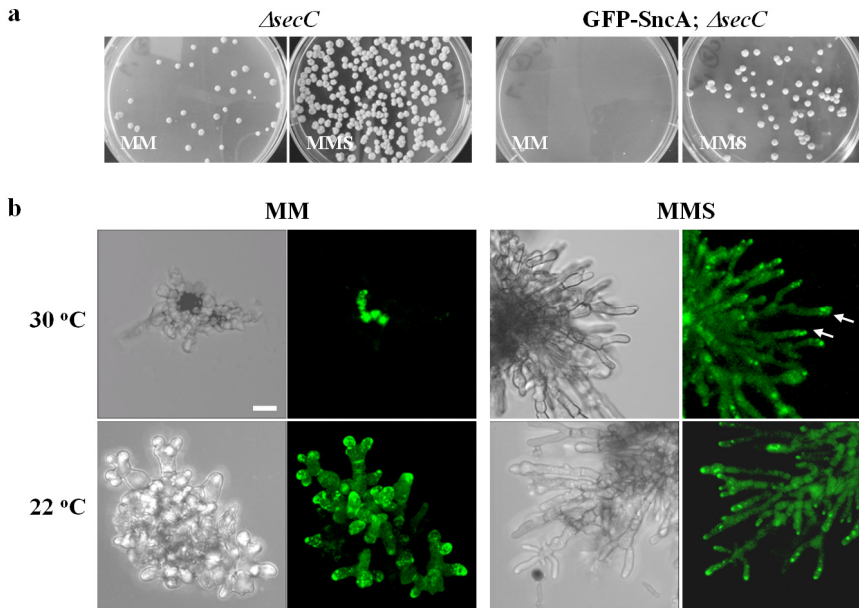


Fig. 4. Phenotypic analysis of *secC* gene deletion mutant. a) Deletions of *secC* in the wild-type and GFP-SncA background show severe growth defect that could be partially rescued by supplementation with 1.2 M Sorbitol (MMS). Deletion of *secC* in GFP-SncA shows a stronger growth defect than in a wild-type background. b) Microscopic picture of colony morphology and localization of GFP-SncA; *ΔsecC* grown on MMS after 4 days at 30°C and 22°C. Arrows indicate GFP-SncA signals at the sub-apical region of the cell. Bar, 20 μ m.

Point mutations in conserved residues of *A. niger ssoA* do not lead to ts-phenotype as in *S. cerevisiae*

Conditional mutants are powerful tools to study gene functions (Li et al. 2011). To obtain a conditional mutant that accumulates secretory vesicles under restrictive temperature, the essential *ssoA* gene was chosen, which encodes the putative target-SNARE (t-SNARE) for fusion of Golgi-derived vesicles to the plasma membrane. In *S. cerevisiae*, temperature sensitive (ts) alleles of *sso1* or *sso2* have been described to result in conditional secretion mutants (Jantti et al., 2002). The protein amino acid sequence alignment of SsoA showed that this t-SNARE is highly conserved from budding yeast to mammals (Fig. 5). A site-directed mutagenesis approach was used to create *A. niger* strains that harbor point mutations in the *ssoA* gene causing a ts-phenotype in *S. cerevisiae*. The arginine to lysine mutation in *sso1* (R196K) or *sso2* (R200K) gives rise to a ts-phenotype (Jantti et al. 2002). As shown in Fig. 5, the arginine residue located at position 212 in the SsoA protein of *A. niger* is conserved from yeast to mammals. In addition, we also applied an algorithm to

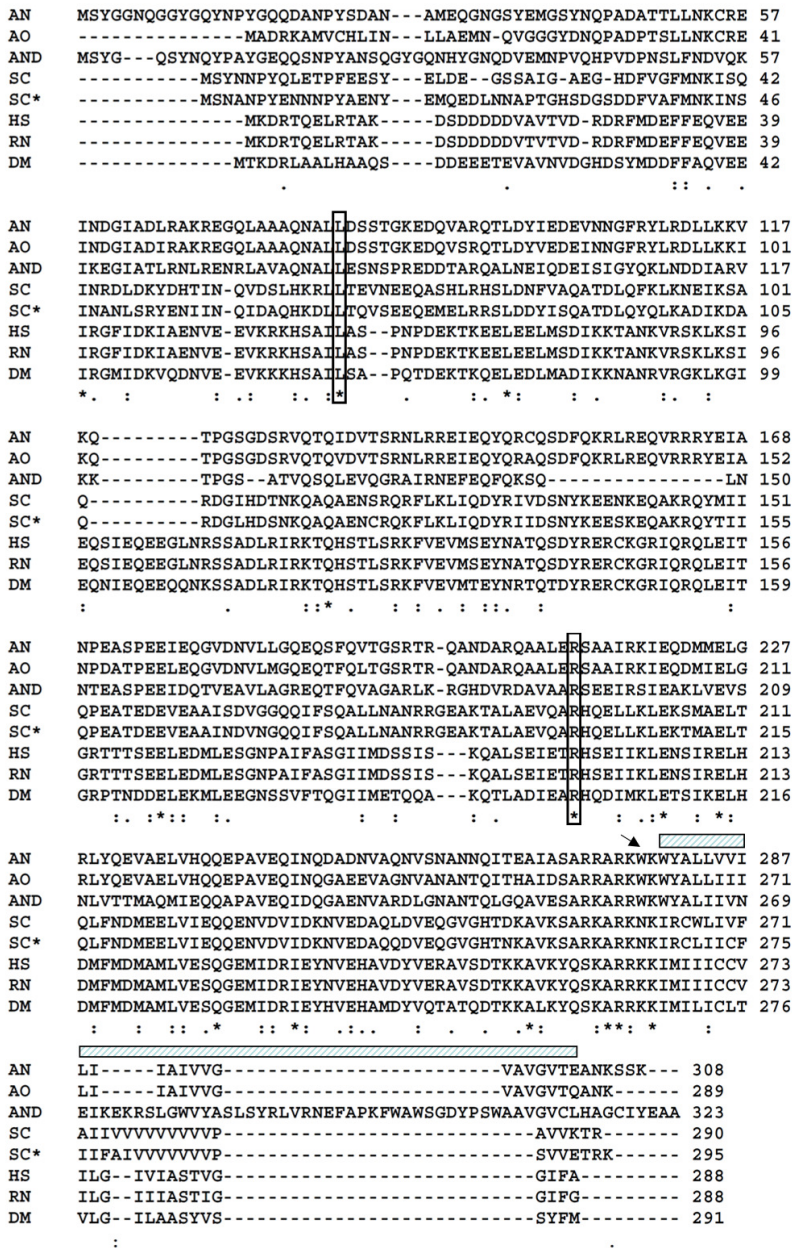


Fig. 5. Protein alignment of eukaryotic SsoA homologs. The amino acids which were chosen for site-directed mutagenesis are indicated by a box. The transmembrane domain is indicated by the hatched box above the sequence. The tryptophan at 278 aa was replaced to a stop codon to remove the transmembrane domain of SsoA; AN (*A. niger*, An12g01190), AO (*A. oryzae*, Q2TX29), AND (*A. nidulans*, Q5B7R4), SC (*S. cerevisiae*, Sso1p, P32867), SC* (*S. cerevisiae*, Sso2p, P39926), HS (*Homo sapiens*, Q16623), RN (*Rattus norvegicus*, P32851) and DM (*Drosophila melanogaster*, Q24547).

predict its mutants based solely on the amino acid sequence (Varadarajan et al. 1996). The program identified a conserved leucine residue at position 81 as a preferred candidate. For both residues (L81 and R212), a conserved and a non-conserved mutation were created. The replacement cassettes consisting of four mutant alleles, L81F, L81G, R212K or R212P and one wild-type allele as a control were constructed and targeted to the *ssmA* locus to replace the resident *ssmA* gene as shown in Fig. 6a. Each of the mutants was verified by Southern blot analysis and the respective *ssmA* allele was re-sequenced from genomic DNAs of the transformants to verify correct replacement of the native *ssmA* gene with its point-mutated alleles (data not shown).

The leucine mutants, L81F and L81G, did not show any obvious phenotype at both 30°C or 37°C (Fig. 6b). Growth of the arginine mutant R212K was unaffected at 30°C, but slightly reduced at 37°C, whereby GFP-SncA fluorescence was still present apically (Fig. 6b). Replacing the arginine at codon 212 with a proline was lethal at both 30°C and 37°C (Fig. 6b), however, the strain survived when cultivated at lower temperature such as 22°C and 25°C (Fig. 6c). The growth defect of R212P mutant was partially complemented by supplementing the medium with sorbitol. Many large and round spots of GFP-SncA signals were observed inside swollen hyphae indicating an accumulation of secretory vesicles in the R212P mutant strain at 30°C (Fig. 6c). By supplementing sorbitol as well as by lowering the temperature, the R212P mutant was able to grow much better, but not as well as the wild-type strain. To examine whether one could use the R212P mutant to accumulate secretory vesicles, the *ssmA* R212P mutant was pre-grown at 22°C to allow the formation of young germlings and then shifted to 30°C for 6 hours. The temperature shift resulted in a variety of pleiotropic phenotypes such as accumulation of vesicles, increased septation, branching and formation of empty cell compartments (Fig. 6d). So although this approach resulted in temperature sensitive mutants, the phenotype of the mutants, either too mild (R212K) or too severe (R212P), did not allow their use to study the secretory pathway in more detail.

Controlled overexpression of SsoA lacking its transmembrane domain does not result in a conditional secretion mutant

Next, another approach to create a conditional mutant was tried by using the Tet-On system which we recently established for *A. niger* (Meyer et al., 2011). The SsoA protein contains a N-terminal syntaxin domain and C-terminal transmembrane domain (TM, 280 - 302 aa, Fig. 5). We aimed to establish a conditional SsoA mutant strain in which overexpression of a truncated SsoA version lacking the TM domain (*ssmA* Δ TM) disturbs fusion of secretory

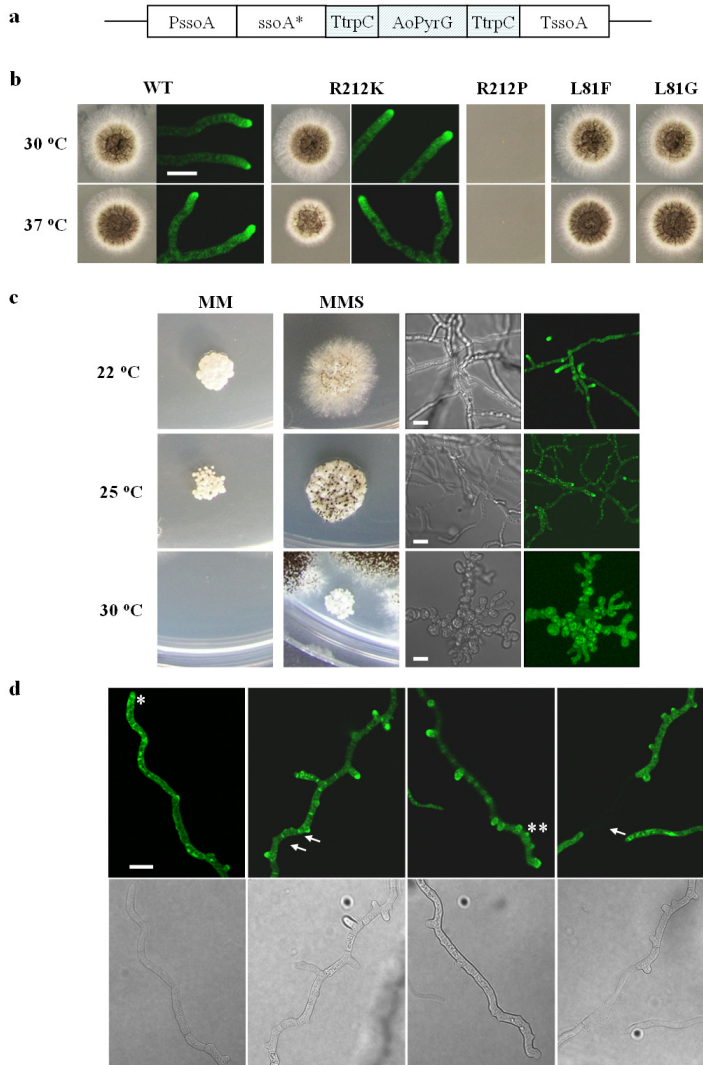


Fig. 6. Colony morphology and GFP-SncA localization in t-SNARE (*ssoA*) mutants.

a) Schematic representation of the approach to replace the wild-type t-SNARE protein (SsoA) with mutant forms of SsoA (labeled *ssoA**). b) 400 spores were point inoculated on CM agar plates and incubated for 3 days at 30°C and 37°C. The R212K mutation in the *ssoA* gene leads to reduced growth at 37°C, but no apparent mislocalization of GFP-SncA; R212P mutation is lethal, whereas the L81F and L81G mutations have no apparent phenotype. Bar, 10 µm. c) Detailed growth analysis of the R212P mutant at various temperatures and in the presence of osmotic stabilizers (MMS). Low temperatures and high osmolarity conditions improve growth. At 30°C, hyphal growth and polarity as well as polarized localization of GFP-SncA is lost. Bar, 20 µm. d) Hyphal morphology and GFP-SncA localization of the R212P mutant after shifting from 22°C to 30°C for 6 hours. The temperature shift results in a variety of phenotypes as depicted; accumulated vesicles (*), increased septation (double arrows), increased branching (**), lysis and formation of empty compartments (a single arrow). Bar, 20 µm.

vesicles with the plasma membrane and thereby provoking accumulation of secretory vesicles. First, we confirmed that expression of *ssoA* under control of the *Ptet* promoter (*Ptet-ssoA-pyrG**) did not affect growth and that *Ptet* controlled expression of *ssoA* rescues the $\Delta ssoA$ strain in a dose-dependent manner (Fig. 7 line a-c and see below). The importance of the TM domain for function of SsoA was verified by deleting the *ssoA* gene in a transformant that contained a *Ptet-ssoA Δ TM* construct at the *pyrG* locus. In this strain, the TM of endogenous *ssoA* gene was removed by replacing it with a *ssoA* gene copy that contained an early stop codon at position 278 of the SsoA protein (Fig. 5). The inability to purify viable transformants in the absence or presence of DOX showed that the TM domain is indeed essential for the function of SsoA (Fig. 7 line e and data not shown). After transformation of the *Ptet-ssoA Δ TM* cassette to the GFP-SncA reporter strain and verification of the correct integration by Southern blot analysis, the growth of *A. niger* and localization of GFP-SncA were examined by the addition of varying amounts of DOX to the growth medium. Unfortunately, overexpression of *ssoA Δ TM* did not result in a conditional mutant by interfering with growth of *A. niger* (Fig. 7 line f).

Controlled down-regulation of SsoA results in a conditional secretion mutant

A transformant containing the *ssoA* gene under the control of *Ptet* promoter present in a $\Delta ssoA$ background strain (MK34.1, Fig. 7 line c) was also analyzed by fluorescence microscopy (Fig. 7 line d). In the absence of DOX, most spores were able to germinate but soon after they lysed, empty germ tubes lacking GFP-SncA signals became visible. At very low DOX concentrations (0.2 $\mu\text{g/ml}$), cells were able to sustain growth, however, hyphal growth speed was considerably reduced and localization of GFP-SncA was severely affected before cells eventually lysed, demonstrating the importance of the t-SNARE SsoA not only for polarized growth and vesicular transport but also for maintaining cell wall integrity of the hyphal tip. Hyphal growth and apical GFP-SncA localization were completely reconstituted and comparable to the wild-type when DOX concentrations of 1.6 $\mu\text{g/ml}$ or higher were added to the growth medium (Fig. 7 line c and d).

To examine whether it was possible to induce accumulation of secretory vesicles by the removal of DOX, spores of strain MK34.1 were germinated in the presence of 2.5 $\mu\text{g/ml}$ DOX for 10 hours before the medium was replaced with DOX-free medium. Three hours after the removal of DOX, some of the germlings showed accumulated GFP-SncA signals or/and swollen hyphal tips (40%, n=10), but also germlings without morphological aberrations were found (Fig. 8a and data not shown). Microscopic analysis after 10 h of growth in the absence of DOX showed a heterogenic mixture of cells. About 25% of young

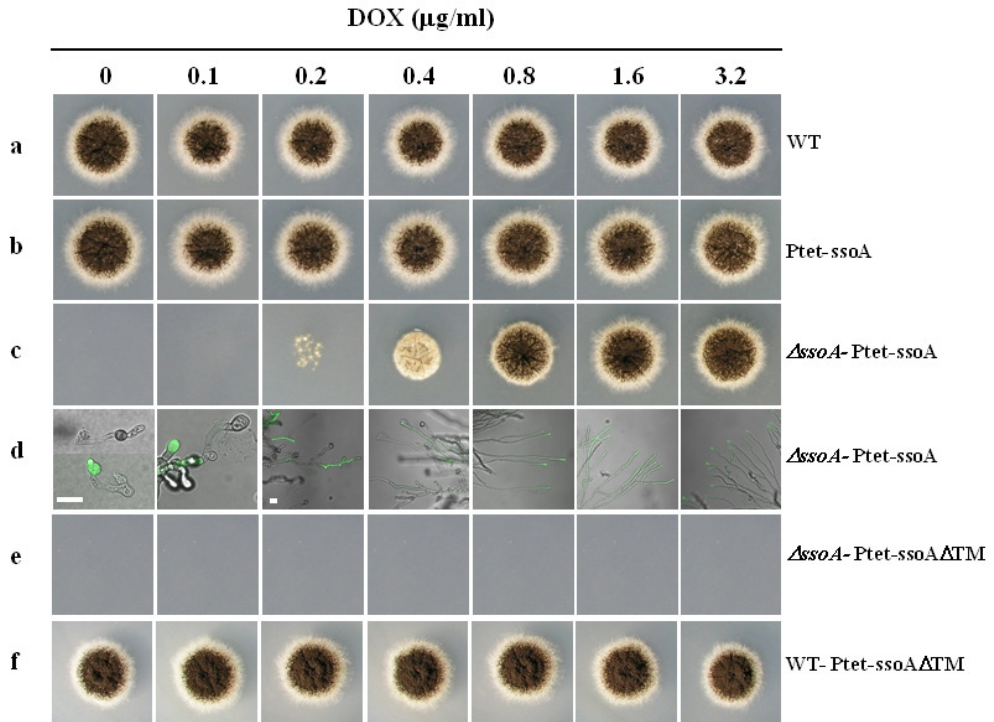


Fig. 7. Growth phenotype of strains overexpressing *ssmA* or *ssmA ΔTM* in wild-type or ΔssmA background. a) Growth of the wild-type is not affected by the presence of DOX; b) overexpression of *ssmA* in wild-type background does not affect growth; c) the lethal phenotype of *ssmA* deletion can be rescued by controlled and tunable expression of *ssmA*; d) microscopic analysis of GFP-SncA localization in hyphae from the ΔssmA -Ptet-*ssmA* strain at various DOX concentrations; e) the transmembrane (TM) domain of SsoA is essential for growth; f) overexpression of the *ssmA ΔTM* in wild-type strain does not interfere with growth; a-f) 10^3 spores were inoculated on MM supplemented with DOX concentrations indicated. Plates were cultivated for 3 days at 30°C. Bar, 20 μm .

germlings showed wild-type morphology, whereas the remaining germlings were characterized by swollen hyphal tips (Fig. 8b and data not shown). Apparently, residual intracellular amounts of SsoA were still present in some cells, which prevented a synchronous response of all germlings.

Discussion

In order to set the basis for systematic analysis of the protein secretion pathway in *A. niger*, we established a GFP-tagged vesicular SNARE reporter strain, GFP-SncA, to visualize the

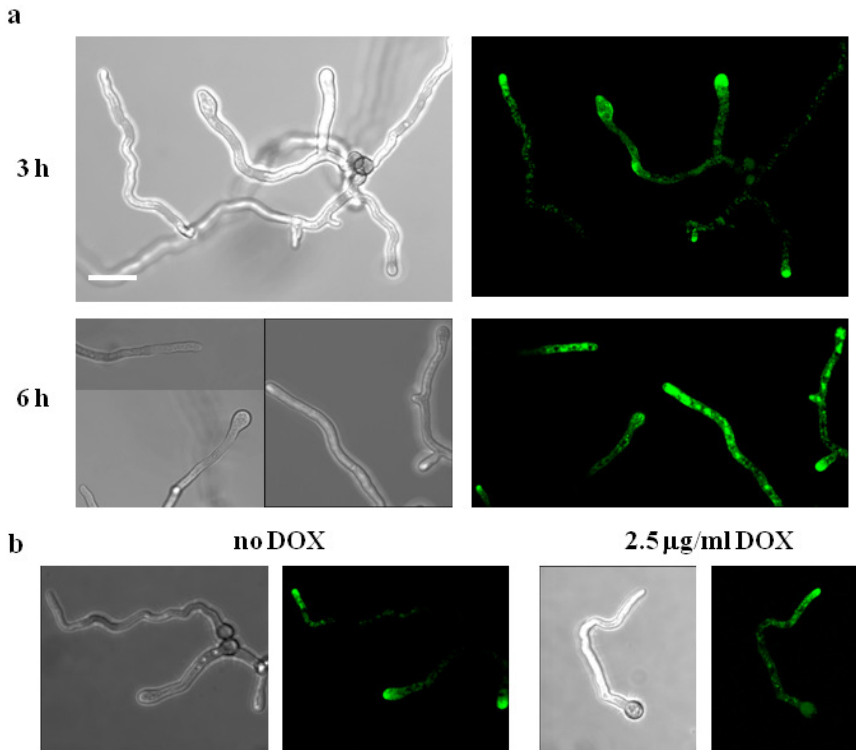


Fig. 8. Morphological phenotype and GFP-SncA localization resulting from controlled down-regulation of *ssoA*. a) Three and six hours after removal of DOX, accumulated GFP-SncA signals in swollen hyphal tips were observed, but also germlings without morphological aberrations were found. Spores were pre-grown on MM supplemented with 2.5 µg/ml of DOX at 30°C for 10 hours after which the medium was replaced with DOX free medium. b) Growth in the absence of DOX showed varying phenotypes after 10 hours of cultivation in DOX-free medium. Bar, 20 µm.

localization and dynamics of secretory vesicles. The localization of SncA homologs was reported in yeast as well as filamentous fungi including *S. cerevisiae*, *T. reesei*, *A. oryzae* and *A. nidulans* (Furuta et al. 2007; Hayakawa et al. 2011; Kuratsu et al. 2007; Taheri-Talesh et al. 2008; Valkonen et al. 2007). Similar to previous studies in filamentous fungi, GFP-SncA is present in intracellular structures representing secretory vesicles and/or endocytic vesicles. High levels of GFP-SncA are also present in the Spitzenkörper of *A. niger* and a tip gradient GFP-SncA localization was observed (Fig. 1). Occasionally, GFP-SncA signals were also observed at septa (data not shown), indicating the involvement of SncA in both hyphal tip secretion as well as septum-directed secretion that has recently been reported for SncA in *A. oryzae* (Hayakawa et al. 2011). In filamentous fungi, it is believed that the long distance transport of secretory vesicles from the sub-apical part to the

apex of hyphal tips takes place along microtubules (MT) powered by kinesin motor proteins. Afterwards, secretory vesicles are transferred either directly to the vesicle supplying center or to actin cables by myosin motor proteins and eventually fuse with the plasma membrane via SNARE complexes to release their cargos into the environment (Saloheimo and Pakula 2012; Steinberg 2007; Taheri-Talesh et al. 2008; Taheri-Talesh et al. 2012). The results shown in Fig. 2 support the importance of both the actin and the tubulin cytoskeletal elements for polarized transport and accumulation of secretory vesicles at hyphal tips of *A. niger*.

The GFP-SncA reporter strain was used to study the function of seven *A. niger* genes, whose orthologs are involved in vesicle transport in *S. cerevisiae*. Unlike *S. cerevisiae*, in which most of the selected candidate genes are essential for growth, *secB* (*SEC2*) and *sncA* (*SNC1*) genes are dispensable for *A. niger*, indicating molecular differences in the organization of secretion processes between yeast and filamentous fungi. Genetic redundancy in *A. niger* might explain this discrepancy, and further analysis of potential candidate genes exerting overlapping functions will require follow-up studies (see below).

It has previously been demonstrated that the *A. niger* SncA protein mediates the fusion of vesicles to the plasma membrane (Sagt et al. 2009). By fusing SncA to the peroxisome membrane using a peroxisomal anchor protein, peroxisomes were targeted to the plasma membrane where they fused with it, resulting in the secretion of peroxisomal cargoes (Sagt et al. 2009). Despite such an important cellular function, deletion of *sncA* had surprisingly only a very small effect on the growth of *A. niger*. A possible explanation for this might be the presence of alternative v-SNAREs, which are functionally redundant with SncA. However, all genome annotations of several filamentous fungi such as *T. reesei*, *Neurospora crassa*, *A. oryzae*, *A. nidulans* and *A. fumigatus* indicate that these fungi contain only a single copy of *sncA* in their genome (Gupta and Brent Heath 2002; Kienle et al. 2009; Kuratsu et al. 2007; Valkonen et al. 2007) as also reported for *A. niger* (Pel et al. 2007). Still, we considered the possibility of a redundant v-SNARE in the *A. niger* genome and searched the genome database for a SncA homolog (Table S2). A potential v-SNARE encoding gene with the highest level of similarity to SncA, and which contains a C-terminal synaptobrevin domain like SncA, is An08g07470 (47% identity, 66% similarity). An08g07470 contains a N-terminal longin domain (Wen et al. 2006) which is not present in SncA, thus making An08g07470 a larger protein (269 amino acids) than SncA (135 aa). Compared to *S. cerevisiae*, An08g07470 is most similar to the vacuolar v-SNARE component Nyv1p which is involved in homotypic vacuolar docking and fusion (Nichols et al. 1997). In *A. oryzae*, this v-SNARE is interestingly also localized to the plasma membrane, although to a lesser extent than the Snc1p homolog (Kuratsu et al. 2007). Hence, An08g07470 of *A. niger* could encode a functionally redundant protein for SncA.

The *S. cerevisiae* Sec2p protein is the guanine exchange factor (GEF) for the secretion related Rab GTPase Sec4p and its function is well characterized (Itzen et al. 2007; Walch-Solimena et al. 1997). GEFs stimulate the exchange of GDP for GTP, thereby activating its corresponding GTPase. Based on the results obtained in *S. cerevisiae*, deletion of the Sec2p ortholog in *A. niger* (SecB) was expected to result in a similar phenotype as the Sec4p ortholog (SrgA). However, deletion of *secB* in *A. niger* resulted in an almost wild-type phenotype in terms of fast hyphal growth and hyphal morphology, which is different from the Δ *srgA* phenotype (Fig. 3). The situation in *A. niger* is already different from that in *S. cerevisiae* as in *A. niger* the Sec4p ortholog itself is not essential for growth as is Sec4p in *S. cerevisiae*. Unlike other protein families, GEFs for different Rab GTPases do not share much sequence identity, making it difficult to predict protein function from sequence data (Segev 2001b). GEFs are considered to be GTPase specific, however, there are examples showing that one GEF complex acts on two GTPases; e.g. the TRAPP complex acts as a GEF for both Ypt1p and Ypt31/32p in *S. cerevisiae* (Jones et al. 2000). We thus assume that the genome of *A. niger* might encode alternative Rab GEF(s) which could activate SrgA in the absence of SecB. A possible candidate protein is An15g06770 which contains a GDP/GTP exchange factor Sec2p domain (pfam06428).

Using the essential *A. niger* *ssoA* gene, orthologous to the *S. cerevisiae* plasma membrane t-SNAREs Sso1/2p, three approaches were followed to create a conditional vesicles transport mutant of *A. niger*. First, we tried to establish a temperature sensitive mutant based on introducing ts-alleles of Sso1/2p in the *A. niger* SsoA ortholog. Despite the high sequence similarity and conservation of amino acid residues, introduction of the respective point mutations in SsoA did not result in a useful phenotype as it was either too mild or too severe (Fig. 6). The second approach focused on the establishment of a mutant which accumulates secretory vesicles via induced overexpression of a truncated SsoA version lacking the essential TM-domain (SsoA Δ TM). Several studies on SNARE-mediated membrane fusion including Sso or Snc proteins demonstrated the importance of the TM domain for facilitating membrane fusion through the interaction of these TM domains (Fdez et al. 2010; Grote et al. 2000; Langosch et al. 2007; Lu et al. 2008). In agreement, this study provides evidence that the TM domain of the *A. niger* SsoA is also essential for its function (Fig. 7 line e). However, our data also clearly shows that a Tet-On based overexpression of SsoA Δ TM, does not affect growth of *A. niger* (Fig. 7 line f). Note that it is unlikely that Tet-On mediated expression is insufficient to induce overexpression of the endogenous *ssoA* expression, as it was previously shown that the Tet-On system enables expression levels similar to *gpdA* expression (Meyer et al., 2011), which in fact would be 80-fold higher than *ssoA* expression (data not shown).

The third approach followed a strategy in which SsoA was down-regulated in a controlled manner using the Tet-On system. For this purpose, a strain was generated, which expressed *ssoA* from the *Ptet* promoter in a Δ *ssoA* background strain. The resulting strain (MK34.1) is only viable in the presence of DOX but not in its absence. A wash-out experiment showed that pre-cultivation in medium containing 2.5 μ g/ml DOX followed by a shift into DOX-free medium resulted in a conditional mutant phenotype characterized by the accumulation of secretory vesicles in the cytosol (Fig. 8a). However, we also observed that the accumulation of secretory vesicles was highly heterogeneous among germlings - some displayed the mutant phenotype and some localized the secretory vesicles still apically. This heterogeneous phenotype might possibly be explained by remnant intracellular concentrations of DOX and/or SsoA, e.g. due to low turnover rates. In both cases, slight amounts of functional SsoA might be still present in some cells thus sustaining normal growth.

Supportive for this explanation is the observation that the concentration of DOX that was used to make the spore plates had an effect on the germination characteristics. Spores that were taken from a plate that contained 100 μ g/ml DOX formed normal germlings after transfer into medium lacking DOX. Apparently, a high concentration of DOX in the spore plates results in high *ssoA* mRNA and/or SsoA protein levels, thereby allowing germination without further induction of *ssoA*. Likewise, we noted that the concentration of DOX in the medium used for the pre-growth affected the outcome of the wash out experiment. A DOX concentration of 20 μ g/ml during pre-growth (instead of the 2.5 μ g/ml as shown in Fig. 8) and subsequent transfer into DOX-free medium increased the time to observe a morphological effect of SsoA depletion dramatically.

Taken together, we showed that controlled downregulation of SsoA via the Tet-On expression system can be used to create a conditional vesicular transport mutant of *A. niger*. However, this strain can display a heterogenous phenotype, which can partially be adjusted by controlling DOX concentrations. Such a conditional mutant will be an important tool for further work to unravel the mechanisms that enable *A. niger* to be an efficient protein secretor.

Methods

Strains, culture conditions and molecular techniques

The *Aspergillus niger* strains used in this study are listed in Table 2. Strains were grown on minimal medium (MM) containing 1% (w v⁻¹) glucose as carbon source (Bennett and

Lasure 1991). Complete medium (CM) consists of MM with the addition of 0.1% (w v⁻¹) casamino acids and 0.5% (w v⁻¹) yeast extract. When required, plates were supplemented with uridine (10 mM), hygromycin (100 µg ml⁻¹), doxycycline (Dox, 1-100 µg ml⁻¹) or sorbitol (1.2 M). Transformation of *A. niger* and fungal chromosomal DNA isolation was performed as described (Meyer et al. 2010b).

Construction of deletion cassettes, mutant alleles and expression cassettes

Standard PCR and cloning procedures were used for the generation of all constructs (Sambrook & Russell, 2001). All PCR amplified DNA sequences and cloned fragments were confirmed by DNA sequencing (Macrogen). All primers used in this study are listed in Table S1 in the supplemental material. Successful deletions or correct integration of GFP-constructs or mutant alleles were verified by Southern analysis.

The GFP-SncA construct was made using a combination of fusion PCR approaches combined with the MultiSite Gateway Three-Fragment Vector Construction Kit (Invitrogen) according to the manufacturer's instructions. Firstly, five individual DNA fragments were amplified by PCR using the primers listed in Table S1. These fragments include two *sncA* promoter regions (~950 bp and ~800 bp in length), the *sncA* ORF and terminator region of *sncA* (~1.2 kb), the *A. oryzae pyrG* (*AopyrG*) fragment (~1.8 kb) and the GFP fragment (~700 bp). The construct is schematically depicted in Fig. 1. The *AopyrG* marker is flanked by two identical promoter regions of *sncA* which allows efficient looping out of the *AopyrG* marker (Meyer et al. 2010b), for subsequent transformations using the *AopyrG* marker. The first promoter fragment was fused to the *AopyrG* fragment and the second promoter fragment was fused to GFP by a fusion PCR. The GFP-SncA final expression cassette was constructed using the three fragments, promoter-*AopyrG*, promoter-GFP and *sncA* ORF and terminator by the MultiSite Gateway Three-Fragment Vector Construction Kit (Invitrogen).

Constructs to delete the *secA*, *secB*, *secC*, *secH*, *ssoA* or *sncA* gene were made as follows: respective 5' flanking sequences (~700 bp) were obtained as *KpnI-XhoI* fragments and 3' flanking sequences (~700 bp) were obtained as *HindIII-NotI* fragments by PCR using genomic DNA from strain N402 as a template. The respective 5' region *KpnI-XhoI* fragments, 3' *HindIII-NotI* fragments and a 1.7 kb *HindIII-XhoI* fragment from pAO4-13 (de Rooter-Jacobs et al. 1989) containing *AopyrG* gene were cloned into the pBluscript-SK⁺ backbone prepared by digestion with *KpnI* and *NotI*. In the case of *sncA*, a 3.1 kb of the hygromycin resistance cassette isolated from pAN7-1 (Punt et al. 1987) was used to replace the *sncA* ORF. For *srgA* gene deletion cassette was kindly provided by Bernhard Seiboth, Vienna, Austria.

Table 2. Strains used in this work.

Strain	Relevant genotype	Source
N402	<i>cspA1</i> (derivative of ATCC9029)	(Bos et al. 1988)
AB4.1	<i>pyrG</i> ⁻	(van Hartingsveldt et al. 1987)
AO4.13	<i>pyrG</i> ⁺ (derivative of AB4.1 containing <i>A. oryzae pyrG</i>)	(Kwon et al. 2011)
MA70.15	Δ <i>kusA pyrG</i> (derivative of AB4.1)	(Meyer et al. 2007a)
MA169.4	<i>kusA::DR-amdS-DR pyrG</i> ⁻	(Carvalho et al. 2010)
MA234.1	<i>kusA::DR-amdS-DR pyrG</i> ⁺	This work
FG7	Δ <i>kusA pyrG</i> ⁺ <i>egfp::sncA</i> (derivative of MA70.15)	This work
MK27.1	<i>kusA::DR-amdS-DR pyrG</i> ⁺ , Δ <i>sncA hyg</i> ^r (derivative of MA234.1)	This work
MK12.1	Δ <i>kusA pyrG</i> <i>egfp::sncA</i> (derivative of FG7)	This work
MA164.1	Heterokaryon Δ <i>kusA</i> , <i>secA/pyrG</i> ⁻ , Δ <i>secA/pyrG</i> ⁺	This work
MK19.1	Δ <i>kusA pyrG</i> ⁺ Δ <i>secB egfp::sncA</i> (derivative of MK12.1)	This work
MA165.1	Δ <i>kusA pyrG</i> ⁺ Δ <i>secB</i> (derivative of MA70.15)	This work
MK20.2	Δ <i>kusA pyrG</i> ⁺ Δ <i>secC egfp::sncA</i> (derivative of MK12.1)	This work
MK16.2	<i>kusA::DR-amdS-DR pyrG</i> ⁺ Δ <i>secC</i> (derivative of MA169.4)	This work
MK17.5	Heterokaryon Δ <i>kusA</i> , <i>secH/pyrG</i> ⁻ , Δ <i>secH/pyrG</i> ⁺	This work
MK18.A	Δ <i>kusA pyrG</i> ⁺ Δ <i>srgA egfp::sncA</i> (derivative of MK12.1)	This work
MK15.A	<i>kusA::DR-amdS-DR pyrG</i> ⁺ Δ <i>srgA</i> (derivative of MA169.4)	This work
MA168.5	Heterokaryon Δ <i>kusA</i> , <i>ssoA/pyrG</i> ⁻ , Δ <i>ssoA/pyrG</i> ⁺	This work
MK28.1	Δ <i>kusA pyrG</i> ⁺ <i>ssoA egfp::sncA</i> (derivative of MK12.1)	This work
MK29.3	Δ <i>kusA pyrG</i> ⁺ <i>ssoAL81F egfp::sncA</i> (derivative of MK12.1)	This work
MK30.1	Δ <i>kusA pyrG</i> ⁺ <i>ssoAL81G egfp::sncA</i> (derivative of MK12.1)	This work
MK31.2	Δ <i>kusA pyrG</i> ⁺ <i>ssoAR212K egfp::sncA</i> (derivative of MK12.1)	This work
MK32.2	Δ <i>kusA pyrG</i> ⁺ <i>ssoAR212P egfp::sncA</i> (derivative of MK12.1)	This work
MK22.3	Δ <i>kusA TetO7::Pmin::ssoA pyrG</i> ⁺ (derivative of MK12.1)	This work
MK24.20	Δ <i>kusA TetO7::Pmin::ssoAΔTM pyrG</i> ⁺ (derivative of MK12.1)	This work
MK34.1	Δ <i>kusA ΔssoA hyg</i> ^r <i>TetO7::Pmin::ssoA pyrG</i> ⁺ (derivative of MK12.1)	This work
MK33.1	Heterokaryon Δ <i>kusA</i> , <i>ssoA/hyg</i> ^r , Δ <i>ssoA/hyg</i> ^{r+} <i>TetO7::Pmin::ssoAΔTM pyrG</i> ⁺ (derivative of MK12.1)	This work

The *P**ssoA::ssoA::TtrpC::AopyrG::TtrpC::T**ssoA* construct for generating mutant alleles of *ssoA* (encoding SsoA^{L81F}, SsoA^{L81G}, SsoA^{R212K} and SsoA^{R212P}) was made by PCR amplification and subsequent cloning of four fragments. The four fragments include the ~0.7 kb promoter of *ssoA* as a *KpnI-XhoI* fragment, the ~1.2 kb ORF of *ssoA* as a *XhoI-EcoRI* fragment, a ~2.8 kb *NotI-AscI* fragment containing *TtrpC-AopyrG-TtrpC* (TPT)

selection marker and a ~0.7 kb *AscI-NotI* fragment containing the terminator region of *ssmA*. The *TrpC* repeats allow efficient loop out of the *pyrG* marker to allow subsequent transformations with the *pyrG* marker. Firstly, the 0.7 kb *KpnI-XhoI* promoter fragment was cloned into the pBluscript-SK⁺ backbone prepared by digestion with *KpnI* and *XhoI* resulting pMK1. Then the fragments *NotI-AscI* TPT and the *AscI-NotI* terminator of *ssmA* were cloned into *NotI* restricted pMK1 to give pMK2. Finally, the *XhoI-EcoRI* ORF of *ssmA* was cloned into *XhoI-EcoRI* restricted pMK2. Mutant alleles of *ssmA* (encoding SsoA^{L81F}, SsoA^{L81G}, SsoA^{R212K} and SsoA^{R212P}) were generated by PCR using primers carrying respective mutations and *XhoI-EcoRI* ends. The DNA fragments encoding the respective mutations were cloned into *XhoI-EcoRI* restricted pMK2.

For the construction of conditional *ssmA* overexpression using the Tet-on system, the *ssmA* ORF or *ssmA* ORF truncated transmembrane domain domain (*ssmAΔTM*) were cloned into pVG2.2 (Meyer et al. 2011a) and the resulting plasmid was transformed for targeted integration at the *pyrG* locus using the *pyrG** marker. After Southern analysis, strains were selected (MK22.3 and MK24.20) that contained with wild-type *ssmA* gene or *ssmAΔTM* gene at the *pyrG* locus under control of the tetracycline inducible promoter. These strains were also used to delete the *ssmA* gene. To do so, the *ssmA::pyrG* disruption cassette (see above) was altered by replacing *AopyrG* selection marker with the *HindIII-XhoI* hygromycin resistance cassette that was obtained from pAN7-1 (Punt et al. 1987).

Microscopy

Light microscopic pictures for the edge of the colony were captured using an Axioplan 2 (Zeiss) equipped with a DKC-5000 digital camera (Sony). For the light and fluorescence images for GFP-SncA, pictures were captured with 40x C-apochromatic objective on an inverted LSM5 microscope equipped with a laser scanning confocal system (Zeiss Observer). LSM5 was also equipped with an incubator to control the cultivation temperature. The observation conditions for the life-imaging of hyphae were the same as described previously (Kwon et al. 2011). For time-lapse microscopy, in total seven z stacks (0.8 μm interval) were taken in 60 s time intervals. The time-lapse movie showing 4 frames per second was assembled using ZEN2009 software (Zeiss).

For the DOX washout experiments, cells were grown and observed on chamber glass slides (Lab-Tek II Chamber #1.5 German Coverglass System) with 2.5 μg/ml of DOX for 10 h at 30°C. Subsequently, the culture medium containing DOX was gently removed from the observation chamber with a transfer pipette and replaced with medium without DOX. This was repeated at least five times. For benomyl and latrunculin B treatments, cells were grown on MM agar plate for 2 days at 22°C to avoid sporulation. The mycelium was cut

with a scalpel, placed upside down on a cover glass bottom culture dish containing one drop of MM containing 5 $\mu\text{g/ml}$ benomyl or 2 $\mu\text{g/ml}$ latrunculin B respectively, and incubated at 22°C for an additional hour before microscopically examined.

Acknowledgements

We acknowledge Sjors Noteboom for his contributions to cloning experiments and Cees van den Hondel for helpful and stimulating discussions. This project was carried out within the research programme of the Kluyver Centre for Genomics of Industrial Fermentation which is part of the Netherlands Genomics Initiative / Netherlands Organization for Scientific Research.

General Discussion

The ability of *Aspergillus niger* to secrete a high quantity and wide range of enzymes and organic acids to the extracellular environment makes this fungus a versatile cell factory (Pel et al. 2007). Due to its well annotated genome sequence, the rapid development of omics technologies (mainly transcriptomics and proteomics), and genetic tools such as newly established gene transfer systems, *A. niger* has become a model fungus for industrially exploited filamentous fungi (Adav et al. 2010; Carvalho et al. 2010; Fleissner and Dersch 2010; Jacobs et al. 2009; Meyer et al. 2011b; Pel et al. 2007). Like other filamentous fungi, a key feature of *A. niger* is the highly polarized growth of its hyphae by apical extension at the hyphal tip. After spore germination, the axis of growth remains fixed in the primary germ tube while the formation of secondary germ tubes and subapical lateral branches establish new growth axes (Momany 2002). This polar or asymmetric cell growth is found not only in filamentous fungi but also ubiquitously throughout other phyla e.g. filamentous bacteria (actinomycetes), pollen tubes, plant root hairs and developing neuronal cells (Horio 2007). Because of the relatively simple cytoskeletal organization and similarity to higher eukaryotic systems, the morphology of filamentous fungi including *A. niger* are important model systems to study polar cell growth (Horio 2007). In addition, fungal morphology is an important factor determining the efficiency of product formation in terms of yield, mixing or mass/oxygen transfer in industrial fermentations (Grimm et al. 2005; McIntyre et al. 2001; Papagianni 2004). Better understanding of the process determining morphology could lead to the improvement of fungal cells for the production of enzymes or acids.

Polarized growth and secretion involve many factors including transport of secretory vesicles containing different cargos to the tip of the cell. Direction of growth is determined by a vesicle-rich region located in the hyphal tip called the Spitzenkörper (Steinberg 2007; Virag and Harris 2006b). Moving the Spitzenkörper from its apical position by optical tweezers has substantial effects on the cell shape, which indicates that the position of the Spitzenkörper is crucial and directs polar growth (Bartnicki-Garcia et al. 1995). Secretory vesicles are transported along the hyphae to the Spitzenkörper via microtubules (MT) powered by kinesin motor proteins while short distance transport from the Spitzenkörper to the plasma membrane is mediated via the actin cables by myosin motor proteins (Fig. 1) (Saloheimo and Pakula 2012; Steinberg 2007; Taheri-Talesh et al. 2008; Taheri-Talesh et al. 2012). Thus the polarity of the cytoskeleton (tubulin and actin filaments) is a crucial factor in establishing and maintaining polar growth and secretion. Rho GTPases present in many systems including mammalian cells are well known to regulate morphology by

organizing the dynamics of the actin cytoskeleton (Bosco et al. 2009; Heasman and Ridley 2008; Park and Bi 2007; Ridley 2006). We systematically investigated the function of all members of the Rho family GTPases present in *A. niger* (Chapter 2). Based on loss-of-function studies, we showed that six Rho GTPases (RacA, CftA, RhoA, RhoB, RhoC, RhoD) exert distinct and overlapping functions during the life cycle of *A. niger*. Additionally the localization of RacA protein was observed as a crescent shape at the actively growing hyphal tips, which is incorporated into Fig. 1.

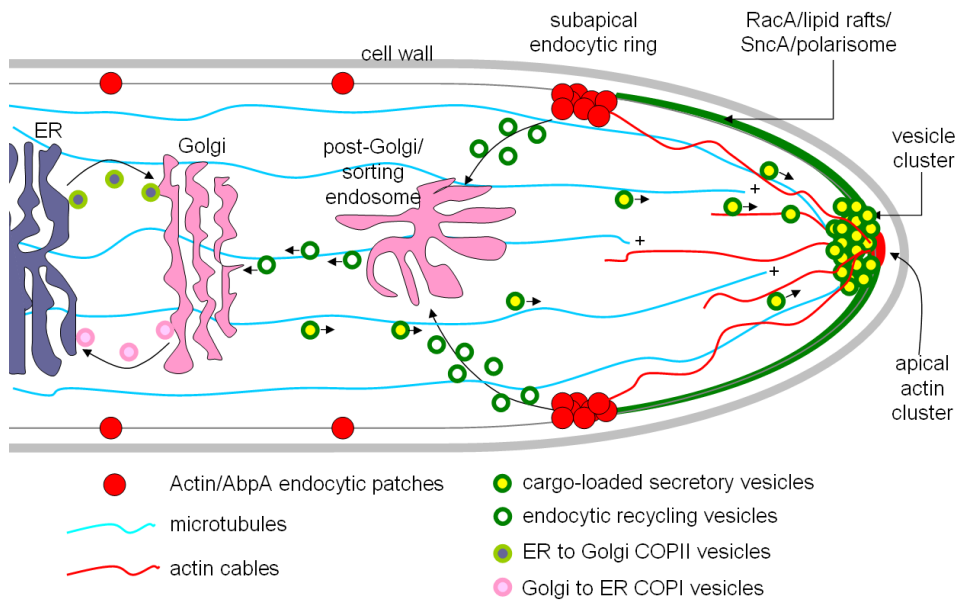


Fig. 1. A schematic model for polarized growth and secretion in *A. niger*. Secretory vesicles move to the Spitzenkörper (vesicle clusters) via the microtubules powered by kinesin motor proteins while short distance transport from the Spitzenkörper to the plasma membrane (PM) acts via the actin cables by myosin motor proteins (Steinberg 2007; Taheri-Talesh et al. 2008; Taheri-Talesh et al. 2012). The transport of the secretory vesicle cargo from the ER to the Golgi is mediated by the COPII carrier while retrieval of escaped luminal proteins as well as other machinery required for optimal anterograde (ER to Golgi) transport is mediated by the COPI carrier. Golgi derived secretory vesicles fuse with the PM, releasing their contents and the components of the membranes of the secretory vesicles. As the tip grows, the ring of actin/AbpA endocytic patches moves forward, removing SncA and other vesicle membrane components from the PM and incorporating them into endocytic vesicles for recycling. Adapted from (Taheri-Talesh et al. 2008).

Interestingly, a gene encoding the predicted acetyl-coenzyme A (CoA) transporter (An02g13410) was consistently up-regulated in all the compared protein overexpression and ER stress conditions transcriptomes (Chapter 4). The putative acetyl-CoA transporter (An0213410) is predicted to contain a transmembrane spanning domain like the acetyl-CoA transporter AT-1 in humans (based on TMHMM) and shares 38% amino acids identity (Pehar and Puglielli 2013). In higher eukaryotes, this protein is shown to be involved in translocation of acetyl-CoA from the cytosol into the ER. The ER localized acetyl-CoA is subsequently used for acetylation of ER-transiting proteins including membrane proteins and possibly secretory proteins, thereby improving the folding efficiency (Fig. 2) (Jonas et al. 2010; Pehar and Puglielli 2013). Only acetylated nascent proteins can leave the ER and enter the Golgi where they are deacetylated (Fig. 2). Interestingly, also in mammalian

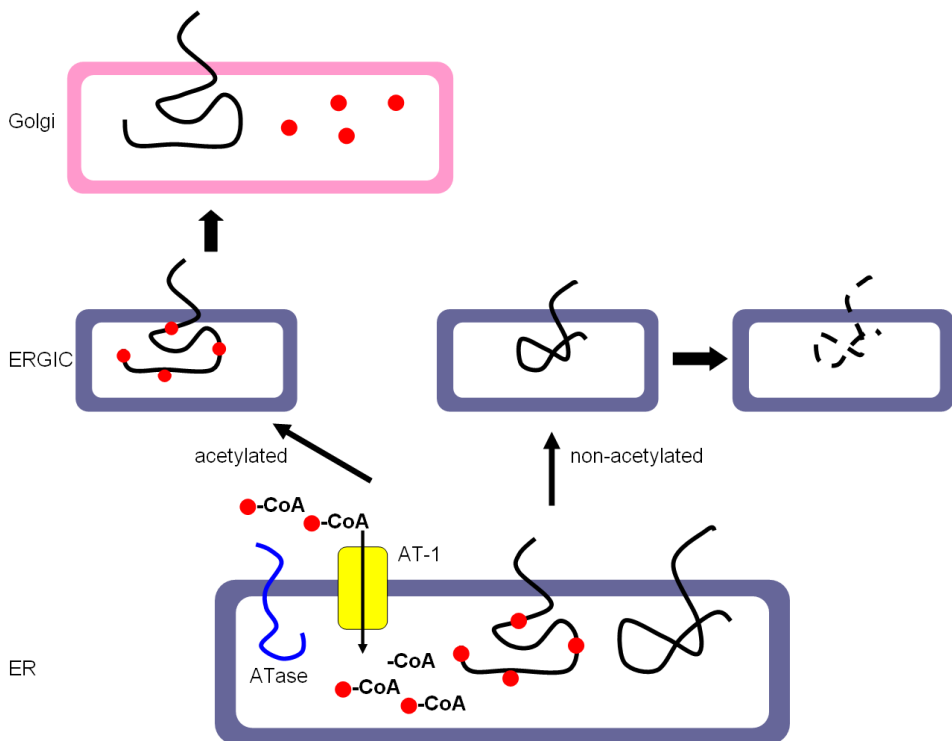


Fig. 2. A schematic view of acetylation in the ER. Acetyl- CoA is translocated from the cytosol into the lumen of the ER by an acetyl-CoA transporter (AT-1) and subsequently used for acetylation of nascent ER-transiting proteins including membrane proteins and possibly secretory proteins by an acetyltransferase (ATase). If acetylated, the nascent proteins can reach the Golgi where they are deacetylated and complete maturation while non-acetylated proteins are retained and degraded in the ER Golgi intermediate compartment (ERGIC). The acetyl group is shown as a red circle. Adapted from (Pehar and Puglielli 2013).

cells the gene encoding the acetyl-CoA transporter (AT-1) is up-regulated in response to ER stress (Shaffer et al. 2004). This suggests conservation of the possible role of acetylation in the ER as a part of the unfolded protein response (UPR) in eukaryotic cells including filamentous fungi.

Growth and secretion in fungi are considered to be tightly linked processes. However, with previous results from our group (Jørgensen et al. 2009) and our current results (Chapter 4), we observed a growth rate independent increase in protein secretion (Kwon et al. 2013b). The mechanism(s) which enables *A. niger* to secrete more proteins although cultivated at the same growth rate is not well known. Some possible mechanisms have been addressed in the general introduction part of this thesis (see Chapter 1). One of the important features in the further research will be based on the dynamics of processes related to the secretion. In the last decade, many proteins involved in hyphal tip growth and the polarized secretory pathway have been identified, analyzed and visualized using fluorescent proteins (FPs) (Sudbery 2011). In addition, some important proteins have been labeled in this thesis and our group: GFP-SncA (secretory vesicles), SlaB-YFP, AbpA-CFP (endocytic actin), CFP-TubA (tubulin), GFP-RacA (RacA) from this thesis and GmtA-GFP (Golgi, (Carvalho et al. 2011b)), SpaA-CFP (polarisome, (Meyer et al. 2008)), GlaA-GFP-HDEL, H2B-GFP, MTS-GFP (ER, nuclei, mitochondria respectively, unpublished data). Actin was visualized indirectly using immunostaining (Chapter 2), as approaches to fuse GFP to actin to perform life imaging of actin dynamics were not successful despite several attempts to fuse GFP either to the N- or C-terminus of actin (data not shown). We showed that the organization of the hyphal tip apparatus (or at least endocytic/exocytic events) is similar to what is observed in *A. nidulans*. To understand the high secretion capacity of *A. niger* or to understand mechanisms to explain different production rates at the same growth rates, the dynamics of the secretion machinery e.g. endo/exocytosis or COPII/COPI turnover rates need to be studied in more detail in the future.

Two major findings have been achieved from this thesis, which will bring further follow-up studies. The first important finding is the acetylation of ER proteins (Chapter 4). The acetylation takes place in the ER involving the protein secretory pathway. This is quite a new finding in filamentous fungi. Since we only have transcriptomic data for this so far, it has to be proven whether the predicted *A. niger* acetyl-CoA transporter fulfills the same function. If acetylation takes place in *A. niger*, it has to be studied whether the acetylation of proteins in *A. niger* is part of the quality control mechanism, and other proteins involved in this process like acetyltransferases or deacetylases need to be identified in future studies.

Possibly this will open a new opportunity to understand and thus improve (heterologous) protein production in *A. niger*.

The second major finding from this thesis is the possible importance of lipid signaling networks and lipid remodeling that are involved in polar tip growth (Chapter 3). The synthesis of important phospho- and sphingolipid molecules functioning as secondary messengers in eukaryotes (DAG, IP, PA, PIP2, S1P) and as components of the plasma membrane (e.g. ergosterol, sphingolipids, glycerophosphocholine) were modulated during apical branching ($\Delta racA$, *ramosa-1*) and apolar growth (*PglaA-racA^{G18V}*). In *S. cerevisiae* and filamentous fungi, sphingolipids and ergosterol concentrate to form lipid rafts in the plasma membrane which organize and regulate signaling cascades involved in polar growth control (Takeshita et al. 2012; Wachtler and Balasubramanian 2006). It is also known that the membrane lipid modification is important for Rho GTPase activity in addition to the GTP/GDP cycle (Casey 1994; Dransart et al. 2005; Ridley 2006), and as a consequence of this, localization of Rho GTPases is also influenced by the lipid composition of the membrane. In this context, it is worth to highlight that RacA localized mainly at the hyphal apex displaying a crescent-like form (Chapter 2, Fig. 5). Since RacA is post-translationally prenylated, RacA seems to be localized at the site with specific lipid compositions. An interesting question for future research is to determine factors to ensure the presence of RacA both at the right place and at the right time and to determine to which extent the lipid composition of the membrane affects RacA localization.

Summary

In **Chapter 1**, a general introduction is given related to enzyme and metabolite production using filamentous fungi, with special attention to some possible mechanisms to explain why *A. niger* is such a good protein secretor.

Chapter 2 describes the systematic investigation of the function of all members of the Rho family GTPases present in *A. niger*. Based on loss-of-function studies, we have showed that six Rho GTPases (RacA, CftA, RhoA, RhoB, RhoC, RhoD) exert distinct and overlapping functions during the life cycle of *A. niger*. Overall, our data show that individual Rho GTPases contribute differently to growth and morphogenesis within fungi. RacA and CftA collectively ensure polarity maintenance, whereby the main protagonist in *A. niger* is RacA. Interestingly, in *A. nidulans* deletion of the *cftA* resulted in a more pronounced effect on morphology compared to the *racA* deletion. The comparison between *A. niger* and *A. nidulans* indicates that the partitioning of the roles between CftA and RacA varies even among closely related filamentous fungi.

In **Chapter 3**, the *racA* mutant was subjected to more detailed studies to elucidate the impact of the altered morphology on the protein production yields as well as on the transcriptome. Surprisingly, physiological profiles including maximum specific growth rates and specific protein production rates were nearly identical despite the significant difference in their morphology. By following exocytotic (SncA-GFP) and endocytotic (SlaB-YFP, AbpA-CFP) markers together with protein yield determination, it was shown that the increase in hyphal tips did not result in an increase of protein production yields. The transcriptomic analysis of three morphological mutants ($\Delta racA$, *ramosa-1* apical branching mutants; PglA-RacAG18V, an apolar growing mutant, in which RacA is trapped in its 'on-state' by mutating the predicted GTP binding and hydrolysis domain) revealed that several signaling and metabolic pathways were altered in these morphological mutants involved in the polar tip growth. With regard to an increase of protein secretion, it would be interesting to challenge the $\Delta racA$ strain to overexpress a certain protein of interest to see the effect of hyperbranching on the protein secretion.

In **Chapter 4**, we performed transcriptome analyses by comparing an *A. niger* wild-type strain to a glucoamylase overexpressing strain under the same growth rate. Using GO term enrichment analysis, four higher-order categories were identified in the up-regulated gene set: i) ER membrane translocation, ii) protein glycosylation, iii) vesicle transport and iv) ion homeostasis. Among these, about 130 genes had predicted functions for the passage of

proteins through the ER and those genes included target genes of the HacA transcription factor that mediates the unfolded protein response (UPR), e.g. *bipA*, *clxA*, *prpA*, *tigA* and *pdiA*. Comparison of this dataset to other datasets in which *A. niger* was triggered to induce an unfolded protein response, a core set of 40 genes was identified which are key for the intensified traffic of proteins through the secretory pathway. The consistent up-regulation of a gene encoding the predicted acetyl-coenzyme A (CoA) transporter suggests a possible role for transient acetylation to ensure correct folding of secreted proteins

In **Chapter 5**, we established a GFP-v-SNARE reporter strain in which the trafficking and dynamics of secretory vesicles can be followed *in vivo* to study the process of protein secretion in *A. niger*. The biological role of seven secretion-specific genes, known to function in key aspects of the protein secretion machinery in *S. cerevisiae*, was analyzed using the GFP-v-SNARE reporter strain. This study revealed that the orchestration of exocyst-mediated vesicle transport is only partially conserved in *S. cerevisiae* and *A. niger* which serves as a basis to understand differences in secretion mechanisms between the species.

In **Chapter 6**, the major findings from the research described in the thesis are summarized, highlighted and interesting topics for future research are discussed.

Samenvatting

In **Hoofdstuk 1** wordt een algemene introductie gegeven over de productie van enzymen en metabolieten door filamenteuze schimmels. In de introductie wordt speciale aandacht geschonken aan een aantal mogelijk mechanismen die kunnen verklaren waarom *A. niger* zo efficiënt is in het uitscheiden van eiwitten .

Hoofdstuk 2 beschrijft de systematische bestudering van de functies van alle GTPases van de Rho familie die in *A. niger* aanwezig zijn. Gebaseerd op het verlies van functie, hebben we hier laten zien dat de zes Rho GTPases (RacA, CftA, RhoA, RhoB, RhoC, RhoD) verschillende en overlappende functies bezitten gedurende de levenscyclus van *A. niger*. Alles bij elkaar genomen laat de data zien dat de individuele Rho GTPases op verschillende manieren bijdragen aan de groei en morfogenese in schimmels. RacA en CftA zorgen samen voor polariteit, waarbij in *A. niger* RacA de belangrijkste rol speelt. In *A. nidulans* zorgt juist de deletie van *cftA* voor een meer uitgesproken effect op de morfologie, vergeleken met de deletie van *racA*. De vergelijking tussen *A. niger* en *A. nidulans* toont aan dat de rolverdeling tussen CftA en RacA zelfs tussen nauw verwante schimmels kan verschillen.

In **Hoofdstuk 3** is de *racA* mutant onderworpen aan een meer gedetailleerde studie, om de impact van veranderde morfologie op de eiwitproductie en op het transcriptoom op te helderen. Tot onze verrassing was het fysiologische profiel, waaronder de maximale specifieke groeisnelheid en de specifieke eiwitproductie, nagenoeg hetzelfde ondanks de significante verschillen in morfologie. Door het volgen van exocytose (SncA-GFP) en endocytose (SlaB-YFP, AbpA-CFP) markers, in combinatie met een bepaling van de eiwitopbrengst, is aangetoond dat de toename in groeitips niet resulteerde in een toename van eiwitproductie. De analyse van het transcriptoom van drie morfologie mutanten (*ΔracA*, *ramosa-1* apicale vertakkingsmutanten; PglA-RacAG18V, een apolair groeiende mutant, waar RacA gevangen is in de ‘aan-status’ door het muteren van het voorspelde GTP bindende en hydrolyse domein) toont aan dat verscheidene signaal- en metabolische routes anders tot expressie komen in deze morfologische mutanten. Met betrekking tot eiwitsecretie zou het interessant zijn om in de *ΔracA* stam een bepaald eiwit to overexpressie te brengen om het effect van hypervertakking op eiwitsecretie te kunnen bestuderen.

In **Hoofdstuk 4** hebben we transcriptoom analyses uitgevoerd door de *A. niger* wildtype stam te vergelijken met de glucoamylase overexpressie stam bij dezelfde groeisnelheid. Met behulp van GO-term verrijkinganalyse zijn vier hogere-orde categorieën geïdentificeerd in de omhoog gereguleerde set van genen i) ER membraan translocatie, ii) eiwit glycosylering, iii) transport van blaasjes, iv) ion homeostase. Binnen deze genenset waren ongeveer 130 genen met een voorspelde functie betrokken bij het passeren van eiwitten door het ER, en in deze genenset waren target genen van de HacA transcriptiefactor, die de Unfolded Protein Response (UPR) medieert, bv. *bipA*, *clxA*, *prpA*, *tigA* and *pdiA*. Deze dataset werd vergeleken met andere datasets waarbij in *A. niger* UPR werd geïnduceerd, resulterend in een kernset van 40 genen die zeer belangrijk zijn voor het geïntensiveerde eiwit transport door de secretieroute. De consistente up-regulatie van een gen coderend voor de voorspelde acetyl-coenzyme A (CoA) transporter suggereert een rol voor transiënte acetylering om te zorgen voor correcte vouwing van uitgescheiden eiwitten.

In **Hoofdstuk 5** hebben we een GFP-v-SNARE reporter stam gemaakt waarin het transport en de dynamiek van secretieblaasjes *in vivo* gevolgd kan worden, om zo het proces van eiwitsecretie in *A. niger* te kunnen bestuderen. De biologische rol van zeven secretie specifieke genen, waarvan bekend is dat ze functioneren in belangrijke aspecten van het eiwit secretie apparaat in *S. cerevisiae*, is geanalyseerd mbv de GFP-v-SNARE reporter stam. Dit onderzoek heeft aangetoond dat de organisatie van exocyst-gemedieerde blaasjestransport maar deels geconserveerd is in *S. cerevisiae* en *A. niger*, wat de basis is voor het begrijpen van de verschillen in de secretiemechanismen tussen de verschillende soorten.

In **Hoofdstuk 6** zijn de belangrijkste ontdekkingen, voortkomend uit het onderzoek beschreven in dit proefschrift, samengevat en uitgelicht, en interessante onderwerpen voor toekomstig onderzoek worden hier besproken.

Supplemental material

The supplemental material of this thesis is comprises the following and available via each website:

Chapter 2: <http://onlinelibrary.wiley.com/doi/10.1111/j.1365-2958.2010.07524.x/supinfo>

Fig. S1. Phylogenetic tree of fungal Rho GTPases.

Fig. S2. Deletion of *rhoD* causes loss of septation in *A. niger*.

Fig. S3. Phenotypes of wt, individual *rho* deletion and complemented strains.

Fig. S4. Phenotypes of wild-type, $\Delta noxR$ and $\Delta noxA$.

Movie S1. Time-lapse movie of *A. niger* expressing eGFP::*RacA*.

Chapter 3:

<http://www.plosone.org/article/info%3Adoi%2F10.1371%2Fjournal.pone.0068946#s6>

Table S1. Complete transcriptome data containing RMA expression values (log₂ scale), mean expression values, p-values, q-values and fold changes

Table S2. Subset of the transcriptome data containing up-down-regulated gene sets.

Table S3. ZIP archive file containing FetGOat enrichment results for the up- and down-regulated gene sets of all six comparisons.

Table S4. Subset of the transcriptome data for selected intersection of the Venn diagram.

Table S5. Primers used in this study.

Chapter 4: <http://www.biomedcentral.com/1471-2164/13/701/additional>

Additional file 1. Differentially expressed genes between B36 and N402 maltose-limited chemostat cultures.

Additional file 2. Network map based on GO-enrichment analysis using the differentially expressed, induced and repressed gene sets in B36/N402 chemostat cultures.

Additional file 3. Enriched-GO terms using the differentially expressed, induced and repressed gene sets in B36/N402 chemostat cultures.

Additional file 4. Four higher-order categories of enriched-GO terms using the induced gene set in B36/N402 chemostat cultures.

Additional file 5. Expression values of iron uptake genes.

Additional file 6. Expression values of protease genes.

Additional file 7. Enriched-GO terms from the comparison between B36/N402 *versus* maltose/xylose.

Additional file 8. Primers used in qPCR and RT PCR.

Chapter 5: http://mic.sgmjournals.org/content/160/Pt_2/316/suppl/DC1

Supplemental Fig. 1. Schematic representations of the wild-type locus and disruptant locus and Southern blot analysis of the *sncA* (A and B) and *secB* (C and D).

Supplemental Fig. 2. Localization of GFP-tubulin (Kwon et al., 2011) and SlaB-YFP (Kwon et al. 2013b) reporter strains after treatment with respectively benomyl (5 µg/ml) or latrunculin B (2 µg/ml).

Supplemental video 1. Time lapse of *A. niger* expressing GFP-SncA.

References

- Adav SS, Li AA, Manavalan A, Punt P, Sze SK. 2010. Quantitative iTRAQ secretome analysis of *Aspergillus niger* reveals novel hydrolytic enzymes. *J Proteome Res* 9(8):3932-40.
- Alic M, Bennett JW, Lasure LL. 1991. More gene manipulations in fungi. San Diego: Academic Press. xxiii, 470 p. p.
- Amanullah A, Christensen LH, Hansen K, Nienow AW, Thomas CR. 2002. Dependence of morphology on agitation intensity in fed-batch cultures of *Aspergillus oryzae* and its implications for recombinant protein production. *Biotechnol Bioeng* 77(7):815-26.
- Araujo-Bazan L, Penalva MA, Espeso EA. 2008. Preferential localization of the endocytic internalization machinery to hyphal tips underlies polarization of the actin cytoskeleton in *Aspergillus nidulans*. *Mol Microbiol* 67(4):891-905.
- Arellano M, Duran A, Perez P. 1996. Rho 1 GTPase activates the (1-3)beta-D-glucan synthase and is involved in *Schizosaccharomyces pombe* morphogenesis. *EMBO J* 15(17):4584-91.
- Banuet F, Quintanilla RH, Jr., Reynaga-Pena CG. 2008. The machinery for cell polarity, cell morphogenesis, and the cytoskeleton in the Basidiomycete fungus *Ustilago maydis*-a survey of the genome sequence. *Fungal Genet Biol* 45 Suppl 1:S3-S14.
- Barlowe C, Orci L, Yeung T, Hosobuchi M, Hamamoto S, Salama N, Rexach MF, Ravazzola M, Amherdt M, Schekman R. 1994. COPII: a membrane coat formed by Sec proteins that drive vesicle budding from the endoplasmic reticulum. *Cell* 77(6):895-907.
- Barlowe C, Schekman R. 1993. SEC12 encodes a guanine-nucleotide-exchange factor essential for transport vesicle budding from the ER. *Nature* 365(6444):347-9.
- Bartnicki-Garcia S, Bartnicki DD, Gierz G, Lopez-Franco R, Bracker CE. 1995. Evidence that Spitzenkorper behavior determines the shape of a fungal hypha: a test of the hyphoid model. *Exp Mycol* 19(2):153-9.
- Beeson WT, Iavarone AT, Hausmann CD, Cate JH, Marletta MA. 2011. Extracellular aldonolactonase from *Myceliophthora thermophila*. *Appl Environ Microbiol* 77(2):650-6.
- Benitah SA, Valeron PF, van Aelst L, Marshall CJ, Lacal JC. 2004. Rho GTPases in human cancer: an unresolved link to upstream and downstream transcriptional regulation. *Biochim Biophys Acta* 1705(2):121-32.
- Benjamini Y, Hochberg Y. 1995. Controlling the False Discovery Rate - a Practical and Powerful Approach to Multiple Testing. *Journal of the Royal Statistical Society Series B-Methodological* 57(1):289-300.
- Bennett JW, Lasure LL. 1991. More gene manipulations in fungi. New York: Academic Press. 441-457 p.
- Berepiki A, Lichius A, Read ND. 2011. Actin organization and dynamics in filamentous fungi. *Nat Rev Microbiol* 9(12):876-87.
- Bergmeyer H, Bernt E, Schmidt F, Stork H. 1974. Glucose. In: Bergmeyer H, editor. *Methods of Enzymatic Analysis*. New York: Academic Press. p 1196-1201.
- Berka RM, Grigoriev IV, Otilar R, Salamov A, Grimwood J, Reid I, Ishmael N, John T, Darmond C, Moisan MC and others. 2011. Comparative genomic analysis of the thermophilic biomass-degrading fungi *Myceliophthora thermophila* and *Thielavia terrestris*. *Nat Biotechnol* 29(10):922-7.
- Bermejo C, Rodriguez E, Garcia R, Rodriguez-Pena JM, Rodriguez de la Concepcion ML, Rivas C, Arias P, Nombela C, Posas F, Arroyo J. 2008. The sequential activation of the yeast HOG and SLT2 pathways is required for cell survival to cell wall stress. *Mol Biol Cell* 19(3):1113-24.
- Bi X, Corpina RA, Goldberg J. 2002. Structure of the Sec23/24-Sar1 pre-budding complex of the COPII vesicle coat. *Nature* 419(6904):271-7.
- Bock JB, Matern HT, Peden AA, Scheller RH. 2001. A genomic perspective on membrane compartment organization. *Nature* 409(6822):839-841.

- Bocking SP, Wiebe MG, Robson GD, Hansen K, Christiansen LH, Trinci AP. 1999. Effect of branch frequency in *Aspergillus oryzae* on protein secretion and culture viscosity. *Biotechnol Bioeng* 65(6):638-48.
- Bonifacino JS, Glick BS. 2004. The Mechanisms of Vesicle Budding and Fusion. *Cell* 116(2):153-166.
- Bos CJ, Debets AJ, Swart K, Huybers A, Kobus G, Slakhorst SM. 1988. Genetic analysis and the construction of master strains for assignment of genes to six linkage groups in *Aspergillus niger*. *Curr Genet* 14(5):437-43.
- Bosco EE, Mulloy JC, Zheng Y. 2009. Rac1 GTPase: a "Rac" of all trades. *Cell Mol Life Sci* 66(3):370-4.
- Boueux A, Vignal E, Faure S, Fort P. 2007. Evolution of the Rho family of ras-like GTPases in eukaryotes. *Mol Biol Evol* 24(1):203-16.
- Boyce KJ, Hynes MJ, Andrianopoulos A. 2003. Control of morphogenesis and actin localization by the *Penicillium marneffei* RAC homolog. *J Cell Sci* 116(Pt 7):1249-60.
- Braaksma M, Martens-Uzunova ES, Punt PJ, Schaap PJ. 2010. An inventory of the *Aspergillus niger* secretome by combining in silico predictions with shotgun proteomics data. *BMC Genomics* 11:584.
- Brandizzi F, Barlowe C. 2013. Organization of the ER-Golgi interface for membrane traffic control. *Nat Rev Mol Cell Biol* 14(6):382-92.
- Braun S, Vecht-Lifshitz SE. 1991. Mycelial morphology and metabolite production. *Trends in Biotechnology* 9(1):63-68.
- Calonge TM, Nakano K, Arellano M, Arai R, Katayama S, Toda T, Mabuchi I, Perez P. 2000. Schizosaccharomyces pombe rho2p GTPase regulates cell wall alpha-glucan biosynthesis through the protein kinase pck2p. *Mol Biol Cell* 11(12):4393-401.
- Cano-Dominguez N, Alvarez-Delfin K, Hansberg W, Aguirre J. 2008. NADPH oxidases NOX-1 and NOX-2 require the regulatory subunit NOR-1 to control cell differentiation and growth in *Neurospora crassa*. *Eukaryot Cell* 7(8):1352-61.
- Carman GM, Han GS. 2007. Regulation of phospholipid synthesis in *Saccharomyces cerevisiae* by zinc depletion. *Biochim Biophys Acta* 1771(3):322-30.
- Carvalho ND, Arentshorst M, Kwon MJ, Meyer V, Ram AF. 2010. Expanding the ku70 toolbox for filamentous fungi: establishment of complementation vectors and recipient strains for advanced gene analyses. *Appl Microbiol Biotechnol* 87(4):1463-73.
- Carvalho ND, Jorgensen TR, Arentshorst M, Nitsche BM, van den Hondel CA, Archer DB, Ram AF. 2012. Genome-wide expression analysis upon constitutive activation of the HacA bZIP transcription factor in *Aspergillus niger* reveals a coordinated cellular response to counteract ER stress. *BMC Genomics* 13:350.
- Carvalho NDSP, Arentshorst M, Kooistra R, Stam H, Sagt CM, van den Hondel CAMJJ, Ram AFJ. 2011a. Effects of a defective ERAD pathway on growth and heterologous protein production in *Aspergillus niger*. *Applied Microbiology and Biotechnology* 89(2):357-373.
- Carvalho NDSP, Arentshorst M, Weenink XO, Punt PJ, van den Hondel CAMJJ, Ram AFJ. 2011b. Functional YFP-tagging of the essential GDP-mannose transporter reveals an important role for the secretion related small GTPase SrgC protein in maintenance of Golgi bodies in *Aspergillus niger*. *Fungal Biology* 115(3):253-264.
- Casey PJ. 1994. Lipid modifications of G proteins. *Curr Opin Cell Biol* 6(2):219-25.
- Chen J, Zheng W, Zheng S, Zhang D, Sang W, Chen X, Li G, Lu G, Wang Z. 2008. Rac1 is required for pathogenicity and Chm1-dependent conidiogenesis in rice fungal pathogen *Magnaporthe grisea*. *PLoS Pathog* 4(11):e1000202.
- Chen YA, Scheller RH. 2001. SNARE-mediated membrane fusion. *Nat Rev Mol Cell Biol* 2(2):98-106.
- Cheng J, Park TS, Chio LC, Fischl AS, Ye XS. 2003. Induction of apoptosis by sphingoid long-chain bases in *Aspergillus nidulans*. *Mol Cell Biol* 23(1):163-77.
- Cheng J, Park TS, Fischl AS, Ye XS. 2001. Cell cycle progression and cell polarity require sphingolipid biosynthesis in *Aspergillus nidulans*. *Mol Cell Biol* 21(18):6198-209.

- Colin VL, Baigori MD, Pera LM. 2013. Tailoring fungal morphology of *Aspergillus niger* MYA 135 by altering the hyphal morphology and the conidia adhesion capacity: biotechnological applications. *AMB Express* 3(1):27.
- Cooper JA. 1987. Effects of cytochalasin and phalloidin on actin. *J Cell Biol* 105(4):1473-8.
- Cowart LA, Shotwell M, Worley ML, Richards AJ, Montefusco DJ, Hannun YA, Lu X. 2010. Revealing a signaling role of phytosphingosine-1-phosphate in yeast. *Mol Syst Biol* 6:349.
- D'Arcangelo JG, Stahmer KR, Miller EA. 2013. Vesicle-mediated export from the ER: COPII coat function and regulation. *Biochim Biophys Acta* 1833(11):2464-72.
- Damveld RA, Arentshorst M, Franken A, vanKuyk PA, Klis FM, van den Hondel CA, Ram AF. 2005. The *Aspergillus niger* MADS-box transcription factor RlmA is required for cell wall reinforcement in response to cell wall stress. *Mol Microbiol* 58(1):305-19.
- Daquinag A, Fadri M, Jung SY, Qin J, Kunz J. 2007. The yeast PH domain proteins Slm1 and Slm2 are targets of sphingolipid signaling during the response to heat stress. *Mol Cell Biol* 27(2):633-50.
- de Bekker C, Bruning O, Jonker MJ, Breit TM, Wosten HA. 2011a. Single cell transcriptomics of neighboring hyphae of *Aspergillus niger*. *Genome Biol* 12(8):R71.
- de Bekker C, van Veluw GJ, Vinck A, Wiebenga LA, Wosten HA. 2011b. Heterogeneity of *Aspergillus niger* microcolonies in liquid shaken cultures. *Appl Environ Microbiol* 77(4):1263-7.
- de Oliveira JM, van Passel MW, Schaap PJ, de Graaff LH. 2011. Proteomic analysis of the secretory response of *Aspergillus niger* to D-maltose and D-xylose. *PLoS One* 6(6):e20865.
- de Ruiter-Jacobs YM, Broekhuijsen M, Unkles SE, Campbell EI, Kinghorn JR, Contreras R, Pouwels PH, van den Hondel CA. 1989. A gene transfer system based on the homologous pyrG gene and efficient expression of bacterial genes in *Aspergillus oryzae*. *Curr Genet* 16(3):159-63.
- de Souza WR, de Gouvea PF, Savoldi M, Malavazi I, de Souza Bernardes LA, Goldman MH, de Vries RP, de Castro Oliveira JV, Goldman GH. 2011. Transcriptome analysis of *Aspergillus niger* grown on sugarcane bagasse. *Biotechnol Biofuels* 4:40.
- Delmas S, Pullan ST, Gaddipati S, Kokolski M, Malla S, Blythe MJ, Ibbett R, Campbell M, Liddell S, Aboobaker A and others. 2012. Uncovering the genome-wide transcriptional responses of the filamentous fungus *Aspergillus niger* to lignocellulose using RNA sequencing. *PLoS Genet* 8(8):e1002875.
- Dolman NJ, Tepikin AV. 2006. Calcium gradients and the Golgi. *Cell Calcium* 40(5-6):505-512.
- Dransart E, Olofsson B, Cherfils J. 2005. RhoGDIs revisited: novel roles in Rho regulation. *Traffic* 6(11):957-66.
- Driouch H, Hansch R, Wucherpennig T, Krull R, Wittmann C. 2012. Improved enzyme production by bio-pellets of *Aspergillus niger*: targeted morphology engineering using titanate microparticles. *Biotechnol Bioeng* 109(2):462-71.
- Driouch H, Sommer B, Wittmann C. 2010. Morphology engineering of *Aspergillus niger* for improved enzyme production. *Biotechnol Bioeng* 105(6):1058-68.
- Dudgeon DD, Zhang N, Ositelu OO, Kim H, Cunningham KW. 2008. Nonapoptotic death of *Saccharomyces cerevisiae* cells that is stimulated by Hsp90 and inhibited by calcineurin and Cmk2 in response to endoplasmic reticulum stresses. *Eukaryot Cell* 7(12):2037-51.
- Ernst R, Klemm R, Schmitt L, Kuchler K. 2005. Yeast ATP-binding cassette transporters: cellular cleaning pumps. *Methods Enzymol* 400:460-84.
- Fadri M, Daquinag A, Wang S, Xue T, Kunz J. 2005. The pleckstrin homology domain proteins Slm1 and Slm2 are required for actin cytoskeleton organization in yeast and bind phosphatidylinositol-4,5-bisphosphate and TORC2. *Mol Biol Cell* 16(4):1883-900.
- Fajardo-Somera RA, Bowman B, Riquelme M. 2013. The plasma membrane proton pump PMA-1 is incorporated into distal parts of the hyphae independently of the Spitzenkörper in *Neurospora crassa*. *Eukaryot Cell* 12(8):1097-105.
- Fdez E, Martinez-Salvador M, Beard M, Woodman P, Hilfiker S. 2010. Transmembrane-domain determinants for SNARE-mediated membrane fusion. *J Cell Sci* 123(Pt 14):2473-80.
- Finkelstein DB, Rambosek J, Crawford MS, Soliday CL, McAda PC, Leach J. 1989. Protein secretion in *Aspergillus niger*. In: Hershberger CL, Queener SW, Hegeman G, editors. *Genetics and*

- Molecular Biology of Industrial Microorganisms*. Washington, DC: Am. Soc. Microbiol. p 295-300.
- Fisher RA. 1922. On the Interpretation of X² from Contingency Tables, and the Calculation of P.
- Fleissner A, Dersch P. 2010. Expression and export: recombinant protein production systems for *Aspergillus*. *Appl Microbiol Biotechnol* 87(4):1255-70.
- Friesen H, Humphries C, Ho Y, Schub O, Colwill K, Andrews B. 2006. Characterization of the yeast amphiphysins Rvs161p and Rvs167p reveals roles for the Rvs heterodimer in vivo. *Mol Biol Cell* 17(3):1306-21.
- Fu Y, Yang Z. 2001. Rop GTPase: a master switch of cell polarity development in plants. *Trends Plant Sci* 6(12):545-7.
- Furuta N, Fujimura-Kamada K, Saito K, Yamamoto T, Tanaka K. 2007. Endocytic recycling in yeast is regulated by putative phospholipid translocases and the Ypt31p/32p-Rcy1p pathway. *Mol Biol Cell* 18(1):295-312.
- Gamarra NN, Villena GK, Gutierrez-Correa M. 2010. Cellulase production by *Aspergillus niger* in biofilm, solid-state, and submerged fermentations. *Appl Microbiol Biotechnol* 87(2):545-51.
- Geysens S, Whyteside G, Archer DB. 2009. Genomics of protein folding in the endoplasmic reticulum, secretion stress and glycosylation in the aspergilli. *Fungal Genetics and Biology* 46(1, Supplement):S121-S140.
- Gibbs PA, Seviour RJ, Schmid F. 2000. Growth of filamentous fungi in submerged culture: problems and possible solutions. *Crit Rev Biotechnol* 20(1):17-48.
- Gordon CL, Khalaj V, Ram AF, Archer DB, Brookman JL, Trinci AP, Jeenes DJ, Doonan JH, Wells B, Punt PJ and others. 2000. Glucoamylase::green fluorescent protein fusions to monitor protein secretion in *Aspergillus niger*. *Microbiology* 146 (Pt 2):415-26.
- Grimm LH, Kelly S, Krull R, Hempel DC. 2005. Morphology and productivity of filamentous fungi. *Appl Microbiol Biotechnol* 69(4):375-84.
- Grote E, Baba M, Ohsumi Y, Novick PJ. 2000. Geranylgeranylated SNAREs are dominant inhibitors of membrane fusion. *J Cell Biol* 151(2):453-66.
- Guest GM, Lin X, Momany M. 2004. *Aspergillus nidulans* RhoA is involved in polar growth, branching, and cell wall synthesis. *Fungal Genet Biol* 41(1):13-22.
- Guillemette T, Ram AF, Carvalho ND, Joubert A, Simoneau P, Archer DB. 2011. Methods for investigating the UPR in filamentous fungi. *Methods Enzymol* 490:1-29.
- Guillemette T, van Peij NN, Goosen T, Lanthaler K, Robson GD, van den Hondel CA, Stam H, Archer DB. 2007. Genomic analysis of the secretion stress response in the enzyme-producing cell factory *Aspergillus niger*. *BMC Genomics* 8:158.
- Gupta GD, Brent Heath I. 2002. Predicting the distribution, conservation, and functions of SNAREs and related proteins in fungi. *Fungal Genet Biol* 36(1):1-21.
- Gusakov AV. 2011. Alternatives to *Trichoderma reesei* in biofuel production. *Trends Biotechnol* 29(9):419-25.
- Hagag S, Kubitschek-Barreira P, Neves GW, Amar D, Nierman W, Shalit I, Shamir R, Lopes-Bezerra L, Osherov N. 2012. Transcriptional and proteomic analysis of the *Aspergillus fumigatus* DeltaprtT protease-deficient mutant. *PLoS One* 7(4):e33604.
- Hall A. 1998. Rho GTPases and the actin cytoskeleton. *Science* 279(5350):509-14.
- Harris SD. 2011. Cdc42/Rho GTPases in fungi: variations on a common theme. *Mol Microbiol* 79(5):1123-7.
- Harris SD, Morrell JL, Hamer JE. 1994. Identification and characterization of *Aspergillus nidulans* mutants defective in cytokinesis. *Genetics* 136(2):517-32.
- Harris SD, Read ND, Roberson RW, Shaw B, Seiler S, Plamann M, Momany M. 2005. Polarisome meets Spitzenkörper: microscopy, genetics, and genomics converge. *Eukaryot Cell* 4(2):225-9.
- Harris SD, Turner G, Meyer V, Espeso EA, Specht T, Takeshita N, Helmstedt K. 2009. Morphology and development in *Aspergillus nidulans*: a complex puzzle. *Fungal Genet Biol* 46 Suppl 1:S82-S92.
- Harsay E, Bretscher A. 1995. Parallel secretory pathways to the cell surface in yeast. *J Cell Biol* 131(2):297-310.

- Hasegawa J, Tokuda E, Tenno T, Tsujita K, Sawai H, Hiroaki H, Takenawa T, Itoh T. 2011. SH3YL1 regulates dorsal ruffle formation by a novel phosphoinositide-binding domain. *J Cell Biol* 193(5):901-16.
- Hawksworth DL. 2001. The magnitude of fungal diversity: the 1.5 million species estimate revisited. *Mycological Research* 105(12):1422-1432.
- Hayakawa Y, Ishikawa E, Shoji JY, Nakano H, Kitamoto K. 2011. Septum-directed secretion in the filamentous fungus *Aspergillus oryzae*. *Mol Microbiol* 81(1):40-55.
- Hazan I, Liu H. 2002. Hyphal tip-associated localization of Cdc42 is F-actin dependent in *Candida albicans*. *Eukaryot Cell* 1(6):856-64.
- Heasman SJ, Ridley AJ. 2008. Mammalian Rho GTPases: new insights into their functions from in vivo studies. *Nat Rev Mol Cell Biol* 9(9):690-701.
- Heider MR, Munson M. 2012. Exorcising the Exocyst Complex. *Traffic*.
- Hordijk PL. 2006. Regulation of NADPH oxidases: the role of Rac proteins. *Circ Res* 98(4):453-62.
- Horio T. 2007. Role of microtubules in tip growth of fungi. *J Plant Res* 120(1):53-60.
- Irizarry RA, Bolstad BM, Collin F, Cope LM, Hobbs B, Speed TP. 2003. Summaries of affymetrix GeneChip probe level data. *Nucleic Acids Research* 31(4).
- Itzen A, Rak A, Goody RS. 2007. Sec2 is a highly efficient exchange factor for the Rab protein Sec4. *J Mol Biol* 365(5):1359-67.
- Iversen J JL, Thomsen JK, Cox RP. 1994. On Line Growth Measurements in Bioreactors by Titrating Metabolic Proton-Exchange. *Applied Microbiology and Biotechnology* 42(2-3):256-262.
- Jacobs DI, Olsthoorn MM, Mailliet I, Akeroyd M, Breestraat S, Donkers S, van der Hoeven RA, van den Hondel CA, Kooistra R, Lapointe T and others. 2009. Effective lead selection for improved protein production in *Aspergillus niger* based on integrated genomics. *Fungal Genet Biol* 46 Suppl 1:S141-52.
- Jantti J, Aalto MK, Oyen M, Sundqvist L, Keranen S, Ronne H. 2002. Characterization of temperature-sensitive mutations in the yeast syntaxin 1 homologues Sso1p and Sso2p, and evidence of a distinct function for Sso1p in sporulation. *J Cell Sci* 115(Pt 2):409-20.
- Johnson DI, Pringle JR. 1990. Molecular characterization of CDC42, a *Saccharomyces cerevisiae* gene involved in the development of cell polarity. *J Cell Biol* 111(1):143-52.
- Johnson JL, Erickson JW, Cerione RA. 2009. New insights into how the Rho guanine nucleotide dissociation inhibitor regulates the interaction of Cdc42 with membranes. *J Biol Chem* 284(35):23860-71.
- Jonas MC, Pehar M, Puglielli L. 2010. AT-1 is the ER membrane acetyl-CoA transporter and is essential for cell viability. *J Cell Sci* 123(Pt 19):3378-88.
- Jones S, Newman C, Liu F, Segev N. 2000. The TRAPP complex is a nucleotide exchanger for Ypt1 and Ypt31/32. *Mol Biol Cell* 11(12):4403-11.
- Jørgensen TR, Goosen T, Hondel CA, Ram AF, Iversen JJ. 2009. Transcriptomic comparison of *Aspergillus niger* growing on two different sugars reveals coordinated regulation of the secretory pathway. *BMC Genomics* 10:44.
- Jørgensen TR, Nitsche BM, Lamers GE, Arentshorst M, van den Hondel CA, Ram AF. 2010. Transcriptomic insights into the physiology of *Aspergillus niger* approaching a specific growth rate of zero. *Appl Environ Microbiol* 76(16):5344-55.
- Joung MJ, Mohan SK, Yu C. 2012. Molecular level interaction of inositol hexaphosphate with the C2B domain of human synaptotagmin I. *Biochemistry* 51(17):3675-83.
- Kaksonen M, Toret CP, Drubin DG. 2006. Harnessing actin dynamics for clathrin-mediated endocytosis. *Nat Rev Mol Cell Biol* 7(6):404-14.
- Kasuga T, Glass NL. 2008. Dissecting colony development of *Neurospora crassa* using mRNA profiling and comparative genomics approaches. *Eukaryot Cell* 7(9):1549-64.
- Kaufman RJ. 1999. Stress signaling from the lumen of the endoplasmic reticulum: coordination of gene transcriptional and translational controls. *Genes Dev* 13(10):1211-33.
- Kaup BA, Ehrlich K, Pescheck M, Schrader J. 2008. Microparticle-enhanced cultivation of filamentous microorganisms: increased chloroperoxidase formation by *Caldariomyces fumago* as an example. *Biotechnol Bioeng* 99(3):491-8.

- Kienle N, Klopper TH, Fasshauer D. 2009. Phylogeny of the SNARE vesicle fusion machinery yields insights into the conservation of the secretory pathway in fungi. *BMC Evol Biol* 9:19.
- Kim HS, Czymmek KJ, Patel A, Modla S, Nohe A, Duncan R, Gilroy S, Kang S. 2012. Expression of the Cameleon calcium biosensor in fungi reveals distinct Ca(2+) signatures associated with polarized growth, development, and pathogenesis. *Fungal Genet Biol* 49(8):589-601.
- Klahre U, Kost B. 2006. Tobacco RhoGTPase ACTIVATING PROTEIN1 spatially restricts signaling of RAC/Rop to the apex of pollen tubes. *Plant Cell* 18(11):3033-46.
- Krijgsheld P, Altaeaf AF, Post H, Ringrose JH, Muller WH, Heck AJ, Wosten HA. 2012. Spatially resolving the secretome within the mycelium of the cell factory *Aspergillus niger*. *J Proteome Res* 11(5):2807-18.
- Kumar P, Satyanarayana T. 2009. Microbial glucoamylases: characteristics and applications. *Crit Rev Biotechnol* 29(3):225-55.
- Kumar R, Singh S, Singh OV. 2008. Bioconversion of lignocellulosic biomass: biochemical and molecular perspectives. *J Ind Microbiol Biotechnol* 35(5):377-91.
- Kuratsu M, Taura A, Shoji JY, Kikuchi S, Arioka M, Kitamoto K. 2007. Systematic analysis of SNARE localization in the filamentous fungus *Aspergillus oryzae*. *Fungal Genet Biol* 44(12):1310-23.
- Kwon MJ, Arentshorst M, Fiedler M, de Groen FL, Punt PJ, Meyer V, Ram AF. 2013a. Molecular genetic analysis of vesicular transport in *Aspergillus niger* reveals partial conservation of the molecular mechanism of exocytosis in fungi. *Microbiology*.
- Kwon MJ, Arentshorst M, Roos ED, van den Hondel CA, Meyer V, Ram AF. 2011. Functional characterization of Rho GTPases in *Aspergillus niger* uncovers conserved and diverged roles of Rho proteins within filamentous fungi. *Mol Microbiol* 79(5):1151-67.
- Kwon MJ, Jorgensen TR, Nitsche BM, Arentshorst M, Park J, Ram AF, Meyer V. 2012. The transcriptomic fingerprint of glucoamylase over-expression in *Aspergillus niger*. *BMC Genomics* 13:701.
- Kwon MJ, Nitsche BM, Arentshorst M, Jorgensen TR, Ram AF, Meyer V. 2013b. The transcriptomic signature of RacA activation and inactivation provides new insights into the morphogenetic network of *Aspergillus niger*. *PLoS One* 8(7):e68946.
- Lambeth JD. 2004. NOX enzymes and the biology of reactive oxygen. *Nat Rev Immunol* 4(3):181-9.
- Langosch D, Hofmann M, Ungermann C. 2007. The role of transmembrane domains in membrane fusion. *Cell Mol Life Sci* 64(7-8):850-64.
- Lanzetti L. 2007. Actin in membrane trafficking. *Curr Opin Cell Biol* 19(4):453-8.
- Lara-Ortiz T, Riveros-Rosas H, Aguirre J. 2003. Reactive oxygen species generated by microbial NADPH oxidase NoxA regulate sexual development in *Aspergillus nidulans*. *Mol Microbiol* 50(4):1241-55.
- Lee J, Paetzel M. 2011. Structure of the catalytic domain of glucoamylase from *Aspergillus niger*. *Acta Crystallogr Sect F Struct Biol Cryst Commun* 67(Pt 2):188-92.
- Leucci MR, Di Sansebastiano GP, Gigante M, Dalessandro G, Piro G. 2007. Secretion marker proteins and cell-wall polysaccharides move through different secretory pathways. *Planta* 225(4):1001-17.
- Levin AM, de Vries RP, Wosten HA. 2007. Localization of protein secretion in fungal colonies using a novel culturing technique; the ring-plate system. *J Microbiol Methods* 69(2):399-401.
- Li S, Du L, Yuen G, Harris SD. 2006. Distinct ceramide synthases regulate polarized growth in the filamentous fungus *Aspergillus nidulans*. *Mol Biol Cell* 17(3):1218-27.
- Li Z, Vizeacoumar FJ, Bahr S, Li J, Warringer J, Vizeacoumar FS, Min R, Vandersluis B, Bellay J, Devit M and others. 2011. Systematic exploration of essential yeast gene function with temperature-sensitive mutants. *Nat Biotechnol* 29(4):361-7.
- Lichius A, Berepiki A, Read ND. 2011. Form follows function -- the versatile fungal cytoskeleton. *Fungal Biol* 115(6):518-40.
- Lill R. 2009. Function and biogenesis of iron-sulphur proteins. *Nature* 460(7257):831-838.
- Lin H, Cheng W, Ding HT, Chen XJ, Zhou QF, Zhao YH. 2010. Direct microbial conversion of wheat straw into lipid by a cellulolytic fungus of *Aspergillus oryzae* A-4 in solid-state fermentation. *Bioresour Technol* 101(19):7556-62.

- Lu X, Sun J, Nimtze M, Wissing J, Zeng AP, Rinas U. 2010. The intra- and extracellular proteome of *Aspergillus niger* growing on defined medium with xylose or maltose as carbon substrate. *Microb Cell Fact* 9:23.
- Lu X, Zhang Y, Shin YK. 2008. Supramolecular SNARE assembly precedes hemifusion in SNARE-mediated membrane fusion. *Nat Struct Mol Biol* 15(7):700-6.
- Maattanen P, Gehring K, Bergeron JJ, Thomas DY. 2010. Protein quality control in the ER: the recognition of misfolded proteins. *Semin Cell Dev Biol* 21(5):500-11.
- Mach-Aigner AR, Omony J, Jovanovic B, van Boxtel AJ, de Graaff LH. 2012. D-xylose concentration-dependent Hydrolase Expression Profiles and the Role of CreA and XlnR in *A. niger*. *Appl Environ Microbiol*.
- Machida M, Yamada O, Gomi K. 2008. Genomics of *Aspergillus oryzae*: learning from the history of Koji mold and exploration of its future. *DNA Res* 15(4):173-83.
- Mahlert M, Leveleki L, Hlubek A, Sandrock B, Bolker M. 2006. Rac1 and Cdc42 regulate hyphal growth and cytokinesis in the dimorphic fungus *Ustilago maydis*. *Mol Microbiol* 59(2):567-78.
- Malagnac F, Lalucque H, Lepere G, Silar P. 2004. Two NADPH oxidase isoforms are required for sexual reproduction and ascospore germination in the filamentous fungus *Podospora anserina*. *Fungal Genet Biol* 41(11):982-97.
- Markina-Inarrairaegui A, Pantazopoulou A, Espeso EA, Penalva MA. 2013. The *Aspergillus nidulans* peripheral ER: disorganization by ER stress and persistence during mitosis. *PLoS One* 8(6):e67154.
- Martens-Uzunova ES, Schaap PJ. 2009. Assessment of the pectin degrading enzyme network of *Aspergillus niger* by functional genomics. *Fungal Genet Biol* 46 Suppl 1:S170-S179.
- Martinez-Rocha AL, Roncero MI, Lopez-Ramirez A, Marine M, Guarro J, Martinez-Cadena G, Di Pietro A. 2008. Rho1 has distinct functions in morphogenesis, cell wall biosynthesis and virulence of *Fusarium oxysporum*. *Cell Microbiol* 10(6):1339-51.
- Martinez IM, Chrispeels MJ. 2003. Genomic analysis of the unfolded protein response in *Arabidopsis* shows its connection to important cellular processes. *Plant Cell* 15(2):561-576.
- Masai K, Maruyama J, Sakamoto K, Nakajima H, Akita O, Kitamoto K. 2006. Square-plate culture method allows detection of differential gene expression and screening of novel, region-specific genes in *Aspergillus oryzae*. *Appl Microbiol Biotechnol* 71(6):881-91.
- Matsui Y, Toh-e A. 1992. Isolation and characterization of two novel ras superfamily genes in *Saccharomyces cerevisiae*. *Gene* 114(1):43-9.
- Matsuoka K, Orci L, Amherdt M, Bednarek SY, Hamamoto S, Schekman R, Yeung T. 1998. COPII-coated vesicle formation reconstituted with purified coat proteins and chemically defined liposomes. *Cell* 93(2):263-75.
- McIntyre M, Muller C, Dynesen J, Nielsen J. 2001. Metabolic engineering of the morphology of *Aspergillus*. *Adv Biochem Eng Biotechnol* 73:103-28.
- Mercier A, Labbe S. 2010. Iron-dependent remodeling of fungal metabolic pathways associated with ferrichrome biosynthesis. *Appl Environ Microbiol* 76(12):3806-17.
- Merkel O, Oskolkova OV, Raab F, El-Toukhy R, Paltauf F. 2005. Regulation of activity in vitro and in vivo of three phospholipases B from *Saccharomyces cerevisiae*. *Biochem J* 387(Pt 2):489-96.
- Meyer V. 2008. Genetic engineering of filamentous fungi--progress, obstacles and future trends. *Biotechnol Adv* 26(2):177-85.
- Meyer V, Arentshorst M, El-Ghezal A, Drews AC, Kooistra R, van den Hondel CA, Ram AF. 2007a. Highly efficient gene targeting in the *Aspergillus niger* kusA mutant. *J Biotechnol* 128(4):770-5.
- Meyer V, Arentshorst M, Flitter SJ, Nitsche BM, Kwon MJ, Reynaga-Pena CG, Bartnicki-Garcia S, van den Hondel CA, Ram AF. 2009. Reconstruction of signaling networks regulating fungal morphogenesis by transcriptomics. *Eukaryot Cell* 8(11):1677-91.
- Meyer V, Arentshorst M, van den Hondel CA, Ram AF. 2008. The polarisome component SpaA localises to hyphal tips of *Aspergillus niger* and is important for polar growth. *Fungal Genet Biol* 45(2):152-64.

- Meyer V, Damveld RA, Arentshorst M, Stahl U, van den Hondel CA, Ram AF. 2007b. Survival in the presence of antifungals: genome-wide expression profiling of *Aspergillus niger* in response to sublethal concentrations of caspofungin and fenpropimorph. *J Biol Chem* 282(45):32935-48.
- Meyer V, Minkwitz S, Schutze T, van den Hondel CA, Ram A. 2010a. The *Aspergillus niger* RmsA protein: A node in a genetic network? *Commun & Integrat Biol* 3(2):1-3.
- Meyer V, Ram AF, Punt PJ. 2010b. Genetics, genetic manipulation and approaches to strain improvement of filamentous fungi. In: AL. D, J. D, editors. *Manual of industrial microbiology and biotechnology*. 3rd ed. NY: Wiley. p 318-29.
- Meyer V, Wanka F, van Gent J, Arentshorst M, van den Hondel CA, Ram AF. 2011a. Fungal gene expression on demand: an inducible, tunable, and metabolism-independent expression system for *Aspergillus niger*. *Appl Environ Microbiol* 77(9):2975-83.
- Meyer V, Wu B, Ram AF. 2011b. *Aspergillus* as a multi-purpose cell factory: current status and perspectives. *Biotechnol Lett* 33(3):469-76.
- Mikoshiba K, Fukuda M, Ibata K, Kabayama H, Mizutani A. 1999. Role of synaptotagmin, a Ca²⁺ and inositol polyphosphate binding protein, in neurotransmitter release and neurite outgrowth. *Chem Phys Lipids* 98(1-2):59-67.
- Miller PJ, Johnson DI. 1994. Cdc42p GTPase is involved in controlling polarized cell growth in *Schizosaccharomyces pombe*. *Mol Cell Biol* 14(2):1075-83.
- Moffett S, Brown DA, Linder ME. 2000. Lipid-dependent targeting of G proteins into rafts. *J Biol Chem* 275(3):2191-8.
- Momany M. 2002. Polarity in filamentous fungi: establishment, maintenance and new axes. *Curr Opin Microbiol* 5(6):580-5.
- Moukha SM, Wosten HA, Mylius EJ, Asther M, Wessels JG. 1993. Spatial and temporal accumulation of mRNAs encoding two common lignin peroxidases in *Phanerochaete chrysosporium*. *J Bacteriol* 175(11):3672-8.
- Mulder HJ, Saloheimo M, Penttila M, Madrid SM. 2004. The transcription factor HACA mediates the unfolded protein response in *Aspergillus niger*, and up-regulates its own transcription. *Mol Genet Genomics* 271(2):130-40.
- Muller C, McIntyre M, Hansen K, Nielsen J. 2002. Metabolic engineering of the morphology of *Aspergillus oryzae* by altering chitin synthesis. *Appl Environ Microbiol* 68(4):1827-36.
- Nakahara K, Ohkuni A, Kitamura T, Abe K, Naganuma T, Ohno Y, Zoeller RA, Kihara A. 2012. The Sjogren-Larsson syndrome gene encodes a hexadecenal dehydrogenase of the sphingosine 1-phosphate degradation pathway. *Mol Cell* 46(4):461-71.
- Nakase M, Tani M, Morita T, Kitamoto HK, Kashiwazaki J, Nakamura T, Hosomi A, Tanaka N, Takegawa K. 2010. Mannosylinositol phosphorylceramide is a major sphingolipid component and is required for proper localization of plasma-membrane proteins in *Schizosaccharomyces pombe*. *J Cell Sci* 123(Pt 9):1578-87.
- Nichols BJ, Ungermann C, Pelham HR, Wickner WT, Haas A. 1997. Homotypic vacuolar fusion mediated by t- and v-SNAREs. *Nature* 387(6629):199-202.
- Nitsche BM, Crabtree J, Cerqueira GC, Meyer V, Ram AF, Wortman JR. 2011. New resources for functional analysis of omics data for the genus *Aspergillus*. *BMC Genomics* 12:486.
- Nitsche BM, Jorgensen TR, Akeroyd M, Meyer V, Ram AF. 2012a. The carbon starvation response of *Aspergillus niger* during submerged cultivation: insights from the transcriptome and secretome. *BMC Genomics* 13:380.
- Nitsche BM, Ram AF, Meyer V. 2012b. The use of open source bioinformatics tools to dissect transcriptomic data. *Methods Mol Biol* 835:311-31.
- Novick P, Ferro S, Schekman R. 1981. Order of events in the yeast secretory pathway. *Cell* 25(2):461-9.
- Novick P, Field C, Schekman R. 1980. Identification of 23 complementation groups required for post-translational events in the yeast secretory pathway. *Cell* 21(1):205-215.
- Nowrousian M, Ringelberg C, Dunlap JC, Loros JL, Kuck U. 2005. Cross-species microarray hybridization to identify developmentally regulated genes in the filamentous fungus *Sordaria macrospora*. *Molecular Genetics and Genomics* 273(2):137-149.

- Nunez LR, Jesch SA, Gaspar ML, Almaguer C, Villa-Garcia M, Ruiz-Noriega M, Patton-Vogt J, Henry SA. 2008. Cell wall integrity MAPK pathway is essential for lipid homeostasis. *J Biol Chem* 283(49):34204-17.
- O'Donnell D, Wang L, Xu J, Ridgway D, Gu T, Moo-Young M. 2001. Enhanced heterologous protein production in *Aspergillus niger* through pH control of extracellular protease activity. *Biochemical Engineering Journal* 8(3):187-193.
- Oda K, Kakizono D, Yamada O, Iefuji H, Akita O, Iwashita K. 2006. Proteomic analysis of extracellular proteins from *Aspergillus oryzae* grown under submerged and solid-state culture conditions. *Appl Environ Microbiol* 72(5):3448-57.
- Otte S, Belden WJ, Heidtman M, Liu J, Jensen ON, Barlowe C. 2001. Erv41p and Erv46p: new components of COPII vesicles involved in transport between the ER and Golgi complex. *J Cell Biol* 152(3):503-18.
- Pakula TM, Laxell M, Huuskonen A, Uusitalo J, Saloheimo M, Penttila M. 2003. The effects of drugs inhibiting protein secretion in the filamentous fungus *Trichoderma reesei* - Evidence for down-regulation of genes that encode secreted proteins in the stressed cells. *Journal of Biological Chemistry* 278(45):45011-45020.
- Pakula TM, Uusitalo J, Saloheimo M, Salonen K, Aarts RJ, Penttila M. 2000. Monitoring the kinetics of glycoprotein synthesis and secretion in the filamentous fungus *Trichoderma reesei*: cellobiohydrolase I (CBHI) as a model protein. *Microbiology* 146 (Pt 1):223-32.
- Palmgren S, Ojala PJ, Wear MA, Cooper JA, Lappalainen P. 2001. Interactions with PIP2, ADP-actin monomers, and capping protein regulate the activity and localization of yeast twinfilin. *J Cell Biol* 155(2):251-60.
- Pantazopoulou A, Penalva MA. 2009. Organization and dynamics of the *Aspergillus nidulans* Golgi during apical extension and mitosis. *Mol Biol Cell* 20(20):4335-47.
- Papagianni M. 2004. Fungal morphology and metabolite production in submerged mycelial processes. *Biotechnol Adv* 22(3):189-259.
- Papagianni M. 2007. Advances in citric acid fermentation by *Aspergillus niger*: biochemical aspects, membrane transport and modeling. *Biotechnol Adv* 25(3):244-63.
- Park HO, Bi E. 2007. Central roles of small GTPases in the development of cell polarity in yeast and beyond. *Microbiol Mol Biol Rev* 71(1):48-96.
- Pehar M, Puglielli L. 2013. Lysine acetylation in the lumen of the ER: a novel and essential function under the control of the UPR. *Biochim Biophys Acta* 1833(3):686-97.
- Pel HJ, de Winde JH, Archer DB, Dyer PS, Hofmann G, Schaap PJ, Turner G, de Vries RP, Albang R, Albermann K and others. 2007. Genome sequencing and analysis of the versatile cell factory *Aspergillus niger* CBS 513.88. *Nat Biotechnol* 25(2):221-31.
- Perez P, Rincon SA. 2010. Rho GTPases: regulation of cell polarity and growth in yeasts. *Biochem J* 426(3):243-53.
- Pfaffl MW. 2001. A new mathematical model for relative quantification in real-time RT-PCR. *Nucleic Acids Research* 29(9).
- Pham CD, Yu Z, Sandrock B, Bolker M, Gold SE, Perlin MH. 2009. *Ustilago maydis* Rho1 and 14-3-3 homologues participate in pathways controlling cell separation and cell polarity. *Eukaryot Cell* 8(7):977-89.
- Philpott CC, Leidgens S, Frey AG. 2012. Metabolic remodeling in iron-deficient fungi. *Biochim Biophys Acta*.
- Philpott CC, Protchenko O. 2008. Response to iron deprivation in *Saccharomyces cerevisiae*. *Eukaryot Cell* 7(1):20-7.
- Pinar M, Pantazopoulou A, Arst HN, Jr., Penalva MA. 2013. Acute inactivation of the *Aspergillus nidulans* Golgi membrane fusion machinery: correlation of apical extension arrest and tip swelling with cysternal disorganization. *Mol Microbiol* 89(2):228-48.
- Posas F, Wurgler-Murphy SM, Maeda T, Witten EA, Thai TC, Saito H. 1996. Yeast HOG1 MAP kinase cascade is regulated by a multistep phosphorelay mechanism in the SLN1-YPD1-SSK1 "two-component" osmosensor. *Cell* 86(6):865-75.

- Protopopov V, Govindan B, Novick P, Gerst JE. 1993. Homologs of the synaptobrevin/VAMP family of synaptic vesicle proteins function on the late secretory pathway in *S. cerevisiae*. *Cell* 74(5):855-61.
- Punt PJ, Oliver RP, Dingemans MA, Pouwels PH, van den Hondel CA. 1987. Transformation of *Aspergillus* based on the hygromycin B resistance marker from *Escherichia coli*. *Gene* 56(1):117-24.
- Punt PJ, Seiboth B, Weenink XO, van Zeijl C, Lenders M, Konetschny C, Ram AF, Montijn R, Kubicek CP, van den Hondel CA. 2001. Identification and characterization of a family of secretion-related small GTPase-encoding genes from the filamentous fungus *Aspergillus niger*: a putative SEC4 homologue is not essential for growth. *Mol Microbiol* 41(2):513-25.
- Punt PJ, van Biezen N, Conesa A, Albers A, Mangnus J, van den Hondel C. 2002. Filamentous fungi as cell factories for heterologous protein production. *Trends Biotechnol* 20(5):200-6.
- Punt PJ, van Gemeren IA, Drint-Kuijvenhoven J, Hessing JG, van Muijlwijk-Hartevelde GM, Beijersbergen A, Verrips CT, van den Hondel CA. 1998. Analysis of the role of the gene *bipA*, encoding the major endoplasmic reticulum chaperone protein in the secretion of homologous and heterologous proteins in black *Aspergilli*. *Appl Microbiol Biotechnol* 50(4):447-54.
- Qadota H, Python CP, Inoue SB, Arisawa M, Anraku Y, Zheng Y, Watanabe T, Levin DE, Ohya Y. 1996. Identification of yeast Rho1p GTPase as a regulatory subunit of 1,3-beta-glucan synthase. *Science* 272(5259):279-81.
- Quintero-Monzon O, Rodal AA, Strokopytov B, Almo SC, Goode BL. 2005. Structural and functional dissection of the Abp1 ADFH actin-binding domain reveals versatile in vivo adapter functions. *Mol Biol Cell* 16(7):3128-39.
- Ram AF, Arentshorst M, Damveld RA, vanKuyk PA, Klis FM, van den Hondel CA. 2004. The cell wall stress response in *Aspergillus niger* involves increased expression of the glutamine : fructose-6-phosphate amidotransferase-encoding gene (*gfaA*) and increased deposition of chitin in the cell wall. *Microbiology* 150(Pt 10):3315-26.
- Ram AF, Klis FM. 2006. Identification of fungal cell wall mutants using susceptibility assays based on Calcofluor white and Congo red. *Nat Protoc* 1(5):2253-6.
- Rasmussen CG, Glass NL. 2005. A Rho-type GTPase, rho-4, is required for septation in *Neurospora crassa*. *Eukaryot Cell* 4(11):1913-25.
- Reynaga-Pena CG, Bartnicki-Garcia S. 1997. Apical branching in a temperature sensitive mutant of *Aspergillus niger*. *Fungal Genet Biol* 22(3):153-67.
- Reynaga-Pena CG, Bartnicki-Garcia S. 2005. Cytoplasmic contractions in growing fungal hyphae and their morphogenetic consequences. *Arch Microbiol* 183(4):292-300.
- Richman TJ, Toenjes KA, Morales SE, Cole KC, Wasserman BT, Taylor CM, Koster JA, Whelihan MF, Johnson DI. 2004. Analysis of cell-cycle specific localization of the Rdi1p RhoGDI and the structural determinants required for Cdc42p membrane localization and clustering at sites of polarized growth. *Curr Genet* 45(6):339-49.
- Ridley AJ. 2001. Rho family proteins: coordinating cell responses. *Trends Cell Biol* 11(12):471-7.
- Ridley AJ. 2006. Rho GTPases and actin dynamics in membrane protrusions and vesicle trafficking. *Trends Cell Biol* 16(10):522-9.
- Riley GL, Tucker KG, Paul GC, Thomas CR. 2000. Effect of biomass concentration and mycelial morphology on fermentation broth rheology. *Biotechnol Bioeng* 68(2):160-72.
- Robertson AS, Allwood EG, Smith AP, Gardiner FC, Costa R, Winder SJ, Ayscough KR. 2009. The WASP homologue Las17 activates the novel actin-regulatory activity of Ysc84 to promote endocytosis in yeast. *Mol Biol Cell* 20(6):1618-28.
- Roca MG, Kuo HC, Lichius A, Freitag M, Read ND. 2010. Nuclear dynamics, mitosis, and the cytoskeleton during the early stages of colony initiation in *Neurospora crassa*. *Eukaryot Cell* 9(8):1171-83.
- Rolke Y, Tudzynski P. 2008. The small GTPase Rac and the p21-activated kinase Cla4 in *Claviceps purpurea*: interaction and impact on polarity, development and pathogenicity. *Mol Microbiol* 68(2):405-23.

- Romisch K. 1999. Surfing the Sec61 channel: bidirectional protein translocation across the ER membrane. *J Cell Sci* 112 (Pt 23):4185-91.
- Rumbold K, van Buijsen HJ, Gray VM, van Groenestijn JW, Overkamp KM, Slomp RS, van der Werf MJ, Punt PJ. 2010. Microbial renewable feedstock utilization: a substrate-oriented approach. *Bioeng Bugs* 1(5):359-66.
- Rumbold K, van Buijsen HJ, Overkamp KM, van Groenestijn JW, Punt PJ, van der Werf MJ. 2009. Microbial production host selection for converting second-generation feedstocks into bioproducts. *Microb Cell Fact* 8:64.
- Sagt CM, ten Haaft PJ, Minneboo IM, Hartog MP, Damveld RA, van der Laan JM, Akeroyd M, Wenzel TJ, Luesken FA, Veenhuis M and others. 2009. Peroxirecretion: a novel secretion pathway in the eukaryotic cell. *BMC Biotechnol* 9:48.
- Saloheimo M, Pakula TM. 2012. The cargo and the transport system: secreted proteins and protein secretion in *Trichoderma reesei* (*Hypocrea jecorina*). *Microbiology* 158(Pt 1):46-57.
- Saloheimo M, Valkonen M, Penttila M. 2003. Activation mechanisms of the HAC1-mediated unfolded protein response in filamentous fungi. *Mol Microbiol* 47(4):1149-61.
- Sambrook J, Russell D. 2001. *Molecular cloning: A laboratory manual*. New York: Cold Spring Harbour Laboratory Press.
- Schekman R. 2010. Charting the secretory pathway in a simple eukaryote. *Mol Biol Cell* 21(22):3781-4.
- Schlessinger K, Hall A, Tolwinski N. 2009. Wnt signaling pathways meet Rho GTPases. *Genes Dev* 23(3):265-77.
- Schuster A, Schmoll M. 2010. Biology and biotechnology of *Trichoderma*. *Appl Microbiol Biotechnol* 87(3):787-99.
- Scott B, Eaton CJ. 2008. Role of reactive oxygen species in fungal cellular differentiations. *Curr Opin Microbiol* 11(6):488-93.
- Segev N. 2001a. Ypt and Rab GTPases: insight into functions through novel interactions. *Current Opinion in Cell Biology* 13(4):500-511.
- Segev N. 2001b. Ypt/rab gtpases: regulators of protein trafficking. *Sci STKE* 2001(100):re11.
- Semighini CP, Harris SD. 2008. Regulation of apical dominance in *Aspergillus nidulans* hyphae by reactive oxygen species. *Genetics* 179(4):1919-32.
- Serrano R, Bernal D, Simon E, Arino J. 2004. Copper and iron are the limiting factors for growth of the yeast *Saccharomyces cerevisiae* in an alkaline environment. *J Biol Chem* 279(19):19698-704.
- Shaffer AL, Shapiro-Shelef M, Iwakoshi NN, Lee AH, Qian SB, Zhao H, Yu X, Yang L, Tan BK, Rosenwald A and others. 2004. XBPI, downstream of Blimp-1, expands the secretory apparatus and other organelles, and increases protein synthesis in plasma cell differentiation. *Immunity* 21(1):81-93.
- Si H, Justa-Schuch D, Seiler S, Harris SD. 2010. Regulation of septum formation by the Bud3-Rho4 GTPase module in *Aspergillus nidulans*. *Genetics* 185(1):165-76.
- Sims RE, Mabee W, Saddler JN, Taylor M. 2010. An overview of second generation biofuel technologies. *Bioresour Technol* 101(6):1570-80.
- Singh A, Del Poeta M. 2010. Lipid signalling in pathogenic fungi. *Cell Microbiol* 13(2):177-85.
- Smyth GK. 2004. Linear models and empirical bayes methods for assessing differential expression in microarray experiments. *Stat Appl Genet Mol Biol* 3:Article3.
- Solovyov A, Gilbert HF. 2004. Zinc-dependent dimerization of the folding catalyst, protein disulfide isomerase. *Protein Sci* 13(7):1902-7.
- Sorimachi K, Jacks AJ, Le Gal-Coeffet MF, Williamson G, Archer DB, Williamson MP. 1996. Solution structure of the granular starch binding domain of glucoamylase from *Aspergillus niger* by nuclear magnetic resonance spectroscopy. *J Mol Biol* 259(5):970-87.
- Steinberg G. 2007. Hyphal growth: a tale of motors, lipids, and the Spitzenkorper. *Eukaryot Cell* 6(3):351-60.
- Stojilkovic SS. 2005. Ca²⁺-regulated exocytosis and SNARE function. *Trends in Endocrinology and Metabolism* 16(3):81-83.

- Su X, Schmitz G, Zhang M, Mackie RI, Cann IK. 2012. Heterologous gene expression in filamentous fungi. *Adv Appl Microbiol* 81:1-61.
- Sudbery P. 2011. Fluorescent proteins illuminate the structure and function of the hyphal tip apparatus. *Fungal Genet Biol* 48(9):849-57.
- Taheri-Talesh N, Horio T, Araujo-Bazan L, Dou X, Espeso EA, Penalva MA, Osmani SA, Oakley BR. 2008. The tip growth apparatus of *Aspergillus nidulans*. *Mol Biol Cell* 19(4):1439-49.
- Taheri-Talesh N, Xiong Y, Oakley BR. 2012. The functions of myosin II and myosin V homologs in tip growth and septation in *Aspergillus nidulans*. *PLoS One* 7(2):e31218.
- Takemoto D, Tanaka A, Scott B. 2006. A p67Phox-like regulator is recruited to control hyphal branching in a fungal-grass mutualistic symbiosis. *Plant Cell* 18(10):2807-21.
- Takeshita N, Dhalluin G, Fischer R. 2012. The role of flotillin FloA and stomatin StoA in the maintenance of apical sterol-rich membrane domains and polarity in the filamentous fungus *Aspergillus nidulans*. *Mol Microbiol* 83(6):1136-52.
- Tanaka A, Takemoto D, Hyon GS, Park P, Scott B. 2008. NoxA activation by the small GTPase RacA is required to maintain a mutualistic symbiotic association between *Epichloe festucae* and perennial ryegrass. *Mol Microbiol* 68(5):1165-78.
- Tcheperegine SE, Gao XD, Bi E. 2005. Regulation of cell polarity by interactions of Msb3 and Msb4 with Cdc42 and polarisome components. *Mol Cell Biol* 25(19):8567-80.
- te Biesebeke R, Boussier A, van Biezen N, van den Hondel CA, Punt PJ. 2006. Identification of secreted proteins of *Aspergillus oryzae* associated with growth on solid cereal substrates. *J Biotechnol* 121(4):482-5.
- te Biesebeke R, Record E, van Biezen N, Heerikhuisen M, Franken A, Punt PJ, van den Hondel CA. 2005. Branching mutants of *Aspergillus oryzae* with improved amylase and protease production on solid substrates. *Appl Microbiol Biotechnol* 69(1):44-50.
- Tiedje C, Sakwa I, Just U, Hofken T. 2008. The Rho GDI Rdi1 regulates Rho GTPases by distinct mechanisms. *Mol Biol Cell* 19(7):2885-96.
- Titorenko VI, Ogrydziak DM, Rachubinski RA. 1997. Four distinct secretory pathways serve protein secretion, cell surface growth, and peroxisome biogenesis in the yeast *Yarrowia lipolytica*. *Mol Cell Biol* 17(9):5210-26.
- Tsukagoshi N, Kobayashi T, Kato M. 2001. Regulation of the amylolytic and (hemi-)cellulolytic genes in aspergilli. *J Gen Appl Microbiol* 47(1):1-19.
- Ungar D, Hughson FM. 2003. SNARE protein structure and function. *Annu Rev Cell Dev Biol* 19:493-517.
- Upadhyay S, Shaw BD. 2008. The role of actin, fimbrin and endocytosis in growth of hyphae in *Aspergillus nidulans*. *Mol Microbiol* 68(3):690-705.
- Ustinov BB, Gusakov AV, Antonov AI, Sinitsyn AP. 2008. Comparison of properties and mode of action of six secreted xylanases from *Chrysosporium lucknowense*. *Enzyme and Microbial Technology* 43(1):56-65.
- Valkonen M, Kalkman ER, Saloheimo M, Penttila M, Read ND, Duncan RR. 2007. Spatially segregated SNARE protein interactions in living fungal cells. *J Biol Chem* 282(31):22775-85.
- van den Berg RA, Braaksma M, van der Veen D, van der Werf MJ, Punt PJ, van der Oost J, de Graaff LH. 2010. Identification of modules in *Aspergillus niger* by gene co-expression network analysis. *Fungal Genet Biol* 47(6):539-50.
- van den Berg RA, Hoefslot HC, Westerhuis JA, Smilde AK, van der Werf MJ. 2006. Centering, scaling, and transformations: improving the biological information content of metabolomics data. *BMC Genomics* 7:142.
- van den Brink J, van Muiswinkel GC, Theelen B, Hinz SW, de Vries RP. 2013. Efficient plant biomass degradation by thermophilic fungus *Myceliophthora heterothallica*. *Appl Environ Microbiol* 79(4):1316-24.
- van Gemeren IA, Punt PJ, Drint-Kuyvenhoven A, Broekhuijsen MP, van't Hoog A, Beijersbergen A, Verrips CT, van den Hondel CA. 1997. The ER chaperone encoding *bipA* gene of black *Aspergilli* is induced by heat shock and unfolded proteins. *Gene* 198(1-2):43-52.

- van Gorcom RF, van den Hondel CA. 1988. Expression analysis vectors for *Aspergillus niger*. *Nucleic Acids Res* 16(18):9052.
- van Hartingsveldt W, Mattern IE, van Zeijl CM, Pouwels PH, van den Hondel CA. 1987. Development of a homologous transformation system for *Aspergillus niger* based on the pyrG gene. *Mol Gen Genet* 206(1):71-5.
- Varadarajan R, Nagarajaram HA, Ramakrishnan C. 1996. A procedure for the prediction of temperature-sensitive mutants of a globular protein based solely on the amino acid sequence. *Proc Natl Acad Sci U S A* 93(24):13908-13.
- Vasara T, Salusjarvi L, Raudaskoski M, Keranen S, Penttila M, Saloheimo M. 2001. Interactions of the *Trichoderma reesei* rho3 with the secretory pathway in yeast and *T. reesei*. *Mol Microbiol* 42(5):1349-61.
- Verdoes JC, Punt PJ, Burlingame R, Bartels J, Van Dijk R, Slump E, Meens M, Joosten R, Emalfarb M. 2007. A dedicated vector for efficient library construction and high throughput screening in the hyphal fungus *Chrysosporium lucknowense*. *Ind Biotechnol* 3:48-57.
- Verdoes JC, Punt PJ, Schrickx JM, Vanverseveld HW, Stouthamer AH, Vandenhondel CAMJJ. 1993. Glucoamylase Overexpression in *Aspergillus-Niger* - Molecular Genetic-Analysis of Strains Containing Multiple Copies of the Glaa-Genes. *Transgenic Research* 2(2):84-92.
- Verdoes JC, Punt PJ, Stouthamer AH, van den Hondel CA. 1994a. The effect of multiple copies of the upstream region on expression of the *Aspergillus niger* glucoamylase-encoding gene. *Gene* 145(2):179-87.
- Verdoes JC, Vandiepeningen AD, Punt PJ, Debets AJM, Stouthamer AH, Vandenhondel CAMJJ. 1994b. Evaluation of Molecular and Genetic Approaches to Generate Glucoamylase Overproducing Strains of *Aspergillus-Niger*. *Journal of Biotechnology* 36(2):165-175.
- Vinck A, de Bekker C, Ossin A, Ohm RA, de Vries RP, Wosten HA. 2011. Heterogenic expression of genes encoding secreted proteins at the periphery of *Aspergillus niger* colonies. *Environ Microbiol* 13(1):216-25.
- Vinck A, Terlouw M, Pestman WR, Martens EP, Ram AF, van den Hondel CA, Wosten HA. 2005. Hyphal differentiation in the exploring mycelium of *Aspergillus niger*. *Mol Microbiol* 58(3):693-9.
- Virag A, Griffiths AJ. 2004. A mutation in the *Neurospora crassa* actin gene results in multiple defects in tip growth and branching. *Fungal Genet Biol* 41(2):213-25.
- Virag A, Harris SD. 2006a. Functional characterization of *Aspergillus nidulans* homologues of *Saccharomyces cerevisiae* Spa2 and Bud6. *Eukaryot Cell* 5(6):881-95.
- Virag A, Harris SD. 2006b. The Spitzenkorper: a molecular perspective. *Mycol Res* 110(Pt 1):4-13.
- Virag A, Lee MP, Si H, Harris SD. 2007. Regulation of hyphal morphogenesis by cdc42 and rac1 homologues in *Aspergillus nidulans*. *Mol Microbiol* 66(6):1579-96.
- Visser H, Joosten V, Punt PJ, Gusakov AV, Olson PT, Joosten R, Bartels J, Visser J, Sinitzyn AP, Emalfarb MA and others. 2011. Development of a mature fungal technology and production platform for industrial enzymes based on a *Myceliophthora thermophila* isolate, previously known as *Chrysosporium lucknowense* C1. *Ind Biotechnol* 7:214-223.
- Wachtler V, Balasubramanian MK. 2006. Yeast lipid rafts?--an emerging view. *Trends Cell Biol* 16(1):1-4.
- Walch-Solimana C, Collins RN, Novick PJ. 1997. Sec2p mediates nucleotide exchange on Sec4p and is involved in polarized delivery of post-Golgi vesicles. *J Cell Biol* 137(7):1495-509.
- Waldron KJ, Rutherford JC, Ford D, Robinson NJ. 2009. Metalloproteins and metal sensing. *Nature* 460(7257):823-830.
- Wang H, Entwistle J, Morlon E, Archer DB, Peberdy JF, Ward M, Jeenes DJ. 2003. Isolation and characterisation of a calnexin homologue, clxA, from *Aspergillus niger*. *Mol Genet Genomics* 268(5):684-91.
- Wang J, Hu H, Wang S, Shi J, Chen S, Wei H, Xu X, Lu L. 2009. The important role of actinin-like protein (AcnA) in cytokinesis and apical dominance of hyphal cells in *Aspergillus nidulans*. *Microbiology* 155(Pt 8):2714-25.
- Warne PH, Viciano PR, Downward J. 1993. Direct interaction of Ras and the amino-terminal region of Raf-1 in vitro. *Nature* 364(6435):352-5.

- Waters BM, Eide DJ. 2002. Combinatorial control of yeast FET4 gene expression by iron, zinc, and oxygen. *J Biol Chem* 277(37):33749-57.
- Wen W, Chen L, Wu H, Sun X, Zhang M, Banfield DK. 2006. Identification of the yeast R-SNARE Nyv1p as a novel longin domain-containing protein. *Mol Biol Cell* 17(10):4282-99.
- Wendland J, Philippsen P. 2001. Cell polarity and hyphal morphogenesis are controlled by multiple rho-protein modules in the filamentous ascomycete *Ashbya gossypii*. *Genetics* 157(2):601-10.
- Withers JM, Swift RJ, Wiebe MG, Robson GD, Punt PJ, van den Hondel CA, Trinci AP. 1998. Optimization and stability of glucoamylase production by recombinant strains of *Aspergillus niger* in chemostat culture. *Biotechnol Bioeng* 59(4):407-18.
- Wongwicharn A, McNeil B, Harvey LM. 1999. Effect of oxygen enrichment on morphology, growth, and heterologous protein production in chemostat cultures of *Aspergillus niger* B1-D. *Biotechnol Bioeng* 65(4):416-24.
- Wösten HA, Moukha SM, Sietsma JH, Wessels JG. 1991. Localization of growth and secretion of proteins in *Aspergillus niger*. *J Gen Microbiol* 137(8):2017-23.
- Wucherpennig T, Kiep KA, Driouch H, Wittmann C, Krull R. 2010. Morphology and rheology in filamentous cultivations. *Adv Appl Microbiol* 72:89-136.
- Xiong L, Lee H, Ishitani M, Zhu JK. 2002. Regulation of osmotic stress-responsive gene expression by the LOS6/ABA1 locus in *Arabidopsis*. *J Biol Chem* 277(10):8588-96.
- Yoshida H, Matsui T, Yamamoto A, Okada T, Mori K. 2001. XBP1 mRNA Is Induced by ATF6 and Spliced by IRE1 in Response to ER Stress to Produce a Highly Active Transcription Factor. *Cell* 107(7):881-891.
- Yoshimori T, Keller P, Roth MG, Simons K. 1996. Different biosynthetic transport routes to the plasma membrane in BHK and CHO cells. *J Cell Biol* 133(2):247-56.
- Youn JY, Friesen H, Kishimoto T, Henne WM, Kurat CF, Ye W, Ceccarelli DF, Sicheri F, Kohlwein SD, McMahon HT and others. 2010. Dissecting BAR domain function in the yeast Amphiphysins Rvs161 and Rvs167 during endocytosis. *Mol Biol Cell* 21(17):3054-69.
- Yuan XL, Goosen C, Kools H, van der Maarel MJ, van den Hondel CA, Dijkhuizen L, Ram AF. 2006. Database mining and transcriptional analysis of genes encoding inulin-modifying enzymes of *Aspergillus niger*. *Microbiology* 152(Pt 10):3061-73.
- Yuan XL, Roubos JA, van den Hondel CA, Ram AF. 2008a. Identification of InuR, a new Zn(II)2Cys6 transcriptional activator involved in the regulation of inulinolytic genes in *Aspergillus niger*. *Mol Genet Genomics* 279(1):11-26.
- Yuan XL, van der Kaaij RM, van den Hondel CAMJJ, Punt PJ, van der Maarel MJEC, Dijkhuizen L, Ram AFJ. 2008b. *Aspergillus niger* genome-wide analysis reveals a large number of novel alpha-glucan acting enzymes with unexpected expression profiles. *Molecular Genetics and Genomics* 279(6):545-561.
- Zheng Y, Yu X, Zeng J, Chen S. 2012. Feasibility of filamentous fungi for biofuel production using hydrolysate from dilute sulfuric acid pretreatment of wheat straw. *Biotechnol Biofuels* 5(1):50.
- Ziman M, O'Brien JM, Ouellette LA, Church WR, Johnson DI. 1991. Mutational analysis of CDC42Sc, a *Saccharomyces cerevisiae* gene that encodes a putative GTP-binding protein involved in the control of cell polarity. *Mol Cell Biol* 11(7):3537-44.

Publications

- Kwon, M. J.**, Arentshorst, M., de Groen F. L. M., Punt, P. J., Meyer, V., Ram, A. F. Establishment of reporter strains for simultaneous detection and functional analysis of secretion-specific genes in *Aspergillus niger*. *Microbiology*, 2014 Feb;160(Pt 2):316-329
- Kwon, M. J.**, Nitsche B. M., Arentshorst, M., Jørgensen, T. R., Ram, A. F., Meyer, V. The transcriptomic signature of RacA activation and inactivation provides new insights into the morphogenetic network of *Aspergillus niger*. *PLoS one*, 2013 Jul 24;8(7).
- Kwon, M. J.**, Jørgensen, T. R., Nitsche B. M., Arentshorst, M., Park J. H., Ram, A. F., Meyer, V., 2012. The transcriptomic fingerprint of glucoamylase over-expression in *Aspergillus niger*. *BMC Genomics*,13, 701.
- Kwon, M. J***, Arentshorst*, M., Roos, E. D., van den Hondel, C. A., Meyer, V., Ram, A. F., 2011. Functional characterization of Rho GTPases in *Aspergillus niger* uncovers conserved and diverged roles of Rho proteins within filamentous fungi. *Mol Microbiol*. 79, 1151-67. (* shared first authors)
- Carvalho, N. D., Arentshorst, M., **Kwon, M. J.**, Meyer, V., Ram, A. F., 2010. Expanding the ku70 toolbox for filamentous fungi: establishment of complementation vectors and recipient strains for advanced gene analyses. *Appl Microbiol Biotechnol*. 87, 1463-73.
- Meyer, V., Arentshorst, M., Flitter, S. J., Nitsche, B. M., **Kwon, M. J.**, Reynaga-Pena, C. G., Bartnicki-Garcia, S., van den Hondel, C. A., Ram, A. F., 2009. Reconstruction of signaling networks regulating fungal morphogenesis by transcriptomics. *Eukaryot Cell*. 8, 1677-91.

Curriculum vitae

Min Jin Kwon was born on 17th January 1978 in Busan, Korea. After graduating high school in 1996, she started to work at Samsung General Chemicals as a technician and in the mean time she enrolled as a student of chemical engineering at Hanbat National University (Daejeon, Korea). During her work as a technician she was involved in synthesis of organic compounds. She transferred the University to Dongseo University (Busan, Korea) due to the working situation at the company. In 2002, she quit the job and continued her studies at Dongseo University and Berlin University of Technology (Master's Dual Degree program in Biotechnology (“Diplom-Ingenieurin der Biotechnologie“)). In 2004, she moved to Berlin to continue her master study at Berlin University of Technology. While completing her degree, in July-September 2006 she did an internship involved in the project “Identification of Zn-finger transcription factors(TXFs) involved in pectin degradation in *Aspergillus niger*” under the supervision of Dr. Arthur Ram in the Institute of Biology Leiden (IBL) at Leiden University in the Netherlands. In 2007 she obtained her Master degree in Biotechnology. From February 2007 until August 2012 she worked as a PhD student in the department of Molecular Microbiology and Biotechnology under the supervision of Dr. Arthur Ram, Prof. Dr. Vera Meyer and Prof. Dr. Cees van den Hondel in the institute above mentioned, and the results are presented in this book.

